UNIVERSITÀ degli STUDI di CATANIA

Dipartimento di Scienze
Biologiche, Geologiche e Ambientali

PhD Course in "Earth and Environmental Science"

Dottorato di Ricerca in "Scienze della Terra e dell'Ambiente"

XXXIV CICLO

Chemical characterization and quantification of metallic nanoparticles (MNPs) in seafood: Dietary exposure and risk assessment

ALFINA GRASSO

Advisor:
Prof.ssa Margherita Ferrante
Co-advisor:
Dott.ssa Chiara Copat

Coordinator:
Prof.ssa Agata di Stefano

Ph. D. attended during 2018/2021

Index

Abstract

The last decade has been characterized by a growing interest in the study of metallic nanoparticles (MNPs) for the various applications in many fields, as they exhibit new and better properties depending on their size, surface area, distribution and morphology. As a result, their increasing use has led to the release into the environment, especially the marine environment. Although nano-based applications have great potential, there are some concerns about the potential adverse effects of nanoparticles on human health and the environment. As a result, food is a potential vehicle for oral exposure to nanoparticles because they can be used directly in food as additives, migrate from packaging and sensors into the food matrix, and food can accumulate nanoparticles from the environment. This can lead to intentional and unintentional human exposure through food ingestion. To date, there is limited data on oral exposure, in vivo and in vitro toxicity studies are not always congruent, the fate of nanoparticles once they enter the gastrointestinal tract is unknown, and there are no provisional oral reference doses to protect consumer health.

This work focuses on the investigation of three commonly used metallic nanoparticles, TiO_2-NPs, Ag-NPs and ZnO-NPs and food additives E171 (TiO_2) and E174 (Ag) in seafood.

The main aspects of this work were:

1) the chemical characterization and quantification of TiO_2-NPs, Ag-NPs and ZnO-NPs and dissolved elements in processed canned seafood (tuna, mackerel, anchovies and clams) using the new single particle inductively coupled plasma technique (spICP- MS) preceded by alkaline digestion;

2) the assessment of an estimated daily intake for adults and children according to the guidelines of EPA;

3) the evaluation of *in-vitro* cytotoxicity and genotoxicity in colon

cancer cells HCT116 and Caco 2 induced by E171 compared to TiO_2 NPs 60 nm;
4) the evaluation of the acute *in-vivo* toxicity of TiO_2-NPs (60 nm), E171, Ag-NPs (40 nm), E174 and ZnO-NPs (30 nm) in zebrafish embryos using a fish embryo toxicity test (FET) (OECD Test Guideline 236);
5) the determination of the biopersistence rate of TiO_2-NPs, Ag-NPs and ZnO-NPs in standards and seafood samples (tuna and shellfish) using an in vitro static digestion system.
All the nanoparticles sought were found to be present in all seafood, indicating environmental contamination by these compounds and a potential risk for the environment and human health.
Estimates of daily oral exposure to nanoparticles suggest that seafood may be an important route for ingestion of these metal compounds, especially for a vulnerable group such as children.
The *in-vitro* study confirmed that food-grade TiO_2 in anatase form (E171) may have stronger genotoxic effects than general TiO_2 (60 nm), while *in-vivo* study showed that Ag-NPs (40 nm) are embryotoxic at a lethal concentration (LC50) of 9.604 mg/L, while TiO_2 (60 nm), E171 and E174 showed no acute embryotoxicity at 100 mg/l. ZnO-NPs (30 nm), revealed a developmental delay at the end of 96 h post fertilization.
The calculated biopersistence rates were always higher than the limit set by EFSA (12%), indicating that the metallic nanoparticles studied are stable under gastrointestinal conditions and cannot be considered as readily degradable and may be able to pass through the gastrointestinal epithelium and enter the bloodstream and other organs.

Riassunto

L'ultimo decennio è stato caratterizzato da un crescente interesse nello studio delle nanoparticelle metalliche per le loro varie applicazioni in molti campi, in quanto presentano nuove e migliori proprietà a seconda di dimensioni, superficie, distribuzione e morfologia. L'incremento nella loro produzione ha portato inevitabilmente al rilascio nell'ambiente, in particolare nell'ambiente marino. Sebbene le applicazioni basate sulle nanoparticelle abbiano un grande potenziale, vi sono alcune preoccupazioni circa i potenziali effetti negativi delle nanoparticelle sulla salute dell'uomo e dell'ambiente.

Il cibo è un potenziale veicolo per l'esposizione orale alle nanoparticelle poiché possono essere utilizzate direttamente negli alimenti come additivi, migrare da imballaggi e sensori nella matrice alimentare, o essere accumulate dall'ambiente. Questo può portare ad un'esposizione umana intenzionale e non intenzionale attraverso l'ingestione di cibo. Ad oggi, i dati sull'esposizione orale, gli studi in di tossicità in vitro e in vivo non sono sempre congruenti. Ad oggi il destino delle nanoparticelle una volta entrate nel tratto gastrointestinale è sconosciuto e non esistono dosi di riferimento tossicologico per proteggere la salute dei consumatori.

Questo lavoro si concentra sullo studio di tre nanoparticelle metalliche comunemente utilizzate, TiO_2, Ag e ZnO, e additivi alimentari E171 (TiO_2) e E174 (Ag) nei prodotti ittici.

Gli aspetti principali di questo lavoro sono stati:

1) la caratterizzazione chimica e la quantificazione di nanoparticelle di TiO_2, Ag e ZnO e di elementi disciolti in prodotti ittici trasformati (tonno, sgombro, acciuga e vongola) mediante spettrometria di massa a plasma accoppiato induttivamente abbinata ad un software per la determinazione delle singole nanoparticelle (spICP- MS), preceduta da una digestione alcalina dei campioni;

2) la valutazione di una dose di esposizione orale giornaliera stimata per adulti e bambini, secondo le linee guida dell'EPA;

3) la valutazione della citotossicità e della genotossicità in vitro indotta da E171 e TiO_2 (60 nm) su linee cellulari tumorali del colon HCT116 e Caco 2;
4) la valutazione della tossicità acuta in vivo di TiO_2 (60 nm), E171, Ag (40 nm), E174 e ZnO (30 nm) mediante un test di tossicità sugli embrioni di zebrafish (FET) (linea guida OCSE 236);
5) la determinazione del tasso di persistenza biologica delle nanoparticelle di TiO_2, Ag e ZnO in soluzioni di standard e campioni di pesce (tonno e molluschi) tramite un modello statico di digestione in vitro.
Le nanoparticelle ricercate sono risultate presenti in tutti i campioni di pesce, indicando una contaminazione ambientale da parte di questi composti e un potenziale rischio per l'ambiente e la salute umana.
Le stime sull' esposizione orale giornaliera alle nanoparticelle suggeriscono che i prodotti ittici trasformati possono essere una via importante per l'ingestione di questi composti metallici, specialmente per un gruppo vulnerabile come i bambini.
Lo studio in vitro ha confermato che il TiO_2 alimentare in forma di anatasio (E171) può avere effetti genotossici più forti del TiO_2 (60 nm), mentre lo studio in vivo ha dimostrato che le nanoparticelle di Ag (40 nm) sono embriotossiche con una concentrazione letale (LC50) di 9,604 mg/L, mentre il TiO_2 (60 nm), E171 e E174 non hanno mostrato tossicità acuta sugli embrioni ad una concentrazione di 100 mg/L. Infine, le nanoparticelle di ZnO (30 nm) hanno mostrato un rallentamento dello sviluppo dopo 96 ore dalla fecondazione.
Le percentuali di biopersistenza calcolate sono sempre state superiori al limite fissato dall'EFSA (12%), indicando che le nanoparticelle metalliche studiate sono stabili in condizioni gastrointestinali e non possono essere considerate facilmente degradabili e possono pertanto essere in grado di passare attraverso l'epitelio gastrointestinale ed entrare nel flusso sanguigno e in altri organi.

1 Introduction

1.1 Background

The history of nanomaterials (NMs) is quite long; nevertheless, important developments in nanoscience have taken place in the last two decades.

The idea of nanotechnology was first proposed by Nobel Laureate Richard Feynman in his famous lecture at the California Institute of Technology, on December 29, 1959.

Nanomaterials are structures that have at least one external dimension in the nanoscale (1-100 nm). Due to their small size and relatively large surface-to-volume ratio, NMs have different physicochemical and optical properties than conventional materials, e.g., different thermal, mechanical, electrical, chemical, catalytic, etc. (Auffan et al. 2009; Kango 2013).

For all these reasons, engineered NMs are attractive for a wide range of applications and offer numerous opportunities in many fields. In recent years, there have been impressive developments in the field of nanotechnology. Numerous methods have been developed for the synthesis of nanoparticles (NPs), which have a specific shape and size depending on the requirements (Stone et al. 2009).

Despite their exceptional properties, there are still "downsides" in terms of their toxicity to living organisms.

For sustainable development and safe use of innovative products based on these materials, it is important to understand the potential risks to human health posed by these novel contaminants.

A crucial point is the determination of a dosage at which a nanomaterial can be considered safe and thus suitable for everyday products.

Humans are exposed to NPs through food and drinking water, as well as through skin products, which are absorbed through the

gastrointestinal tract and the skin, respectively. Other relevant routes of entry are the respiratory tract and the bloodstream.

In the food industry, nanotechnology can be used to improve the quality, shelf life, safety, cost and nutritional value of food (Sekhon 2010). In some cases, nanomaterials used in the food industry are not intended to enter the final product, such as in packaging, sensors, and antimicrobial treatments used to disinfect food manufacturing equipment. In other cases, nanomaterials are specifically intended for use in food, such as nanoparticles used as delivery systems or to alter optical, rheological, or flow properties.

Although there are a number of publications on the adverse effects of NPs, there are still some knowledge gaps regarding the inherent hazards of NPs, the potential human exposure to NPs, and the relationship between exposure and adverse health effects (risks) of NPs (Oberdorster et al. 2007; Hussain et al. 2015).

The United States of America (U.S.A.) and Europe have developed many approaches to regulating nanomaterials.

In the U.S.A., the Environmental Protection Agency (EPA), in collaboration with other federal agencies such as the Food and Drug Administration (FDA), regulateS the use of NPs. In Europe, the handling of chemicals is regulated by the 'Registration, Evaluation, Authorisation and Restriction of Chemicals' (REACH). Thus, there is no proper distinction between nanomaterials and chemicals.

The existing information on possible adverse health effects is mainly based on animal experiments and in vitro studies with cell lines.

For example, nanomaterials have been shown to induce cytotoxic, genotoxic, inflammatory and oxidative stress responses in various mammalian cell lines (Elsabahy et al. 2013, Watson et al. 2014).

Several specific biological responses resulting from exposure to NPs, such as reduction in cell viability, have been shown to be influenced by the physicochemical properties of NP such as size, surface charge, and surface area (Duran et al. 2015, Recordati et al. 2016).

Due to their small size, there is concern that nanoparticles inadvertently cross the barriers of the human body.

Several in vivo studies have been conducted to evaluate the distribution of nanoparticles after inhalation, oral exposure, skin exposure and intravenous injection (Geraets et al. 2012, Leite-Silva et al. 2013, van der Zande et al., 2014).
These studies show that nanoparticles can cross the lung, intestinal, skin and placental barriers, depending on the route, time and concentration of exposure and their properties.
To provide a realistic and reliable risk assessment for NPs, knowledge of their concentrations in the diet is needed.
This is possible if robust, reliable, and accurate methods are developed for characterizing NPs in complex matrices.

1.2 Nanomaterials

The definition of a nanomaterial as used by the European Commission: a natural, incidental or manufactured material containing particles in an unbound state or as an aggregate or agglomerate and in which, for 50% or more of the particles in the number size distribution, one or more external dimensions are in the size range 1 nm - 100 nm.
Nanomaterials can be classified in many different ways, one of which is shown in the following figure (Borm and Müller-Schulte, 2006).

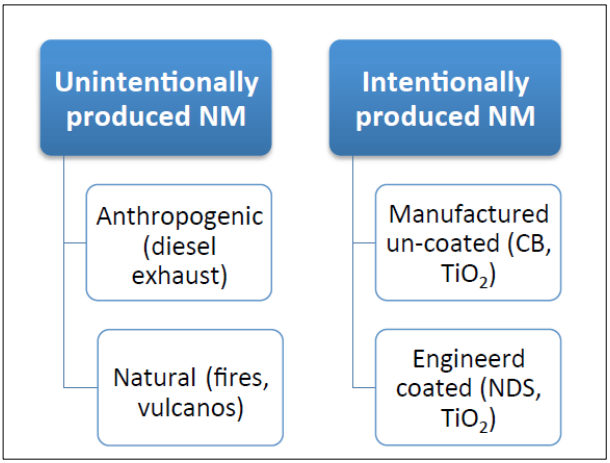

Figure 1. Categories of nanomaterial. Abbreviations: NM, Nanomaterial; CB, Carbon Black; TiO2, Titanium Dioxide; NDS, Nano Delivery Systems.

Nano-sized particles are important components of the Earth biogeochemical system, being produced by various natural processes, such as volcanic eruptions and dust storms. Human industrial activities disturbed their natural cycle and increased their abundance, producing also anthropogenic nanoparticles ANPs (Lespes et al., 2020).

The term "engineered nanoparticles" (ENPs) was introduced to distinguish natural particles from man-made particles of similar size. ENPs are produced by different chemical synthetic methods: the bottom-up method, which starts from molecules, atoms or ions to obtain ENPs, or the top-down method, which uses bulk materials that are reduced to ENPs by physical, chemical or mechanical processes (Sharma et al., 2015). As mentioned earlier, ENPs are structures with at least one dimension between 1 and 100 nm.

They can be categorized based on their shape (Tiede et al., 2008).

- Nanofilms/nanocoatings: 1-100 nm in one dimension.
- Nanowires/nanotubes: 1-100 nm in two dimensions. These can be

mm in length.
- Nanoparticles: 1-100 nm in three dimensions.
- Quantum dots: the smallest nanoparticles with a size of 1-10 nm (10-50 atoms).

It is not easy to distinguish the health effects of ENPs from the health effects caused by NPs of natural or anthropogenic origin.

Size is generally inversely related to reactivity. This is due to the fact that smaller particles have a larger surface area relative to mass ratio and the number of atoms on their surface increases exponentially, which increases reactivity (Borm and Müller-Schulte, 2006).

Crucial to the fate and effect of NPs is their tendency to agglomerate, one of the complicating factors in nanoscience. Agglomerated particles can dissociate depending on factors such as pH, ion concentration, zeta potential of the particle, and surrounding proteins (Keller et al., 2021). Furthermore, depending on their surface properties, primary particles can form larger structures called secondary particles. Agglomerates form between primary particles that are loosely held together by van der Waals interactions. The surface area of an agglomerate is approximately equal to the sum of the primary particles that form the agglomerate because they are not tightly bound together (Powell et al., 2010). This is important to know because it has implications for reactivity. One cannot assume lower reactivity of agglomerates just because they are larger structures. It depends on what particles or structures are being studied and in what context. It is said that the pores within an agglomerate can hold particles of 1-2 nm (depending on the particle) and that the immersed smaller particles would be exposed to both the inner and outer surfaces (Sharma et al., 2015).

Therefore, it is quite difficult to predict the stability of NPs in media.

Studies have provided compelling evidence that the interaction of NPs with biological media and biomolecules is complicated and can lead to particle agglomeration, aggregation, and dissolution (Stebounova et al., 2011).

1.2.1 *Titanium dioxide nanoparticles*

Titanium is one of the most abundant elements in the earth's crust, occurring in nature only in its oxidized form as titanium dioxide or Ti(IV)oxide.

Titanium dioxide (TiO_2) is a fine, white, crystalline, odorless, poorly soluble powder that has relatively low toxicity (Sager et al., 2008).

TiO_2-NPs are used in numerous products due to their ability to impart opacity and whiteness (Weir et al., 2012). It is usually present in a mixture of anatase and rutile crystals, with the anatase form being more chemically reactive (Warheit et al., 2007).

TiO_2 is also used in food as a colorant (E171) and therefore can enter the food in the nanoform (Periasamy et al., 2015). It has been shown that 25-38% of a food grade TiO_2 was in the form of NPs less than 100 nm in size (Weir et al., 2012). TiO_2 is also commonly used as a food additive and antimicrobial agent for food packaging and storage containers (EFSA Panel on Food Contact Materials, Enzymes and Processing Aids (CEP) et al., 2019).

Concerns have been raised that the NPs of TiO_2 may have different bioactivity than solid TiO_2 and may have adverse effects on human health.

TiO_2-NPs have been found to induce genotoxicity, cytotoxicity, reactive oxygen species formation (ROS), and cytokine production, as demonstrated in vitro and in vivo (Gerloff et al., 2012).

Exposure to food-grade TiO_2, which contained approximately 25% of TiO_2 as NPs < 100 nm, also resulted in loss of microvilli from Caco-2BBe1 cells (Faust et al., 2014).

Although TiO_2-NPs have been extensively studied in recent years, many questions regarding potential health effects remain to be addressed to support risk assessment and management.

1.2.2 *Silver nanoparticles*

Silver nanoparticles (Ag-NPs) can be synthesized by various physical, chemical, and biological methods. However, in recent

years, various rapid chemical methods have been replaced by green synthesis because the toxicity of the process could be avoided and the quality could be increased.

Biologically synthesized Ag-NPs have many applications, such as coatings for solar energy absorption and intercalation materials for electric batteries, optical receptors, catalysts in chemical reactions, bio-labelling, and antimicrobial agents (Zhang et al., 2019).

Ag is authorized as food additive in its elemental form (E174) to be used to color the external coating of confectionery, for decoration of chocolates and in liqueurs according to the Regulation (EC) No. 1129/2011 and specification to the Regulation (EC) No. 231/2012 (EFSA Panel on Food Additives and Nutrient Sources added to Food (ANS), 2016). Furthermore, Ag-NPs are used in the form of aqueous suspensions in food supplements, which are claimed to boost the body's immune system and have an antimicrobial effect on various types of pathogens (Ferdous and Nemmar, 2020). In addition, they are used as antibacterial coatings in refrigerators and packaging materials for food, wound dressings, clothing, and deodorants, due to because of their broad spectrum killing against both Gram-positive and Gram-negative bacteria, fungi, viruses, and even against multidrug resistant bacteria (Kim et al., 2018).

In vitro studies have reported several adverse effects of Ag-NPs, including, for example, a decrease in cell viability (McShan et al., 2014), increased ROS production (Rahman et al., 2009), DNA damage (Huk et al., 2014), cell cycle changes (Asharani et al., 2009), apoptosis (Foldbjerg et al., 2009), and inhibition of stem cell differentiation (Park et al., 2011).

In vivo studies with Ag-NPs have been performed in rats and mice (Falconer and Grainger, 2018; Grosse et al., 2013). In a 28-day repeated-dose toxicity study in rats, intravenous administration of Ag NPs resulted in suppression of the functional immune system (Vandebriel et al., 2014).

Factors known to influence toxicity include the concentration, dispersion, size, and surface functionalization of Ag NPs (Recordati et al., 2016).
The literature also indicates that the dissolution of silver nanoparticles may play a key role in their toxicity (Maurer et al., 2014).

1.2.3 Zinc oxide nanoparticles

ZnO occurs in the earth's crust as the mineral zincite; however, most commercial ZnO is produced synthetically.
To synthesize ZnO-NPs, chemical vapor method, spray pyrolysis, laser synthesis technique, and vapor condensation method may all be applied. It's usually in the form of a white powder that's practically water insoluble. Plastics, ceramics, glass, cement, rubber (e.g., car tires), lubricants, paints, ointments, adhesives, sealants, pigments, food (source of Zn nutrition), batteries, ferrites, fire retardants, and other materials and products use the powder as an addition (Sabir et al., 2014).
ZnO-NPs have made their way into industry and are currently one of the most essential building blocks of modern civilization due to their ability to absorb ultraviolet light, broad chemical spectrum, piezoelectricity, and luminescence at high temperatures (Girigoswami et al., 2015).
Zinc and zinc oxide nanoparticles can be used as an additive in food supplements and functional foods, as it is an essential trace element required for the maintenance of human health and well-being (MacDonald, 2000; Nutrition, 2021).
The antibacterial activity of the ZnO nanoparticles was likewise higher than that of the microparticles against both Gram-positive and Gram-negative bacteria. Nevertheless, antibacterial activity's specific mechanisms are yet unknown (Sirelkhatim et al., 2015). In their investigation, some researchers believed that the production of hydrogen peroxide is the key mechanism for antibacterial activity

(Sawai et al., 1998), while others stated that particle adherence to the bacterial surface owing to electrostatic forces might also be a component (Stoimenovet et. al., 2002).

Research has focused on the cytotoxic and genotoxic potential of ZnO-NPs in eukaryotic cells. The toxicity of ZnO-NPs was studied in human cervical cancer cell line (HEp-2), human hepatocyte cell line HEK 293 and human bronchial epithelial cells. The observed results of the study showed that the zinc oxide nanoparticles were toxic to the cells and caused DNA damage and a decrease in cell viability (Osman et al., 2010).

In addition, the ZnO-NPs delayed the development of Danio rerio embryos, caused tissue damage, and decreased survival and hatching (Zhu et al., 2009).

Although the mechanisms behind the properties of ZnO-NPs are not fully understood, it has been shown that ZnO-NPs can increase the intracellular concentration of reactive oxygen species (ROS), leading to genotoxicity and cell death (Cardozo et al., 2019).

2 Analytical technique to characterize nanoparticles

2.1 Characterization of nanoparticles

Due to the increasing use of engineered nanomaterials in consumer products and toxicity studies of engineered nanomaterials, regulatory agencies and other research organizations have determined that the development of robust, reliable, and accurate methods for characterizing NPs in complex matrices is a top priority and urgently needed (Clemente et al., 2013).

The most important properties of NPs include particle size, size distribution, chemical composition, particle concentration, aggregation state, shape, crystallinity, surface charge, specific area, surface speciation, and functionality, etc.

Different techniques and tools are required to characterize the various properties of NPs. There is no single technique that can fully characterize all the above main properties of NPs. For NPs, the size, size distribution and chemical composition are of primary interest for many purposes.

Electron microscopy, field flow fractionation (FFF), and light scattering are the most widely used methods to characterize the size of ENPs, although some other techniques exist.

Electron microscopy is a powerful technique for characterizing the size of ENPs and analyzing their chemical composition in conjunction with an energy dispersive spectroscopy detector. However, its application is usually limited by its sensitivity to environmental and biological samples. Characterization of NPs in biological matrices also requires extensive sample preparation, usually involving fixation, dehydration, sectioning, and staining. Electron microscopy examines only a tiny portion of the entire sample and is therefore sometimes unrepresentative.

FFF is a technique for particle separation. Particle size can be calculated either by FFF theory or by creating a calibration curve between particle size and retention time. In FFF, a physical field is applied perpendicular to a solution pumped through a long and narrow channel to separate the particles/macromolecules in the solution according to their different "mobility" under the force applied by the field. Based on the different applied fields, FFF can be divided into symmetric FFF, asymmetric FFF, centrifugal/sedimentation FFF, thermal FFF, electrical FFF, etc. After FFF separation, UV/Vis detectors, light scattering detectors and element based detectors (ICP-OES /ICP- MS) are usually used to detect the analyte either alone or coupled online.

UV/MALS-ICP-MS has shown great potential for particle characterization, especially for studying the interactions between particles/colloids and other chemicals.

For example, FFF-ICP-MS has recently been successfully used to study the interactions between toxic elements and environmental colloids/NPs or humic acid, such as the sorption of U(VI) on nano-hematite, the interaction of bentonite colloids with Cs, Eu, Th and U in the presence of humic acid, NOM metal complexes in water (Lesher et al., 2009).

Although FFF coupling with multidetectors offers some analytical advantages, there are still some challenges. For example, each analysis usually takes 1 hour or even longer if the particle size range is large, which does not make FFF a high-throughput technique. Another challenge with FFF is the non-specific interactions between analyte particles and FFF membranes, which can lead to retention time shifts and sample loss (Nischwitz and Goenaga-Infante, 2012).

2.2 *Single Particle-Inductively Coupled Plasma Mass Spectrometry*

Single particle inductively coupled plasma- mass spectrometry (sp-ICP-MS) is an emerging technique for NP characterization and

quantification, especially at low NPs concentrations and in complex matrices, due to the sensitivity of the technique. This is the first analytical technique that can determine all three nano-specific metrics from a single sample: particle size, mass and number distribution.

The use of sp-ICP-MS to detect NPs in aqueous samples is straightforward, as sample preparation consists only of dilution prior to analysis. However, analysis of NPs in tissues is more difficult and requires a digestion step prior to analysis.

Traditional digestion methods focus on using strong acids to dissolve the desired elements from the tissues. However, this type of digestion is incompatible with the analysis of NPs, as the ENPs present would likely dissolve.

Another approach is to digest tissues with strong bases or enzymes, which ideally release the NPs without altering them.

In sp-ICP-MS analysis, the NP suspensions enter the plasma and are ionized individually. They are then detected as pulse signals by the mass spectrometer, making sp-ICP-MS a powerful technique to determine the masses of the metal elements in each NP (Laborda et al., 2014). At the same time, the corresponding dissolved analyte is detected as a continuous signal, which means that sp-ICP-MS is able to detect both the particle analyte and the dissolved analyte simultaneously.

In sp-ICP-MS analysis, the signal intensity of NP depends on the particle size, and the signal frequency is proportional to the particle concentration in the samples. In the early days, sp-ICP-MS was a rather qualitative technique, as there were no well-characterized NPs standards. More recently, quantitative results have been obtained with sp-ICP-MS after some well-defined NPs standards and fast scanning techniques ICP-MS, such as NexION 350 ICP-MS, became commercially available.

The most important factor in measuring individual particles is the speed at which data can be acquired: since particle ionization events are on the order of microseconds, fast data acquisition and elimination of settling time between measurements are critical. Continuous measurement allows multiple measurements per particle ionization event, resulting in more accurate sizing. With sp-ICP-MS, continuous data acquisition with a dwell time of 100 μs or less is the most important instrumental requirement for accurate nanoparticle counting and sizing.

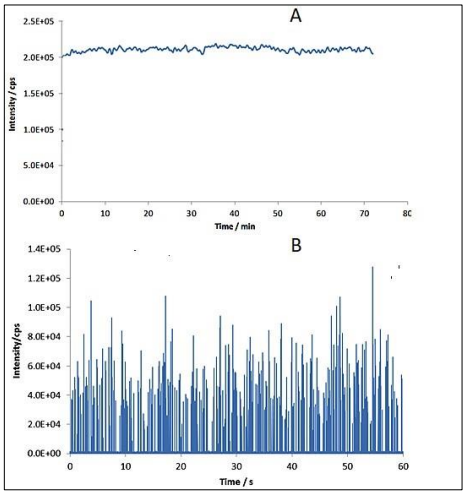

Figure 2. A) Continuous signal from measuring a dissolved analyte; B) A signal from measuring nanoparticles.

2.3 Sample preparation

While sizing NPs suspended in water is relatively straightforward using ICP-MS, accurate mass determination of NPs in complex media such as consumer products and natural systems remains a challenge. When NPs are suspended in a complex medium, the

matrix can affect the sensitivity of the analyte and lead to inaccurate NP size determination.

One approach for extracting NPs is chemical digestion with the strong base tetramethylammonium hydroxide (TMAH).

Our experiments prove that extraction with TMAH in combination with sp-ICP-MS can be successfully used to release NPs from tissues.

TMAH extraction has been shown to provide high yields in both particle number and total mass compared to tissue disruption with ultrasound and water, and is a promising technique for the analysis of NPs in biological samples (Gray et al., 2013).

Moreover, TMAH digestion does not affect particle stability by aggregation and settling of particles (loss of pulses).

In short, tissue digestion was performed according to the method described by Gray et al. 2013.

Briefly, organic base (TMAH) was used to digest tissues and release NPs from the tissues at a solvent to tissue ratio of 20:1, and the TMAH digestion solution consisted of 20% TMAH w/w. Digestion of the samples was carried out for 24 hours at room temperature. The digested tissues were diluted to 1% TMAH prior to analysis. This TMAH concentration was maintained if further dilution was required.

3 Techniques for determining the toxicity and genotoxicity of nanoparticles in cells in vitro

Nanoparticles have attracted much attention because of their toxicity. They cause toxicity through various processes. Nanoparticles can easily cross cell membranes and disrupt intracellular metabolism (Hanley et al., 2009).
The formation of ROS is one of the mechanisms for the toxicity of nanoparticles (Wang et al., 2013).
After internalization of nanoparticles, phagocytosis induces pro-oxidant effects leading to the formation of ROS, mitochondrial respiration and NADPH-dependent enzyme systems (Regoli and Giuliani, 2014).
In vitro assessment of nanoparticle toxicity is one of the most important methods. Advantages include lower cost, speed, and minimal ethical concerns. The assessment can be divided into proliferation, apoptosis and DNA damage assays.
They have also been shown to enter cells via various endocytotic processes (Dusinska and Collins, 2008). These processes are most likely dependent on surface properties that may be directly related to their genotoxic potential. It is therefore imperative to investigate the direct effects on DNA in order to obtain initial information on the potential genotoxicity of these materials.

3.1 Microculture Tetrazolium Assay (MTA)

The MTT assay to assess cell viability has become a widely used, standard technique in recent nanoparticle research.
Short-term MTAs are metabolic assays that do not provide direct information on the total number of cells, but measure the viability of a cell population compared to untreated control cells.

Cells are treated with particles for various times before soluble yellow tetrazolium salts such as MTS (3-(4,5-dimethylthiazol-2-yl)-5-(3-carboxymethoxyphenyl)-2-(4-sulfophenyl)-2H-tetrazolium) or MTT (3-(4, 5-dimethylthiazol-2-yl)-2, 5-diphenyltetrazolium bromide) are used for 2-4 hours at 37°C.
During this process, viable cells with active mitochondrial respiratory activity bioreduce MTS or MTT via mitochondrial succinic acid dehydrogenases to an insoluble purple formazan product, which is subsequently solubilized by dimethyl sulfoxide (DMSO) or detergents and quantified using a visible light spectrophotometer. Data are reported as optical density (OD)/control group.

3.2 Clonogenic Assay

The clonogenic assay allows evaluation of decreased or increased survival and proliferation over extended periods of time (weeks). After plating at a very low density, the cells are allowed to grow until colonies are observed, i.e. from 10 days to 3 weeks. The cells can either be pre-treated with the desired particles or treated after plating out. Each colony is assumed to originate from a single plated cell, hence the name "clonogenic assay". Colonies can be stained with crystal violet or nuclear stain and quantified by number and/or size.

3.3 Comet Assay

The single cell gel electrophoresis (SCGE) assay, also known as the comet assay, can detect single and double DNA strand breaks and alkali-labile sites in single cells. This assay is based on the simple principle that DNA containing strand breaks migrates into the agarose gel faster than intact DNA when an electric field is applied. Therefore, the extent of DNA damage is directly related to the length of the "comet tail" that becomes visible after exposure to test materials. Staining with a fluorescent dye allows visualization of

comet tails. Various parameters of these structures are usually determined using image analysis software and then used to calculate an olive tail moment (OTM) defined by both the tail length and the distribution of DNA in the tail parameter.

3.4 Western Blot

The Western blot is commonly used in research to separate and identify proteins. In this technique, a mixture of proteins is separated by gel electrophoresis according to their molecular weight and thus their type. These results are then transferred to a membrane, creating a band for each protein. The membrane is then incubated with labelled antibodies specific for the protein of interest.
The unbound antibody is washed off, leaving only the antibody bound to the protein of interest. The bound antibodies are then detected by developing the film.
Since the antibodies bind only to the protein of interest, only one band should be visible. The thickness of the band corresponds to the amount of protein present. Thus, a standard can indicate the amount of protein present.

4 Assay for alteration in gene expression

4.1 Real time-PCR (Bcl-2 and Bax)

Bcl-2 and Bax are two important regulatory genes in the mitochondrial apoptotic signaling pathway.
The gene product Bcl-2 is thought to contribute to oncogenesis by suppressing signals that initiate apoptotic cell death.
Bax, a major homolog of Bcl-2, is a promoter of apoptosis. It has been proposed that the sensitivity of cells to apoptosis stimuli is closely related to the ratio of Bcl-2/Bax and other Bcl-2 homologs. When Bcl-2 is present in excess, cells are protected. However, when Bax is in excess and Bax homodimers are dominant, cells are susceptible to apoptosis.
One technique for assessing gene expression is polymerase chain reaction (qRT-PCR).
Real-time PCR is a quantitative method for determining the copy number of PCR templates such as DNA or cDNA and consists of two types: probe-based and intercalator-based.
Probe-based real-time PCR requires a pair of PCR primers (as in normal PCR) and an additional fluorogenic oligonucleotide probe to which both a fluorescent reporter and a quencher dye are bound. The intercalator-based (SYBR Green) method requires a double-stranded DNA dye in the PCR reaction to bind to newly synthesized double-stranded DNA and produce fluorescence. Both methods require a dedicated thermal cycler equipped with a sensitive camera that monitors fluorescence in each well of a 96-well plate at regular intervals during the PCR reaction.

5 Routes of Exposure to Nanoparticles and toxicology

Various natural processes and industrial activities of humans produce NPs. As a result, living organisms are constantly exposed to NPs that enter the human body through various pathways (Buzea et al., 2007)).
TiO_2-NPs and ZnO-NPs are used in commercial products such as sunscreens, food additives, and paints (Chen and Mao, 2007). Ingestion and skin penetration are inevitably the main, although not the only, routes by which they enter the human body.

Ag-NPs are used in food, antibacterial products, water disinfectants, the textile industry, diagnostic biosensors, imaging probes, and conductive inks (Marin et al., 2015). For these reasons, they can enter the human body through inhalation, ingestion, and skin penetration.

The various physicochemical properties of NPs (size, shape, charge, surface coating, stability, crystallinity, agglomeration state, and dosage) have been shown to have adverse effects on biological systems (Gatoo et al., 2014).

In fact, the shape and size of NPs are key parameters regardless of the exposure route, as rods have a higher penetration rate than spheres and triangles (Sergent et al., 2012).

The properties of NPs can be modified by functionalization processes to alter or reduce the toxicity of the chemical materials used to produce them (Oberdörster et al., 2007).

In addition to physicochemical properties, the interaction between NPs and the culture medium or biological fluids is another important parameter to be considered in toxicological studies. This

interaction could promote NP aggregation and dispersion, both of which affect cell uptake, which in turn influences the toxicity of NPs.

5.1 Ingestion

The human gastrointestinal tract is divided into the upper (esophagus, stomach, and duodenum) and lower gastrointestinal tracts (small intestine and the entire colon), each of which has specific functions (Reinus and Simon, 2014). This apparatus forms a mucosal barrier that selectively promotes the breakdown and absorption of nutrients.

Humans can directly ingest a variety of food ingredients, additives, and supplements that contain NP. As a consequence, NPs can affect gastrointestinal tract motility, the mucus layer covering the lumen, and the microbiota (Kararli, 1995).

In the gastrointestinal tract, there is a modulation of pH, which changes along the different sections of the apparatus (Fröhlich and Fröhlich, 2016). In addition to pH, peristalsis can also affect physicochemical properties NP.

The stomach is characterized by an acidic environment with an early pH range of 1.2-2.0. Dissolution of NPs at low pH promotes their further degradation in the digestive fluids.

It has been observed that the uptake of NPs less than 100 nm in diameter occurs mainly by endocytosis in "normal" epithelial cells (Axson et al., 2015).

The digestion and absorption processes are carried out by the small intestine, which has a typical pH between six and seven in the duodenal region.

Large NPs and microparticles can also cross the intestinal epithelium by transcytosis via the uptake of M cells and villi through the gaps formed in their apical zone, due to a dysfunction process induced by NPs that alters the morphology of the epithelium (Elder et al., 2009).

Recent studies show that inorganic NPs, which include quantum dots (QDs), metal oxide NPs such as SiO2NPs, TiO_2-NPs, ZnO-NPs,

and metallic NPs such as silver NPs (Ag-NPs), are less well tolerated even at low concentrations because they are susceptible to low pH, which initiates a degradation process. The deposition of Ag-NPs in the gastrointestinal tract has been widely demonstrated in various studies (Loeschner et al., 2018). TiO_2-NPs induce a change in microvilli on the apical surface of the epithelium and an increase in calcium levels (Koeneman et al., 2010). ZnO-NPs (8-10 nm) and micro ZnO (< 44 μm) induce mithocondrial dysfunction on human colon carcinoma cells (Moos et al., 2011). The adverse effects were associated with the interactions between the particles and the cells; the toxicity did not depend on the zinc ions in the cell culture medium and the NPs were found to be more toxic than microparticles.

5.2 Skin penetration

The skin has several functions, such as protection from external agents, UV protection, and a selective permeable barrier. In addition, the skin plays a critical role in regulating human body temperature and immunological response.

The skin is structurally divided into three layers: Epidermis, Dermis, and Hypodermis (Visscher et al., 2014). The cosmetics contain TiO_2-NPs (70/80%), ZnO-NPs (70%) and Ag-NPs (20%).

In some studies, the NPs were found to be unable to cross the skin barrier. In contrast, other studies showed penetration of metal NPs.

The available data show that the penetration of NPs through the skin is mainly influenced by size.

In addition, the penetration of TiO_2-NPs was studied on pig skin under light and dark conditions. In the presence of light, 200 mg/kg were found in the skin, while only 75 mg/kg were found under dark conditions, suggesting that photoinduction may promote NP dermal penetration (Bennett et al., 2012).

Crosera et al. (2009) studied the toxicity of TiO_2-NPs to human epidermal keratinocytes (HaCaT cells) over 24, 48 hours and seven

days and observed low cytotoxicity, suggesting that the potential toxic effects occur only after exposure to high concentrations (0.007-50 μg/cm2) for up to seven days.
Another study by Rancan and Vogt (2014) showed that only smaller NPs were able to penetrate the damaged statum cornum and may have various toxic effects, such as inducing ROS production.

5.3 Inhalation

The respiratory system consists of two parts: the upper airways (nasal cavity, pharynx, and larynx) and the lower airways (trachea, bronchi, and lungs). The size distribution of NPs plays an important role in their ability to enter the human respiratory tract (Bakand et al., 2016). Small particles can enter the alveolar region by gravity sedimentation and Brownian diffusion, triggering inflammation and production of ROS. Once NPs settle, the excretion mechanisms are not rapid and many toxins may be produced.

In addition, smaller diameter particles can migrate into the blood capillaries because the epithelium separating the inhaled air from the blood is very thin.
Biodistribution and toxicity depend on the size, shape and surface properties. Small Ag-NPs accumulated in different organs, while the larger ones preferred the liver and spleen (Chaigneau et al., 2021).
Xu et al. confirmed the occurrence of lung tumors, broncho-alveolar adenomas, and cystic keratinizing squamous cell carcinomas after inhalation and instillation of rutile and anatase TiO_2-NPs.
The exposure of primary human bronchial epithelial cells (BEAS-2B) to ZnO-NPs triggered cytotoxicity, oxidative stress, high intracellular Ca2+ levels, and alteration of mitochondrial membrane potential.
Lee et al. (2011) exposed A549 cells to increasing concentrations of Ag-NPs for 24 h and observed dose-dependent morphological changes and cell death.

Ag-NPs (20 nm) induced DNA damage and overexpression of metallothioneins in A549 cells at a concentration of 0.6 nM for up to 48 hours (Nguyen et al., 2014).
The work of Nguyen et al. (2014) also demonstrates that the coating induces other cell effects.

6 Nanoparticles in the aquatic environment

Given the increasing load of NPs in the environment, a thorough understanding of the behaviour of NPs in the aquatic environment is essential.

NPs are transported to receiving waters through atmospheric deposition, surface runoff, wastewater treatment plants, and direct input.

Ultimately, aquatic systems, particularly sediments, are the primary sink for NPs (Klaine et al., 2008).

Understanding the fate of NPs requires the concepts of colloid chemistry, as NPs are comparable to colloidal systems.

The formation of aggregates depends on binding efficiency and collision frequency. Binding efficiency describes the probability that particles will bind to each other and form an aggregate when they collide. It depends on various factors such as electrostatic and van der Waals forces, steric hindrances, magnetic and hydration forces (Petosa et al., 2010).

The collision frequency between particles depends on Brownian motion, fluid motion and differential deposition (Handy et al., 2008).

NPs can aggregate with other NPs (homoaggregation), but also associate or aggregate (heteroaggregation) with organic material or other particles present in the water such as natural colloids (NC), suspended solids, and dissolved compounds. Depending on the binding efficiency and collision frequency, larger aggregates can be formed, which can lead to sedimentation.

In addition, chemical transformations of NPs are possible, including oxidation/reduction, dissolution, hydrolysis, and biodegradation (Klaine et al., 2008). These transformations are highly dependent on the composition of the NPs.

In addition, the nature of the receiving water body affects the fate of ENPs due to differences in the composition of substances in the water (e.g., natural organic matter (NOM), NC, dissolved molecules,

pollutants), pH, turbulence (e.g., deep or shallow lake or river), and salinity (freshwater vs. seawater).
Because available analytical methods generally cannot distinguish between pristine ENPs, natural nanoparticles, and nanoparticles produced by mass production or combustion, measured concentrations are expected to be higher than predicted concentrations because most fate model predictions are based on the engineered fraction of the total nanosize (Gottschalk et al., 2013).
In aquatic systems, NPs are likely to interact with natural colloids, suspended solids, and other contaminants, including other NPs. Therefore, it is important to study not only ENPs in their pure form, but also their fate and toxicity in the receiving environment, where background chemicals may adsorb to ENPs (Nowack et al., 2012).
However, the risks of NPs may also be related to the risks of the associated toxicant, a phenomenon known as the "Trojan horse".
NPs can release toxins when ingested by marine organisms.
In addition, inorganic ENPs can release ions, but other chemical or biological transformations are also possible that can affect exposure and toxicity (Wiesner et al., 2009).
However, for NPs, the standard toxicity tests used for conventional organic pollutants are not always appropriate, and development of more suitable tests for individual species is ongoing.
Natural processes may occur that can influence the effect of ENPs on biota and may not be accounted for, or may be less well accounted for, in short-term laboratory tests with individual species.

For example, increasing the ionic strength and pH of NaCl suspensions has been shown to increase the aggregation rate and size of TiO2-NP, which in turn can affect bioavailability in the marine ecosystem (Handy et al., 2008).
Although nanomaterials are theoretically thought to be more toxic than their massive counterparts due to their greater surface reactivity, in reality they can form aggregates that approach the size

of massive materials and therefore may not be more effective in the marine environment.

NP aggregates could pose an ecotoxicological risk to both pelagic and, once deposited in sediment, benthic species. Despite this concern, few studies have been conducted on the ecotoxicological effects of NP on the oceans.

Most studies on the toxicity of NPs have used exposure times of 48, 72 or 96 hours, all of which can be considered short-term tests and involve high doses that are unrealistic from an ecological perspective (Handy et al., 2012). Nevertheless, such tests are essential to assess the hazards of ENPs, to establish the dose-response relationships needed for risk assessment, and to identify the mechanisms of toxicity at the species level (Handy et al. 2012).

For NPs, there are few chronic effect studies, community studies, model ecosystems, or field studies.

7 Application of Nanoparticles in Food

The application of nanocompounds plays a crucial role in the food industry.
The food market is demanding new technologies which are essential to maintain leadership in the food industry to produce fresh, authentic, convenient and tasty food, extend shelf life and freshness of products and improve food quality.
New nanomaterials are being developed that not only change the taste of food, but also improve the safety and health benefits of food.
According to a definition in a report by the European Nanotechnology Gateway, a food is called a nanofood if nanoparticles or nanotechnological techniques are used in the cultivation, production, processing or packaging of the food (Sekhon, 2010).
Generally, a distinction is made between two forms of nanofood application:
- Food additives (nano inside)
- Food packaging (nano outside).

Nanoparticles present in foods can be easily categorized based on their composition (organic or inorganic), as this factor has a great influence on their gastrointestinal effects and potential toxicity (McClements et al., 2017).
Inorganic nanoparticles such as silver, silica, iron oxide, titanium dioxide or zinc oxide can be spherical or non-spherical with different surface properties and sizes depending on the precursor materials and preparation conditions during manufacture.
Organic nanoparticles are essentially composed of organic substances, such as carbohydrates, proteins or lipids. These substances are liquid, semi-liquid or solid (crystalline or amorphous) at room temperature, depending on their composition and the processing conditions.

7.1 Food processing

Food processing can be greatly enhanced by intelligent delivery of nutrients, nano-encapsulation of dietary supplements, bioseparation of proteins, rapid removal of biological and chemical contaminants, solubilization, delivery, and coloring of foods.

These are just some of the emerging applications of nanotechnology in food science (Ravichandran, 2010).

Nanoencapsulation is a technology for packaging substances in miniature form using techniques such as nanocomposite, nanoemulsification, and nanostructuring to ensure the functionality of the final product, including controlled release of the core (Sekhon, 2010).

Nanosized dispersions, emulsions and filled micelles have the advantage of non-sedimentation which leads to better shelf life and storage of the product. Since the size of these nanoadditives is much smaller compared to the wavelength of light, they can even be incorporated into clear and transparent foods without causing color problems. Substances that are difficult for the body to dissolve can be absorbed more easily in nano size due to their larger surface area.

Nanocapsulation can improve the bioavailability of bioactive compounds after oral administration through targeted delivery systems. Such nanocapsulation allows the release of flavors to be controlled at the desired time and also protects the degradation of these flavors during processing and storage (Yu et al., 2018).

Nanoparticles can act as antioxidant carriers and are considered suitable for the encapsulation of bioactive compounds such as flavonoids and vitamins that are released in the acidic environment of the stomach (Pool et al., 2012).

Other developments in food processing include the addition of nanoparticles to existing foods to enhance the absorption of nutrients and to extend the shelf life of the product (Jampilek et al., 2019).

A number of metal and metal oxide nanomaterials have been shown to be effective antimicrobial agents that have the potential to extend

food shelf life by preventing microbial growth. They interact with various microbial cells, killing them and have the potential to prevent biofilm formation (Ahmed et al., 2017).

Silver nanoparticles and their nanocomposites are the most commonly used nanomaterials as antimicrobial agents in the food industry (He and Hwang, 2016).

It has been claimed that silver nanocomposites are quite safe for food packaging as no detectable or negligible amounts of silver nanoparticles are released to pass from the containers into the actual food samples and food stimulants (Addo Ntim et al., 2015).

There is an opportunity to combine biology and nanotechnology in the fabrication of sensors that offer great potential for increased sensitivity and shorter response times.

Nanosensors are used as tiny crisps, invisible to the human eye, embedded in foods to act as electronic barcodes and are used to detect food contaminants, especially microbes. These devices are characterized by exceptional sensitivity, rapid response and rescue because they are very small, where pathogens often hide (Ameta et al., 2020).

Mostly, nanosensors are used to detect pesticides such as organophosphates in plants, fruits and aquatic plants. It is well known that pesticides are highly permeable and soluble and they are harmful. They are widely used in agricultural science.

Another aspect is smart packaging, where a nano-biosensor is designed to fluoresce in different colors when it interacts with different pathogens in food.

Nanoparticles are also used to enhance physical properties such as color and flavor.

TiO_2 is approved as a color additive for food, but the amount must not exceed 1% (w/w) (Shi et al., 2013).

The technique of nanocapsulation is widely used to improve the release and retention of flavors and to provide a balanced diet. SiO2 nanomaterials can also serve as carriers for these fragrances or flavors in food and non-food products (Dekkers et al., 2011). As a

result, it has been used in food products and is registered as a food additive E551 in the EU.
However, there is still a debate on the health and safety issues related to the use of such engineered nanoparticles in consumer products.

7.2 Packaging

Food is perishable. They can be contaminated and/or degraded at any stage of the food chain. The process can be chemical, physical or biological.
Therefore, it is important that food is protected at all levels. Nanosensors for smart packaging are being developed to detect food spoilage and release nano-antimicrobials to extend shelf life.
In addition, this technology can reduce the cost of food additives and extend the shelf life of food.
A number of packaging materials are used in the food industry, including active packaging and smart packaging (Rai et al., 2019).
Active packaging refers to the use of active nanomaterials such as antimicrobial agents and oxygen binding materials. Some nanomaterials can impart antimicrobial properties to food packaging. Some of them are nano silver, nano titanium dioxide, nano magnesium oxide, nano copper oxide, carbon nanotubes etc.
These packaging allow slow but continuous release of antimicrobial agents from the packaging material to the food surfaces, so that high concentration of these agents is not present for a long period of time (Quintavalla and Vicini, 2002).
Advances in active packaging result in delayed oxidation, controlled respiration rate, microbial growth and moisture migration (Brody et al., 2008).
When nanomaterials are used to improve packaging, they are blended into the polymer matrix to improve the gas barrier properties and the resistance of the packaging to temperature and moisture. The US Food and Drug Administration has also approved

the use of these nanocomposites in contact with food.
Smart packaging is designed to detect microbial or biochemical changes in food because it can detect the growth of pathogens in food.
They are capable of detecting food spoilage and releasing nanoantimicrobials to extend the shelf life of food.
Smart packaging is also being developed with special preservatives that release preservatives as soon as food begins to spoil.

8 Zebrafish embryos (*Danio rerio*) as a Model Organism

The zebrafish (*Danio rerio*) has recently become an important model organism in biological research. The zebrafish is a tropical freshwater fish that lives in the rivers (mainly the Ganges) of the Himalayan region of South Asia, particularly India, Nepal, Bhutan, Pakistan, Bangladesh and Myanmar. It is a bony fish (teleost) and belongs to the family Cyprinidae in the class Actinopterygii.

The zebrafish shares many physiological and genetic similarities with humans, including the brain, digestive tract, musculature, vascular system, and innate immune system. In addition, 70% of human disease genes share functional similarities with those of zebrafish (Santoriello and Zon, 2012).

D. Rario is preferred by scientists because of its diverse characteristics that make it useful as a model organism. The embryo develops rapidly outside the mother and is optically clear, making it easily accessible for experimentation and observation. The blastula stage takes only 3 hours, while gastrulation is completed in 5 hours. With an embryo about 18 hours old, very well developed ears, eyes, segmentation muscles and brain can be seen as the embryo is transparent. After 24 hours, segmentation is complete and most of the primary organ systems are formed. After 72 hours, the embryo hatches from the eggshell and goes in search of food within the next 2 days. Over a period of only 4 days, the embryo rapidly develops into a small version of the adult.

The adult zebrafish reaches sexual maturity very quickly, with a generation time of about 10 weeks, and this tiny fish also has a good fertility rate.

In addition to the above characteristics of the zebrafish, it requires very little space and incurs very low maintenance costs. These characteristics make this fish an attractive model organism for developmental, toxicological and transgenic studies (Lele and Krone, 1996).

Embryos are used for an acute toxicity assessment of test substances, determined according to the OECD test guideline (TG) 236. Due to the short analysis time, transparency of embryos, short life cycle, high fecundity and similarity of genetic data, this test is at the forefront of toxicological research.

The endpoints indicated by OECD TG 236 that can be analysed with the inverted microscope are: (1) coagulation of fertilised eggs, (2) lack of somite formation, (3) lack of tail bud detachment, and (4) lack of heartbeat (OECD, 2013), any other observation is recorded as additional lethal or sublethal endpoints. Common examples include: decreased heartbeat or blood flow, inhibited or absent pigmentation, delayed or altered development, altered movement(s), spinal deformities, and the formation of various types of edema.

References

- Addo Ntim, S., Thomas, T.A., Begley, T.H., Noonan, G.O., 2015. Characterisation and potential migration of silver nanoparticles from commercially available polymeric food contact materials. Food Addit Contam Part A Chem Anal Control Expo Risk Assess 32, 1003–1011. https://doi.org/10.1080/19440049.2015.1029994
- Ahmed, D., Anwar, A., Khan, A.K., Ahmed, A., Shah, M.R., Khan, N.A., 2017. Size selectivity in antibiofilm activity of 3-(diphenylphosphino)propanoic acid coated gold nanomaterials against Gram-positive Staphylococcus aureus and Streptococcus mutans. AMB Express 7, 210. https://doi.org/10.1186/s13568-017-0515-x
- Ameta, S.K., Rai, A.K., Hiran, D., Ameta, R., Ameta, S.C., 2020. Use of Nanomaterials in Food Science. Biogenic Nano-Particles and their Use in Agro-ecosystems 457–488. https://doi.org/10.1007/978-981-15-2985-6_24
- Asharani, P.V., Hande, M.P., Valiyaveettil, S., 2009. Anti-proliferative activity of silver nanoparticles. BMC Cell Biol 10, 65. https://doi.org/10.1186/1471-2121-10-65
- Auffan, M., Rose, J., Bottero, J.-Y., Lowry, G.V., Jolivet, J.-P., Wiesner, M.R., 2009. Towards a definition of inorganic nanoparticles from an environmental, health and safety perspective. Nat Nanotechnol 4, 634–641. https://doi.org/10.1038/nnano.2009.242
- Axson, J.L., Stark, D.I., Bondy, A.L., Capracotta, S.S., Maynard, A.D., Philbert, M.A., Bergin, I.L., Ault, A.P., 2015. Rapid Kinetics of Size and pH-Dependent Dissolution and Aggregation of Silver Nanoparticles in Simulated Gastric Fluid. J Phys Chem C Nanomater Interfaces 119, 20632–20641. https://doi.org/10.1021/acs.jpcc.5b03634
- Bakand, S., Hayes, A., 2016. Toxicological Considerations, Toxicity Assessment, and Risk Management of Inhaled Nanoparticles. Int J Mol Sci 17, E929. https://doi.org/10.3390/ijms17060929
- Bennett, S.W., Zhou, D., Mielke, R., Keller, A.A., 2012. Photoinduced disaggregation of TiO_2 nanoparticles enables transdermal penetration. PLoS One 7, e48719. https://doi.org/10.1371/journal.pone.0048719
- Borm, P.J.A., Müller-Schulte, D., 2006. Nanoparticles in drug delivery and environmental exposure: same size, same risks? Nanomedicine (Lond) 1, 235–249. https://doi.org/10.2217/17435889.1.2.235
- Brody, A.L., Bugusu, B., Han, J.H., Sand, C.K., McHugh, T.H., 2008. Scientific Status Summary. Journal of Food Science 73, R107–R116. https://doi.org/10.1111/j.1750-3841.2008.00933.x
- Buzea, C., Pacheco, I.I., Robbie, K., 2007. Nanomaterials and nanoparticles: sources and toxicity. Biointerphases 2, MR17-71. https://doi.org/10.1116/1.2815690

- Cardozo, T.R., De Carli, R.F., Seeber, A., Flores, W.H., da Rosa, J.A.N., Kotzal, Q.S.G., Lehmann, M., da Silva, F.R., Dihl, R.R., 2019. Genotoxicity of zinc oxide nanoparticles: an in vivo and in silico study. Toxicology Research 8, 277–286. https://doi.org/10.1039/c8tx00255j
- Chaigneau, T., Pallotta, A., Benaddi, F.Z., Sancey, L., Chakir, S., Boudier, A., Clarot, I., 2021. Monitoring of Gold Biodistribution from Nanoparticles Using a HPLC-Visible Method. Separations 8, 215. https://doi.org/10.3390/separations8110215
- Chen, X., Mao, S.S., 2007. Titanium Dioxide Nanomaterials: Synthesis, Properties, Modifications, and Applications. Chem. Rev. 107, 2891–2959. https://doi.org/10.1021/cr0500535
- Clemente, Z., Castro, V.L., Feitosa, L.O., Lima, R., Jonsson, C.M., Maia, A.H.N., Fraceto, L.F., 2013. Fish exposure to nano-TiO_2 under different experimental conditions: methodological aspects for nanoecotoxicology investigations. Sci Total Environ 463–464, 647–656. https://doi.org/10.1016/j.scitotenv.2013.06.022
- Crosera, M., Bovenzi, M., Maina, G., Adami, G., Zanette, C., Florio, C., Filon Larese, F., 2009. Nanoparticle dermal absorption and toxicity: a review of the literature. Int Arch Occup Environ Health 82, 1043–1055. https://doi.org/10.1007/s00420-009-0458-x
- Dekkers, S., Krystek, P., Peters, R.J.B., Lankveld, D.P.K., Bokkers, B.G.H., van Hoeven-Arentzen, P.H., Bouwmeester, H., Oomen, A.G., 2011. Presence and risks of nanosilica in food products. Nanotoxicology 5, 393–405. https://doi.org/10.3109/17435390.2010.519836
- Durán, N., Durán, M., de Jesus, M.B., Seabra, A.B., Fávaro, W.J., Nakazato, G., 2016. Silver nanoparticles: A new view on mechanistic aspects on antimicrobial activity. Nanomedicine 12, 789–799. https://doi.org/10.1016/j.nano.2015.11.016
- Dusinska, M., Collins, A.R., 2008. The comet assay in human biomonitoring: gene-environment interactions. Mutagenesis 23, 191–205. https://doi.org/10.1093/mutage/gen007
- EFSA Panel on Food Additives and Nutrient Sources added to Food (ANS), 2016. Scientific opinion on the re-evaluation of silver (E 174) as food additive. EFSA Journal 14, 4364. https://doi.org/10.2903/j.efsa.2016.4364
- EFSA Panel on Food Contact Materials, Enzymes and Processing Aids (CEP), Silano, V., Barat Baviera, J.M., Bolognesi, C., Brüschweiler, B.J., Chesson, A., Cocconcelli, P.S., Crebelli, R., Gott, D.M., Grob, K., Lampi, E., Mortensen, A., Steffensen, I.-L., Tlustos, C., Van Loveren, H., Vernis, L., Zorn, H., Castle, L., Cravedi, J.-P., Kolf-Clauw, M., Milana, M.R., Pfaff, K., Tavares Poças, M. de F., Svensson, K., Wölfle, D., Barthélémy, E., Rivière, G., 2019. Safety assessment of the substance, titanium dioxide surface treated with fluoride-modified alumina, for use in food contact materials. EFSA Journal 17, e05737. https://doi.org/10.2903/j.efsa.2019.5737

- Elder, A., Vidyasagar, S., DeLouise, L., 2009. Physicochemical Factors that Affect Metal and Metal Oxide Nanoparticle Passage Across Epithelial Barriers. Wiley Interdiscip Rev Nanomed Nanobiotechnol 1, 434–450. https://doi.org/10.1002/wnan.44
- Elsabahy, M., Zhang, S., Zhang, F., Deng, Z.J., Lim, Y.H., Wang, H., Parsamian, P., Hammond, P.T., Wooley, K.L., 2013. Surface Charges and Shell Crosslinks Each Play Significant Roles in Mediating Degradation, Biofouling, Cytotoxicity and Immunotoxicity for Polyphosphoester-based Nanoparticles. Sci Rep 3, 3313. https://doi.org/10.1038/srep03313
- Falconer, J.L., Grainger, D.W., 2018. In vivo comparisons of silver nanoparticle and silver ion transport after intranasal delivery in mice. J Control Release 269, 1–9. https://doi.org/10.1016/j.jconrel.2017.10.018
- Faust, J.J., Doudrick, K., Yang, Y., Westerhoff, P., Capco, D.G., 2014. Food grade titanium dioxide disrupts intestinal brush border microvilli in vitro independent of sedimentation. Cell Biol Toxicol 30, 169–188. https://doi.org/10.1007/s10565-014-9278-1
- Ferdous, Z., Nemmar, A., 2020. Health Impact of Silver Nanoparticles: A Review of the Biodistribution and Toxicity Following Various Routes of Exposure. Int J Mol Sci 21, 2375. https://doi.org/10.3390/ijms21072375
- Foldbjerg, R., Olesen, P., Hougaard, M., Dang, D.A., Hoffmann, H.J., Autrup, H., 2009. PVP-coated silver nanoparticles and silver ions induce reactive oxygen species, apoptosis and necrosis in THP-1 monocytes. Toxicol Lett 190, 156–162. https://doi.org/10.1016/j.toxlet.2009.07.009
- Fröhlich, E.E., Fröhlich, E., 2016. Cytotoxicity of Nanoparticles Contained in Food on Intestinal Cells and the Gut Microbiota. Int J Mol Sci 17, 509. https://doi.org/10.3390/ijms17040509
- Gatoo, M.A., Naseem, S., Arfat, M.Y., Mahmood Dar, A., Qasim, K., Zubair, S., 2014. Physicochemical Properties of Nanomaterials: Implication in Associated Toxic Manifestations. BioMed Research International 2014, e498420. https://doi.org/10.1155/2014/498420
- Geraets, L., Oomen, A.G., Schroeter, J.D., Coleman, V.A., Cassee, F.R., 2012. Tissue distribution of inhaled micro- and nano-sized cerium oxide particles in rats: results from a 28-day exposure study. Toxicol Sci 127, 463–473. https://doi.org/10.1093/toxsci/kfs113
- Gerloff, K., Fenoglio, I., Carella, E., Kolling, J., Albrecht, C., Boots, A.W., Förster, I., Schins, R.P.F., 2012. Distinctive toxicity of TiO_2 rutile/anatase mixed phase nanoparticles on Caco-2 cells. Chem Res Toxicol 25, 646–655. https://doi.org/10.1021/tx200334k
- Girigoswami, K., Viswanathan, M., Murugesan, R., Girigoswami, A., 2015. Studies on polymer-coated zinc oxide nanoparticles: UV-blocking efficacy and in vivo toxicity. Materials Science and Engineering: C 56, 501–510. https://doi.org/10.1016/j.msec.2015.07.017

- Gottschalk, F., Sun, T., Nowack, B., 2013. Environmental concentrations of engineered nanomaterials: review of modeling and analytical studies. Environ Pollut 181, 287–300. https://doi.org/10.1016/j.envpol.2013.06.003
- Gray, E.P., Coleman, J.G., Bednar, A.J., Kennedy, A.J., Ranville, J.F., Higgins, C.P., 2013. Extraction and Analysis of Silver and Gold Nanoparticles from Biological Tissues Using Single Particle Inductively Coupled Plasma Mass Spectrometry. Environ. Sci. Technol. 47, 14315–14323. https://doi.org/10.1021/es403558c
- Grosse, S., Evje, L., Syversen, T., 2013. Silver nanoparticle-induced cytotoxicity in rat brain endothelial cell culture. Toxicol In Vitro 27, 305–313. https://doi.org/10.1016/j.tiv.2012.08.024
- Handy, R.D., Cornelis, G., Fernandes, T., Tsyusko, O., Decho, A., Sabo-Attwood, T., Metcalfe, C., Steevens, J.A., Klaine, S.J., Koelmans, A.A., Horne, N., 2012. Ecotoxicity test methods for engineered nanomaterials: practical experiences and recommendations from the bench. Environ Toxicol Chem 31, 15–31. https://doi.org/10.1002/etc.706
- Handy, R.D., Henry, T.B., Scown, T.M., Johnston, B.D., Tyler, C.R., 2008. Manufactured nanoparticles: their uptake and effects on fish--a mechanistic analysis. Ecotoxicology 17, 396–409. https://doi.org/10.1007/s10646-008-0205-1
- Hanley, C., Thurber, A., Hanna, C., Punnoose, A., Zhang, J., Wingett, D.G., 2009. The Influences of Cell Type and ZnO Nanoparticle Size on Immune Cell Cytotoxicity and Cytokine Induction. Nanoscale Res Lett 4, 1409–1420. https://doi.org/10.1007/s11671-009-9413-8
- He, X., Hwang, H.-M., 2016. Nanotechnology in food science: Functionality, applicability, and safety assessment. Journal of Food and Drug Analysis 24, 671–681. https://doi.org/10.1016/j.jfda.2016.06.001
- Huk, A., Izak-Nau, E., Reidy, B., Boyles, M., Duschl, A., Lynch, I., Dušinska, M., 2014. Is the toxic potential of nanosilver dependent on its size? Part Fibre Toxicol 11, 65. https://doi.org/10.1186/s12989-014-0065-1
- Hussain, I., Singh, N.B., Singh, A., Singh, H., Singh, S.C., 2016. Green synthesis of nanoparticles and its potential application. Biotechnol Lett 38, 545–560. https://doi.org/10.1007/s10529-015-2026-7
- Jampilek, J., Kos, J., Kralova, K., 2019. Potential of Nanomaterial Applications in Dietary Supplements and Foods for Special Medical Purposes. Nanomaterials (Basel) 9, E296. https://doi.org/10.3390/nano9020296
- Kararli, T.T., 1995. Comparison of the gastrointestinal anatomy, physiology, and biochemistry of humans and commonly used laboratory animals. Biopharm Drug Dispos 16, 351–380. https://doi.org/10.1002/bdd.2510160502
- Keller, J.G., Persson, M., Müller, P., Ma-Hock, L., Werle, K., Arts, J., Landsiedel, R., Wohlleben, W., 2021. Variation in dissolution behavior among different nanoforms and its implication for grouping approaches in

inhalation toxicity. NanoImpact 23, 100341. https://doi.org/10.1016/j.impact.2021.100341
- Kim, D., Kwon, S.-J., Wu, X., Sauve, J., Lee, I., Nam, J., Kim, J., Dordick, J.S., 2018. Selective Killing of Pathogenic Bacteria by Antimicrobial Silver Nanoparticle—Cell Wall Binding Domain Conjugates. ACS Appl. Mater. Interfaces 10, 13317–13324. https://doi.org/10.1021/acsami.8b00181
- Klaine, S.J., Alvarez, P.J.J., Batley, G.E., Fernandes, T.F., Handy, R.D., Lyon, D.Y., Mahendra, S., McLaughlin, M.J., Lead, J.R., 2008. Nanomaterials in the environment: Behavior, fate, bioavailability, and effects. Environmental Toxicology and Chemistry 27, 1825–1851. https://doi.org/10.1897/08-090.1
- Koeneman, B.A., Zhang, Y., Westerhoff, P., Chen, Y., Crittenden, J.C., Capco, D.G., 2010. Toxicity and cellular responses of intestinal cells exposed to titanium dioxide. Cell Biol Toxicol 26, 225–238. https://doi.org/10.1007/s10565-009-9132-z
- Laborda, F., Bolea, E., Jiménez-Lamana, J., 2014. Single Particle Inductively Coupled Plasma Mass Spectrometry: A Powerful Tool for Nanoanalysis. Anal. Chem. 86, 2270–2278. https://doi.org/10.1021/ac402980q
- Lee, Y.S., Kim, D.W., Lee, Y.H., Oh, J.H., Yoon, S., Choi, M.S., Lee, S.K., Kim, J.W., Lee, K., Song, C.-W., 2011. Silver nanoparticles induce apoptosis and G2/M arrest via PKCζ-dependent signaling in A549 lung cells. Arch Toxicol 85, 1529–1540. https://doi.org/10.1007/s00204-011-0714-1
- Leite-Silva, V.R., Le Lamer, M., Sanchez, W.Y., Liu, D.C., Sanchez, W.H., Morrow, I., Martin, D., Silva, H.D.T., Prow, T.W., Grice, J.E., Roberts, M.S., 2013. The effect of formulation on the penetration of coated and uncoated zinc oxide nanoparticles into the viable epidermis of human skin in vivo. Eur J Pharm Biopharm 84, 297–308. https://doi.org/10.1016/j.ejpb.2013.01.020
- Lele, Z., Krone, P.H., 1996. The zebrafish as a model system in developmental, toxicological and transgenic research. Biotechnol Adv 14, 57–72. https://doi.org/10.1016/0734-9750(96)00004-3
- Lesher, E.K., Ranville, J.F., Honeyman, B.D., 2009. Analysis of pH Dependent Uranium(VI) Sorption to Nanoparticulate Hematite by Flow Field-Flow Fractionation - Inductively Coupled Plasma Mass Spectrometry. Environ. Sci. Technol. 43, 5403–5409. https://doi.org/10.1021/es900592r
- Lespes, G., Faucher, S., Slaveykova, V.I., 2020. Natural Nanoparticles, Anthropogenic Nanoparticles, Where Is the Frontier? Frontiers in Environmental Science 8, 71. https://doi.org/10.3389/fenvs.2020.00071
- Loeschner, K., Correia, M., López Chaves, C., Rokkjær, I., Sloth, J.J., 2018. Detection and characterisation of aluminium-containing nanoparticles in Chinese noodles by single particle ICP-MS. Food Additives & Contaminants. Part A, Chemistry, Analysis, Control, Exposure & Risk Assessment 35, 86–93. https://doi.org/10.1080/19440049.2017.1382728
- MacDonald, R.S., 2000. The role of zinc in growth and cell proliferation. J Nutr 130, 1500S–8S. https://doi.org/10.1093/jn/130.5.1500S

- Marin, S., Vlasceanu, G.M., Tiplea, R.E., Bucur, I.R., Lemnaru, M., Marin, M.M., Grumezescu, A.M., 2015. Applications and toxicity of silver nanoparticles: a recent review. Curr Top Med Chem 15, 1596–1604. https://doi.org/10.2174/1568026615666150414142209
- Maurer, E.I., Sharma, M., Schlager, J.J., Hussain, S.M., 2014. Systematic analysis of silver nanoparticle ionic dissolution by tangential flow filtration: toxicological implications. Nanotoxicology 8, 718–727. https://doi.org/10.3109/17435390.2013.824127
- McClements, D.J., Xiao, H., 2017. Is nano safe in foods? Establishing the factors impacting the gastrointestinal fate and toxicity of organic and inorganic food-grade nanoparticles. NPJ Sci Food 1, 6. https://doi.org/10.1038/s41538-017-0005-1
- McShan, D., Ray, P.C., Yu, H., 2014. Molecular toxicity mechanism of nanosilver. J Food Drug Anal 22, 116–127. https://doi.org/10.1016/j.jfda.2014.01.010
- Moos, P.J., Olszewski, K., Honeggar, M., Cassidy, P., Leachman, S., Woessner, D., Cutler, N.S., Veranth, J.M., 2011. Responses of human cells to ZnO nanoparticles: a gene transcription study. Metallomics 3, 1199–1211. https://doi.org/10.1039/c1mt00061f
- Nguyen, D.T., Kim, K.-S., 2014. Functionalization of magnetic nanoparticles for biomedical applications. Korean J. Chem. Eng. 31, 1289–1305. https://doi.org/10.1007/s11814-014-0156-6
- Nischwitz, V., Goenaga-Infante, H., 2012. Improved sample preparation and quality control for the characterisation of titanium dioxide nanoparticles in sunscreens using flow field flow fractionation on-line with inductively coupled plasma mass spectrometry. J. Anal. At. Spectrom. 27, 1084–1092. https://doi.org/10.1039/C2JA10387G
- Nowack, B., Ranville, J.F., Diamond, S., Gallego-Urrea, J.A., Metcalfe, C., Rose, J., Horne, N., Koelmans, A.A., Klaine, S.J., 2012. Potential scenarios for nanomaterial release and subsequent alteration in the environment. Environ Toxicol Chem 31, 50–59. https://doi.org/10.1002/etc.726
- Nutrition, C. for F.S. and A., 2021. Food Additive Status List. FDA.
- Oberdörster, G., Stone, V., Donaldson, K., 2007. Toxicology of nanoparticles: A historical perspective. Nanotoxicology 1, 2–25. https://doi.org/10.1080/17435390701314761
- Osman, I.F., Baumgartner, A., Cemeli, E., Fletcher, J.N., Anderson, D., 2010. Genotoxicity and cytotoxicity of zinc oxide and titanium dioxide in HEp-2 cells. Nanomedicine (Lond) 5, 1193–1203. https://doi.org/10.2217/nnm.10.52
- Park, M.V.D.Z., Neigh, A.M., Vermeulen, J.P., de la Fonteyne, L.J.J., Verharen, H.W., Briedé, J.J., van Loveren, H., de Jong, W.H., 2011. The effect of particle size on the cytotoxicity, inflammation, developmental toxicity and genotoxicity of silver nanoparticles. Biomaterials 32, 9810–9817. https://doi.org/10.1016/j.biomaterials.2011.08.085

- Periasamy, V.S., Athinarayanan, J., Al-Hadi, A.M., Juhaimi, F.A., Alshatwi, A.A., 2015. Effects of titanium dioxide nanoparticles isolated from confectionery products on the metabolic stress pathway in human lung fibroblast cells. Arch Environ Contam Toxicol 68, 521–533. https://doi.org/10.1007/s00244-014-0109-4
- Petosa, A.R., Jaisi, D.P., Quevedo, I.R., Elimelech, M., Tufenkji, N., 2010. Aggregation and deposition of engineered nanomaterials in aquatic environments: role of physicochemical interactions. Environ Sci Technol 44, 6532–6549. https://doi.org/10.1021/es100598h
- Pool, H., Quintanar, D., de Dios Figueroa, J., Mano, C.M., Bechara, J.E.H., Godínez, L.A., Mendoza, S., 2012. Antioxidant effects of quercetin and catechin encapsulated into PLGA nanoparticles. J. Nanomaterials 2012, 86:86.
- Powell, J.J., Faria, N., Thomas-McKay, E., Pele, L.C., 2010. Origin and fate of dietary nanoparticles and microparticles in the gastrointestinal tract. J Autoimmun 34, J226-233. https://doi.org/10.1016/j.jaut.2009.11.006
- Quintavalla, S., Vicini, L., 2002. Antimicrobial food packaging in meat industry. Meat Science 62, 373–380. https://doi.org/10.1016/S0309-1740(02)00121-3
- Rahman, M.F., Wang, J., Patterson, T.A., Saini, U.T., Robinson, B.L., Newport, G.D., Murdock, R.C., Schlager, J.J., Hussain, S.M., Ali, S.F., 2009. Expression of genes related to oxidative stress in the mouse brain after exposure to silver-25 nanoparticles. Toxicol Lett 187, 15–21. https://doi.org/10.1016/j.toxlet.2009.01.020
- Rai, M., Ingle, A.P., Gupta, I., Pandit, R., Paralikar, P., Gade, A., Chaud, M.V., dos Santos, C.A., 2019. Smart nanopackaging for the enhancement of food shelf life. Environ Chem Lett 17, 277–290. https://doi.org/10.1007/s10311-018-0794-8
- Rancan, F., Vogt, A., 2014. Getting under the skin: what is the potential of the transfollicular route in drug delivery? Ther Deliv 5, 875–877. https://doi.org/10.4155/tde.14.56
- Ravichandran, R., 2010. Nanotechnology Applications in Food and Food Processing: Innovative Green Approaches, Opportunities and Uncertainties for Global Market. International Journal of Green Nanotechnology: Physics and Chemistry 1, P72–P96. https://doi.org/10.1080/19430871003684440
- Recordati, C., De Maglie, M., Bianchessi, S., Argentiere, S., Cella, C., Mattiello, S., Cubadda, F., Aureli, F., D'Amato, M., Raggi, A., Lenardi, C., Milani, P., Scanziani, E., 2016. Tissue distribution and acute toxicity of silver after single intravenous administration in mice: nano-specific and size-dependent effects. Part Fibre Toxicol 13, 12. https://doi.org/10.1186/s12989-016-0124-x

- Regoli, F., Giuliani, M.E., 2014. Oxidative pathways of chemical toxicity and oxidative stress biomarkers in marine organisms. Mar Environ Res 93, 106–117. https://doi.org/10.1016/j.marenvres.2013.07.006
- Reinus, J.F., Simon, D., 2014. Gastrointestinal anatomy and physiology: The essentials. Wiley-Blackwell. https://doi.org/10.1002/9781118833001
- Sabir, S., Arshad, M., Chaudhari, S.K., 2014. Zinc Oxide Nanoparticles for Revolutionizing Agriculture: Synthesis and Applications. The Scientific World Journal 2014, e925494. https://doi.org/10.1155/2014/925494
- Sager, T.M., Kommineni, C., Castranova, V., 2008. Pulmonary response to intratracheal instillation of ultrafine versus fine titanium dioxide: role of particle surface area. Part Fibre Toxicol 5, 17. https://doi.org/10.1186/1743-8977-5-17
- Santoriello, C., Zon, L.I., 2012. Hooked! Modeling human disease in zebrafish. J Clin Invest 122, 2337–2343. https://doi.org/10.1172/JCI60434
- Sawai, J., Shoji, S., Igarashi, H., Hashimoto, A., Kokugan, T., Shimizu, M., Kojima, H., 1998. Hydrogen peroxide as an antibacterial factor in zinc oxide powder slurry. Journal of Fermentation and Bioengineering 86, 521–522. https://doi.org/10.1016/S0922-338X(98)80165-7
- Sekhon, B.S., 2010. Food nanotechnology – an overview. Nanotechnol Sci Appl 3, 1–15.
- Sergent, J.-A., Paget, V., Chevillard, S., 2012. Toxicity and genotoxicity of nano-SiO2 on human epithelial intestinal HT-29 cell line. Ann Occup Hyg 56, 622–630. https://doi.org/10.1093/annhyg/mes005
- Sharma, V.K., Filip, J., Zboril, R., Varma, R.S., 2015. Natural inorganic nanoparticles – formation, fate, and toxicity in the environment. Chem. Soc. Rev. 44, 8410–8423. https://doi.org/10.1039/C5CS00236B
- Shi, H., Magaye, R., Castranova, V., Zhao, J., 2013. Titanium dioxide nanoparticles: a review of current toxicological data. Part Fibre Toxicol 10, 15. https://doi.org/10.1186/1743-8977-10-15
- Sirelkhatim, A., Mahmud, S., Seeni, A., Kaus, N.H.M., Ann, L.C., Bakhori, S.K.M., Hasan, H., Mohamad, D., 2015. Review on Zinc Oxide Nanoparticles: Antibacterial Activity and Toxicity Mechanism. Nanomicro Lett 7, 219–242. https://doi.org/10.1007/s40820-015-0040-x
- Stebounova, L.V., Guio, E., Grassian, V.H., 2011. Silver nanoparticles in simulated biological media: a study of aggregation, sedimentation, and dissolution. J Nanopart Res 13, 233–244. https://doi.org/10.1007/s11051-010-0022-3
- Stoimenovet et. al., 2002. Metal Oxide Nanoparticles as Bactericidal Agents | Langmuir [WWW Document]. URL https://pubs.acs.org/doi/10.1021/la0202374 (accessed 11.14.21).
- Tiede, K., Boxall, A.B.A., Tear, S.P., Lewis, J., David, H., Hassellov, M., 2008. Detection and characterization of engineered nanoparticles in food and the

environment. Food Addit Contam Part A Chem Anal Control Expo Risk Assess 25, 795–821. https://doi.org/10.1080/02652030802007553

- van der Zande, M., Vandebriel, R.J., Groot, M.J., Kramer, E., Herrera Rivera, Z.E., Rasmussen, K., Ossenkoppele, J.S., Tromp, P., Gremmer, E.R., Peters, R.J.B., Hendriksen, P.J., Marvin, H.J.P., Hoogenboom, R.L.A.P., Peijnenburg, A.A.C.M., Bouwmeester, H., 2014. Sub-chronic toxicity study in rats orally exposed to nanostructured silica. Part Fibre Toxicol 11, 8. https://doi.org/10.1186/1743-8977-11-8
- Vandebriel, R.J., Tonk, E.C., de la Fonteyne-Blankestijn, L.J., Gremmer, E.R., Verharen, H.W., van der Ven, L.T., van Loveren, H., de Jong, W.H., 2014. Immunotoxicity of silver nanoparticles in an intravenous 28-day repeated-dose toxicity study in rats. Part Fibre Toxicol 11, 21. https://doi.org/10.1186/1743-8977-11-21
- Vigneshwaran, N., Kumar, S., Kathe, A.A., Varadarajan, P.V., Prasad, V., 2006. Functional finishing of cotton fabrics using zinc oxide–soluble starch nanocomposites. Nanotechnology 17, 5087–5095. https://doi.org/10.1088/0957-4484/17/20/008
- Visscher, M., Narendran, V., 2014. The Ontogeny of Skin. Adv Wound Care (New Rochelle) 3, 291–303. https://doi.org/10.1089/wound.2013.0467
- Wang, F., Yu, L., Monopoli, M.P., Sandin, P., Mahon, E., Salvati, A., Dawson, K.A., 2013. The biomolecular corona is retained during nanoparticle uptake and protects the cells from the damage induced by cationic nanoparticles until degraded in the lysosomes. Nanomedicine 9, 1159–1168. https://doi.org/10.1016/j.nano.2013.04.010
- Warheit, D.B., Webb, T.R., Reed, K.L., Frerichs, S., Sayes, C.M., 2007. Pulmonary toxicity study in rats with three forms of ultrafine-TiO_2 particles: differential responses related to surface properties. Toxicology 230, 90–104. https://doi.org/10.1016/j.tox.2006.11.002
- Watson, C., Ge, J., Cohen, J., Pyrgiotakis, G., Engelward, B.P., Demokritou, P., 2014. High-Throughput Screening Platform for Engineered Nanoparticle-Mediated Genotoxicity Using CometChip Technology. ACS Nano 8, 2118–2133. https://doi.org/10.1021/nn404871p
- Weir, A., Westerhoff, P., Fabricius, L., Hristovski, K., von Goetz, N., 2012. Titanium dioxide nanoparticles in food and personal care products. Environ Sci Technol 46, 2242–2250. https://doi.org/10.1021/es204168d
- Wiesner, M.R., Lowry, G.V., Jones, K.L., Hochella, Jr., Michael F., Di Giulio, R.T., Casman, E., Bernhardt, E.S., 2009. Decreasing Uncertainties in Assessing Environmental Exposure, Risk, and Ecological Implications of Nanomaterials. Environ. Sci. Technol. 43, 6458–6462. https://doi.org/10.1021/es803621k
- Yadav, A., Prasad, V., Kathe, A.A., Raj, S., Yadav, D., Sundaramoorthy, C., Vigneshwaran, N., 2006. Functional finishing in cotton fabrics using zinc

oxide nanoparticles. Bull Mater Sci 29, 641–645. https://doi.org/10.1007/s12034-006-0017-y

- Yu, H., Park, J.-Y., Kwon, C.W., Hong, S.-C., Park, K.-M., Chang, P.-S., 2018. An Overview of Nanotechnology in Food Science: Preparative Methods, Practical Applications, and Safety. Journal of Chemistry 2018, e5427978. https://doi.org/10.1155/2018/5427978
- Zhang, W., Ke, S., Sun, C., Xu, X., Chen, J., Yao, L., 2019. Fate and toxicity of silver nanoparticles in freshwater from laboratory to realistic environments: a review. Environ Sci Pollut Res 26, 7390–7404. https://doi.org/10.1007/s11356-019-04150-0
- Zhu, X., Wang, J., Zhang, X., Chang, Y., Chen, Y., 2009. The impact of ZnO nanoparticle aggregates on the embryonic development of zebrafish (Danio rerio). Nanotechnology 20, 195103. https://doi.org/10.1088/0957-4484/20/19/195103

9 Objectives

The aims of this thesis were different:

1) To chemically characterise and quantify titanium dioxide nanoparticles (TiO_2-NPs), silver nanoparticles (Ag-NPs), and zinc oxide nanoparticles (ZnO-NPs) in processed canned fish by single particle ICP-MS;
We selected canned seafood for this assessment study because it is an essential component of the human diet and an important source of inorganic NPs intake due to its high accumulation in aquatic organisms (Chen et al., 2018). In addition, the most commonly used nanoparticles in the food industry were selected.
2) Optimization of an alkaline digestion for the extraction of TiO_2-NPs, Ag-NPs and ZnO-NPs from seafood samples from two different trophic levels (pelagic: tuna, mackerel and anchovy; benthic: canned mussels).
3) Provide estimated daily intake data for adults and children that may be useful for risk assessors to develop a provisional tolerable daily intake for all three nanoparticles studied.
4) Evaluate the in-vivo toxicity of TiO_2-NPs, Ag-NPs, ZnO-NPs and food additives (TiO_2 - E171 - and Ag - E174);
5) Evaluate the in-vitro toxicity of TiO_2-NPs and food additives (TiO_2 - E171);
6) Re-evaluation of the safety of titanium dioxide (TiO_2, E 171) when used as a food additive, following concerns expressed bythe European Food Safety Authority (EFSA) in the last safety assessment in 2021.
7) Investigation of the fate of TiO_2-NPs, Ag-NPs and ZnO-NPs under intestinal conditions, accepting possible agglomeration of NPs over time.

9.1 Outline of the thesis

In order to facilitate the reading of the work and to find a common thread between the result chapters (1-6), a brief overview of the outline of the work is given here.

Chapter 1: provides a chemical characterization and quantification of TiO_2-NPs (< 100 nm), total TiO_2 particles (TiO_2-Ps-Tot, all size ranges of particles), dissolved Ti and total Ti in processed canned seafood belonging to different trophic positions of the pelagic compartment (tuna, mackerel and anchovy) and in canned shellfish. The new emerging technique of Single Particle - Inductively Coupled Plasma (spICP- MS) was applied, which allows the determination of nanoparticle number-based concentration as well as the dissolved titanium. Prior to performing sp-ICP-MS analysis, alkaline digestion of the samples was performed using the method described by Gray et al. (2013). In addition, data on estimated daily intake for adults and children were provided.

Chapter 2: provides a chemical characterization and quantification of AgNPs and dissolved Ag in the same processed canned seafood as in Chapter 1, as well as estimated daily intake data for adults and children. The analytical method and procedure are the same as in Chapter 1.

Chapter 3: provides a chemical characterization and quantification of ZnO-NPs in processed canned seafood as in Chapter 1 and a first esteem of ZnO-NPs daily intake derived from consumption of seafood products. The analytical method and procedure are the same as in Chapter 1.

Chapter 4: investigates the genotoxic potential of TiO_2-NPs in colorectal cancer cells, HCT-116 and Caco-2, including their potential

to induce DNA damage and apoptosis.
The correlation between DNA damage and reduction in cell viability was investigated using genomics and proteomics approaches. The following experiments were performed and analyzed: Cytotoxicity assays (MTT assay), genotoxicity assays (Comet assay), gene expression (real-time PCR), apoptosis markers (Western blot assay) and proliferation assay (Clonigenic assay).

Chapter 5: provides preliminary results of Fish Embryo Toxicity Test (FET) on zebrafish (*Danio rerio*) exposed to TiO_2-NPs, TiO_2 used as a food additive (E171), ZnO-NPs, Ag-NPs and Ag used as a food additive (E174). Fish Embryo Toxicity (FET) test was performed according to OECD guideline (2013).

Chapter 6: samples of canned tuna and meckarel were subjected to in vitro digestion in the human gastrointestinal tract. The same study was performed for standards of TiO_2-NPs, Ag-NPs and Zn-NPs at one concentration levels. The changes in number concentration, size distribution and dissolved content were studied during the digestion process (30, 60 and 120 min of gastric phase and 30, 60, 120 min of intestinal phase). Measurements were performed using sp-ICP-MS.

10 Results

CHAPTER 1: Chemical characterization and quantification of titanium dioxide nanoparticles (TiO_2-NPs) in seafood by single particle ICP-MS: assessment of dietary exposure

CHAPTER 2: Chemical characterization and quantification of silver nanoparticles (Ag-NPs) and dissolved Ag in seafood by single particle ICP-MS: assessment of dietary exposure.

CHAPTER 3: Dietary exposure of zinc oxide nanoparticles (ZnO-NPs) from canned seafood by single particle ICP-MS: balancing of risks and benefits for human health.

CHAPTER 4: DNA damage, and apoptosis induced by titanium dioxide nanoparticles and the food additive E171 in colon cancer cells: HCT-116 and Caco-2

CHAPTER 5: Preliminary results of Fish Embryo test (FET) on zebrafish (*Danio rerio*) exposed to metallic nanoparticles (Titanium dioxide - TiO_2, Silver – Ag - and Zinc Oxide – ZnO) and food additive (TiO_2 - E171 - and Ag - E174)

CHAPTER 6: Behaviour and fate of Ag-NPs, TiO_2-NPs and ZnO-NPs in an in vitro digestion model of the human gastrointestinal tract and calculation of the biopersistence rate.

10.1 CHAPTER 1: Chemical characterization and quantification of titanium dioxide nanoparticles (TiO_2-NPs) in seafood by single particle ICP-MS: assessment of dietary exposure

Alfina Grasso[1], Margherita Ferrante[1], Pietro Zuccarello[1], Tommaso Filippini[2], Giovanni Arena[3], Maria Fiore[1], Antonio Cristaldi[1], Gea Oliveri Conti[1], Chiara Copat[1]

[1] Department of Medical, Surgical and Advanced Technologies "G.F Ingrassia", University of Catania, Catania, Italy.

[2] Department of Biomedical, Metabolic and Neural Sciences, Section of Public Health, University of Modena and Reggio Emilia, Modena, Italy.

[3] Freelance chemist.

Publisehd in: International Journal of Environmental Research and Public Health, 2020, 17, 9547; doi:10.3390/ijerph17249547

Abstract

The significant increase in the production and variety of nanoparticles (NPs) led to their release into the environment, especially into the marine environment. Titanium dioxide nanoparticles (TiO_2-NPs) is used in different industrial sectors, from food industry to several consumer and household products. Since the aquatic environment is highly sensitive to contamination by TiO_2-NPs, this work allowed to give a preliminary assessment on the contamination of packaged seafood, where the food additive TiO_2 (E171) is not be intentionally added. It is aimed to provide a chemical characterization and quantification of TiO_2-NPs in processed canned fish products belonging to different trophic position of the pelagic compartment and in canned clam. It was applied the new emerging technique of Single Particle - Inductively Coupled Plasma (spICP-MS), which allows the determination of nanoparticle number-based concentration as well as the dissolved titanium. This study highlights how processed food, where the pigment E171 is not intentionally added, could contain amount of TiO_2 in its nanoparticles form, as well as dissolved titanium. Processed clam represents the seafood with the higher content of TiO_2-NPs. In pelagic fish species we found a progressively higher levels and smaller sizes of TiO_2-NPs from smaller to larger fish. Our results highlight the importance to plan the characterization and quantification of TiO_2-NPs in food both processing and not, and where the pigment E171 is intentionally added and not, as it is not the only source of TiO_2-NPs. This result would be a solid step to be able to estimate the real TiO_2-NPs dietary exposure for the general population and their related health risks.

Keywords: Titanium dioxide; Nanoparticle; spICP-MS; Processed Food; Dietary Intake; E171.

1.1 Introduction

In Earth science, nanoparticles (1-100 nm) are important components of the biogeochemical system, but human impact on the environment altered their natural cycle (Lespes et al., 2020) by introducing engineered nanoparticles with several physicochemical characteristics and applications (Ziental et al., 2020). Nanoparticles represents a blooming industrial sector destined to increase, because of the numerous investments that it is able to attract. Due to their peculiar characteristics (e.g. different optical properties, greater flexibility, resistance, reactivity, electrical conductivity or absorption), nanoparticles (NPs) find more and more applications in many consumer products, such as conductors, in cosmetics, plastics and as agents used in environmental recovery, and in various sectors such as the pharmaceutical, food, biomedical, military and automotive industries (Boverhof and David, 2010; Piccinno et al., 2012).

Our study focuses on titanium dioxide (TiO_2), a metal oxide naturally occurring in three polymorphic forms known as rutile, anatase and brookite (Ziental et al., 2020). It is synthetized as titanium dioxide nanoparticles (TiO_2-NPs) for several industrial sectors. In food industry, TiO_2 is authorised as a food additive (E 171) in accordance to the European Regulation (EC) No. 1333/2008, in both anatase and rutile forms (Commission Regulation (EU) No. 231/2012) (EFSA, 2016). It is added for whitening and brightening purpose in many foods including milk and dairy products, chewing-gum, ice-cream, and all sweets when it constitutes the coating of sugar confectionary (EFSA, 2016; Filippini et al., 2019). Nevertheless, it is not considered a nanomaterial by the current "European Commission recommendation for the definition of nanomaterial". Accordingly, a nanomaterial should consist for 50% or more of particles having a size between 1-100 nm (Regulation 211/696/EU), but E171 may contain up to 3.2% of its weight in nanoparticles. TiO_2 in its nanoform is also used in plastic packaging, as titanium dioxide

surface treated with fluoride-modified alumina, to improve the quality and the shelf-life of the product. According to EFSA safety assessment, the substance does not raise safety concern for the consumer if used as an additive up to 25% w/w in polymers in contact with all food types for any time and temperature conditions (Silano et al., 2019). TiO_2-NPs is also used in several consumer and household products which potentially can expose human such as toothpaste, sun cream, creams, and lip balm (Rompelberg et al., 2016; Ruszkiewicz et al., 2017; Schneider and Lim, 2019). Other uses of manufacturer TiO_2 nanomaterial known as P25 include antimicrobial applications, paints, catalysts for air and water purification, medical applications, and energy storage (Weir et al., 2012). Despite their favourable properties, NPs are known to cause local adverse effects and/or systemic toxicity (Bostan et al., 2016).

The significant increase in the production and variety of NMs led to their release into the environment (Klaine et al., 2008), especially into the marine environment, as the NPs are not completely removed from domestic and industrial wastes after water treatment (Carmo et al., 2018; Westerhoff et al., 2011). It increases both the ecological risks for the ecosystems and the likelihood of inhalation, dermal and oral exposure risk for humans (Borm et al., 2006). In toxicological studies concerning TiO_2-NPs, most researchers have utilized industrial grade nano form of TiO_2, though food grade one represents the majority of TiO2 containing materials that enter the ecosystem today (Chen et al., 2018). The choice depends on the fact that it is commonly used, due to the primary crystals being relatively uniform and less than 50 nm in size. Results in literature studies demonstrate also that exists a difference in the removal efficiency of food grade TiO_2, which is lower than industrial grade TiO_2. For this reason food grade TiO_2 accumulates preferably in the environment, involving an environmental and human health risk (Chen et al., 2018).

The oral exposure route of TiO_2-NPs is the least investigated. To date, despite the existing numerous applications of TiO_2-NPs, little

or nothing is known about the bioaccumulation potential of TiO_2-NPs along the food chain and the dietary exposure dose to the general population. Nevertheless, as this compound has a limited elimination rate and it can be absorbed by the gastrointestinal tract in a size-dependent manner and pass through the mucus pores to enter other organs (Jovanović, 2015), some studies suggest a potential health risk such as disorders of gut microbiota and gut-associated metabolism in vivo (Chen et al., 2019a), apoptosis induction (Schneider et al., 2017), hepatic toxicity (Chen et al., 2019b), a potential risk for liver, ovaries and testes (Heringa et al., 2016), an impact on lipid metabolism (Chen et al., 2020) and an increase abundance of pro-inflammatory immune cells and cytokines in the colonic mucosa (Cao et al., 2020).

The risk to human is through food chain transport because TiO_2 has a high attitude to bio-accumulate in aquatic organism and this implies that TiO_2 particles could be bio-concentrated from one species to another (Chen et al., 2018).

Since the aquatic environment is highly sensitive to contamination by TiO_2-NPs (Klaine et al., 2008), this work allowed to give a preliminary assessment on the contamination of packaged food derived from marine environment. According to literature, very few studies report the levels of nanoparticles in marine organisms (Taboada-López et al., 2019, 2018; Xu et al., 2020; Yin et al., 2017; Zhou et al., 2020).

With this study, we wanted to provide a chemical characterization and quantification of TiO_2-NPs (<100 nm), TiO_2 total particles (TiO_2-Ps-Tot, all size range of particles), dissolved Ti and Total Ti, in processed canned seafood products belonging to different trophic position. Our choice to use canned seafood for this evaluation study was because it is a fundamental component in human nutrition, representing an important source of unsaturated fatty acids, protein and different micronutrient (Domingo et al., 2007).

Furthermore, we also provided data related to the estimated daily intake for both adults and children, which may be useful to risk assessors, to develop a provisional tolerable daily intake for TiO_2-NPs.

1.2 Methods

1.2.1 Experimental by alkaline digestion and spICP-MS analysis

Different brands of canned tuna (5), mackerel (4), anchovy (3) and clam (3), among the best-selling and low cost brands, were purchased from the main Italian supermarket chains in the city of Catania, (Italy), in the period between June and July 2019 and stored at -80° until analysis. For each brand of seafood product we chose to purchase also three different batches, which were extracted and processed in triplicate. Thus we performed a total of 45 extraction for canned tuna, 36 for canned mackerel, 27 for canned anchovy and 37 for canned clam.

Assessment of TiO_2 has been performed with a NexION® 350D (Perkin Elmer, USA) with the Syngistix Nano Application software. The instrumental operating conditions for the determination of TiO_2 are listed in Table 1.1. The dwell time used was chosen based on other studies (Wu et al., 2020; Xu et al., 2020).

Table 1.1. NexION® 350D ICP-MS instrumental condition for single particles analysis.

Parameter	Value
Nebulizer, flow	Meinhard, 1 mL/min
Spray chamber	Glass cyclonic
Sample uptake rate	0.26–0.28 mL/min
RF power	1600 W
Analysis mode	Standard
Quadrupole settling time	0 µs
Analyte	Ti 48.9
Dwell time	50 µs
Data acquisition time	60 s
Density	4.23 g/cm^3
Ti mass fraction	60%

The new emerging technique of Single Particle - Inductively Coupled Plasma (spICP-MS) allows the determination of particle number-based concentration, with rapid simultaneous characterization of its elemental composition, number of particles, size and size distribution, in addition to the dissolved concentration. Furthermore, by modifying the integration window, it is possible to collect data related to a specific size distribution. Accordingly, for each sample we captured data on the total TiO_2 particles (Ps-Tot) and TiO_2 nanoparticles (NPs<100 nm) only.

Titanium nanoparticle stock solution was prepared from a TiO2-NPs standard (60 nm TiO_2 Nano Powder, rutile, 99.9%, AEM) purchased from Nanovision (Brugherio, MB, Italy), while Ti ion standard (1000 mg/L, CPAchem) was used for spICP-MS calibration of titanium.

To support the quality of spICP-MS measurements, the particle size distribution of the powder TiO_2-NPs standard was assessed as follows. A TiO_2-NPs stock suspension (215 ng/L or 4.5×10^5 particles/mL) was prepared in ultrapure water and dispersed for 30 minutes a 37°C by an ultrasonic bath, to maximize a homogenous dispersion. The transport efficiency was calculated with the certified reference material PELCO (Ag-NPs, 39 ± 5nm, 110 ng/L, monitoring m/z 107) under the same instrumental conditions as the samples, obtaining a value of TE% 2.54. This solution gave a TiO_2-NPs concentration of $4.6 \times 10^5 \pm 0.16 \times 10^5$ particles/mL (n=10), in agreement to the particle concentration prepared. TiO_2-NPs showed a size range of 44-85 nm with a mean size of 66.2 ± 3.0 (n=10) and a most frequent size of 56.6 ± 4.4 (n=10). The results obtained were in compliance with the size of TiO_2-NPs standard supplied by the manufacturer (60 nm).

Before performing the spICP-MS analysis, an alkaline digestion of the samples was performed using the method described by Gray et al., (2013) (Gray et al., 2013). Approximately 0.5 gr of wet sample tissue was weighed in DigiTUBEs (SCP Science, Canada) and mixed

with 5 mL of tetramethylammonium hydroxide (TMHA, 20% v/v) that is a strong organic base capable of digesting tissues and releasing nanoparticles without altering them. A vortex was used, at first, to prevent the tissues from sticking to the walls of the container used for digestion. The TiO_2 extraction was obtain through sonication for 30 min at 37°C by an ultrasonic bath to accelerate tissue breakdown and prevent particle aggregation. Subsequently the samples were left to digest for another 24 hours at room temperature. At the end of digestion, samples were diluted with MilliQ water (Millipore, Bedford, MA, USA) to 1% TMAH concentration before analysis, and 0.1% Triton X-100 to allow the detection of single particles.

All samples and calibration solutions were sonicated for 30 minutes before being analyzed. To avoid contamination between samples, the system was rinsed with nitric acid (2%, v/v) prior to the measurement. TiO_2-NPs standard was used also for the determination of the transport efficiency that was within the 3%-8% range, in agreement with TE obtained with Ag certified reference material.

The effect of the extracting solution on the size distribution and particle concentration was studied in triplicate, spiking simultaneously TiO_2 standard to ultrapure water (n1=3) and to TMAH 1% (n2=3), at the same concentration (215 ng/L or 4.5×10^5 particles/mL) we used for determining the transport efficiency. We obtained a particles concentration of $4.3 \times 10^5 \pm 5.0 \times 10^4$ in water and $4.9 \times 10^5 \pm 3.6 \times 10^4$ in TMAH 1%, with a recovery of 97.6% ± 10.5 and 108.8 % ± 7.2, respectively. In addition, results revealed that the alkaline digestion in TMAH 1% does not affect TiO_2 particles size distribution (mean size and most frequent size). Mean size of TiO_2 in ultrapure water (63.8 nm ± 3.0) and mean size of TiO_2 in TMAH 1% (61.1 nm ± 4.3) are statistically homogeneous if applied a two tailed t-test (p=95%; n1 + n2 − 2) (tcalculated = 1.5 < ttabulated = 2.8). Also, the most frequent size is statistically homogeneous in ultrapure

water (57.6 ± 3.2) and in TMAH 1% (56.0 ±4.0) (tcalculated = 0.88; ttabulated = 2.8).

The limit of detection (LOD) and the limit of quantification (LOQ) were calculated by analyzing ten alkaline extract blanks, in the same analytical condition of the samples, and based respectively on the mean ± 3 SD and the mean ± 10 SD criterion of the number of particles/mL obtained. LOD was 1.3×10^3 particles/mL, while LOQ was 2.5×10^3 particles/mL. Referring to the sample weight and digestion volume used, they resulted 2.6×10^5/g and 5.0×10^5/g, respectively.

In addition LOD in size (LODnm) was estimated 35 nm applying the following equation (1) (Lee et al., 2014; Taboada-López et al., 2018):

$$\mathrm{LODnm} = \sqrt[3]{\frac{6 \times 3\sigma_{blank}}{R \times f_a \times \rho \times \pi}} \quad (1)$$

Where, 3σ blank is three times the standard deviation of counts/dwell time of alkaline blanks (1% TMAH), R is the slope of the calibration curve of ionic Ti solutions, fa is the mass fraction of analyzed metallic element in the TiO_2-NPs, and ρ is the density of the TiO_2-NPs.

For each batch of analysis, a quality control was performed with analytical recovery before and after spiking with 60 nm TiO_2-NPs at concentration of 5 µg/L, corresponding to a concentration of 1.1×10^6 part/mL. The values (range 90-95%) were calculated on the whole size distribution by dividing TiO_2-NPs concentration by the TiO_2-NPs concentration found in the solution of TiO_2-NPs used for spiking and multiplying by 100.

Accuracy was tested by a Laboratory Fortified Matrix with a seafood sample spiked with 5 µg/L of TiO_2-NPs (60 nm). An LFM was processed at each batch of digestion, obtaining a concentration of 9.8

$\times 10^5 \pm 4.6 \times 10^5$ particles/mL ($1.9 \times 10^8 \pm 9.3 \times 10^7$ particles/g) and a recovery range from 87-121% (n= 5). The measured mean size of TiO_2-NPs in alkaline digested samples was 64.2 ± 5.1 nm.

1.2.2 Experimental by acid digestion and ICP-MS analysis of Total Ti

For the determination of total titanium, the same samples were processed by acid digestion. Aliquots of 0.5 g of wet samples were weighed in Teflon reactors using an analytical balance (Mettler Toledo) and then digested in a microwave oven (Ethos, TC, Milestone), by adding 6 mL of 67% super pure nitric acid (HNO3; Carlo Erba, Italy) and 2 mL of 30% hydrogen peroxide (H2O2; Carlo Erba, Italy) for 1 h at 80 °C. After acid digestion all samples were diluted to 50 mL with ultrapure water and were filtrated through 0.45 μm membrane filter before analysis. Total Ti was quantified with the same Inductively Coupled Plasma – Mass Spectrometer (ICP-MS NexION® 350D, Perkin Elmer, USA), in the standard mode, by using the standard addition technique covering the concentration from 0 to 50 μg/L.

Single element standard solution Ti (1000 mg/L in 5 % di HNO3, 0.5% HF) was purchased from CPAchem. Standard for the instrument calibration were prepared in the same acid matrix and Yttrium (Y) was used as an internal standard to verify the accuracy.

To verify if acid digestion of the samples allows the total dissolution of TiO_2 particles, and then the quantification of total Ti, we conducted a preliminary acid digestion of 4 μg/L ionic Ti (n=6), canned clam (n=6) and canned tuna (n=6). The quantification of TiO_2 particles was detected by Syngistix Nano Application software and the resulting background signals, expressed as particles/mL, are showed in Table 1.2.

Table 1.2. Descriptive statistics concerning the quantification of TiO_2 particles (Ps-Tot) expressed as Particles/mL detected with Syngistix Nano Application software after acid digestion of the samples.

Parameter	Value
Nebulizer, flow	Meinhard, 0.89 mL/min
Spray chamber	Glass cyclonic
RF power	1600 W
Analogic phase voltage	−1950 V
Pulses voltage	1300 V
Discriminator threshold	12
Deflector voltage	−12 V
Analysis mode	Standard
Analyte	Ti 48.9
Internal standard	Y

Threshold value of TiO_2 particles was estimated as the mean + 3SD given by ionic Ti, which resulted 1029 particles/mL. Digested samples of canned clam and canned tuna did not show background values of TiO_2 particles higher than the calculated threshold, demonstrating the effectiveness of the acid digestion in dissolving all TiO_2 particles.

The LOD and LOQ, were calculated by analyzing ten acid extract blanks based on the mean ± 3 SD / mean ± 10 SD criterion. They resulted 0.06 and 0.16 mg/kg, respectively.

For each batch of analysis, a quality control was performed with analytical recovery after spiking with 20 μg/L of ionic Ti.

Accuracy was tested by a Laboratory Fortified Matrix with a seafood sample (use of ionic Ti at 20 μg/L) processed at each batch of digestion, obtaining a recovery range of ionic Ti from 92-115%.

Table 1.3. NexION® 350D ICP-MS instrumental condition for Total Ti in standard mode.

Statistics	4 µg/L Ionic Ti (n = 6)	Canned Clam (n = 6)	Canned Tuna (n = 6)
Mean of particles/mL	564	588	653
SD	155	267	237
Min	324	267	252
Max	758	901	918
Mean + 3 SD	1029	-	-

1.2.3 Estimated Meal Intake

An exposure assessment derived from consumption of selected seafood products was conducted for TiO_2-NPs (TiO_2 particles <100 nm), TiO_2-Ps-Tot (TiO_2 total particles) and dissolved Ti according to the method described in a previous paper [35]. Briefly, it was provided the Estimated Meal Intake (EDI) (µg/Kg bw per day) according the following equation (3):

EMI = (C × M) / BW (3)

Where C is the TiO_2-NPs, TiO_2-Ps-Tot or dissolved Ti (mg/Kg w.w.); M is the meal size (227 g for adults and 114 g for child) (Copat et al., 2013); BW is the body weight, considered as 16 Kg for child (6 years) and 70 Kg for adult (70 years) (US-EPA, 2000).

1.2.4 Statistical analysis

The statistical software package IBM SPSS 20.0 was used for statistical analysis. One-way ANOVA and post hoc Tukey test were performed to evaluate differences in TiO_2 and dissolved Ti levels among canned products. We processed a total of 45 samples of canned tuna, 36 of canned mackerel, 27 of canned anchovy and 37 of canned clam.

1.3 Results

The total TiO_2 particles present (Ps-Tot size), as well as the level of Ti in its dissolved form, were analysed with the NexION® 350D (Perkin Elmer, USA) with the Syngistix Nano Application software, by processing the samples with the ultrasound assisted alkaline digestion. In a separate working session, we also provide the level of total Ti measured with ICP-MS in standard mode, by processing the samples digested with acid. As showed in Table 1.4, the quantification of dissolved Ti did not differ significant with the total Ti. The result of Total Ti slightly higher can be related to the acid dissolution of the Ti bonded into the particles, as supported in the experimental showed in Table 1.2. As showed in Table 1.4 and Figure 1.1, canned anchovy and canned clam revealed the highest mean diameters of Ps-Tot size, close to 140 nm, significantly higher than the mean diameters found in canned tuna and canned mackerel, close to 100 nm. The most frequent size was found significantly higher in canned anchovy versus the other seafood products, followed by canned mackerel, canned clam and canned tuna. As regard the Ps-Tot level, the samples of canned clam had the highest levels of TiO_2-NPs than the fish species, with a mean value of 0.326 mg/kg. Among fish species, canned tuna had levels of TiO_2-NPs significantly higher than canned mackerel and anchovy, with a mean value of 0.117 mg/Kg. As regard the ionic Ti performed with the single particle technique, canned clam and canned anchovy had higher level than the other seafood products, with mean values of 1.31 and 1.22 mg/kg respectively.

Table 1.4. Descriptive statistics concerning the chemical characterization and quantification of total TiO_2 particles (Ps-Tot), dissolved Ti (mg/Kg) and total Ti in packaged seafood products.

Canned Tuna	Most Frequent Size Ps-Tot. (nm)	Mean Diameter Ps-Tot. (nm)	Number of Ps-Tot/g.	Ps-Tot. mg/kg	Dissolved Ti [a] mg/kg	Total Ti [b] mg/kg
Mean	73	104	9.77×10^7	0.117	0.851	1.015
SD	11	12	6.27×10^7	0.156	0.099	0.121
Min.	59	87	1.93×10^7	0.029	0.752	0.857
Max.	98	126	2.86×10^8	0.634	1.052	1.152
Canned Mackerel	**Most Frequent size Ps-Tot. (nm)**	**Mean Diameter Ps-Tot. (nm)**	**Number of Ps-Tot/g.**	**Ps-Tot. mg/kg**	**Dissolved Ti [a] mg/kg**	**Total Ti [b] mg/kg**
Mean	85	112	1.47×10^7	0.025	0.835	1.154
SD	11	11	7.17×10^6	0.021	0.095	0.108
Min.	69	95	8.15×10^6	0.007	0.669	0.951
Max.	104	133	2.72×10^7	0.068	1.003	1.185
Canned Anchovy	**Most Frequent size Ps-Tot. (nm)**	**Mean Diameter Ps-Tot. (nm)**	**Number of Ps-Tot/g.**	**Ps-Tot. mg/kg**	**Dissolved Ti [a] mg/kg**	**Total Ti [b] mg/kg**
Mean	113	141	1.67×10^7	0.059	1.223	1.385
SD	7	8	3.12×10^6	0.019	0.051	0.148
Min.	101	127	1.06×10^7	0.026	1.141	0.985
Max.	122	150	2.02×10^7	0.087	1.312	1.485
Canned Clam	**Most Frequent size Ps-Tot. (nm)**	**Mean Diameter Ps-Tot. (nm)**	**Number of Ps-Tot/g.**	**Ps-Tot. mg/kg**	**Dissolved Ti [a] mg/kg**	**Total Ti [b] mg/kg**
Mean	82	138	1.05×10^8	0.326	1.313	1.458
SD	6	13	1.52×10^7	0.084	0.210	0.341
Min.	75	124	7.00×10^7	0.162	1.005	1.145
Max.	91	167	1.00×10^8	0.451	1.735	1.915

[a] Ultrasound assisted alkaline digestion and *sp*ICP-MS determination;
[b] Microwave assisted acid digestion and ICP-MS determination in standard mode.

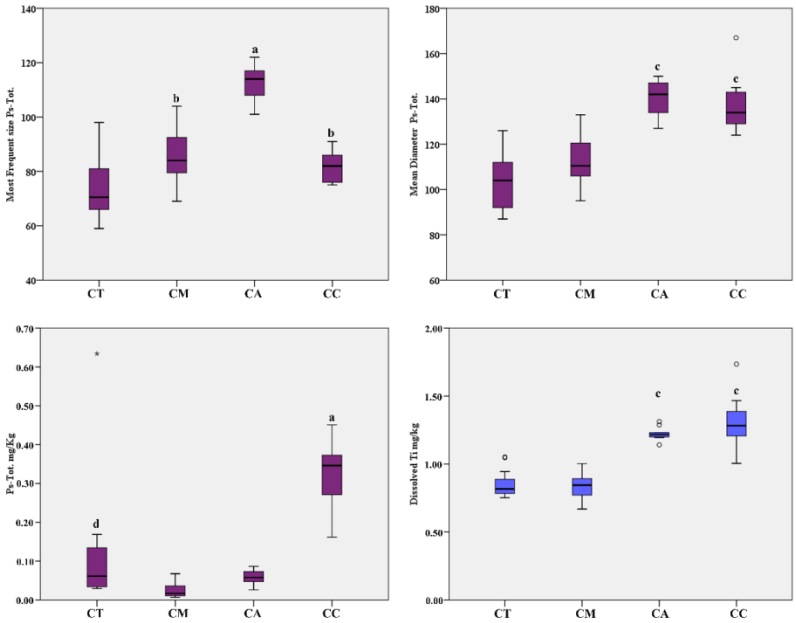

Figure 1.1. Box Plot distribution of TiO_2-Ps-Tot most frequent size (nm), mean diameter (nm), level of Ps-Tot and dissolved Ti (mg/Kg) in packaged seafood products. Legend: CT, Canned Tuna; CM, Canned Mackerel; CA, Canned Anchovy; CC, Canned Clam; a, $p<0.001$ vs all; b, $p< 0.05$ vs CT, c, $p<0.001$ vs CT and CM; d $p<0.05$ vs CM and CA.

For each sample, by reducing the integration window of particle size, we selected the particle size distribution <100 nm to quantify the nanoparticles only. The analyses carried out showed the presence of TiO_2-NPs, with a diameter lower than 100 nm, in all the seafood samples. As showed in Table 1.5 and Figure 1.2, with regard to NPs size, canned anchovy and canned clam revealed the highest mean diameters, close to 90 nm, higher than the mean diameters found in canned tuna and canned mackerel (both below 80 nm). The most frequent size was found significantly higher in canned anchovy versus the other seafood products with mean value of 93 nm,

followed by canned mackerel, canned clam and canned tuna. As regard the NPs level, the samples of canned clam had the highest levels of TiO_2-NPs than the fish species, with a mean value of 0.112 mg/kg. Among fish species, canned tuna had levels of TiO_2-NPs four-fold higher than canned mackerel and anchovy, with a mean value of 0.038 mg/Kg. Furthermore, the percentage of TiO_2-NPs in the TiO_2 total particles is close to 60% in all seafood products but canned anchovy, which showed a percentage close to 30% (Table 1.5 and Figure 1.2).

Table 1.5. Descriptive statistics concerning the chemical characterization and quantification of TiO_2-NPs (< 100 nm) in packaged seafood products.

Canned Tuna	Most Frequent Size NPs (nm)	Mean Diameter NPs (nm)	Number of NPs/g	NPs mg/kg	%NPs on Ps-Tot.
Mean	66	72	5.26×10^7	0.0380	58.5
SD	7	4	2.19×10^7	0.0298	13.3
Min.	56	65	9.34×10^6	0.0062	32
Max.	82	79	1.02×10^8	0.1251	76
Canned Mackerel	**Most Frequent size NPs (nm)**	**Mean Diameter NPs (nm)**	**Number of NPs/g**	**NPs mg/Kg**	**%NPs on Ps-Tot.**
Mean	77	78	7.84×10^6	0.0085	57.4
SD	11	8	2.42×10^6	0.0053	12.2
Min.	48	54	5.24×10^6	0.0020	39
Max.	91	86	1.23×10^7	0.0206	73
Canned Anchovy	**Most Frequent size NPs (nm)**	**Mean Diameter NPs (nm)**	**Number of NPs/g**	**NPs mg/Kg**	**%NPs on Ps-Tot.**
Mean	93	89	5.16×10^6	0.0092	31.6
SD	2	1	9.30×10^5	0.0019	6.78
Min.	91	88	4.36×10^6	0.0078	23
Max.	96	92	7.24×10^6	0.0137	43
Canned Clam	**Most Frequent size NPs (nm)**	**Mean Diameter NPs (nm)**	**Number of NPs/g**	**NPs mg/Kg**	**%NPs on Ps-Tot.**
Mean	72	89	5.37×10^7	0.1116	51.4
SD	5	6	8.34×10^6	0.0254	5.70
Min.	63	81	4.00×10^7	0.0650	41
Max.	81	97	7.00×10^7	0.1403	61

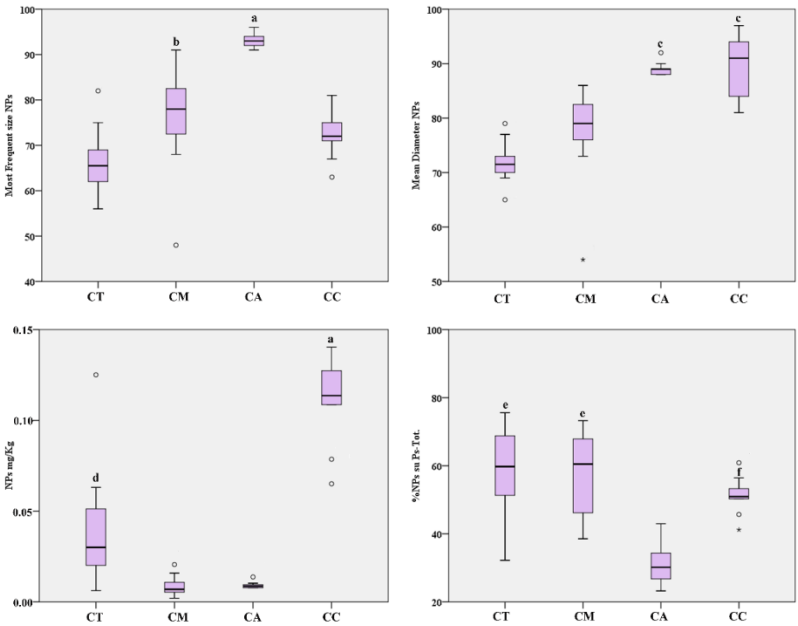

Figure 1.2. Box Plot distribution of TiO_2-NPs most frequent size (nm), mean diameter (nm), %NPs on Ps-Tot and level (mg/Kg) in packaged seafood products. Legend: CT, Canned Tuna; CM, Canned Mackerel; CA, Canned Anchovy; CC, Canned Clam; a, $p<0.001$ vs all; b, $p<0.01$ vs CT; C, $p<0.001$ vs CT and CM; d, $p<0.01$ vs CM and CA; e, $p<0.001$ vs CA, f, $p<0.01$ vs CA.

Regarding the Estimated Meal Intake, as it is shown in Table 1.6 and Figure 1.3, based on levels found, it resulted obviously significantly higher in child than in adult, due to the low body weight of the considered age class. According to the different seafood products, the EMI of both NPs and Ps-Tot form is highest with a meal of canned clam, followed by the EMI calculated for canned tuna, significantly higher than the EMI derived from a meal of canned mackerel or canned anchovy. As concern the dissolved Ti, the EMI calculated for canned clam and canned anchovy are both significantly higher than the EMI calculated for the other fish species ($p<0.001$).

Table 1.6. Descriptive statistics of Estimated Meal Intake (EMI μg/Kg b.w.) calculated for adult (70 years) and child (6 years) concerning the TiO_2-NPs, TiO_2-Ps-Tot and dissolved Ti.

Canned Tuna	EMI Adult NPs	EMI Child NPs	EMI Adult Ps-Tot.	EMI Child Ps-Tot.	EMI Adult Dissolved Ti	EMI Child Dissolved Ti
Mean	0.124	0.272	0.379	0.832	2.759	6.063
SD	0.097	0.212	0.507	1.113	0.321	0.706
Min.	0.020	0.044	0.095	0.209	2.438	5.357
Max.	0.406	0.891	2.056	4.517	3.412	7.497
Canned Mackerel	**EMI Adult NPs**	**EMI Child NPs**	**EMI Adult Ps-Tot.**	**EMI Child Ps-Tot.**	**EMI Adult Dissolved Ti**	**EMI Child Dissolved Ti**
Mean	0.028	0.060	0.082	0.180	2.709	5.952
SD	0.017	0.038	0.066	0.146	0.307	0.674
Min.	0.007	0.014	0.021	0.046	2.171	4.769
Max.	0.067	0.147	0.219	0.482	3.253	7.147
Canned Anchovy	**EMI Adult NPs**	**EMI Child NPs**	**EMI Adult Ps-Tot.**	**EMI Child Ps-Tot.**	**EMI Adult Dissolved Ti**	**EMI Child Dissolved Ti**
Mean	0.030	0.066	0.191	0.419	3.967	8.716
SD	0.006	0.013	0.062	0.135	0.164	0.361
Min.	0.025	0.055	0.084	0.184	3.699	8.129
Max.	0.044	0.098	0.280	0.616	4.254	9.346
Canned Clam	**EMI Adult NPs**	**EMI Child NPs**	**EMI Adult Ps-Tot.**	**EMI Child Ps-Tot.**	**EMI Adult Dissolved Ti**	**EMI Child Dissolved Ti**
Mean	0.362	0.795	1.056	2.319	4.259	9.358
SD	0.082	0.181	0.273	0.600	0.681	1.496
Min.	0.211	0.464	0.524	1.152	3.259	7.162
Max.	0.455	0.999	1.462	3.211	5.628	12.36

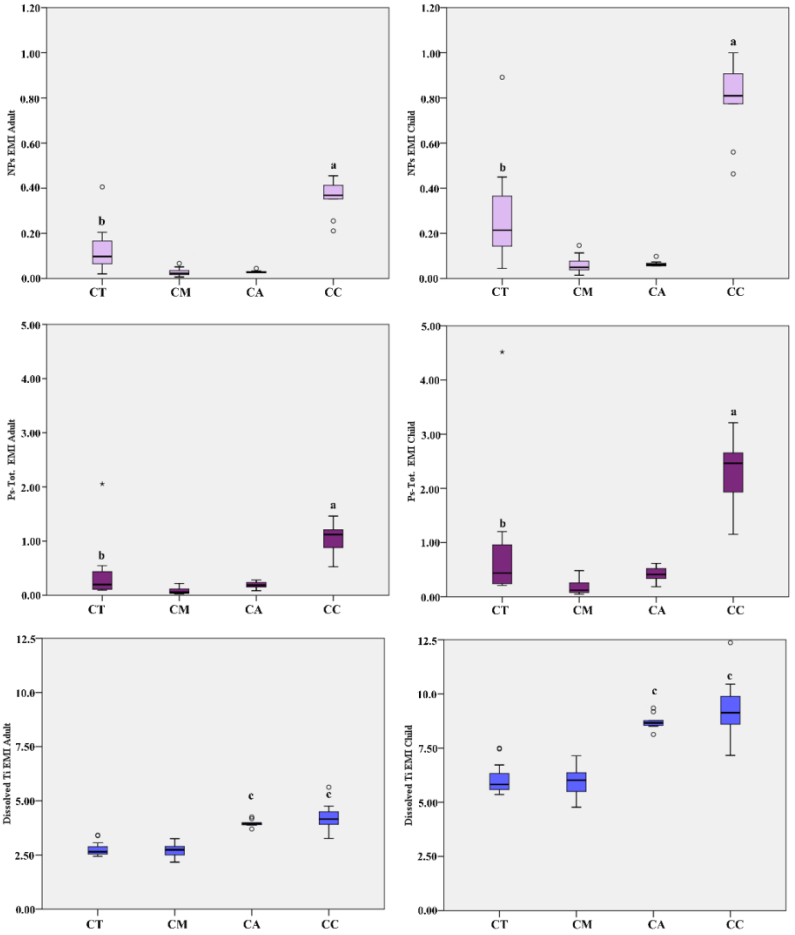

Figure 1.3. Box Plot distribution of Estimated Meal Intake (EMI μg/Kg b.w.) of TiO_2-NPs, TiO_2-Ps-Tot and dissolved Ti concentration calculated for adult (70 years) and child (6 years). Legend: CT, Canned Tuna; CM, Canned Mackerel; CA, Canned Anchovy; CC, Canned Clam; a, $p<0.001$ vs all; b, $p< 0.01$ vs CM and CA; c, $p<0.001$ vs CT and CM.

1.3 Discussion

Our results are the first to provide a quantitative analysis of TiO_2-Ps-Tot in packaged pelagic fish, and deepen findings related to bivalve molluscs. It is important to specify that in all the products we have chosen, the use of the additive E171 was not indicated on the label, indicating that it should not be intentionally added during food processing. Thus, the presence of titanium dioxide in particle or nanoparticle form may be attributed to a contamination within the food industry, but above all to levels related to the bioaccumulation of organisms in their natural environment. As showed in Table 1.5 and Figure 1.2, our findings highlighted how the longest-lived and larger-sized organisms, such as tuna and mackerel, had the lower TiO_2 nanoparticle diameter than anchovy, a small pelagic fish, and clams, as well the highest percentage of NPs on the total particles. Accordingly, it seems that nanoparticles of smaller diameter have a higher potential of bioaccumulation and biomagnification along the food chain in aquatic systems. This environmental behaviour of TiO_2-NPs seems promoted by their poor water solubility and long-term persistence in aquatic systems (Gupta et al., 2016).

Nevertheless, both TiO_2-Ps-Tot and TiO_2-NPs concentrations were found significantly higher in clam, surely due to their filter feeding behaviour, making it a great biological model to test for the bioavailability of contamination at the sediment-water interface. The sedimentation capacity of TiO_2-NPs is strictly related to the availability and characteristic of natural organic matters (NOM). NOM can act to maintain smaller particles sizes and more negative surface charges on the NPs (Zhang et al., 2009) reducing the rate of sedimentation of metal oxide NPs (Keller et al., 2010; Pettibone et al., 2008). As it has been experimentally proven, low NOM content and high ionic strength conditions of seawater promote high rate of sedimentation of metal oxide nanoparticles (Keller et al., 2010). In this way, NPs are less mobile and their interaction with filter feeders and sediment-dwelling organisms is favoured (Farré et al., 2009),

supporting our findings in stating that benthic molluscs are more exposed to TiO_2-NPs bioaccumulation.

First occurrence data related to single particle characterization and quantification of TiO_2-Ps-Tot in shellfish are reported in literature (Taboada-López et al., 2018; Xu et al., 2020), although the authors did not reduce the particle acquisition spectrum to the nano-fraction of 100 nm in diameter. Taboada-López et al. (2018) processed different shellfish species collected both fresh and frozen at supermarket, by applying an ultrasound assisted enzyme digestion and spICP-MS analysis. The levels range of dissolved Ti they found in fresh clam species (0.802-1.31 mg/kg w.w.) are comparable with our ones (1.31 ± 0.21 mg/kg w.w.), while they found a slightly lower number of particle concentration (4.16-7.56 x 10^7 Part/g vs 10.5 ± 1.52 x 10^7 Part/g). Furthermore, Taboada-López et al. (2018) by analyzing the variegated scallop found a significant higher concentration of TiO_2 particles and dissolved Ti in frozen samples than fresh ones, as if there were a contamination by food industry. Overall, the mean size of TiO_2-NPs diameter given for these shellfish is in the range of 60-84 nm versus a mean size of 89.8 ± 6 nm found in our packaged clams. Xu et al. (2018), also performed an enzyme digestion and spICP-MS analysis in shellfish collected from an offshore aquaculture farm. In clams they found comparable concentrations of dissolved Ti (1.11 ± 0.35 mg/kg w.w.) and mean size of TiO_2-NPs (70.9 ± 12.4 nm), but a lower concentration of TiO_2-NPs (2.10 ± 0.31 x 10^7 Part/g). Furthermore, they did not find any significant differences with the other shellfish species analysed.

We also provided a first esteem of TiO_2-NPs, TiO_2-Ps-Tot and dissolved Ti intake derived from a meal of the different packaged seafood, both for adult of 70 years and child of 6 years. It resulted obviously significantly higher in child than in adult, due to the low body weight of the considered age class.

Based on carcinogenicity study with TiO_2 (as E171) in mice and in

rats, the EFSA Panel on Food Additives and Nutrient Sources added to Food (ANS) chose the lowest no observed adverse effects levels (NOAEL), which was 2,250 mg TiO_2/kg bw/day (EFSA, 2016), but it may contain up to 3.2% of its weight in nanoparticles. For these reason E171 as a food additive would not be considered as a nanomaterial according to the EU Recommendation on the definition of a nanomaterial. In our samples we found a high occurrence of TiO_2 in its nanoparticle structure, with the lowest in canned anchovy (32%) and the highest in canned tuna (59%), thus we cannot refer to the established NOAEL for toxicological evaluation.

Most studies available are referred to the oral intake of total TiO2 and TiO_2-NPs for TiO_2 added during the production process in food, toothpaste and supplements (Bachler et al., 2015; Rompelberg et al., 2016; Weir et al., 2012). Bachler et al. (2015), by developing a physiologically based pharmacokinetic (PBPK) model, calculated the dietary intake of total titanium for the German population between 0.5 and 1.0 mg/kg b.w. for all age groups except the age group ''Other Children', who have the highest titanium intake of all age classes (approximately 2.0 mg/kg b.w.). Furthermore, by assuming that 10% of the total titanium intake is in the nano-range, which is a conservative estimation based on the ratio of ionic to particulate titanium intake (1:19) and the amount of TiO_2-NPs in E171 (approximately 11% by weight) (Weir et al., 2012), they calculated the 95th percentile of TiO2-NPs dietary intake below 170 ng/g for all age groups. As well, Rompelberg et al., (2016) estimated the long-term intake of TiO_2-NPs for the Dutch population ranged from 0.19 μg/kg bw/day for elderly, 0.55 μg/kg bw/day for 7–69-year-old people, to 2.16 μg/kg bw/day for young children. The results found in literature are significantly lower the potential exposure calculated in this study. Nevertheless, considering that presence of E171 as food additive in canned fish is not expected, our results give an esteem of dietary intake probably related to TiO_2-NPs bioaccumulation in fish and seafood species through environmental contamination.

Nonetheless, we cannot be sure regarding the potential total amount of TiO_2-NPs which can be accumulated in human tissue after an oral ingestion, considering that part of the compound can be altered in the gastrointestinal environment by extreme pH and co-ingested food (Walczak et al., 2015), although intestinal epithelial cells are affected at a functional level (Guo et al., 2017). Finally, a study limitation is the inability to discern the origin of TiO_2-NPs, if natural or anthropogenic. Taking into account the numerous applications of TiO_2-NPs, a proper improvement of wastewater depuration process could be a step to prevent the contamination of the water bodies.

1.4 Conclusion

This study provides for the first time an evaluation of the estimated daily intake of TiO_2-NPs starting from quantitative measured data. Our findings highlight how processed seafood where the pigment E171 is not intentionally added, could contain amount of TiO_2 in its particle and nanoparticles form, as well as dissolved titanium. In particular, our results reveal that the consumption of the selected types of foods could be an important route for the uptake of TiO_2, especially for a vulnerable group like children. Processed clam was the seafood with the higher content of TiO_2-NPs, while among pelagic fish species, we found progressively higher levels and smaller sizes from small to large fish. Nevertheless, seafood consumption represents only a small part of the human total diet, thus, to provide a realistic exposure assessment it is important recommend TiO_2-NPs characterization and quantification in a large number of food items, both processing and not, and where the pigment E171 is intentionally added and not, as it is not the only source of TiO_2-NPs. This information would be a solid step to be able to actually estimate the TiO_2-NPs dietary exposure of populations and related health risks. The new emerging technique of spICP-MS, being able to distinguish between the particulate and the dissolved fraction, is crucial to better understand the fate and transport characteristics of the particles and ionic forms and their possible

(independent or synergistic) environmental and (eco) toxicological impacts.

References

- Bachler, G., Goetz, N. von, Hungerbuhler, K., 2015. Using physiologically based pharmacokinetic (PBPK) modeling for dietary risk assessment of titanium dioxide (TiO_2) nanoparticles. Nanotoxicology 9, 373–380. https://doi.org/10.3109/17435390.2014.940404
- Borm, P.J.A., Robbins, D., Haubold, S., Kuhlbusch, T., Fissan, H., Donaldson, K., Schins, R., Stone, V., Kreyling, W., Lademann, J., Krutmann, J., Warheit, D., Oberdorster, E., 2006. The potential risks of nanomaterials: a review carried out for ECETOC. Part Fibre Toxicol 3, 11. https://doi.org/10.1186/1743-8977-3-11
- Bostan, H.B., Rezaee, R., Valokala, M.G., Tsarouhas, K., Golokhvast, K., Tsatsakis, A.M., Karimi, G., 2016. Cardiotoxicity of nano-particles. Life Sci 165, 91–99. https://doi.org/10.1016/j.lfs.2016.09.017
- Boverhof, D.R., David, R.M., 2010. Nanomaterial characterization: considerations and needs for hazard assessment and safety evaluation. Anal Bioanal Chem 396, 953–961. https://doi.org/10.1007/s00216-009-3103-3
- Cao, X., Han, Y., Gu, M., Du, H., Song, M., Zhu, X., Ma, G., Pan, C., Wang, W., Zhao, E., Goulette, T., Yuan, B., Zhang, G., Xiao, H., 2020. Foodborne Titanium Dioxide Nanoparticles Induce Stronger Adverse Effects in Obese Mice than Non-Obese Mice: Gut Microbiota Dysbiosis, Colonic Inflammation, and Proteome Alterations. Small e2001858. https://doi.org/10.1002/smll.202001858
- Carmo, T.L.L., Azevedo, V.C., Siqueira, P.R., Galvão, T.D., Santos, F.A., Martinez, C.B.R., Appoloni, C.R., Fernandes, M.N., 2018. Mitochondria-rich cells adjustments and ionic balance in the Neotropical fish Prochilodus lineatus exposed to titanium dioxide nanoparticles. Aquatic Toxicology 200, 168–177. https://doi.org/10.1016/j.aquatox.2018.05.006
- Chen, C., Marcus, I.M., Waller, T., Walker, S.L., 2018. Comparison of filtration mechanisms of food and industrial grade TiO_2 nanoparticles. Anal Bioanal Chem 410, 6133–6140. https://doi.org/10.1007/s00216-018-1132-5
- Chen, Z., Han, S., Zheng, P., Zhou, D., Zhou, S., Jia, G., 2020. Effect of oral exposure to titanium dioxide nanoparticles on lipid metabolism in Sprague-Dawley rats. Nanoscale 12, 5973–5986. https://doi.org/10.1039/c9nr10947a
- Chen, Z., Han, S., Zhou, D., Zhou, S., Jia, G., 2019a. Effects of oral exposure to titanium dioxide nanoparticles on gut microbiota and gut-associated metabolism in vivo. Nanoscale 11, 22398–22412. https://doi.org/10.1039/c9nr07580a
- Chen, Z., Zhou, D., Zhou, S., Jia, G., 2019b. Gender difference in hepatic toxicity of titanium dioxide nanoparticles after subchronic oral exposure in Sprague-Dawley rats. J Appl Toxicol 39, 807–819. https://doi.org/10.1002/jat.3769

- Copat, C., Arena, G., Fiore, M., Ledda, C., Fallico, R., Sciacca, S., Ferrante, M., 2013. Heavy metals concentrations in fish and shellfish from eastern Mediterranean Sea: Consumption advisories. Food and Chemical Toxicology 53, 33–37. https://doi.org/10.1016/j.fct.2012.11.038
- Domingo, J.L., Bocio, A., Falcó, G., Llobet, J.M., 2007. Benefits and risks of fish consumption: Part I. A quantitative analysis of the intake of omega-3 fatty acids and chemical contaminants. Toxicology 230, 219–226. https://doi.org/10.1016/j.tox.2006.11.054
- EFSA, 2016. Re-evaluation of titanium dioxide (E 171) as a food additive. EFSA Journal 14, e04545. https://doi.org/10.2903/j.efsa.2016.4545
- Farré, M., Gajda-Schrantz, K., Kantiani, L., Barceló, D., 2009. Ecotoxicity and analysis of nanomaterials in the aquatic environment. Anal Bioanal Chem 393, 81–95. https://doi.org/10.1007/s00216-008-2458-1
- Filippini, T., Tancredi, S., Malagoli, C., Malavolti, M., Bargellini, A., Vescovi, L., Nicolini, F., Vinceti, M., 2019. Dietary Estimated Intake of Trace Elements: Risk Assessment in an Italian Population. Expo Health. https://doi.org/10.1007/s12403-019-00324-w
- Gray, E.P., Coleman, J.G., Bednar, A.J., Kennedy, A.J., Ranville, J.F., Higgins, C.P., 2013. Extraction and Analysis of Silver and Gold Nanoparticles from Biological Tissues Using Single Particle Inductively Coupled Plasma Mass Spectrometry. Environ. Sci. Technol. 47, 14315–14323. https://doi.org/10.1021/es403558c
- Guo, Z., Martucci, N.J., Moreno-Olivas, F., Tako, E., Mahler, G.J., 2017. Titanium Dioxide Nanoparticle Ingestion Alters Nutrient Absorption in an In Vitro Model of the Small Intestine. NanoImpact 5, 70–82. https://doi.org/10.1016/j.impact.2017.01.002
- Gupta, G.S., Kumar, A., Shanker, R., Dhawan, A., 2016. Assessment of agglomeration, co-sedimentation and trophic transfer of titanium dioxide nanoparticles in a laboratory-scale predator-prey model system. Sci Rep 6. https://doi.org/10.1038/srep31422
- Heringa, M.B., Geraets, L., van Eijkeren, J.C.H., Vandebriel, R.J., de Jong, W.H., Oomen, A.G., 2016. Risk assessment of titanium dioxide nanoparticles via oral exposure, including toxicokinetic considerations. Nanotoxicology 10, 1515–1525. https://doi.org/10.1080/17435390.2016.1238113
- Jovanović, B., 2015. Critical review of public health regulations of titanium dioxide, a human food additive: Titanium Dioxide in Human Food. Integrated Environmental Assessment and Management 11, 10–20. https://doi.org/10.1002/ieam.1571
- Keller, A.A., Wang, H., Zhou, D., Lenihan, H.S., Cherr, G., Cardinale, B.J., Miller, R., Ji, Z., 2010. Stability and Aggregation of Metal Oxide Nanoparticles in Natural Aqueous Matrices. Environ. Sci. Technol. 44, 1962–1967. https://doi.org/10.1021/es902987d

- Klaine, S.J., Alvarez, P.J.J., Batley, G.E., Fernandes, T.F., Handy, R.D., Lyon, D.Y., Mahendra, S., McLaughlin, M.J., Lead, J.R., 2008. Nanomaterials in the environment: behavior, fate, bioavailability, and effects. Environ. Toxicol. Chem. 27, 1825–1851. https://doi.org/10.1897/08-090.1
- Lee, S., Bi, X., Reed, R.B., Ranville, J.F., Herckes, P., Westerhoff, P., 2014. Nanoparticle Size Detection Limits by Single Particle ICP-MS for 40 Elements. Environ. Sci. Technol. 48, 10291–10300. https://doi.org/10.1021/es502422v
- Lespes, G., Faucher, S., Slaveykova, V.I., 2020. Natural Nanoparticles, Anthropogenic Nanoparticles, Where Is the Frontier? Front. Environ. Sci. 8. https://doi.org/10.3389/fenvs.2020.00071
- Pettibone, J.M., Cwiertny, D.M., Scherer, M., Grassian, V.H., 2008. Adsorption of Organic Acids on TiO_2 Nanoparticles: Effects of pH, Nanoparticle Size, and Nanoparticle Aggregation. Langmuir 24, 6659–6667. https://doi.org/10.1021/la7039916
- Piccinno, F., Gottschalk, F., Seeger, S., Nowack, B., 2012. Industrial production quantities and uses of ten engineered nanomaterials in Europe and the world. J Nanopart Res 14, 1109. https://doi.org/10.1007/s11051-012-1109-9
- Rompelberg, C., Heringa, M.B., van Donkersgoed, G., Drijvers, J., Roos, A., Westenbrink, S., Peters, R., van Bemmel, G., Brand, W., Oomen, A.G., 2016. Oral intake of added titanium dioxide and its nanofraction from food products, food supplements and toothpaste by the Dutch population. Nanotoxicology 10, 1404–1414. https://doi.org/10.1080/17435390.2016.1222457
- Ruszkiewicz, J.A., Pinkas, A., Ferrer, B., Peres, T.V., Tsatsakis, A., Aschner, M., 2017. Neurotoxic effect of active ingredients in sunscreen products, a contemporary review. Toxicol Rep 4, 245–259. https://doi.org/10.1016/j.toxrep.2017.05.006
- Schneider, S.L., Lim, H.W., 2019. A review of inorganic UV filters zinc oxide and titanium dioxide. Photodermatology, Photoimmunology & Photomedicine 35, 442–446. https://doi.org/10.1111/phpp.12439
- Schneider, T., Westermann, M., Glei, M., 2017. In vitro uptake and toxicity studies of metal nanoparticles and metal oxide nanoparticles in human HT29 cells. Arch. Toxicol. 91, 3517–3527. https://doi.org/10.1007/s00204-017-1976-z
- Silano, V., Baviera, J.M.B., Bolognesi, C., Tlustos, C., Loveren, H.V., Vernis, L., Zorn, H., Castle, L., Cravedi, J.-P., Kolf-Clauw, M., Milana, M.R., Pfaff, K., Poças, M. de F.T., Svensson, K., Wölfle, D., Barthélémy, E., Rivière, G., 2019. Safety assessment of the substance, titanium dioxide surface treated with fluoride-modified alumina, for use in food contact materials. EFSA Journal 17, e05737. https://doi.org/10.2903/j.efsa.2019.5737

- Taboada-López, M.V., Herbello-Hermelo, P., Domínguez-González, R., Bermejo-Barrera, P., Moreda-Piñeiro, A., 2019. Enzymatic hydrolysis as a sample pre-treatment for titanium dioxide nanoparticles assessment in surimi (crab sticks) by single particle ICP-MS. Talanta 195, 23–32. https://doi.org/10.1016/j.talanta.2018.11.023
- Taboada-López, M.V., Iglesias-López, S., Herbello-Hermelo, P., Bermejo-Barrera, P., Moreda-Piñeiro, A., 2018. Ultrasound assisted enzymatic hydrolysis for isolating titanium dioxide nanoparticles from bivalve mollusk before sp-ICP-MS. Anal. Chim. Acta 1018, 16–25. https://doi.org/10.1016/j.aca.2018.02.075
- US-EPA, 2000. Guidance for Assessing Chemical Contamination Data for Use in Fish Advisories, vol. II. Risk Assessment and Fish Consumption Limits EPA/823-B94- 004.
- Walczak, A.P., Kramer, E., Hendriksen, P.J.M., Helsdingen, R., van der Zande, M., Rietjens, I.M.C.M., Bouwmeester, H., 2015. In vitro gastrointestinal digestion increases the translocation of polystyrene nanoparticles in an in vitro intestinal co-culture model. Nanotoxicology 9, 886–894. https://doi.org/10.3109/17435390.2014.988664
- Weir, A., Westerhoff, P., Fabricius, L., von Goetz, N., 2012. Titanium Dioxide Nanoparticles in Food and Personal Care Products. Environ Sci Technol 46, 2242–2250. https://doi.org/10.1021/es204168d
- Westerhoff, P., Song, G., Hristovski, K., Kiser, M.A., 2011. Occurrence and removal of titanium at full scale wastewater treatment plants: implications for TiO_2 nanomaterials. J Environ Monit 13, 1195–1203. https://doi.org/10.1039/c1em10017c
- Wu, S., Zhang, S., Gong, Y., Shi, L., Zhou, B., 2020. Identification and quantification of titanium nanoparticles in surface water: A case study in Lake Taihu, China. Journal of Hazardous Materials 382, 121045. https://doi.org/10.1016/j.jhazmat.2019.121045
- Xu, L., Wang, Z., Zhao, J., Lin, M., Xing, B., 2020. Accumulation of metal-based nanoparticles in marine bivalve mollusks from offshore aquaculture as detected by single particle ICP-MS. Environmental Pollution 260, 114043. https://doi.org/10.1016/j.envpol.2020.114043
- Yin, C., Zhao, W., Liu, Rui, Liu, Rong, Wang, Z., Zhu, L., Chen, W., Liu, S., 2017. TiO_2 particles in seafood and surimi products: Attention should be paid to their exposure and uptake through foods. Chemosphere 188, 541–547. https://doi.org/10.1016/j.chemosphere.2017.08.168
- Zhang, Y., Chen, Y., Westerhoff, P., Crittenden, J., 2009. Impact of natural organic matter and divalent cations on the stability of aqueous nanoparticles. Water Research 43, 4249–4257. https://doi.org/10.1016/j.watres.2009.06.005
- Zhou, Q., Liu, L., Liu, N., He, B., Hu, L., Wang, L., 2020. Determination and characterization of metal nanoparticles in clams and oysters. Ecotoxicology

and Environmental Safety 198, 110670. https://doi.org/10.1016/j.ecoenv.2020.110670

- Ziental, D., Czarczynska-Goslinska, B., Mlynarczyk, D.T., Glowacka-Sobotta, A., Stanisz, B., Goslinski, T., Sobotta, L., 2020. Titanium Dioxide Nanoparticles: Prospects and Applications in Medicine. Nanomaterials (Basel) 10. https://doi.org/10.3390/nano10020387

10.2 CHAPTER 2: Chemical characterization and quantification of silver nanoparticles (Ag-NPs) and dissolved Ag in seafood by single particle ICP-MS: assessment of dietary exposure.

Alfina Grasso[1], Margherita Ferrante[1], Giovanni Arena[2], Rossella Salemi[3], Pietro Zuccarello[1], Maria Fiore[1] and Chiara Copat[1]

[1] Department of Medical, Surgical and Advanced Technologies "G.F. Ingrassia", University of Catania, Catania, Italy.

[2] Freelance chemist.

[3] Department of Biomedical and Biotechnological Sciences, University of Catania, Catania, Italy.

Published in: International Journal of Environmental Research and Public Health, 2021, 18, 4076. https://doi.org/10.3390/ijerph18084076

Abstract

This study provides a first insight on the chemical characterization and quantification of silver nanoparticles (AgNPs) and dissolved Ag in processed canned seafood products, where food-grade E174 is not intentionally added nor is the nanoparticle contained in the food contact material. The aim was to evaluate the bioaccumulation potential of AgNPs and to contribute to the assessment of AgNPs and ionic Ag human dietary intake from processed seafood. It is known how seafood, and in particular pelagic fish, is a precious nutritional source of unsaturated fatty acids, protein, and different micronutrients. Nevertheless, it may cause possible health problems due to the intake of toxic compounds coming from environmental pollution. Among emerging contaminants, AgNPs are widely applied in several fields such as biomedicine, pharmaceutical, food industry, health care, drug-gene delivery, environmental study, water treatments, and many others, although its primary application is in accordance with its antimicrobial property. As a consequence, AgNPs are discharged into the aquatic environment, where the colloidal stability of these NPs is altered by chemical and physical environmental parameters. Its toxicity was demonstrated in in-vitro and in-vivo studies, although some findings are controversial because toxicity depends by several factors such as size, concentration, chemical composition, surface charge, Ag+ ions released, and hydrophobicity. The new emerging technique called single-particle inductively coupled plasma mass spectrometry (spICP-MS) was applied, which allows the determination of nanoparticle number-based concentration and size distribution, as well as the dissolved element. Our findings highlighted comparable mean sizes across all species analysed, although AgNPs concentrations partly follow a trophic level-dependent trend. The low mean size detected could be of human health concern, since, smaller is the diameter higher is the toxicity. Dietary intake from a meal calculated for adults and children seems to be very low.

Although seafood consumption represents only a small part of the human total diet, our findings represent a first important step to understand the AgNPs dietary exposure of the human population. Further studies are needed to characterize and quantify AgNPs in a large number of food items, both processing and not, and where AgNPs are added at the industrial level. They will provide a realistic exposure assessment, useful to understand if AgNPs toxicity levels observed in literature are close to those estimable through food consumption and implement data useful for risk assessors in developing AgNPs provisional tolerable daily intake.

Keywords: Ag; Nanoparticle; spICP-MS; Processed Food; Seafood; Dietary Intake

2.1. Introduction

The last decade is characterized by a growing concern in the research field of nanoparticles (NPs) for their several applications, because of their new and better properties dependent on size, surface area, distribution and morphology.

In particular, silver nanoparticles (AgNPs) are widely applied for more than 244 consumer products (Zhang et al., 2019) in several fields such as biomedicine, pharmaceutical, food industry, health care, drug-gene delivery, environmental study, water treatments, and many others, although its primary application is in accordance with its antimicrobial propriety (Fontecha-Umaña et al., 2020; Jha et al., 2017; Li et al., 2018; Shimabuku et al., 2017; Valsalam et al., 2019; Vines et al., 2018).

In the food industry, AgNPs have a wide spectrum of action in favor of the greatest safety and longest shelf life of food (Simbine et al., 2019). Ag is authorized as a food additive in its elemental form (E174) to be used to color the external coating of confectionery, for decoration of chocolates and in liqueurs according to the Regulation (EC) No. 1129/2011 and specification to the Regulation (EC) No. 231/2012. Nevertheless, according to the EFSA Panel on Food Additives and Nutrient Sources added to Food (EFSA, 2016), several pieces of information need to be addressed to deep scientific knowledge on E174 particle size distribution, the release of Ag ions from elemental silver, and data on toxicity studies on elemental silver. Furthermore, AgNPs is widely used in food-contact plastics in order to provide an antimicrobial activity to the food product as well improve its properties (Han et al., 2011), being the efficiency of AgNPs much stronger compared to the bulk Ag such as Ag-binding zeolites, based on the surface area to volume ratio (Rai et al., 2009). Currently, AgNPs are not included among the authorized substances given in Commission Regulation (EU) No. 10/2011. Accordingly, a maximum level of 0.01 mg/kg in food should be established for the migration of a non-authorized substance through a functional

barrier.

As a consequence of their numerous uses, AgNPs are discharged into the aquatic environment, where the colloidal stability of this NP is altered by chemical and physical environmental parameters (Gunsolus et al., 2015), thus influencing AgNPs dissolution to give Ag+ when the temperature increase or the pH decrease (Liu and Hurt, 2010), or depending by the available natural organic matter (NOM) (Huang et al., 2018). The dispersion of AgNPs into the natural environment could lead to the bioaccumulation process and determine trophic transfer to food webs, thus implying also risks for human health (Zhang et al., 2019).

Nevertheless, in addition to the engineered metal nanoparticles (ENPs), AgNPs exists also as naturally occurring. Since natural waters contain Ag(I) ions, in the presence of natural organic matter such as humic acids (Akaighe et al., 2011), AgNPs are formed under thermal, non-thermal, and photochemical conditions (Sharma et al., 2015). Furthermore, they can be released by erosion, geological weathering, and other phenomena such as fires (Ghosn et al., 2020).

Consequently, humans could be exposed to NPs every day through food, water, air, and dermal contact. From the literature is known that silver in the human body does not play any biological role and the majority is removed, while 1-2% is accumulated in the organism (Kowalska et al., 2020).

The toxicity of AgNPs has been studied in the laboratory with concentrations typically higher (10 mg/L) than those found in the natural environment and concerning also several form and size (Zhang et al., 2019). The AgNPs act decreasing the antioxidant enzymes, imbalance the oxidative status, altering the mitochondrial membrane potential, inducing cell death, DNA damage, and cytokines secretion (AshaRani et al., 2009; Das et al., 2017; De Matteis et al., 2018; Song et al., 2012). On the other hand, it is poorly understood if the toxicity of AgNPs can be attributable to its particulate form combined with the ionic silver released, since NPs facilitates more rapid dissolution of ions than the equivalent bulk

material (Reidy et al., 2013). Accordingly, results from the literature are controversial, suggesting that both ionic and particulate Ag should be taken into consideration in the toxicological evaluation of AgNPs (Qin et al., 2017).
With this study, we wanted to provide a chemical characterization and quantification of AgNPs and dissolved Ag, in processed canned seafood products belonging to different trophic positions with the emerging technique of Single Particle - Inductively Coupled Plasma (spICP-MS), which allows the determination of particle number-based concentration, with rapid simultaneous characterization of its elemental composition, number of particles, size and size distribution, in addition to the dissolved concentration. Our choice to carry out this study using canned seafood was because it is a product that makes up a significant contribution to the diet (unsaturated fatty acids, protein, and different micronutrients), nevertheless, it may cause possible health problems due to the intake of toxic compounds. Furthermore, we also provided data related to the estimated daily intake for both adults and children, which may be useful to risk assessors, to develop a provisional tolerable daily intake for AgNPs.

2.2. Materials and method

2.2.1. Sample collection, handling and preparation

The research material consisted of canned seafood products belonging to three different fish species and one mollusc species, purchased in the period between June and July 2019, from Italian supermarkets chains in the city of Catania (Italy). Different brands for canned tuna (5), mackerel (4), anchovy (3), and clam (3) were chosen among the more popular ones and three different batches have been selected for each brand. The extraction and analysis procedure on each sample was carried on in triplicate, obtaining 45 extractions for canned tuna, 36 for canned mackerel, 27 for canned

anchovy, and 27 for canned clam. The content of every can was homogenized and next the samples were frozen at – 80°C until analysis.

2.2.2. Alkaline digestion and spICP-MS analysis of silver nanoparticles (AgNPs) and dissolved silver (Ag)

The method described by Gray et al. (2013), was used to allow an alkaline digestion of the samples. Briefly, 0.25 gr of the wet sample was weighed directly in graduated polypropylene tubes (DigiTUBEs, SCP Science, Canada) using an analytical balance, and mixed with 5 mL of tetramethylammonium hydroxide (TMAH, 20% v/v). Firstly, a vortex was used to facilitate the separation of tissues from the walls of containers used for digestion.
The extraction was obtained through sonication for 30 minutes at 37°C by an ultrasonic bath, which allows the destruction of tissues and to release of nanoparticles without altering them. Next, the samples were left to digest another 24 hours at room temperature. Finally, the digested solutions were diluted to 50 mL using high purity water 0.22μm filtered (Millipore, Bedford, MA, USA) to 1% TMAH concentration and 0,1% Triton X-100, useful to prevent particle aggregation.
AgNPs and dissolved silver were analyzed with the Syngistix Nano application software supported by the ICP-MS (NexION® 350D, Perkin Elmer), which is gaining increasing popularity for the characterization of particles concentration and size distribution at a short dwell time, in addition to the dissolved concentration. The instrumental condition for the determination AgNPs and dissolved Ag are reported in Table 2.1.

Table 2.1. NexION® 350D ICP-MS instrumental condition for single particles analysis.

Parameter	Value
Nebulizer, Flow	Meinhard, 1 mL/min
Spray chamber	Glass cyclonic
Sample uptake rate	0.26–0.28 mL/min
RF power	1600 W
Analysis mode	Standard
Quadrupole settling time	0 µs
Analyte	Ag 107
Dwell time	50 µs
Data acquisition time	60 sec
Density	10.49 g/cm^3
Ag mass fraction	100%

All digested samples and calibration solutions were sonicated for 30 minutes before analysis to maximize a homogeneous dispersion. Calibration standards for analysis of dissolved Ag were prepared from a single standard solution (1000 mg/L, CPAchem).

The transport efficiency was determined using a certified reference material (AgNPs 39±5 nm, 6.1 x 10^{10} particles/mL, monitoring m/z 10^7), obtaining values in the range 1.8-4.6%; while for the preparation of calibration standards was used AgNPs of 80 nm (AgNPs 80 ± 9 nm, 7.4 x 10^9 particles/mL). Both AgNPs reference materials (PELCO® 40 nm and 80 nm, Citrate, NanoXactTM, Ted Pella Inc.) used were purchased from Nanovision (Brugherio, MB, Italy).

Firstly, it was evaluated an analytical recovery by spiking 40 nm Ag standard to ultrapure water, at a concentration of 20 µg/L or 5.7 x 10^7 particles/mL, and obtaining a median diameter around 41.8 ± 3.5 nm and a recovery of 94.1 % (5.4 x 10^7 ± 3.1 x 10^6 particles/mL), following the manufacturer's declaration.

Furthermore, it was studied the effect of the extracting solution on the particle's concentration and size distribution, spiking the AgNPs standard in both ultrapure water (n1=7) and TMAH 1% (n2=7), at the same concentration of 150 ng/L or 4.5 particles/mL x 105.

The results obtained were very similar and statistically homogeneous if applied a two tailed t-test (p=95%; $\nu = n1 + n2 - 2 = 14$), and showing no effect from the extraction solution on the

nanoparticles concentration or on size distribution (mean size: tcalculated = 0.69 < ttabulated = 2.14 ; particles/mL: tcalculated = 1.67 < ttabulated = 2.14): 4.2 x 10^5 ± 4.9 x 10^4 particles/mL and 42.1± 3.3 nm of mean size in water and 3.8 x 10^5 ± 3.6 x 10^4 particles/mL and 43.1 ± 1.90 nm of mean size in TMAH 1%, with a recovery of 97.0 % and 88.4 % respectively.

The limit of detection (LOD) and the limit of quantification (LOQ) were calculated by analyzing ten alkaline extract blanks, in the same analytical condition of the samples, and based respectively on the mean ± 3 SD and the mean ± 10 SD criterion of the number of particles/mL obtained. LOD was 1.5x10^3 particles/mL, while LOQ was 3.0x10^3 particles/mL. Referring to the sample weight and digestion volume used, they resulted in 3.3 x 10^5 particles/g and 5.9 x 10^5 particles/g, respectively.

Besides, LOD in size (LOD nm) was estimated at 20 nm applying the following equation (1) (Lee et al., 2014; Taboada-López et al., 2018).

$$\mathrm{LODnm} = \sqrt[3]{\frac{6 \times 3\sigma_{blank}}{R \times f_a \times \rho \times \pi}} \quad (1)$$

Where: 3σ_blank is three times the standard deviation of counts/dwell time of alkaline blanks (1% TMAH); R is the slope of the calibration curve of ionic Ag solutions; fa is the mass fraction of analyzed metallic element in the AgNPs; ρ is the density of the AgNPs.

Accuracy has been assessed spiking silver NPs 40 nm, at a concentration of 20 μg/L or 5.7 x 10^7 particles/mL, in seafood samples (Laboratory Fortified Matrix), one for each batch of analysis, obtaining a mean particles recovery of 88.5 % ± 4.2%.

As can be inferred from the results obtained, the recovery of AgNPs particles in extracting solution is significantly lower than those in ultrapure water, probably depending by an agglomeration phenomenon.

For this reason, we performed also the evaluation of total silver, after acid digestion, intending to confirm the characterization of AgNPs using spICP-MS analysis.

2.2.3. Acid digestion and ICP-MS analysis of total silver (Ag)

To confirm the efficiency of alkaline digestion on the extraction of AgNPs, an assisted microwave acid digestion was performed for the evaluation of total silver.
About 0.5 gr of the wet sample were weighed directly in Teflon vessels and then 6 mL of 67% super pure nitric acid (HNO3, Carlo Erba, Italy) and 2 mL of 30% hydrogen peroxide (H2O2, Carlo Erba, Italy) were added to each sample. A blank sample containing only the reagents was prepared for every mineralization batch.
The microwave mineralization was performed stepwise up to 200 °C in 10 min (1000 W), followed by a 15 min rest at 200°C (1000 W).
After, the cooled samples digested were transferred into graduated polypropylene tubes and diluted to 50 mL using high purity deionized water. Before analysis, all samples were filtrated through 0.45 μm nylon filters, pre-washed with 5 ml 10% v/v HNO3, and rinsed with 5 ml ultrapure water.
For the determination of total silver an inductively coupled plasma mass spectrometer was used (ICP-MS NexION® 350D, Perkin Elmer, USA), and the instrumental conditions are reported in Table 2.2.

Table 2.2. NexION® 350D ICP-MS instrumental condition for Total Ag in standard mode.

Parameter	Value
Nebulizer, Flow	Meinhard, 0.89 mL/min
Spray chamber	Glass cyclonic
RF power	1600 W
Analogic phase voltage	−1950 V
Pulses voltage	1300 V
Discriminator threshold	12
Deflector voltage	−12 V
Analysis mode	Standard
Analyte	Ag 107
Internal standard	Y

ICP-MS quantification of total Ag was carried out, in the standard mode, using the standard addition technique, covering a concentration range from 1 to 10 μg/L, using the same single standard solution (1000 mg/L, CPAchem). Yttrium (Y89) was selected as the internal standard. The analytical process was controlled using the measurement of Laboratory Fortified Matrix (LFM) with a seafood sample (spike of ionic silver at 20 μg/L) processed at each batch of digestion. The recoveries calculated are all in the range 94-117%.
The LOD and LOQ were calculated by analyzing ten acid extract blanks based on the mean ± 3 SD/mean ± 10 SD criterion. They resulted in 0.012 and 0.025 mg/kg, respectively.

2.2.4. Dietary exposure

The Estimated Meal Intake (EMI) (μg/Kg b.w. per day) derived from the consumption of selected seafood products was conducted for AgNPs and dissolved Ag according to the following equation (Grasso et al., 2020):
EMI = (C × M) / BW (2)
Where C is the AgNPs or dissolved Ag (mg/Kg w.w.); M is the meal size (227g for adults and 114g for child); BW is the body weight, considered as 16 Kg for child (6 years) and 70 Kg for adult (70 years) (Pappalardo et al., 2020; US-EPA, 2000).
To evaluate if the intake of dissolved Ag derived from seafood consumption could represent a risk for a human to develop chronic systemic effects, we estimated the Target Hazard Quotient (THQ). When THQ reports a value below 1 means that the level of exposure is smaller than the oral reference dose (RfD), otherwise a daily exposure at this level is not likely to cause any deleterious effects during their exposure duration for the human population. THQ is calculated according to the following equation (Pappalardo et al., 2017):

$$THQ = (EF \times ED \times IR \times C)/(RfD \times BW \times AT) \quad (3)$$

where EF is the exposure frequency or the number of exposure events per year of exposure (350 days/year); ED is the exposure duration (adults 26 years; children 6 years); IR is the average consumption of seafood for the Italian population (applied as 12.16 g/capita/day for pelagic fish CT, CM, and CA; 12.34 for molluscs CC); C is the metal concentration in the food (mg/Kg w.w.); RfD is the oral reference dose (0.005 mg/Kg day)(US EPA, 2013); BW is the body weight (the same used for EDI); and AT is the averaging time (equal to EF × ED).

2.2.5. Determination of packaging composition

To verify the percent presence of Ag in packaging composition, fragments of them were analyzed by scanning electron microscopy coupled with microanalysis using a "Cambridge Instruments Mod. Stereoscan 360" combined with an X Energy Dispersion Detector (SEM-EDX) "Diffractometer Rigaku Miniflex" having the Inca software. For each brand and for each species of canned product, four representative points were scanned for a qualitative analysis, taking into account the internal intact layer, two breaking points, and the external intact layer**.**

2.2.6. Statistical analysis

The statistical software package IBM SPSS 20.0 was used for statistical analysis. Differences in AgNPs and dissolved Ag levels among selected seafood products were studied, and One-Way Analysis of Variance ANOVA coupled with a post hoc Tukey test were applied.

2.3. Results

The AgNPs, as well as the level of Ag in its dissolved form, were analysed with the Syngistix Nano Application software supported by the ICP-MS NexION® 350D (Perkin Elmer, USA), by processing the samples with the ultrasound-assisted alkaline digestion. The total Ag was measured with ICP-MS measurements after acid digestion of the samples and, as shown in Table 2.3, there are no significant differences between dissolved fraction and total Ag, highlighting the efficiency of a properly NPs extraction during the first experimental procedure. As shown in Table 2.3 and Figure 2.1, selected seafood products did not show differences regarding the most frequent size and mean diameter. Only two samples of canned mackerel have the most frequent size below LOD (20 nm). The highest most frequent size was measured for another sample of canned mackerel (39 nm) and, the mean of most frequent size is in the range of 26-28 nm for all the seafood products analysed. Regarding the mean diameter, it was measured a size range of 31-36 nm among selected seafood products, with values progressively higher according to the following order: canned anchovy < canned clam < canned mackerel < canned tuna.

As regards the AgNPs level, in term of number of AgNPs/g and AgNPs mg/Kg, the samples of canned tuna and canned mackerel had the higher levels than canned anchovy and canned clam, with a mean value of 2.28E+07 and 1.86E+07 number of AgNPs/g respectively, which correspond to a concentration of 0.0014 and 0.0012 mg/kg respectively. In canned clam and canned anchovy, these concentrations were in the range of 0.44E+07 – 0.91E+07 number of AgNPs/g, which correspond to a concentration of 0.0004 and 0.0005 mg/kg. Although all the reported values seem to be very low, none of the measured samples had a concentration lower than LOD (3.3E+05 number of AgNPs/g; 3.4E-05 mg/Kg). Dissolved Ag was found with concentration progressively higher with the following order: canned clam < canned mackerel < canned anchovy < canned tuna. Canned tuna and canned anchovy did not report

significant differences in concentration, with values of 0.0346 and 0.0455 mg/Kg respectively. Nevertheless, values measured in canned tuna are significantly higher than canned mackerel (0.0245 mg/Kg) and canned clam (0.0148 mg/Kg), whereas concentrations measured in canned anchovy were significantly higher only versus canned calm. For few values were measures concentrations below LOD (0.012 mg/Kg). These were reported for 4 samples of canned mackerel, 2 samples of canned clam, and 1 sample of canned anchovy.

Table 2.3. Descriptive statistics concerning the chemical characterization and quantification of AgNPs and dissolved Ag (mg/Kg) in packaged seafood products.

Canned Tuna	Most Frequent Size AgNPs (nm)	Mean Diameter AgNPs (nm)	Number of AgNPs/g	AgNPs mg/Kg	Dissolved Ag [a] mg/kg	Total Ag [b] mg/kg
Mean	27.7	35.8	2.28×10^7	0.0014	0.0455	0.0594
S.D.	4.76	5.13	0.88×10^7	0.0008	0.0119	0.0409
Min.	<20	26.0	0.46×10^7	0.0005	0.0251	0.0521
Max.	35.0	45.1	3.13×10^7	0.0028	0.0652	0.0781
Canned Mackerel	**Most Frequent Size AgNPs (nm)**	**Mean Diameter AgNPs (nm)**	**Number of AgNPs/g**	**AgNPs mg/Kg**	**Dissolved Ag [a] mg/kg**	**Total Ag [b] mg/kg**
Mean	26.2	34.1	1.86×10^7	0.0012	0.0245	0.0374
S.D.	5.13	3.65	0.69×10^7	0.0007	0.0219	0.0316
Min.	<20	31.2	1.18×10^7	0.0005	<0.012	<0.012
Max.	39.3	42.3	3.04×10^7	0.003	0.0850	0.0990
Canned Anchovy	**Most Frequent Size AgNPs (nm)**	**Mean Diameter AgNPs (nm)**	**Number of AgNPs/g**	**AgNPs mg/Kg**	**Dissolved Ag[a] mg/kg**	**Total Ag [b] mg/kg**
Mean	26.4	31.1	0.91×10^7	0.0005	0.0346	0.0480
S.D.	3.81	4.37	0.31×10^7	0.0008	0.0129	0.0228
Min.	21.2	27.4	0.49×10^7	0.0001	<0.012	<0.012
Max.	35.4	41.5	1.40×10^7	0.0028	0.0550	0.0810
Canned Clam	**Most Frequent Size AgNPs (nm)**	**Mean Diameter AgNPs (nm)**	**Number of AgNPs/g**	**AgNPs mg/Kg**	**Dissolved Ag[a] mg/kg**	**Total Ag [b] mg/kg**
Mean	26.6	32.9	0.44×10^7	0.0004	0.0148	0.0206
S.D.	2.72	1.76	0.17×10^7	0.0001	0.0024	0.0133
Min.	23.2	31.2	0.14×10^7	0.0002	<0.012	<0.012
Max.	31.4	36.3	0.64×10^7	0.0006	0.0190	0.0321

a Ultrasound-assisted alkaline digestion and spICP-MS determination.
b Microwave-assisted acid digestion and ICP-MS determination in standard mode.

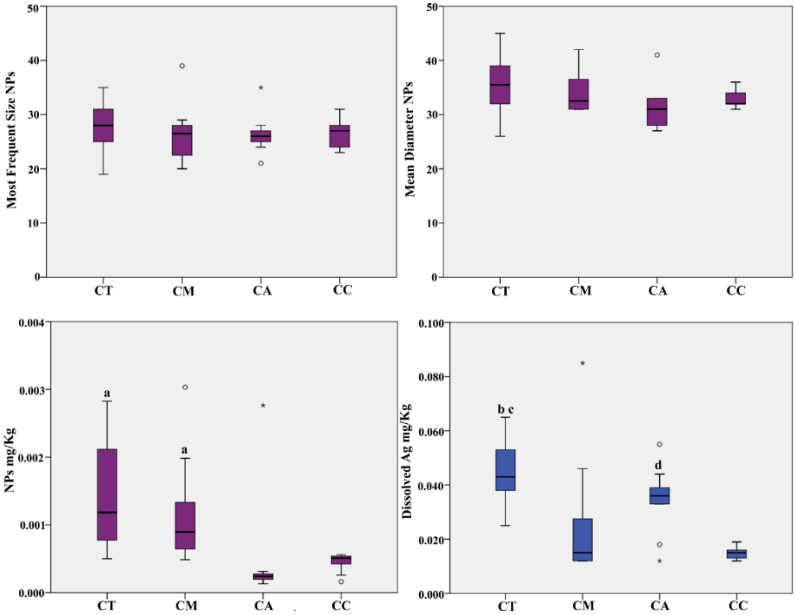

Figure 2.1. Box Plot distribution of AgNPs most frequent size (nm), mean diameter (nm), level of NPs, and dissolved Ag (mg/Kg) in packaged seafood products. Legend: CT, Canned Tuna; CM, Canned Mackerel; CA, Canned Anchovy; CC, Canned Clam; a, $p<0.05$ vs CA and CC; b, $p<0.01$ vs CM; c, $p<0.001$ vs CC; d, $p<0.05$ vs CC. ° Outliers values of the distribution. * Extreme values of the distribution.

In Table 2.4 and Figure 2.2 are shown results regarding the Estimated Meal Intake (EMI) of AgNPs and dissolved Ag, calculated both for adult (70 years old) and child (6 years old), deriving from consumption of the selected seafood products. Since exposure dose reflects both concentrations measured in seafood products, body weight, and meal ingestion rate, EMI is significantly higher in the child than in adults, both for AgNPs and dissolved Ag.

As regard AgNPs, in both age classes, EMI is significantly higher if consuming canned tuna and canned mackerel than canned anchovy and canned clam. We obtained EDI mean values of 0.0047 and 0.0102 μg/Kg b.w. deriving from a meal of canned tuna, respectively for

adult and child, and EDI mean values of 0.0037 and 0.0082 μg/Kg b.w., deriving from a meal of canned mackerel, respectively for adult and child.

Concerning dissolved Ag, EMI is significantly higher if consuming canned tuna and canned anchovy than canned mackerel and canned clam. We obtained EMI mean values of 0.1474 and 0.3238 μg/Kg b.w. deriving from a meal of canned tuna, respectively for adult and child, and EMI mean values of 0.1108 and 0.2435 μg/Kg b.w. deriving from a meal of canned anchovy, respectively for adult and child. These values are below the oral daily reference dose set for inorganic Ag (5 μg/Kg b.w.) and, THQ results below 1 for both adults and children, if an exposure scenario of 6 and 26 years of duration is chosen for the two age groups respectively.

Table 2.4. Descriptive statistics of Estimated Meal Intake (EMI μg/Kg b.w.) calculated for adult (70 years) and child (6 years) concerning the AgNPs and dissolved Ag and, THQ calculation concerning dissolved Ag for adult (70 years) and child (6 years).

Canned Tuna	EMI Adult AgNPs	EMI Child AgNPs	EMI Adult Dissolved Ag	THQ Adult Dissolved Ag	EMI Child Dissolved Ag	THQ Child Dissolved Ag
Mean	0.0047	0.0102	0.1474	1.58×10^{-3}	0.3238	6.92×10^{-3}
S.D.	0.0026	0.0056	0.0391	/	0.0861	/
Min.	0.0021	0.0040	0.0802	/	0.1752	/
Max.	0.0092	0.0202	0.2113	/	0.4641	/
Canned Mackerel	**EMI Adult AgNPs**	**EMI Child AgNPs**	**EMI Adult Dissolved Ag**	**THQ Adult Dissolved Ag**	**EMI Child Dissolved Ag**	**THQ Child Dissolved Ag**
Mean	0.0037	0.0082	0.0781	8.51×10^{-4}	0.1713	3.72×10^{-3}
S.D.	0.0023	0.0054	0.0717	/	0.1574	/
Min.	0.0022	0.0030	<0.038	/	<0.085	/
Max.	0.0100	0.0221	0.2752	/	0.6034	/
Canned Anchovy	**EMI Adult AgNPs**	**EMI Child AgNPs**	**EMI Adult Dissolved Ag**	**THQ Adult Dissolved Ag**	**EMI Child Dissolved Ag**	**THQ Child Dissolved Ag**
Mean	0.0016	0.0036	0.1108	1.20×10^{-3}	0.2435	5.26×10^{-3}
S.D.	0.0028	0.0061	0.0431	/	0.0946	/
Min.	0.0004	0.0009	<0.038	/	<0.085	/
Max.	0.0092	0.0197	0.1769	/	0.3887	/
Canned Clam	**EMI Adult AgNPs**	**EMI Child AgNPs**	**EMI Adult Dissolved Ag**	**THQ Adult Dissolved Ag**	**EMI Child Dissolved Ag**	**THQ Child Dissolved Ag**
Mean	0.0017	0.0033	0.0467	5.22×10^{-4}	0.1024	2.28×10^{-3}
S.D.	0.0005	0.0011	0.0084	/	0.0188	/
Min.	0.0010	0.0013	<0.038	/	<0.085	/
Max.	0.0022	0.0042	0.0601	/	0.1332	/

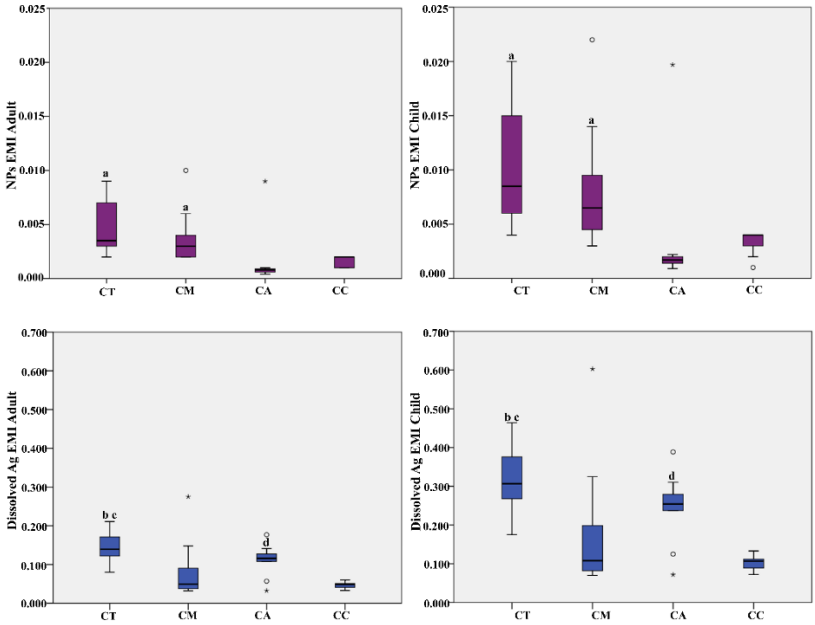

Figure 2.2. Box Plot distribution of Estimated Meal Intake (EMI μg/Kg b.w.) of AgNPs and dissolved Ag concentration calculated for adult (70 years) and child (6 years). Legend: CT. Canned Tuna; CM, Canned Mackerel; CA, Canned Anchovy; CC, Canned Clam; a. $p<0.05$ vs CA and CC; b $p<0.01$ vs CM; c $p<0.001$ vs CC; d $p<0.05$ vs CC. ° Outliers values of the distribution. * Extreme values of the distribution.

The SEM analysis on packaging did not show the presence of Ag in any of the scanned points. Microanalysis mainly highlighted, in addition to the presence of oxygen (O), the presence of iron (Fe), tin (Sn) and zinc (Zn) (Table 2.5). On the inner surface of the packaging, that is the one in contact with food, the predominant presence of carbon (C) makes the use of organic coatings, such as epoxy resins, likely.

Table 2.5. Data about packaging microanalysis for main revealed elements: mean percentage values, standard deviation (SD), minimum (Min) and maximum (Max) values.

Descriptive Statistics	%C	%Fe	%Zn	%Sn	%O
Mean	25.1	5.18	0.10	0.40	68.9
SD	2.22	6.61	0.13	0.29	4.25
Min	22.7	0.20	0.00	0.00	64.2
Max	27.0	12.4	0.24	0.68	72.2

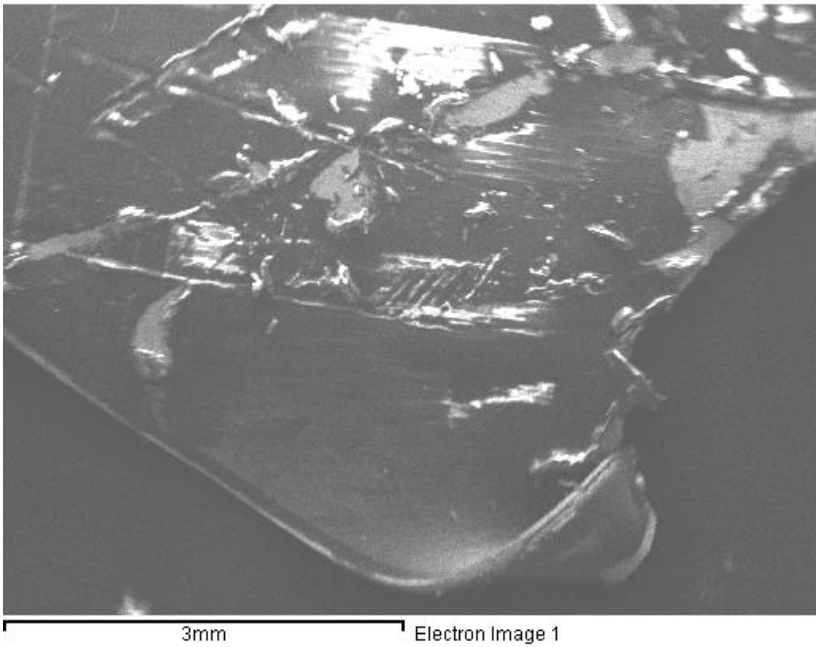

Figure 2.3. Example of a box fragment scanned by a Stereoscan 360" combined with an X Energy Dispersion Detector (SEM-EDX).

2.4. Discussion

This study provides for the first time the characterization and quantification of AgNPs, as well as the quantification of dissolved Ag, in processed canned seafood belonging to the best-selling brands available in large supermarket chains. The additive E174, based on Ag in its elemental form, was not intentionally added in none of the chosen products. As well, since the packages of all the selected canned products were made of metal, they do not fall within active packages obtained by the addition of nano compounds with antimicrobial properties, such as AgNPs (Simbine et al., 2019). Moreover, the SEM analysis performed in our study did not show the presence of Ag in their composition. For the above reasons, we supposed that a bioaccumulation process of Ag as nanoparticles and/or ionic form was occurred in the natural environment of seafood and/or during a contamination in the food processing at the industrial level.

Once discharged in the marine environment, the fate, distribution, and environmental impact of AgNPs is poorly understood yet. Nevertheless, it seems that environmental matrices influence particle dissolution and aggregation (Pasricha et al., 2012), undergoing to a chemical modification such as adsorption of organic molecules or reaction with dissolved species (Wimmer et al., 2020). When AgNPs are dispersed in a saline environment, and thus with high ionic strength, the aggregation is favoured (Lodeiro et al., 2016). Conversely, the high chloride content in seawater paired with the natural organic matter (NOM), favours AgNPs dissolution (Wimmer et al., 2020). Otherwise, most AgNPs remain suspended when a low ionic strength occurs, representing a potentially negative threat to the biota in an ionic or nanoscale form, while in a more saline environment nanoparticles agglomerate and precipitate on the surface of the sediment (Salari Joo et al., 2013). The results obtained from Xu et al. (2020) on seawater analyses showed a particle concentration (0.54×10^7 particles/mL) and a size distribution of

AgNPs (30.5 nm) similar to those obtained in our research, suggesting the possibility of environmental contamination. Nevertheless, because in seawater chlorides precipitate as AgCl(s), and if in excess they form the dissolved ion $AgCl_2^-$, most of the intake may have occurred in the seafood under this chemical form. Subsequently, in the gastric tract characterized by an acidic pH, Ag^+ can be released, and when enters the basic intestinal environment or the blood circulation, the AgNPs could be formed again.

Bioaccumulation of total Ag is not extensively studied in seafood of marine environment as other metals and metalloids (Copat et al., 2020; Ferrante et al., 2017; Salvaggio et al., 2019; Tigano et al., 2009), and the available concentrations from the literature are highly variable. For instance, in coastal sharks from The Bahamas, Ag in muscle tissue was found at a concentration between 0.055 and 0.518 mg/Kg w.w., with no accumulation trend associated with size (Shipley et al., 2021). In the Indian Mackerel captured along the coastal waters of Visakhapatnam, India, Ag in muscle tissue was found with concentrations ranging from 0.10 to 1.20 mg/Kg w.w. (Mangalagiri et al., 2020). A bioaccumulation study conducted in commercial marine fish from Brazil revealed Ag concentrations in muscle tissue ranging from 0.055 to 0.166 mg/Kg d.w. (Cardoso et al., 2019). Trace levels of Ag were also found in the muscle of fish from the Gulf of Lions (North-West Mediterranean Sea) and the Bay of Biscay (North-East Atlantic Ocean), with a concentration between 0.008 and 0.026 mg/Kg d.w. (Mille et al., 2018). In canned fish of 6 different fish species were found a mean concentration of 0.0053 mg/Kg w.w. (Kowalska et al., 2020). In freshwater environments, the main fishery from the La Plata basin (South America) revealed muscle levels of Ag below the limit of detection (Avigliano et al., 2019). Similar results were reported for freshwater fish from the New Caledonia lagoon (Metian et al., 2013), in fish collected from a fish farm located in Nahuel Huapi National Park in the northern Patagonia Andes Mountains, Argentina (Bubach et al., 2018) and in fish collected from a fish farm from Beijing (Jiang et al., 2016).

Irrelevant levels of Ag bioaccumulation described for freshwater ecosystems can be accountable to a low bioavailability of Ag or to the impact of low salinity on Ag bioaccumulation potential. A study conducted along Tunis lagoon, revealed high bioaccumulation concentration in clams sampled during the warmest seasons (0.34-0.60 mg/Kg d.w.) compared to the coldest ones (<LOD – 0.41 mg/Kg d.w.), the latest associated with low water salinity (Chalghmi et al.,. 2016).

The concentration of Ag we found in processed fish falls within the range provided by the literature for the marine ecosystem, and results do not show a trend associated with the trophic level, being Ag of canned tuna > canned anchovy > canned mackerel. To the best of our knowledge, our study is the first to deal with the characterization and quantification of AgNPs in seafood. As it is described in the results section, the mean size of AgNPs (31.1-35.8 nm), as well the most frequent size (26.2-27.7 nm), are comparable for all fish studied and, they did not show a trend associated with the trophic level, as it was observed for TiO_2-NPs (Grasso et al., 2020). Conversely, the number of AgNPs/g is significantly higher in fish with a larger size, tuna, and mackerel, than anchovy, as we partially reported also for TiO_2-NPs (Grasso et al., 2020). Accordingly, if an accumulation of NPs will be verified in humans, being at the top of the food chain, we are potentially exposed to higher concentration than those found in nature.

Only one study in literature reports concentration and characterization of both AgNPs and Total Ag in marine bivalve collected from an offshore aquaculture farm. Clam samples belonging to the species Ruditapes philippinarum revealed an Ag concentration of 0.90 mg/Kg w.w., a mean size of AgNPs of 44.8 nm, and an AgNPs/g number of 2.07E+07 (Xu et al., 2020). Compared to our study, the results we reported are lower for both Ag (0.015 mg/Kg w.w.), number of AgNPs/g (0.44E+07), and mean size (32.9 nm). Furthermore, the mean size of AgNPs in the canned clam is in the same diameter range found for fish species, and the number of

AgNPs/g is the lowest value among all canned seafood analysed. However, despite the concentrations of Ag+ and AgNPs found in our study have been lower than ones reported in other studies, the ratio between the number of AgNPs and milligrams of dissolved Ag (very close to the total) is about 10 times greater in our results compared to those reported in the literature. Therefore, even if the total Ag amount has been lower, in our study Ag showed proportionally a greater tendency to aggregate into NPs having smaller sizes. The slight discrepancy observed between measurements can be linked to the variation of water chemistry, including ionic strength, natural organic matter, pH, and dissolved oxygen (Xu et al., 2020). The low mean size detected could be of human health concern, since, as it was shown from literature data, smaller is the diameter higher is the toxicity following oral exposure, given the ability of nanoparticles to move better into the circulatory system (Xu et al., 2020).

Although the number of AgNPs reported for canned seafood seems very high, its corresponded concentration in terms of mg/Kg w.w., as well the estimated daily intake for adults and children, is very low. It ranges from 0.0016 to 0.0047 μg/Kg b.w. for adults and from 0.0033 to 0.0102 to 0.0047 μg/Kg b.w. for children. Conversely, the estimated daily intake of the dissolved ion fraction is significantly higher, ranging from 0.0047 to 0.147 μg/Kg b.w. for adults and from 0.102 to 0.324 μg/Kg b.w. for children. Nevertheless, these concentrations are lower than the oral Reference Dose (RfDo) set for the inorganic silver (0.005 mg/Kg day b.w.) (US EPA, 2013; US-EPA, 2021) and, according to the results of THQ, there is no risk to develop chronic systemic effects due to dissolved Ag intake during the exposure duration applied.

Scientific opinion shows a great concern regarding the risk for human and environmental health, even at low concentrations, deriving from the toxicity of AgNPs which depend on several factors such as size, concentration, chemical composition, surface charge, Ag+ ions released, and hydrophobicity (Gaillet and Rouanet, 2015;

Park et al., 2010). That said, chemical features and behavior of AgNPs in the different exposure matrices can result in contrasting findings relating to toxicity.

Literature data report in-vitro genotoxicity of AgNPs, for eg. in human bronchial epithelial cells HBEC3-kt, human TK6 cells, human keratinocytes (SVK14), and mouse fibroblasts (NIH3T3) (Jiravova et al., 2016; Lebedová et al., 2018; Li et al., 2017), nevertheless, genotoxicity depend on the characteristics of NPs and the type of cells exposed (Jiravova et al. 2016). Regarding Ag+, no genotoxicity was found nor in vitro (Li et al., 2017) and after oral exposure in a mouse model (Nallanthighal et al., 2017).

In-vivo studies revealed how AgNPs can enter the blood circulation, cross the blood-brain barrier and bioaccumulate in different organs after oral administration (Boudreau et al., 2016; Gan et al., 2020; Kim et al., 2009; Park et al., 2010). A dose-dependent accumulation was observed in rats exposed to AgNPs, with higher bioaccumulation in females than males (Boudreau et al., 2016; Kim et al., 2009). Oral exposure to AgNPs in mice showed a size-dependent accumulation of AgNPs, with higher bioaccumulated concentrations for smaller diameters of NPs, as well as adverse health effects on liver and kidney and inflammatory responses when mice were exposed for 28 days to 1.00 mg/kg of AgNPs of 42 nm (Park et al., 2010). High subacute toxicity and oxidative damage were also observed in mice after oral exposure to 10-250 mg/kg body weight per day for 28 days, with significant pathological changes in the lung and liver (Gan et al., 2020). Weight loss, altered liver enzymes, altered blood biochemistry values, and some loss of renal function were also observed (Gaillet and Rouanet, 2015; Tiwari et al., 2017). In-vivo experiments on plants (Allium cepa and Nicotiana tabacum) and animals (Swiss albino male mice) showed impairment of nuclear DNA (Ghosh et al., 2012). Furthermore, it was shown that AgNPs caused genotoxicity in the bone marrow of rats (Dobrzyńska et al., 2014; Kovvuru et al., 2015) and reticulocytes of mice (Song et al., 2012) after oral exposure. Nevertheless, particle coatings can

modulate nanoparticles behavior in the gastrointestinal tract and change genotoxicity effects. It was observed in a mouse model, where citrate-coated AgNPs in digestive juices tends to agglomerate much more than polyvinylpyrrolidone (PVP)-coated AgNPs becoming more genotoxic (Nallanthighal et al., 2017). Furthermore, once ingested, AgNPs could play a role in the dysregulation of gastrointestinal functions by altering mRNA expression that regulates intestinal permeability (Orr et al., 2019).

In-vitro and in-vivo studies suggest that the toxicity of AgNPs is dependent on the silver ion fraction in the AgNPs suspension (Beer et al., 2012; van der Zande et al., 2012). Differences between oral exposure to AgNPs and ionic Ag have been studied and a greater bioaccumulation was observed for the ionic form (Boudreau et al., 2016; Loeschner et al., 2011; van der Zande et al., 2012). Nevertheless, high fecal excretion following oral administration of AgNPs was observed (Gan et al., 2020; Loeschner et al., 2011), whereas that of ionic Ag is significantly lower (Loeschner et al., 2011).

Conversely, other studies did not show any adverse effects in liver and kidney, or hematological and histopathological changes in animals treated with polyvinyl pyrrolidone coated AgNPs (PVP-AgNPs) after sub-chronic oral exposure (Garcia et al., 2016). Acute oral exposure to 2000 mg/kg of AgNPs in rats did not show genotoxicity or mortality (Kim et al., 2013), whereas the LD50 of the AgNPs synthesized from Elaeodendron croceumin in Wister rats was determined to be greater than 2000 mg/kg body weight. As well, in-vivo one-month exposure of adult zebrafish to concentrations of AgNPs (8, 45, and 70 μg/L) did not show evident morphological and ultrastructural organization in cornea epithelium (Pecoraro et al., 2019).

Several issues still need to be better addressed such as the capacity of AgNPs to enter the body themselves reaching the various body districts or if only the silver ions issuing from the NPs are absorbed and which chemical reactions undergo in the digestive tract based on their chemical composition (Gaillet and Rouanet, 2015). Accordingly,

it was observed that AgNPs capped with citrate and not, aggregate and partially react to form silver chloride during exposure to synthetic stomach fluid (Mwilu et al., 2013; Rogers et al., 2012) and, the aggregation of nanoparticles is favoured by smaller diameters, prolonged period, as well as by the surface features of NPs (Mwilu et al., 2013).Concerning the capacity of nanoparticles to interact with the biomolecules, the study of Marchiore et al., (2017) investigated the migration of added silver nanoparticles from antimicrobial edible coating to sausages. They showed as silver ions, slowly released from AgNPs, are able to interact with proteins and lipids, generating a lipid oxidation and suggesting that silver may act as an activation factor in the free radical reaction.

The studies aimed to verify bioaccumulation of AgNPs after oral administration (Boudreau et al., 2016; Gan et al., 2020; Kim et al., 2009; Park et al., 2010) did not quantify the specific accumulation of AgNPs in animal body district. Indeed, they analysed total Ag content with the standard technique of atomic absorption spectrometer or inductively coupled plasma. Therefore, one of the most important challenges in the field of AgNPs toxicity, or more, in general, the NPs toxicity, is a better understanding of the chemical transformations occurring once the gastrointestinal system is reached and chemical features paired with concentrations of NPs once they are translocated in tissues and organs.

2.5. Conclusions

In this study, we provided a first quantification and characterization of AgNPs in canned seafood where food-grade E174 is not intentionally added nor is the nanoparticle contained in the food contact material. Thus, it is supposed that concentrations found originate from bioaccumulation of AgNPs in the marine environment or a chemical transformation of accumulated Ag compounds once entered in organism body districts. Alternatively, the presence of AgNPs in analysed processed food could arise from

contamination during food processing, at the industrial level.
Our findings highlighted comparable mean sizes across all species analysed, regardless of trophic level, although AgNPs concentrations partly follow a trophic level-dependent trend. The low mean size detected could be of human health concern, as well as the bioaccumulation potential along the food chain. Nevertheless, the concentration of AgNPs and dissolved Ag found in muscle tissue of processed seafood and the resulting EMI calculated for adults and children seems to be very low. Although seafood consumption represents only a small part of the human total diet, our findings represent a first important step to understand the AgNPs dietary exposure of the human population. Further studies are needed to characterize and quantify AgNPs in a large number of food items, both processing and not, and where AgNPs are added at the industrial level. They will provide a realistic exposure assessment, useful to understand if AgNPs toxicity levels observed in literature are close to those really estimable through food consumption and implement data useful for risk assessors in developing AgNPs provisional tolerable daily intake.

.

References

- Akaighe, N., Maccuspie, R.I., Navarro, D.A., Aga, D.S., Banerjee, S., Sohn, M., Sharma, V.K., 2011. Humic acid-induced silver nanoparticle formation under environmentally relevant conditions. Environ. Sci. Technol. 45, 3895–3901. https://doi.org/10.1021/es103946g
- AshaRani, P., Hande, M.P., Valiyaveettil, S., 2009. Anti-proliferative activity of silver nanoparticles. BMC Cell Biol. 10, 65. https://doi.org/10.1186/1471-2121-10-65
- Avigliano, E., Monferrán, M.V., Sánchez, S., Wunderlin, D.A., Gastaminza, J., Volpedo, A.V., 2019. Distribution and bioaccumulation of 12 trace elements in water, sediment and tissues of the main fishery from different environments of the La Plata basin (South America): Risk assessment for human consumption. Chemosphere 236, 124394. https://doi.org/10.1016/j.chemosphere.2019.124394
- Beer, C., Foldbjerg, R., Hayashi, Y., Sutherland, D.S., Autrup, H., 2012. Toxicity of silver nanoparticles—Nanoparticle or silver ion? Toxicol. Lett. 208, 286–292. https://doi.org/10.1016/j.toxlet.2011.11.002
- Boudreau, M.D., Imam, M.S., Paredes, A.M., Bryant, M.S., Cunningham, C.K., Felton, R.P., Jones, M.Y., Davis, K.J., Olson, G.R., 2016. Differential Effects of Silver Nanoparticles and Silver Ions on Tissue Accumulation, Distribution, and Toxicity in the Sprague Dawley Rat Following Daily Oral Gavage Administration for 13 Weeks. Toxicol. Sci. Off. J. Soc. Toxicol. 150, 131–160. https://doi.org/10.1093/toxsci/kfv318
- Bubach, D.F., Catán, S.P., Baez, V.H., Arribére, M.A., 2018. Elemental composition in rainbow trout tissues from a fish farm from Patagonia, Argentina. Environ. Sci. Pollut. Res. Int. 25, 6340–6351. https://doi.org/10.1007/s11356-017-0898-x
- Cardoso, M., de Faria Barbosa, R., Torrente-Vilara, G., Guanaz, G., Oliveira de Jesus, E.F., Mármy, E.T., de Oliveira Resende Ribeiro, R., Gusmão, F., 2019. Multielemental composition and consumption risk characterization of three commercial marine fish species. Environ. Pollut. 252, 1026–1034. https://doi.org/10.1016/j.envpol.2019.06.039
- Chalghmi, H., Zrafi, I., Gourves, P.-Y., Bourdineaud, J.-P., Saidane-Mosbahi, D., 2016. Combined effects of metal contamination and abiotic parameters on biomarker responses in clam Ruditapes decussatus gills: an integrated approach in biomonitoring of Tunis lagoon. Environ. Sci. Process. Impacts 18, 895–907. https://doi.org/10.1039/c6em00139d
- Copat, C., Rizzo, M., Zuccaro, A., Grasso, A., Zuccarello, P., Fiore, M., Mancini, G., Ferrante, M., 2020. Metals/Metalloids and Oxidative Status Markers in Saltwater Fish from the Ionic Coast of Sicily, Mediterranean Sea. Int. J. Environ. Res. 14, 15–27. https://doi.org/10.1007/s41742-019-00237-1

- Das, B., Tripathy, S., Adhikary, J., Chattopadhyay, S., Mandal, D., Dash, S.K., Das, S., Dey, A., Dey, S.K., Das, D., Roy, S., 2017. Surface modification minimizes the toxicity of silver nanoparticles: an in vitro and in vivo study. J. Biol. Inorg. Chem. JBIC Publ. Soc. Biol. Inorg. Chem. 22, 893–918. https://doi.org/10.1007/s00775-017-1468-x
- De Matteis, V., Cascione, M., Toma, C.C., Leporatti, S., 2018. Silver Nanoparticles: Synthetic Routes, In Vitro Toxicity and Theranostic Applications for Cancer Disease. Nanomater. Basel Switz. 8. https://doi.org/10.3390/nano8050319
- Dobrzyńska, M.M., Gajowik, A., Radzikowska, J., Lankoff, A., Dušinská, M., Kruszewski, M., 2014. Genotoxicity of silver and titanium dioxide nanoparticles in bone marrow cells of rats in vivo. Toxicology 315, 86–91. https://doi.org/10.1016/j.tox.2013.11.012
- EFSA, 2016. Scientific opinion on the re-evaluation of silver (E 174) as food additive. EFSA J. 14, 4364. https://doi.org/10.2903/j.efsa.2016.4364
- Ferrante, M., Pappalardo, A.M., Ferrito, V., Pulvirenti, V., Fruciano, C., Grasso, A., Sciacca, S., Tigano, C., Copat, C., 2017. Bioaccumulation of metals and biomarkers of environmental stress in Parablennius sanguinolentus (Pallas, 1814) sampled along the Italian coast. Mar. Pollut. Bull. 122, 288–296. https://doi.org/10.1016/j.marpolbul.2017.06.060
- Fontecha-Umaña, F., Ríos-Castillo, A.G., Ripolles-Avila, C., Rodríguez-Jerez, J.J., 2020. Antimicrobial Activity and Prevention of Bacterial Biofilm Formation of Silver and Zinc Oxide Nanoparticle-Containing Polyester Surfaces at Various Concentrations for Use. Foods Basel Switz. 9. https://doi.org/10.3390/foods9040442
- Gaillet, S., Rouanet, J.-M., 2015. Silver nanoparticles: Their potential toxic effects after oral exposure and underlying mechanisms – A review. Food Chem. Toxicol. 77, 58–63. https://doi.org/10.1016/j.fct.2014.12.019
- Gan, J., Sun, J., Chang, X., Li, W., Li, J., Niu, S., Kong, L., Zhang, T., Wu, T., Tang, M., Xue, Y., 2020. Biodistribution and organ oxidative damage following 28 days oral administration of nanosilver with/without coating in mice. J. Appl. Toxicol. JAT 40, 815–831. https://doi.org/10.1002/jat.3946
- Garcia, T., Lafuente, D., Blanco, J., Sánchez, D.J., Sirvent, J.J., Domingo, J.L., Gómez, M., 2016. Oral subchronic exposure to silver nanoparticles in rats. Food Chem. Toxicol. Int. J. Publ. Br. Ind. Biol. Res. Assoc. 92, 177–187. https://doi.org/10.1016/j.fct.2016.04.010
- Ghosh, M., J, M., Sinha, S., Chakraborty, A., Mallick, S.K., Bandyopadhyay, M., Mukherjee, A., 2012. In vitro and in vivo genotoxicity of silver nanoparticles. Mutat. Res. 749, 60–69. https://doi.org/10.1016/j.mrgentox.2012.08.007
- Ghosn, M., Mahfouz, C., Chekri, R., Khalaf, G., Guérin, T., Jitaru, P., Amara, R., 2020. Seasonal and Spatial Variability of Trace Elements in Livers and

Muscles of Three Fish Species from the Eastern Mediterranean. Environ. Sci. Pollut. Res. Int. 27, 12428–12438. https://doi.org/10.1007/s11356-020-07794-5

- Grasso, A., Ferrante, M., Zuccarello, P., Filippini, T., Arena, G., Fiore, M., Cristaldi, A., Conti, G.O., Copat, C., 2020. Chemical Characterization and Quantification of Titanium Dioxide Nanoparticles (TiO_2-NPs) in Seafood by Single-Particle ICP-MS: Assessment of Dietary Exposure. Int. J. Environ. Res. Public. Health 17, 9547. https://doi.org/10.3390/ijerph17249547
- Gunsolus, I.L., Mousavi, M.P.S., Hussein, K., Bühlmann, P., Haynes, C.L., 2015. Effects of Humic and Fulvic Acids on Silver Nanoparticle Stability, Dissolution, and Toxicity. Environ. Sci. Technol. 49, 8078–8086. https://doi.org/10.1021/acs.est.5b01496
- Han, W., Yu, Y., Li, N., Wang, L., 2011. Application and safety assessment for nano-composite materials in food packaging. Chin. Sci. Bull. 56, 1216–1225. https://doi.org/10.1007/s11434-010-4326-6
- Huang, Z., Zeng, Z., Chen, A., Zeng, G., Xiao, R., Xu, P., He, K., Song, Z., Hu, L., Peng, M., Huang, T., Chen, G., 2018. Differential behaviors of silver nanoparticles and silver ions towards cysteine: Bioremediation and toxicity to Phanerochaete chrysosporium. Chemosphere 203, 199–208. https://doi.org/10.1016/j.chemosphere.2018.03.144
- Jha, P.K., Jha, R.K., Rout, D., Gnanasekar, S., Rana, S.V.S., Hossain, M., 2017. Potential targetability of multi-walled carbon nanotube loaded with silver nanoparticles photosynthesized from Ocimum tenuiflorum (tulsi extract) in fertility diagnosis. J. Drug Target. 25, 616–625. https://doi.org/10.1080/1061186X.2017.1306534
- Jiang, H., Qin, D., Mou, Z., Zhao, J., Tang, S., Wu, S., Gao, L., 2016. Trace elements in farmed fish (Cyprinus carpio, Ctenopharyngodon idella and Oncorhynchus mykiss) from Beijing: implication from feed. Food Addit. Contam. Part B Surveill. 9, 132–141. https://doi.org/10.1080/19393210.2016.1152597
- Jiravova, J., Tomankova, K.B., Harvanova, M., Malina, L., Malohlava, J., Luhova, L., Panacek, A., Manisova, B., Kolarova, H., 2016. The effect of silver nanoparticles and silver ions on mammalian and plant cells in vitro. Food Chem. Toxicol. 96, 50–61. https://doi.org/10.1016/j.fct.2016.07.015
- Kim, J.S., Song, K.S., Sung, J.H., Ryu, H.R., Choi, B.G., Cho, H.S., Lee, J.K., Yu, I.J., 2013. Genotoxicity, acute oral and dermal toxicity, eye and dermal irritation and corrosion and skin sensitisation evaluation of silver nanoparticles. Nanotoxicology 7, 953–960. https://doi.org/10.3109/17435390.2012.676099
- Kim, W.-Y., Kim, J., Park, J.D., Ryu, H.Y., Yu, I.J., 2009. Histological study of gender differences in accumulation of silver nanoparticles in kidneys of Fischer 344 rats. J. Toxicol. Environ. Health A 72, 1279–1284. https://doi.org/10.1080/15287390903212287

- Kovvuru, P., Mancilla, P.E., Shirode, A.B., Murray, T.M., Begley, T.J., Reliene, R., 2015. Oral ingestion of silver nanoparticles induces genomic instability and DNA damage in multiple tissues. Nanotoxicology 9, 162–171. https://doi.org/10.3109/17435390.2014.902520
- Kowalska, M., Skrzypek, M., Kowalski, M., Cyrys, J., 2020. Effect of NOx and NO2 Concentration Increase in Ambient Air to Daily Bronchitis and Asthma Exacerbation, Silesian Voivodeship in Poland. Int. J. Environ. Res. Public. Health 17. https://doi.org/10.3390/ijerph17030754
- Lebedová, J., Hedberg, Y.S., Odnevall Wallinder, I., Karlsson, H.L., 2018. Size-dependent genotoxicity of silver, gold and platinum nanoparticles studied using the mini-gel comet assay and micronucleus scoring with flow cytometry. Mutagenesis 33, 77–85. https://doi.org/10.1093/mutage/gex027
- Lee, S., Bi, X., Reed, R.B., Ranville, J.F., Herckes, P., Westerhoff, P., 2014. Nanoparticle Size Detection Limits by Single Particle ICP-MS for 40 Elements. Environ. Sci. Technol. 48, 10291–10300. https://doi.org/10.1021/es502422v
- Li, C., Yang, X.-Q., Zhang, M.-Z., Song, Y.-Y., Cheng, K., An, J., Zhang, X.-S., Xuan, Y., Liu, B., Zhao, Y.-D., 2018. In vivo Imaging-Guided Nanoplatform for Tumor Targeting Delivery and Combined Chemo-, Gene- and Photothermal Therapy. Theranostics 8, 5662–5675. https://doi.org/10.7150/thno.28241
- Li, Y., Qin, T., Ingle, T., Yan, J., He, W., Yin, J.-J., Chen, T., 2017. Differential genotoxicity mechanisms of silver nanoparticles and silver ions. Arch. Toxicol. 91, 509–519. https://doi.org/10.1007/s00204-016-1730-y
- Liu, J., Hurt, R.H., 2010. Ion Release Kinetics and Particle Persistence in Aqueous Nano-Silver Colloids. Environ. Sci. Technol. 44, 2169–2175. https://doi.org/10.1021/es9035557
- Lodeiro, P., Achterberg, E.P., Pampín, J., Affatati, A., El-Shahawi, M.S., 2016. Silver nanoparticles coated with natural polysaccharides as models to study AgNP aggregation kinetics using UV-Visible spectrophotometry upon discharge in complex environments. Sci. Total Environ. 539, 7–16. https://doi.org/10.1016/j.scitotenv.2015.08.115
- Loeschner, K., Hadrup, N., Qvortrup, K., Larsen, A., Gao, X., Vogel, U., Mortensen, A., Lam, H.R., Larsen, E.H., 2011. Distribution of silver in rats following 28 days of repeated oral exposure to silver nanoparticles or silver acetate. Part. Fibre Toxicol. 8, 18. https://doi.org/10.1186/1743-8977-8-18
- Mangalagiri, P., Bikkina, A., Sundarraj, D.K., Thatiparthi, B.R., 2020. Bioaccumulation of heavy metals in Rastrelliger kanagurta along the coastal waters of Visakhapatnam, India. Mar. Pollut. Bull. 160, 111658. https://doi.org/10.1016/j.marpolbul.2020.111658
- Marchiore, N.G., Manso, I.J., Kaufmann, K.C., Lemes, G.F., Pizolli, A.P. de O., Droval, A.A., Bracht, L., Gonçalves, O.H., Leimann, F.V., 2017. Migration evaluation of silver nanoparticles from antimicrobial edible coating to

sausages. LWT - Food Sci. Technol., SLACA 2015: "Food Science for quality of life and health ageing" 76, 203–208. https://doi.org/10.1016/j.lwt.2016.06.013

- Metian, M., Warnau, M., Chouvelon, T., Pedraza, F., Rodriguez y Baena, A.M., Bustamante, P., 2013. Trace element bioaccumulation in reef fish from New Caledonia: Influence of trophic groups and risk assessment for consumers. Mar. Environ. Res. 87–88, 26–36. https://doi.org/10.1016/j.marenvres.2013.03.001
- Mille, T., Cresson, P., Chouvelon, T., Bustamante, P., Brach-Papa, C., Bruzac, S., Rozuel, E., Bouchoucha, M., 2018. Trace metal concentrations in the muscle of seven marine species: Comparison between the Gulf of Lions (North-West Mediterranean Sea) and the Bay of Biscay (North-East Atlantic Ocean). Mar. Pollut. Bull. 135, 9–16. https://doi.org/10.1016/j.marpolbul.2018.05.051
- Mwilu, S.K., El Badawy, A.M., Bradham, K., Nelson, C., Thomas, D., Scheckel, K.G., Tolaymat, T., Ma, L., Rogers, K.R., 2013. Changes in silver nanoparticles exposed to human synthetic stomach fluid: effects of particle size and surface chemistry. Sci. Total Environ. 447, 90–98. https://doi.org/10.1016/j.scitotenv.2012.12.036
- Nallanthighal, S., Chan, C., Bharali, D.J., Mousa, S.A., Vásquez, E., Reliene, R., 2017. Particle coatings but not silver ions mediate genotoxicity of ingested silver nanoparticles in a mouse model. NanoImpact 5, 92–100. https://doi.org/10.1016/j.impact.2017.01.003
- Orr, S.E., Gokulan, K., Boudreau, M., Cerniglia, C.E., Khare, S., 2019. Alteration in the mRNA expression of genes associated with gastrointestinal permeability and ileal TNF-α secretion due to the exposure of silver nanoparticles in Sprague-Dawley rats. J. Nanobiotechnology 17, 63. https://doi.org/10.1186/s12951-019-0499-6
- Pappalardo, A.M., Copat, C., Ferrito, V., Grasso, A., Ferrante, M., 2017. Heavy metal content and molecular species identification in canned tuna: Insights into human food safety. Mol. Med. Rep. 15, 3430–3437. https://doi.org/10.3892/mmr.2017.6376
- Pappalardo, A.M., Copat, C., Raffa, A., Rossitto, L., Grasso, A., Fiore, M., Ferrante, M., Ferrito, V., 2020. Fish-Based Baby Food Concern—From Species Authentication to Exposure Risk Assessment. Molecules 25, 3961. https://doi.org/10.3390/molecules25173961
- Park, E.-J., Bae, E., Yi, J., Kim, Y., Choi, K., Lee, S.H., Yoon, J., Lee, B.C., Park, K., 2010. Repeated-dose toxicity and inflammatory responses in mice by oral administration of silver nanoparticles. Environ. Toxicol. Pharmacol. 30, 162–168. https://doi.org/10.1016/j.etap.2010.05.004
- Pasricha, A., Jangra, S.L., Singh, N., Dilbaghi, N., Sood, K.N., Arora, K., Pasricha, R., 2012. Comparative study of leaching of silver nanoparticles

from fabric and effective effluent treatment. J. Environ. Sci. 24, 852–859. https://doi.org/10.1016/S1001-0742(11)60849-8
- Pecoraro, R., Salvaggio, A., Scalisi, E.M., Iaria, C., Lanteri, G., Copat, C., Ferrante, M., Fragalà, G., Zimbone, M., Impellizzeri, G., Brundo, M.V., 2019. Evaluation of the effects of silver nanoparticles on Danio rerio cornea: Morphological and ultrastructural analysis. Microsc. Res. Tech. 82, 1297–1301. https://doi.org/10.1002/jemt.23280
- Qin, G., Tang, S., Li, S., Lu, H., Wang, Y., Zhao, P., Li, B., Zhang, J., Peng, L., 2017. Toxicological evaluation of silver nanoparticles and silver nitrate in rats following 28 days of repeated oral exposure. Environ. Toxicol. 32, 609–618. https://doi.org/10.1002/tox.22263
- Rai, M., Yadav, A., Gade, A., 2009. Silver nanoparticles as a new generation of antimicrobials. Biotechnol. Adv. 27, 76–83. https://doi.org/10.1016/j.biotechadv.2008.09.002
- Reidy, B., Haase, A., Luch, A., Dawson, K.A., Lynch, I., 2013. Mechanisms of Silver Nanoparticle Release, Transformation and Toxicity: A Critical Review of Current Knowledge and Recommendations for Future Studies and Applications. Materials 6, 2295–2350. https://doi.org/10.3390/ma6062295
- Rogers, K.R., Bradham, K., Tolaymat, T., Thomas, D.J., Hartmann, T., Ma, L., Williams, A., 2012. Alterations in physical state of silver nanoparticles exposed to synthetic human stomach fluid. Sci. Total Environ. 420, 334–339. https://doi.org/10.1016/j.scitotenv.2012.01.044
- Salari Joo, H., Kalbassi, M.R., Yu, I.J., Lee, J.H., Johari, S.A., 2013. Bioaccumulation of silver nanoparticles in rainbow trout (Oncorhynchus mykiss): influence of concentration and salinity. Aquat. Toxicol. Amst. Neth. 140–141, 398–406. https://doi.org/10.1016/j.aquatox.2013.07.003
- Salvaggio, A., Tiralongo, F., Krasakopoulou, E., Marmara, D., Giovos, I., Crupi, R., Messina, G., Lombardo, B.M., Marzullo, A., Pecoraro, R., Scalisi, E.M., Copat, C., Zuccarello, P., Ferrante, M., Brundo, M.V., 2019. Biomarkers of Exposure to Chemical Contamination in the Commercial Fish Species Lepidopus caudatus (Euphrasen, 1788): A Particular Focus on Plastic Additives. Front. Physiol. 10, 905. https://doi.org/10.3389/fphys.2019.00905
- Sharma, V.K., Filip, J., Zboril, R., Varma, R.S., 2015. Natural inorganic nanoparticles--formation, fate, and toxicity in the environment. Chem. Soc. Rev. 44, 8410–8423. https://doi.org/10.1039/c5cs00236b
- Shimabuku, Q.L., Arakawa, F.S., Fernandes Silva, M., Ferri Coldebella, P., Ueda-Nakamura, T., Fagundes-Klen, M.R., Bergamasco, R., 2017. Water treatment with exceptional virus inactivation using activated carbon modified with silver (Ag) and copper oxide (CuO) nanoparticles. Environ. Technol. 38, 2058–2069. https://doi.org/10.1080/09593330.2016.1245361
- Shipley, O.N., Lee, C.-S., Fisher, N.S., Sternlicht, J.K., Kattan, S., Staaterman, E.R., Hammerschlag, N., Gallagher, A.J., 2021. Metal concentrations in

coastal sharks from The Bahamas with a focus on the Caribbean Reef shark. Sci. Rep. 11, 218. https://doi.org/10.1038/s41598-020-79973-w

- Simbine, E.O., Rodrigues, L. da C., Lapa-Guimarães, J., Kamimura, E.S., Corassin, C.H., Oliveira, C.A.F. de, Simbine, E.O., Rodrigues, L. da C., Lapa-Guimarães, J., Kamimura, E.S., Corassin, C.H., Oliveira, C.A.F. de, 2019. Application of silver nanoparticles in food packages: a review. Food Sci. Technol. 39, 793–802. https://doi.org/10.1590/fst.36318
- Song, M.-F., Li, Y.-S., Kasai, H., Kawai, K., 2012. Metal nanoparticle-induced micronuclei and oxidative DNA damage in mice. J. Clin. Biochem. Nutr. 50, 211–216. https://doi.org/10.3164/jcbn.11-70
- Taboada-López, M.V., Iglesias-López, S., Herbello-Hermelo, P., Bermejo-Barrera, P., Moreda-Piñeiro, A., 2018. Ultrasound assisted enzymatic hydrolysis for isolating titanium dioxide nanoparticles from bivalve mollusk before sp-ICP-MS. Anal. Chim. Acta 1018, 16–25. https://doi.org/10.1016/j.aca.2018.02.075
- Tigano, C., Tomasello, B., Pulvirenti, V., Ferrito, V., Copat, C., Carpinteri, G., Mollica, E., Sciacca, S., Renis, M., 2009. Assessment of environmental stress in Parablennius sanguinolentus (Pallas, 1814) of the Sicilian Ionian coast. Ecotoxicol. Environ. Saf. 72, 1278–1286. https://doi.org/10.1016/j.ecoenv.2008.09.028
- Tiwari, R., Singh, R.D., Khan, H., Gangopadhyay, S., Mittal, S., Singh, V., Arjaria, N., Shankar, J., Roy, S.K., Singh, D., Srivastava, V., 2017. Oral subchronic exposure to silver nanoparticles causes renal damage through apoptotic impairment and necrotic cell death. Nanotoxicology 11, 671–686. https://doi.org/10.1080/17435390.2017.1343874
- US EPA, 2013. Risk Assessment [WWW Document]. US EPA. URL https://www.epa.gov/risk (accessed 1.28.21).
- US-EPA, 2021. Silver CASRN 7440-22-4 | DTXSID4024305 | IRIS | US EPA, ORD [WWW Document]. URL https://cfpub.epa.gov/ncea/iris2/chemicalLanding.cfm?substance_nmbr=99 (accessed 1.13.21).
- US-EPA, 2000. Guidance for Assessing Chemical Contamination Data for Use in Fish Advisories, vol. II. Risk Assessment and Fish Consumption Limits EPA/823-B94- 004.
- Valsalam, S., Agastian, P., Esmail, G.A., Ghilan, A.-K.M., Al-Dhabi, N.A., Arasu, M.V., 2019. Biosynthesis of silver and gold nanoparticles using Musa acuminata colla flower and its pharmaceutical activity against bacteria and anticancer efficacy. J. Photochem. Photobiol. B 201, 111670. https://doi.org/10.1016/j.jphotobiol.2019.111670
- van der Zande, M., Vandebriel, R.J., Van Doren, E., Kramer, E., Herrera Rivera, Z., Serrano-Rojero, C.S., Gremmer, E.R., Mast, J., Peters, R.J.B., Hollman, P.C.H., Hendriksen, P.J.M., Marvin, H.J.P., Peijnenburg, A.A.C.M., Bouwmeester, H., 2012. Distribution, elimination, and toxicity of

silver nanoparticles and silver ions in rats after 28-day oral exposure. ACS Nano 6, 7427–7442. https://doi.org/10.1021/nn302649p

- Vines, J.B., Lim, D.-J., Park, H., 2018. Contemporary Polymer-Based Nanoparticle Systems for Photothermal Therapy. Polymers 10. https://doi.org/10.3390/polym10121357
- Wimmer, A., Urstoeger, A., Funck, N.C., Adler, F.P., Lenz, L., Doeblinger, M., Schuster, M., 2020. What happens to silver-based nanoparticles if they meet seawater? Water Res. 171, 115399. https://doi.org/10.1016/j.watres.2019.115399
- Xu, L., Wang, Z., Zhao, J., Lin, M., Xing, B., 2020. Accumulation of metal-based nanoparticles in marine bivalve mollusks from offshore aquaculture as detected by single particle ICP-MS. Environ. Pollut. 260, 114043. https://doi.org/10.1016/j.envpol.2020.114043
- Zhang, W., Ke, S., Sun, C., Xu, X., Chen, J., Yao, L., 2019. Fate and toxicity of silver nanoparticles in freshwater from laboratory to realistic environments: a review. Environ. Sci. Pollut. Res. 26, 7390–7404. https://doi.org/10.1007/s11356-019-04150-0

10.3 CHAPTER 3: Dietary exposure of zinc oxide nanoparticles (ZnO-NPs) from canned seafood by single particle ICP-MS: balancing of risks and benefits for human health.

Alfina Grasso[1], Margherita Ferrante[1], Antonio Moreda-Piñeiro[2], Giovanni Arena[3], Riccardo Magarini[4], Gea Oliveri Conti[1], Antonio Cristaldi[1], Chiara Copat[1].

[1] Department of Medical, Surgical and Advanced Technologies "G.F. Ingrassia", University of Catania, Catania, Italy.

[2] Trace Element, Spectroscopy and Speciation Group (GETEE), Health Research Institute of Santiago de Compostela (IDIS). Department of Analytical Chemistry, Nutrition and Bromatology. Faculty of Chemistry. Universidade de Santiago de Compostela, Santiago de Compostela, Spain.

[3] Freelance chemist.

[4]PerkinElmer (Italia), Milano, Italy

Published in: Ecotoxicology and Environmental Safety, 2022, 231, https://doi.org/10.1016/j.ecoenv.2022.113217

Abstract

The present study aims to give information regarding the quantification of ZnO-NPs in canned seafood, which may be intentionally or unintentionally added, and to provide a first esteem of dietary exposure. Samples were subjected to an alkaline digestion and assessment of ZnO-NPs was performed by the single particle ICP-MS technique. ZnO-NPs were found with concentrations range from 0.003 to 0.010 mg/kg and a size mean range from 61.3 and 78.6 nm. It was not observed a clear bioaccumulation trend according to trophic level and size of seafood species, although the mollusk species has slightly higher concentrations and larger size. The number of ZnO-NPs/g does not differ significantly among food samples, observing an average range of 5.51×10^6 - 9.97×10^6. Dissolved Zn determined with spICP-MS revealed comparable concentration to total Zn determined with ICP-MS in standard mode, confirming the efficiency of alkaline digestion on the extraction of the Zn. The same accumulation trend found for ZnO-NPs was observed more clearly for dissolved Zn. The ZnO-NPs intake derived from a meal does not differ significantly among seafood products and it ranges from 0.010 to 0.031 μg/kg b.w. in adult, and from 0.022 to 0.067 μg/kg b.w. in child. Conversely, the intake of dissolved Zn is significantly higher if it is assumed a meal of mollusks versus the fish products, with values of 109.3 μg/kg b.w. for adult and 240.1 μg/kg b.w. for child. Our findings revealed that ZnO-NPs have the potential to bioaccumulate in marine organisms, and seafood could be an important uptake route of ZnO-NPs. These results could be a first important step to understand the ZnO-NPs human dietary exposure, but the characterization and quantification of ZnO-NPs is necessary for a large number of food items.

Keywords: ZnO; Nanoparticles; spICP-MS; Food; Dietary Intake; Exposure Assessment

3.1 Introduction

Over the last few decades, intense research in the area of nanoparticles (NPs) is rapidly growing due to their applications in biomedical, industrial and agricultural field. Despite their useful properties, nanoparticle hazards on the biological system are poorly understood up to now and their potential detrimental effects to living organisms are studied (Chakraborty et al., 2016; Hou et al., 2018; Król et al., 2017; Vandebriel and De Jong, 2012). As defined by European Commission (EC, 2013) nanomaterial is 'a natural, incidental or manufactured material containing particles, in an unbound state or as an aggregate or as an agglomerate and where, for 50 % or more of the particles in the number size distribution, one or more external dimensions is in the size range 1–100 nm. In specific cases and where warranted by concerns for the environment, health, safety or competitiveness, the number size distribution threshold of 50 % may be replaced by a threshold between 1 and 50 %". The surface of nanomaterials, as well as the optimization of coating parameters, can be modulated according to their application (Jue et al., 2019; Raliya et al., 2016). This may leads to changes on nanomaterials (NMs) solubility which represents a key factor of NMs toxicity when modulating the interactions with organic compounds in the environment (proteins, amino acids, natural organic matter, humic substances) since NMs coating changes dispersion and complexation with metallic ions (Bondarenko et al., 2013).

ZnO-NPs have received much attention since their usage in several applications, such as cancer therapy (Akhtar et al., 2012; Chandrasekaran and Pandurangan, 2016), the development of electrochemical DNA biosensors (Abu-Salah et al., 2010) or biofilms with antimicrobial and antifungal properties (Barros et al., 2017; Chu et al., 2017; He et al., 2011), as well as in industrial packaging to extending and improving food shelf life (Ahmed et al., 2016; Arfat et al., 2017; Beak et al., 2017; Chia and Leong, 2016; Díez-Pascual and

Díez-Vicente, 2014; Emamifar and Mohammadizadeh, 2015), in renewable biofuels (Gurunathan and Ravi, 2015), wastewater treatment (Dehghani et al., 2018), seed and plants treatment (Elhaj Baddar and Unrine, 2018; Tighe-Neira et al., 2018), and UV blocking products (Girigoswami et al., 2015). Furthermore, ZnO can be added to foods as nutritional fortifier because Zn play a role as a trace element in enzyme activity, cell function and in the immune system (MacDonald, 2000). However, NMs that range in size from 1 to 100 nm are not intended to be used as food additives, and current regulations do not specify the size distribution of NPs (FDA, 2021). ZnO-NPs are heat stable and they are found to have a large surface to volume ratio, increased surface reactivity, and unique thermal, mechanical and electrical properties (Król et al., 2017). Although ZnO-NPs are generally recorded as safe (GRAS) substances approved by Food and Drug Administration (FAO, 2018), the research field of nanotoxicology is a rapidly maturing emerging issue because of their widespread use, the toxicity and biological applicability of ZnO nanoparticles, along with other frequently used nanoparticles like TiO2, SiO2, and carbon nanoparticles.

It was calculated that the sums of NPs derived from consumer products and discharged into the natural environment, in particular the aquatic environment, were within the extend of several hundred tons per year (Zhang et al., 2015). Nevertheless, accumulation of metal-based NPs in organisms from the aquatic environment and their concentrations in water bodies are unknown. Very few studies report concentrations of NPs in marine organisms (Taboada-López et al., 2019, 2018a; Xu et al., 2020; Yin et al., 2017; Zhou et al., 2020), and only one of these reports is related to ZnO-NPs characterization in molluscs species (Xu et al., 2020).

With this study, we would like to provide new information regarding the characterization and quantification of ZnO-NPs in processed canned seafood products, thanks to the emerging and valuable technique of the Single Particle - Inductively Coupled Plasma – Mass Spectrometer (spICP-MS), which allows to identify

number of particles, size and size distribution of metallic NPs with the simultaneous quantification of the dissolved elemental concentration.
This is challenging because food samples are heterogeneous matrices in terms of composition, structure and properties and, consequently food matrix may alter the original properties of NPs. Furthermore, due to the limited literature information related to the human oral exposure to metallic NPs, we would like to provide a first esteem of ZnO-NPs daily intake derived from consumption of seafood products, data that could be useful for risk assessors for developing provisional tolerable intake.

3.2 Material and methods

3.2.1. Reagents

Ultrapure water, 0.22µm filtered, was obtained from a Milli-Q purification device (Merck Millipore, Bedford, MA, USA). Samples acid digestion was performed with HNO3 (65%, w/w) and H2O2 (30%, w/w) from Carlo Erba Reagents S.r.l. (Cornaredo, MI, Italy). Tetramethylammonium hydroxide (25 % solution in water, for synthesis) and Triton X-100 for analysis were purchased from Merck Millipore (Bedford, MA, USA) and were used for the alkaline digestion.
Zinc (Zn) ionic standard solution (1000 mg/L) was purchased from CPAchem S.r.l. (Roma, Italy) and was used for ICP-MS and spICP-MS calibration. Yttrium (Y) ionic standard solution (1000 mg/L), used as an internal standard for the determination of total Zn by ICP-MS, was purchased from CPAchem S.r.l. Zinc Oxide nanoparticles (ZnO-NPs) Nano Powder reference material (AEM®, Purity 98.8%, Size 30 nm, Changsha, Hunan, China) was purchased from Nanovision S.r.l. (Brugherio, MB, Italy), and was used for spICP-MS calibration. Silver nanoparticles (Ag-NPs) certified reference material (PELCO® 39±5 nm, Citrate, NanoXactTM, 6.1 ◎

1010 particles/mL, monitoring m/z 107, Ted Pella Inc., Redding, CA, U.S.A.) was purchased from Nanovision S.r.l (Brugherio, MB, Italy), and used for the calculation of the transport efficiency.

3.2.2. Sampling

The extraction, the analytical determination procedures, and the accuracy of the method are described in detail in previous works (Grasso et al., 2021, 2020). Briefly, different brands of canned seafood samples, among tuna (CT: 5 brands), mackerel (CM, 4 brands), anchovy (CA, 3 brands) and clam (CC, 3 brands) were purchased from local Italian supermarkets chains and each sample was homogenized, stored at −80 °C until analysis, and then processed in triplicate.

3.2.3. Acid digestion and analytical determination of total Zn with ICP-MS

Microwave assisted acid digestion of the samples (0.5 g, wet weight) was carried out with a Microwave Ethos TC (Milestone, Sorisole, BG, Italy), by adding 6.0 mL of HNO3 (65%, w/w) and 2.0 mL of H2O2 (30%, w/w). The digestion was performed stepwise up to 200 °C in 10 min (1000 W), followed by a 15 min hold at 200 °C (1000 W). At the end of mineralization, the digested solutions were transferred into graduated polypropylene tubes DigiTUBEs from SCP SCIENCE Class "A" volumetric standards (Quebec, Canada) verified for leachable metals by ICP-MS, and then diluted to 50 mL using Milli-Q water and filtrated through 0.45 μm nylon filters before analysis.
For each set of digestion, a blank and a real sample, spiked with ionic zinc at 25 μg/L (assessment of the analytical recovery and interferences depending on the matrix) were processed. Zn concentrations of digestion blanks, if detectable, were subtracted to the Zn concentrations of real samples. The recoveries calculated are all in the range 96–111%, thus demonstrating the absence of the matrix effects. The LOD and LOQ were calculated by analyzing ten

acid digested blanks based on the mean + 3 SD and mean + 10 SD criterion, respectively. They resulted in 0.61 and 1.04 mg/kg, respectively.
Total Zn was determined by inductively coupled plasma mass spectrometer (ICP-MS NexION® 350D, Perkin Elmer, USA) on the sample solution diluted 1:10 with ultrapure water. The instrument was calibrated using the external standard technique covering a concentration range from 1 to 50 μg/L, with the addition of 25 μg/L Y, to be used as internal standard.
The operating conditions for total Zn determination are listed in Table 3.1.

Table 3.1. NexION® 350D ICP-MS instrumental condition for total zinc determination.

Parameter	Value
Nebulizer type and flow	Meinhard, 0.92 mL/min
Spray chamber	Glass cyclonic
Sample uptake rate	0.26–0.28 mL/min
RF power	1600W
Analysis mode	Standard (no gas)
Quadrupole Rod Offset	0
Zn (m/z)	64
Exit Cell Voltage	- 7 V
Entrance Cell Voltage	-7 V
Discriminator Threshold	12
Pulse Stage Voltage	1300 V
Analog Stage Voltage	-1959 V
Internal Standard	^{89}Y
Data acquisition times	1000 ms

3.2.4. Alkaline digestion and analytical determination of dissolved Zn and ZnO-NPs with single particle ICP-MS

The alkaline digestion of blanks and real samples (0.25 g, wet weight) was carried out with an ultrasonic bath by adding 5 mL of TMAH (20% v/v) for 30 min at 37 °C. The digestion was prolonged another 24 h at room temperature and then the alkaline digest was separate from any left undissolved residue by centrifugation (7°C,

3500 rpm) for 10 min and protected from light with aluminum foil before analysis. The extracts were kept into polyethylene graduated tubes and were diluted to 50 mL using an aqueous solution containing 1% TMAH and 0.1% Triton X-100 to prevent particle aggregation. All samples and calibration solutions were sonicated (60% amplitude, continuous sonication) for 20 min before analysis to maximize a homogeneous dispersion.

ZnO-NPs and dissolved Zn were determined with the Syngistix Nano application software supported by the ICP-MS (NexION® 350D, Perkin Elmer, Waltham, MA, USA) after 1:10 dilution with ultrapure water. ZnO-NPs and dissolved Zn concentrations of digestion blanks were subtracted to the concentrations detected in the real samples.

According to the principle of the technique, when the suspension of NPs enters the plasma, each NP is individually ionized, and recorded as a (discontinuous) pulse signal by a mass spectrometer (Figure 3.1a), making sp-ICP-MS very powerful in determining the mass of metal elements of all NPs. Meanwhile, the corresponding dissolved analyte is recorded as a continuous signal (Figure 3.1b). This means that sp-ICP-MS can detect both particle and dissolved analytes simultaneously (Figure 3.1c). In sp-ICP-MS analysis, the signal strength of NPs depends on the particle size, while the signal frequency is proportional to the particle concentration in the sample.

Figure 3.1. a) Example of real time data showing individual pulses of ZnO-NPs signaling; b) Example of real time data showing a continuous signal from measuring dissolved Zn; c) Example of real time data showing ZnO particles and dissolved Zn recorded simultaneously.

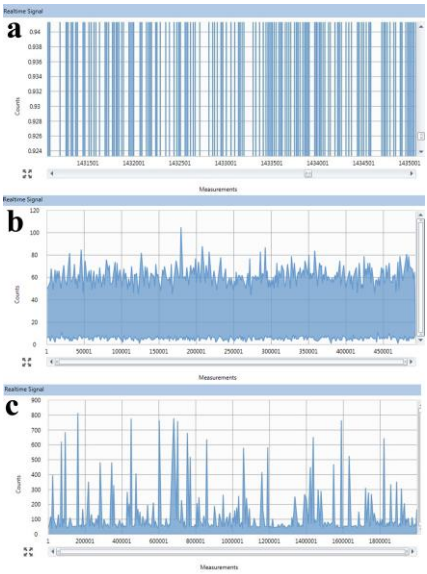

In sp-ICP-MS analysis, the Zn mass was measured first and then a mass fraction of 80% was used to convert the Zn mass to ZnO mass since the ratio of Zn/ZnO is 80%. The ZnO mass (m) was then converted into ZnO particle size diameter with the knowledge of ZnO density (7.14 g/cm3) and by assuming the spherical ZnO particle, according to the sp-ICP-MS theory (Pace et al., 2011).

To evaluate the extent of possible isobaric interference of ^{64}Ni on ^{64}Zn, a microwave acid digestion was performed in triplicate on samples of tuna and clam to determine the other Ni isotopes (60 and 62) and Zn isotopes (66 and 68), with ^{62}Ni and ^{68}Zn used for confirmation. The obtained concentrations were used to calculate the ^{60}Ni/^{66}Zn ratio of the analysed samples, which was in the range of 0.1-0.3% for the tuna sample and 3.2-5.6% for the clam sample,

indicating that the amount of nickel is negligible compared to the amount of zinc and that the possible interference with the analytical determination can also be considered negligible.
The instrumental conditions are reported in Table 3.2.

Table 3.2. NexION® 350D ICP-MS instrumental condition for single particles analysis.

Parameter	Value
Nebulizer, Flow	Meinhard, 0.92 mL/min
Spray chamber	Glass cyclonic
Sample uptake rate	0.26–0.28 mL/min
RF power	1600W
Analysis mode	Standard (no gas)
Quadrupole Rod Offset	0
Zn (m/z)	64
Dwell time	50 µs
Data acquisition time	60 s
Density ZnO	5.61 g/cm^3
Zn mass fraction	80%

Transport efficiency was determined for each batch of analysis using the certified Ag-NPs reference material after appropriate dilution (510 ng/L, 1.5 × 106 particles/mL) under the same instrumental conditions and in the same reagent matrix as for the samples. TE values in the range of 2.3-5.9% were supported by good accuracy results for standard solutions of ZnO-NPs and ionic Zn, within a maximum error of 10% of the expected value for each analytical batch. TE value depends on the sample introduction system and also on various operating parameters. Moreover, the TE % values calculated in the current research were in good agreement with values typically reported in the literature (from 1 to 5%) (Pace et al., 2011).
The effect of the extracting solution on the ZnO recovery was studied. Analytical recovery was performed both in Milli-Q water (n1 = 7) and in TMAH 1% (n2 = 7) by spiking 30 nm ZnO-NPs

standard at a concentration of 210 ng/L or 2.6 × 106 particles/mL. A median diameter around 33.1 ± 5.0 nm and a recovery of 89.7.1% (2.3 × 106 ± 4.6 × 105 particles/mL) was obtained in ultrapure water; whereas a median diameter around 28.3 ± 4,7 nm and a recovery of 91.0% (2.4 × 106 ± 3.7 × 105 particles/mL) was obtained for TMAH 1% experiments. Results obtained were found to be statistically homogeneous when applying a two tailed t-test (p = 95%; $\nu = n1 + n2 - 2 = 14$), and showing no effect from the extraction solution on the nanoparticles concentration or on size distribution (mean size: tcalculated = 1.95 < ttabulated = 2.14; particles/mL: tcalculated = 2.07 < ttabulated = 2.14). One more test was performed to evaluate the stability of ZnO-NPs in 20% TMAH and to verify the possibility of dissolution of ZnO-NPs under the same sample preparation conditions. Experiments were performed in both Milli-Q water and 0.1% Triton X-100 (n1 = 8) and 20% TMAH (n2 = 8) by spiking 30 nm ZnO-NPs at the same concentration as in the previous experiment in 1% TMAH. The results in terms of mean size and particle concentration were statistically homogeneous using a two-tailed t-test (p = 95%; $\nu = n1 + n2 - 2 = 14$) and showed no significant dissolution phenomena of ZnO-NPs (mean size: $t_{calculated} = 1.48 < t_{tabulated} = 2.14$; particles/mL: $t_{calculated} = 1.3 < t_{tabulated} = 2.14$).

Additional experiments were performed to verify that alkaline sample preparation does not produce NPs by spiking alkaline extracts extract from tuna samples with a concentration of 50 μg/L ionic zinc standard. The experiments included sp-ICP-MS measurement of the un-spiked alkaline extracts (n1=3) and the spiked alkaline extracts (n2=6). An average analytical recovery of 100% ± 11% was obtained, indicating that nanoparticles do not form during alkaline digestion. Moreover, the mean size of ZnO NPs was found to be similar in the spiked and un-spiked samples, implying that the sample preparation protocol does not affect the size of ZnO-NPs. This result was verified by applying a pooled t-test (p=95%; n1 + n2 - 2) (tcalculated = 2.12 < ttabulated = 2.36, degree of freedom = 7). The limit of detection (LOD) and the limit of quantification (LOQ)

were calculated as previously described (Grasso et al., 2021, 2020). They resulted in 3.0 × 105 particles/g and 6.8 × 105 particles/g, respectively.
For the determination LOD in size the following equation (Lee et al., 2014; Taboada-López et al., 2018b) was applied to determine the smallest ZnO-NPs size:

$$LODnm = \sqrt[3]{\frac{6 \times 3\sigma_{blank}}{R \times f_a \times \rho \times \pi}} \quad (1)$$

where 3σblank is three times the standard deviation of counts of ultrapure water blanks, R is the sensitivity of the detector (slope of the calibration curve of ionic Zn standard solutions), fa is the mass fraction of analysed metallic element in the nanoparticles, and ϱ is the density of the ZnO NPs
LOD value in ZnO-NPs size was 27 nm.
Accuracy has been assessed by spiking seafood samples with 30 nm ZnO-NPs at a concentration of 450 ng/L or 5.7 × 106 particles/mL, one for each batch of analysis, obtaining a mean particles recovery of 84.7±3% (4.8 × 106 detected for 5.7 × 106 spiked), confirming the effective characterization of NPs using spICP-MS analysis.

3.2.5 Dietary exposure

The estimated intake of ZnO-NPs and dissolved Zn calculated by assuming a meal of selected seafood products was evaluated for adults and children according to the method described in a previous paper (Grasso et al., 2020). Briefly, the estimated meal intake (EMI) (μg/kg b.w. per day) was determined according to the following equation.

$$EMI = (C \times MS)/BW$$

where C is the ZnO-NPs or dissolved Zn (mg/kg wet weight), M is the meal size (227 g for adults and 114 g for children), and BW is the body weight, considered as 16 kg for children (6 years) and 70 kg for adults (70 years)(Grasso et al., 2020; Pappalardo et al., 2020).
The Target Hazard Quotient (THQ) was used for evaluating if the intake of dissolved Zn derived from seafood consumption could represent a risk for human to develop chronic systemic effects during the lifetime, or if the ingestion rate is within the dietary reference intake needed to meet its physiological requirements. A THQ value below 1 means that the level of exposure is smaller than the oral reference dose (RfD), otherwise a daily exposure at this level is not likely to cause any deleterious effects during lifetime for human population. THQ is calculated according the following equation (3)(Pappalardo Am et al., 2017):

$$THQ = (EF \times ED \times IR \times C)/ (RfD \times BW \times AT)$$

where EF is the exposure frequency or number of exposure events per year of exposure (350 days/year); ED is the exposure duration (adults 26 years; children 6 years); IR is the average consumption of seafood for Italian population (applied as 12.16 g/capita/day for pelagic fish CT, CM and CA; 12.34 for molluscs CC); C is the metal concentration in the food (mg/Kg w.w.); RfD is the oral reference dose (0.3 mg/Kg day); BW is the body weight (the same used for EDI); and AT is the averaging time (equal to EF × ED).

3.2.6 Migration test for zinc and ZnO-NPs

According with decree of the Minister of Health of 21 March 1973 and its amendments, a migration test was performed to evaluate the contribution of the containers in releasing Zn or ZnO-NPs from the metal packages. Each packaging was subjected to a ten-day test at 40° C with the distilled water as a food simulant suitable for non-

acid food.
ICP-MS (NexION® 350D) was used to confirm the presence of Zn and ZnO-NPs in the aqueous simulant extract. The calibration standards were prepared covering the same range previously described and operation parameters are the same reported in Tables 1 and 2.
The reliability of ICP-MS method was evaluated by spiking a known concentration of Zn (10 μg/L) and ZnO-NPs (510 ng/L or 2.6 x 106 particles/mL) into the food simulant, obtaining recoveries of 92-95 % and 85-88 %, respectively.

3.2.7 Statistical Analysis

The IBM SPSS 20.0 software package (IBM, Armonk, NY, USA) was used to perform One-Way ANOVA and a post hoc Tukey test. Differences in ZnO-NPs, dissolved Zn levels, and estimated meal intake (EMI) were evaluated among processed seafood products.

3.3 Results and discussion

Currently, scientific knowledge about levels of human exposure from NPs, as well as their bioaccumulation and/or biomagnification potential along the food chain and the levels of exposure which could potentially harm human health, remains unknown. With this study we want to supply information regarding the characterization and quantification of ZnO-NPs, as well as the quantification of dissolved Zn, in canned seafood products belonging to different trophic level of the food chain. Furthermore, we provided the dietary exposure to ZnO-NPs and dissolved Zn of human population, adults of 70 years old and children of 6 years old, derived from consumption of the selected seafood.
All the chosen products were stored in metal packages, whereby they did not fall within active packages obtained by the introduction of engineered functional additives, such as ZnO-NPs

(Bumbudsanpharoke and Ko, 2015). Furthermore, the migration test did not revealed traces of ZnO-NPs and dissolved Zn and all the results were lower than the limit of detection achieved for both analytes, suggesting any migration from packages under the test conditions.

For the above reason, we supposed that the presence of ZnO-NPs, was driven by a bioaccumulation process which occurred in the species natural environment, where NPs can be found as naturally occurring or discharged by man-made materials, or by contamination during food processing at industrial level.

Table 3.3 and Figure 3.1 show results concerning the descriptive statistics of ZnO-NPs size distribution, ZnO-NPs concentrations, dissolved Zn and total Zn in the selected packaged seafood products. None of the samples reported concentrations below the calculated limit of detection in term of both size and concentration. Trace amounts of ZnO-NPs were found with concentrations range from 0.003 to 0.010 mg/Kg, and a mean size range from 61.3 and 78.6 nm. A clear bioaccumulation trend according to trophic level and size of seafood species was not observed, although mollusc were found to contain slightly higher concentrations and larger NPs size than other seafood species. In particular, CM revealed a most frequent size and a mean diameter significantly lower than those found in other seafood samples, with values of 50.8 and 61.3 nm, respectively. No significant differences have been found for the other seafood products, at most a weak trend highlighting a distribution size progressively higher according to the following order: CA < CT< CC. About ZnO-NPs concentrations, the number of ZnO-NPs/g does not differ significantly among food samples, observing a mean range of 5.51×10^6 - 9.97×10^6. This finding is in contrast to the ZnO-NPs concentration expressed as mg/Kg which resulted slightly higher in CC versus fish species. Although this result may appear conflicting, the conversion is de facto very affected by the mean diameter in addition to other factors.

Dissolved Zn determined by assessed with spICP-MS revealed

comparable concentrations to total Zn analysed with ICP-MS, confirming the efficiency of the alkaline digestion on the extraction of ionic Zn and ZnO-NPs. The same accumulation trend found for ZnO-NPs was observed more clearly for dissolved Zn, with similar concentrations in fish species (21.9-24.6 mg/kg) and higher concentrations in clam (33.7 mg/kg) were found. Although the concentrations of total Zn in the acid digests are slightly lower than those found in the alkaline digests, they are not statistically different when the mean values are compared.

Table 3.3. Descriptive statistics concerning the chemical characterization and quantification of ZnO-NPs in term of Most Frequent size, Mean Diameter, Number of ZnO particles/gram (ZnO-Ps/g), dissolved Zn (mg/Kg) and total Zn in packaged seafood products.

Canned Tuna	**Most Frequent size (nm)**	**Mean Diameter (nm)**	**Number of ZnO-Ps/g**	**ZnO-NPs mg/Kg**	**Dissolved[a] Zn mg/kg**	**Total[b] Zn mg/kg**
Mean	68.4	75.2	5.71×10^6	0.006	24.64	23.55
S.D.	4.48	3.40	1.23×10^6	0.002	1.771	2.745
Min.	60.0	69.0	4.03×10^6	0.003	21.09	19.14
Max.	75.0	80.0	8.13×10^6	0.010	27.52	28.41
Canned Mackerel	**Most Frequent size (nm)**	**Mean Diameter (nm)**	**Number of ZnO-Ps/g**	**ZnO-NPs mg/Kg**	**Dissolved[a] Zn mg/kg**	**Total[b] Zn mg/kg**
Mean	50.8	61.3	5.51×10^6	0.003	24.57	22.94
S.D.	10.9	7.20	0.98×10^6	0.001	4.390	1.458
Min.	31.0	47.0	4.28×10^6	0.001	18.51	18.84
Max.	71.0	73.0	7.65×10^6	0.005	31.99	25.45
Canned Anchovy	**Most Frequent size (nm)**	**Mean Diameter (nm)**	**Number of ZnO-Ps/g**	**ZnO-NPs mg/Kg**	**Dissolved[a] Zn mg/kg**	**Total[b] Zn mg/kg**
Mean	62.8	72.3	9.97×10^6	0.009	21.95	19.41
S.D.	5.31	3.81	13.1×10^6	0.010	2.578	3.415
Min.	56.0	67.0	4.23×10^6	0.003	17.44	16.94
Max.	71.0	78.0	44.7×10^6	0.035	25.95	24.25
Canned Clam	**Most Frequent size (nm)**	**Mean Diameter (nm)**	**Number of ZnO-Ps/g**	**ZnO-NPs mg/Kg**	**Dissolved[a] Zn mg/kg**	**Total[b] Zn mg/kg**
Mean	69.6	78.6	8.44×10^6	0.010	33.70	31.15
S.D.	3.57	2.70	0.94×10^6	0.001	2.180	2.415
Min.	65.0	75.0	7.16×10^6	0.008	28.94	27.41
Max.	77.0	83.0	10.6×10^6	0.011	36.61	39.24

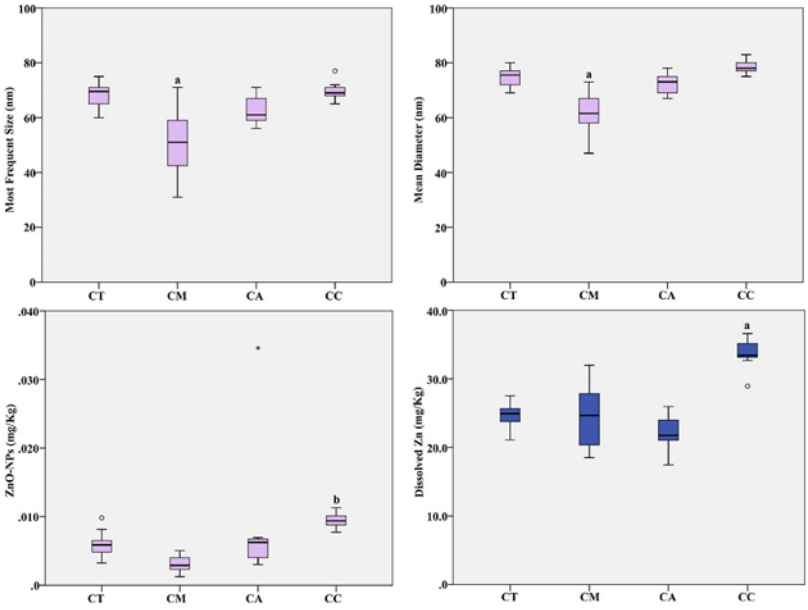

Figure 3.1. Box-plot distribution of ZnO-NPs most frequent size (nm), mean diameter (nm), ZnO-NPs (mg/Kg) and dissolved Zn (mg/Kg). Legend: CT, canned tuna; CM, canned mackerel; CA, canned anchovy; CC, canned clam; a, $p < 0.001$ vs. all; b, $p < 0.05$ vs. all. °Outliers values of the distribution. *Extreme values of the distribution.

There are scarce literature regarding ZnO-NPs concentrations in the natural environment and nothing about the toxic effects of naturally occurring NPs based on their actual size. Only one published study deals with the quantification and characterization of ZnO-NPs in living organisms. Xu et al. (2020) investigated on metal-based NPs in mollusks specie from an offshore aquaculture facility by performing an enzyme digestion and spICP-MS analysis. The authors have reported ZnO-NPs concentrations (ZnO-NPs/g) in clams comparable to those found in the clam samples analysed in our study (8.80 × 106 vs 8.44 × 106) in terms of number, but they have reported a slightly higher diameter (97.8 ± 6.3 vs 78.6 ± 2.7 nm) and a lower content of dissolved Zn (13.8 ± 0.69 vs 33.7 ± 2.18 mg/kg). Taking into account data from seawater bioconcentration factor, where ZnO-NPs were

found at concentration of 4.6 × 106 particle/g and with a mean size of 126 nm, the authors suggested that the smaller is the NPs diameter in the surrounding seawater and the easier is the accumulation in mollusks tissues, especially in the gills and digestive glands. Furthermore, clam has the lower NPs bioconcentration factor when comparing to other mollusks species such as oysters, mussels, scallops and ark shells, probably due to their highest efflux rate.

On the other hand, total Zn is among the most studied micronutrients in seafood. A wide range of Zn concentrations in fresh and canned seafood has been reported in the literature, depending on the fishing area and the degree of environmental contamination. For example, concentrations ranging from 2 to 37 mg/kg w.w. have been reported for fresh fish (Bilandžić et al., 2014; Canli and Atli, 2003; Copat et al., 2018; Guérin et al., 2011; Leblanc et al., 2005) to levels of 106 mg/kg in most industrialized coastal areas (Uluozlu et al., 2007). Similarly, Zn concentration in shellfish ranges from 7 to 30 mg/kg w.w. (Bilandžić et al., 2014; Copat et al., 2018; Guérin et al., 2011; Liu et al., 2018), while in canned seafood it ranges from 12 to 65 mg/kg w.w.,(Bilandžić et al., 2014; Hosseini et al., 2015; Noël et al., 2012; Yabanlı et al., 2021). Overall, the total Zn content in the analysed seafood products is in the average of the concentrations reported in the literature. Nevertheless, we cannot estimate how much industrial processing has contributed to increasing or decreasing the original Zn contents of the concerned products.

In this study, we also estimated the intake of ZnO-NPs and dissolved Zn derived from a meal (EMI), calculated for adults (70 years old) and children (6 years old), and results are showed in Table 4 and Figure 3. The ZnO-NPs intake derived from a meal does not differ significantly among seafood products and it ranges from 0.010 to 0.031 μg/kg b.w. in adults, and from 0.022 to 0.067 μg/kg b.w. in children. Conversely, the intake of dissolved Zn is significantly higher if a meal of CC versus the fish products is assumed, with values of 109.3 μg/kg b.w. for adults, and 240.1 μg/kg b.w. for children. The intake of dissolved Zn does not differ significantly

among the other processed seafood, and the results range from 71.7 to 79.9 μg/kg b.w. for adults, and from 156.4 to 175.6 μg/kg b.w. for children. Furthermore, the chosen lifetime exposure scenario highlights an intake of dissolved Zn below the oral daily reference dose (300 μg/kg b.w.) and no risk to develop chronic systemic effects due to an over intake of Zn during the exposure duration (THQ below 1).

Table 3.4. Descriptive statistics of estimated meal intake (EMI μg/Kg b.w.) calculated for adults (70 years) and children (6 years) concerning the ZnO-NPs and dissolved Zn and, THQ calculated for dissolved Zn.

Canned Tuna	**EMI Adult ZnO-NPs**	**EMI Child ZnO-NPs**	**EMI Adult Dissolved Zn**	**THQ Adult Dissolved Zn**	**EMI Child Dissolved Zn**	**THQ Child Dissolved Zn**
Mean	0.019	0.042	79.90	1.43×10^{-3}	175.6	6.24×10^{-3}
S.D.	0.006	0.012	5.743	/	12.62	/
Min.	0.011	0.023	68.41	/	150.3	/
Max.	0.032	0.070	89.25	/	196.1	/
Canned Mackerel	**EMI Adult ZnO-NPs**	**EMI Child ZnO-NPs**	**EMI Adult Dissolved Zn**	**THQ Adult Dissolved Zn**	**EMI Child Dissolved Zn**	**THQ Child Dissolved Zn**
Mean	0.010	0.022	79.67	1.42×10^{-3}	175.0	6.22×10^{-3}
S.D.	0.004	0.008	14.24	/	31.28	/
Min.	0.004	0.009	60.03	/	131.9	/
Max.	0.016	0.036	103.7	/	227.9	/
Canned Anchovy	**EMI Adult ZnO-NPs**	**EMI Child ZnO-NPs**	**EMI Adult Dissolved Zn**	**THQ Adult Dissolved Zn**	**EMI Child Dissolved Zn**	**THQ Child Dissolved Zn**
Mean	0.028	0.061	71.17	1.27×10^{-3}	156.4	5.56×10^{-3}
S.D.	0.032	0.071	8.360	/	18.37	/
Min.	0.009	0.021	56.56	/	124.3	/
Max.	0.112	0.246	84.14	/	184.9	/
Canned Clam	**EMI Adult ZnO-NPs**	**EMI Child ZnO-NPs**	**EMI Adult Dissolved Zn**	**THQ Adult Dissolved Zn**	**EMI Child Dissolved Zn**	**THQ Child Dissolved Zn**
Mean	0.031	0.067	109.3	1.95×10^{-3}	240.1	8.54×10^{-3}
S.D.	0.004	0.008	7.070	/	15.53	/
Min.	0.025	0.055	93.84	/	206.2	/
Max.	0.037	0.080	118.7	/	260.9	/

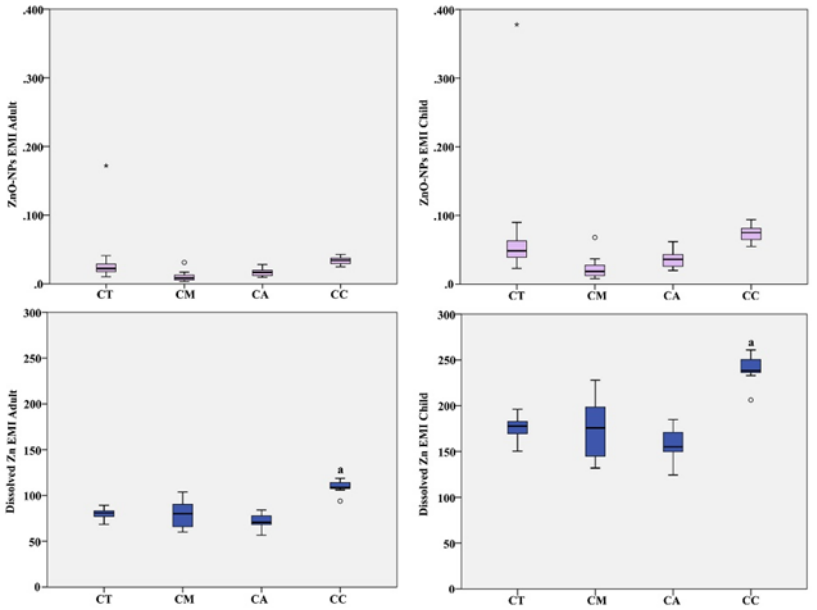

Figure 3.2. Box-plot distribution of estimated meal intake (EMI μg/Kg b.w.) of ZnO-NPs and dissolved Zn concentration calculated for adults (70 years) and children (6 years). Legend: CT, canned tuna; CM, canned mackerel; CA, canned anchovy; CC, canned clam; a, $p < 0.001$ vs. all. ° Outliers values of the distribution. * Extreme values of the distribution.

In vivo and in vitro studies have pointed out that ZnO-NPs have great effects on the activity of antioxidant enzymes and on the mRNA expression. ZnO-NPs exert toxicity in different ways such as production of ROS and inhibition or enhancement of the cells antioxidant system (Asghar et al., 2018; Hao and Chen, 2012; Khosravi-Katuli et al., 2018). Under ZnO-NPs exposure, lipid peroxidation (LPO) levels are also frequently used as a biomarker of the oxidative stress through malondialdehyde (MDA) and the thiobarbituric acid reactive substances (TBARS), which was found to be usually increased moreover the exposure time was longer (Abdelazim et al., 2018; Alkaladi, 2019; Ghafari Farsani et al., 2017; Hao et al., 2013; Hao and Chen, 2012; Kaya et al., 2015; Miranda et

al., 2016). Furthermore, ZnO-NPs showed more potent oxidative effects than bulk-ZnO at the same exposure dose (Hao et al., 2013). A dose-dependent toxicity was also found for ZnO-NPs (<35 nm and <100 nm) and for bulk ZnO, but the highest dependence was found for NPs with the lowest diameter (Kaya et al., 2015; Xiong et al., 2011).

Adverse health effects due to exposure to nanoparticles are poorly understood, in particular those resulting from oral exposure, which is expected to increase as a result of a wider commercialization of NMs as part of the modern diet (Anastasi et al., 2019). In vivo studies on mammals highlighted ZnO-NPs hepatotoxicity after oral exposure (Jia et al., 2017; Wei et al., 2016) since their ability to cross the placental barrier and to be accumulated into fetuses (Teng et al., 2019). In case of metal-based and metal oxide-based NPs, toxicity is at least partly due to the specific properties related to the small size and consequent high surface activity of NPs, while effects may be further enhanced by the release of free metal ions (Auffan et al., 2009). Furthermore, the formation of NPs aggregates increases during the exposure period (Benavides et al., 2016), and it is dependent on the NP nature (Vale et al., 2016) and on the presence of organic matter (Grillo et al., 2015; Jeon et al., 2020; Ju-Nam and Lead, 2008).

Beyond the toxicity studied in the laboratory, the most important open question is what happens if the ingested ZnO-NPs enters in the gastrointestinal tissues, where their composition, size and aggregation state may be altered. In addition, the effect of food matrix on the properties of gastrointestinal fluids can lead to changes on the NPs fate after oral ingestion (McClements et al., 2017). Interactions between ZnO and food components, such as proteins and saccharides, have been demonstrated, forming particle–matrix corona (nanocorona covered by matrices) (Jeon et al., 2020). The same studies highlighted complete dissolution of ZnO-NPs in simulated gastric fluid or under fluid at low pHs (Cho et al., 2013; Gomez-Gomez et al., 2020; He et al., 2020; Sohal et al., 2018), and

have reported a faster dissolution for ZnO-NPs of smaller sizes (He et al., 2020). The high dissolution rate of ZnO-NPs allows a better tissue adsorption and a more extensive organ distribution if compared with other metallic NPs (Cho et al., 2013; He et al., 2020). As a consequence, the ionization of ZnO-NPs in biological fluids can be the main cause of toxicity (Cho et al., 2011), but potential toxicity resulting from ZnO particles cannot be completely excluded since a small portion of ZnO particles fate was also observed after intestinal transit (Jeon et al., 2020).

On the other end, Zn is a well-known micronutrient involved in several cellular and metabolic functions (Andreini and Bertini, 2012; Lambert et al., 2018), and the balance between essentiality and toxicity is regulated through the binding to specific cellular sites (Fan et al., 2013). Adequate intake of Zn are particularly recommended in the early stages of life for the normal growth and development, and for the cognitive function (Ackland and Michalczyk, 2016).Adequate Zn levels are also crucial for a proper functioning of a large number of macromolecules and enzymes (over 300 enzymic reactions) (Król et al., 2017). This element is found in all body tissues, i.e. in muscle and bone (85% of the whole body zinc content), in the skin (11%) and in all other tissues; and is located at intracellular level, mainly in the nucleus, cytoplasm and cell membrane (Tapiero and Tew, 2003). Zn stabilizes the cell membrane structure, contributing to the structure of the SOD and maintaining the metallothionein tissue concentrations. Two mechanisms have been elucidated for its action as an antioxidant: the protection of sulfhydryl groups against oxidation, and the inhibition of the production of reactive oxygens by transition metals (Bray and Bettger, 1990). Zn ensures a proper functioning of the immune system response, being involved in generating innate as well as acquired antiviral immune response (Read et al., 2019). Conversely, Zn dietary deficiency is associated with development of cardiovascular diseases (Choi et al., 2018), chronic liver damage, and metabolic abnormalities (Himoto and Masaki, 2018). In addition, subcellular and organ distribution of

metals in the organism may reflect the internal processing of metal accumulation and provide valuable information about metal toxicity and tolerance.

3.4 Conclusions

What about the balance between benefit and risk derived from the ingestion of Zn in its several form? The question is still open since the total amount of human oral intake of Zn derived from a nanoparticle structure is still unexplored. To date, with the available scientific literature and the analytical instrumentation available in the market, it is not possible to discern the fraction of ion Zinc released by the nanoparticle, which is notably more reactive than other chemical forms. Thus, although the Target Hazard Quotient indicate no risk to develop chronic systemic effects during the lifetime, a specific reference dose for ion Zn derived from a nanoparticle structure should be estimated. Overall, these findings on seafood show how trace amount ZnO-NPs can be bioaccumulated and then transferred to human, representing a first step in oral exposure evaluation.

The determination of the fate of ZnO-NPs, ZnO-NP aggregates/agglomerates, and Zn ions will be important to better understand resulting toxic effects and also the relationship with the matrix type. Indeed, separating NPs and ionized forms from complex food without affecting intact particle size and morphology is challenging because there are numerous factors that can influence the NPs behavior: amount of composite, extraction time, sample pH. For this reason, the development of sensitive advanced methodologies, such as spICP-MS, plays a predominant role in this analytical research.

References

- Abdelazim, A.M., Saadeldin, I.M., Swelum, A.A.-A., Afifi, M.M., Alkaladi, A., 2018. Oxidative Stress in the Muscles of the Fish Nile Tilapia Caused by Zinc Oxide Nanoparticles and Its Modulation by Vitamins C and E. Oxid. Med. Cell. Longev. 2018, 6926712. https://doi.org/10.1155/2018/6926712
- Abu-Salah, K.M., Alrokyan, S.A., Khan, M.N., Ansari, A.A., 2010. Nanomaterials as analytical tools for genosensors. Sensors 10, 963–993. https://doi.org/10.3390/s100100963
- Ackland, M.L., Michalczyk, A.A., 2016. Zinc and infant nutrition. Arch. Biochem. Biophys., The Cutting Edge of Zinc Biology 611, 51–57. https://doi.org/10.1016/j.abb.2016.06.011
- Ahmed, J., Arfat, Y.A., Castro-Aguirre, E., Auras, R., 2016. Mechanical, structural and thermal properties of Ag-Cu and ZnO reinforced polylactide nanocomposite films. Int. J. Biol. Macromol. 86, 885–892. https://doi.org/10.1016/j.ijbiomac.2016.02.034
- Akhtar, M.J., Ahamed, M., Kumar, S., Khan, M.M., Ahmad, J., Alrokayan, S.A., 2012. Zinc oxide nanoparticles selectively induce apoptosis in human cancer cells through reactive oxygen species. Int. J. Nanomedicine 7, 845–857. https://doi.org/10.2147/IJN.S29129
- Alkaladi, A., 2019. Vitamins E and C ameliorate the oxidative stresses induced by zinc oxide nanoparticles on liver and gills of Oreochromis niloticus. Saudi J. Biol. Sci. 26, 357–362. https://doi.org/10.1016/j.sjbs.2018.07.001
- Andreini, C., Bertini, I., 2012. A bioinformatics view of zinc enzymes. J. Inorg. Biochem. 111, 150–156. https://doi.org/10.1016/j.jinorgbio.2011.11.020
- Arfat, Y.A., Ahmed, J., Al Hazza, A., Jacob, H., Joseph, A., 2017. Comparative effects of untreated and 3-methacryloxypropyltrimethoxysilane treated ZnO nanoparticle reinforcement on properties of polylactide-based nanocomposite films. Int. J. Biol. Macromol. 101, 1041–1050. https://doi.org/10.1016/j.ijbiomac.2017.03.176
- Asghar, M.S., Qureshi, N.A., Jabeen, F., Khan, M.S., Shakeel, M., Chaudhry, A.S., 2018. Ameliorative Effects of Selenium in ZnO NP-Induced Oxidative Stress and Hematological Alterations in Catla catla. Biol. Trace Elem. Res. 186, 279–287. https://doi.org/10.1007/s12011-018-1299-9
- Auffan, M., Rose, J., Wiesner, M.R., Bottero, J.-Y., 2009. Chemical stability of metallic nanoparticles: a parameter controlling their potential cellular toxicity in vitro. Environ. Pollut. Barking Essex 1987 157, 1127–1133. https://doi.org/10.1016/j.envpol.2008.10.002
- Barros, J., Grenho, L., Fontenente, S., Manuel, C.M., Nunes, O.C., Melo, L.F., Monteiro, F.J., Ferraz, M.P., 2017. Staphylococcus aureus and Escherichia

coli dual-species biofilms on nanohydroxyapatite loaded with CHX or ZnO nanoparticles. J. Biomed. Mater. Res. A 105, 491–497. https://doi.org/10.1002/jbm.a.35925

- Beak, S., Kim, H., Song, K.B., 2017. Characterization of an Olive Flounder Bone Gelatin-Zinc Oxide Nanocomposite Film and Evaluation of Its Potential Application in Spinach Packaging. J. Food Sci. 82, 2643–2649. https://doi.org/10.1111/1750-3841.13949
- Benavides, M., Fernández-Lodeiro, J., Coelho, P., Lodeiro, C., Diniz, M.S., 2016. Single and combined effects of aluminum (Al2O3) and zinc (ZnO) oxide nanoparticles in a freshwater fish, Carassius auratus. Environ. Sci. Pollut. Res. Int. 23, 24578–24591. https://doi.org/10.1007/s11356-016-7915-3
- Bondarenko, O., Juganson, K., Ivask, A., Kasemets, K., Mortimer, M., Kahru, A., 2013. Toxicity of Ag, CuO and ZnO nanoparticles to selected environmentally relevant test organisms and mammalian cells in vitro: a critical review. Arch. Toxicol. 87, 1181–1200. https://doi.org/10.1007/s00204-013-1079-4
- Bray, T.M., Bettger, W.J., 1990. The physiological role of zinc as an antioxidant. Free Radic. Biol. Med. 8, 281–291. https://doi.org/10.1016/0891-5849(90)90076-U
- Bumbudsanpharoke, N., Ko, S., 2015. Nano-Food Packaging: An Overview of Market, Migration Research, and Safety Regulations. J. Food Sci. 80, R910–R923. https://doi.org/10.1111/1750-3841.12861
- Chakraborty, C., Sharma, A.R., Sharma, G., Lee, S.-S., 2016. Zebrafish: A complete animal model to enumerate the nanoparticle toxicity. J. Nanobiotechnology 14, 65. https://doi.org/10.1186/s12951-016-0217-6
- Chandrasekaran, M., Pandurangan, M., 2016. In Vitro Selective Anti-Proliferative Effect of Zinc Oxide Nanoparticles Against Co-Cultured C2C12 Myoblastoma Cancer and 3T3-L1 Normal Cells. Biol. Trace Elem. Res. 172, 148–154. https://doi.org/10.1007/s12011-015-0562-6
- Chia, S.L., Leong, D.T., 2016. Reducing ZnO nanoparticles toxicity through silica coating. Heliyon 2, e00177. https://doi.org/10.1016/j.heliyon.2016.e00177
- Cho, W.-S., Duffin, R., Howie, S.E.M., Scotton, C.J., Wallace, W.A.H., Macnee, W., Bradley, M., Megson, I.L., Donaldson, K., 2011. Progressive severe lung injury by zinc oxide nanoparticles; the role of Zn2+ dissolution inside lysosomes. Part. Fibre Toxicol. 8, 27. https://doi.org/10.1186/1743-8977-8-27
- Cho, W.-S., Kang, B.-C., Lee, J.K., Jeong, J., Che, J.-H., Seok, S.H., 2013. Comparative absorption, distribution, and excretion of titanium dioxide and zinc oxide nanoparticles after repeated oral administration. Part. Fibre Toxicol. 10, 9. https://doi.org/10.1186/1743-8977-10-9

- Choi, S., Liu, X., Pan, Z., 2018. Zinc deficiency and cellular oxidative stress: prognostic implications in cardiovascular diseases. Acta Pharmacol. Sin. 39, 1120–1132. https://doi.org/10.1038/aps.2018.25
- Chu, Z., Zhao, T., Li, L., Fan, J., Qin, Y., 2017. Characterization of Antimicrobial Poly (Lactic Acid)/Nano-Composite Films with Silver and Zinc Oxide Nanoparticles. Mater. Basel Switz. 10. https://doi.org/10.3390/ma10060659
- Dehghani, M.H., Mahdavi, P., Heidarinejad, Z., 2018. The experimental data of investigating the efficiency of zinc oxide nanoparticles technology under ultraviolet radiation (UV/ZnO) to remove Acid - 32 - Cyanine 5R from aqueous solutions. Data Brief 21, 767–774. https://doi.org/10.1016/j.dib.2018.10.037
- Díez-Pascual, A.M., Díez-Vicente, A.L., 2014. ZnO-reinforced poly(3-hydroxybutyrate-co-3-hydroxyvalerate) bionanocomposites with antimicrobial function for food packaging. ACS Appl. Mater. Interfaces 6, 9822–9834. https://doi.org/10.1021/am502261e
- EC, 2013. Communication from the Commission to the European Parliament, the Council and the European Economic and Social Committee. Second regulatory review on nanomaterials. Brussels, 3.10.2012, COM(2012) 572 final.
- Elhaj Baddar, Z., Unrine, J.M., 2018. Functionalized-ZnO-Nanoparticle Seed Treatments to Enhance Growth and Zn Content of Wheat (Triticum aestivum) Seedlings. J. Agric. Food Chem. 66, 12166–12178. https://doi.org/10.1021/acs.jafc.8b03277
- Emamifar, A., Mohammadizadeh, M., 2015. Preparation and Application of LDPE/ZnO Nanocomposites for Extending Shelf Life of Fresh Strawberries. Food Technol. Biotechnol. 53, 488–495. https://doi.org/10.17113/ftb.53.04.15.3817
- Fan, W., Li, Q., Yang, X., Zhang, L., 2013. Zn subcellular distribution in liver of goldfish (carassius auratus) with exposure to zinc oxide nanoparticles and mechanism of hepatic detoxification. PloS One 8, e78123. https://doi.org/10.1371/journal.pone.0078123
- FAO, 2018. CFR - Code of Federal Regulations Title 21 [WWW Document]. URL https://www.accessdata.fda.gov/scripts/cdrh/cfdocs/cfcfr/CFRSearch.cfm?CFRPart=182 (accessed 3.21.19).
- FDA, 2021. Food Additive Status List [WWW Document]. FDA. URL https://www.fda.gov/food/food-additives-petitions/food-additive-status-list (accessed 9.23.21).
- Ghafari Farsani, H., Binde Doria, H., Jamali, H., Hasanpour, S., Mehdipour, N., Rashidiyan, G., 2017. The protective role of vitamin E on Oreochromis niloticus exposed to ZnONP. Ecotoxicol. Environ. Saf. 145, 1–7. https://doi.org/10.1016/j.ecoenv.2017.07.005

- Girigoswami, K., Viswanathan, M., Murugesan, R., Girigoswami, A., 2015. Studies on polymer-coated zinc oxide nanoparticles: UV-blocking efficacy and in vivo toxicity. Mater. Sci. Eng. C Mater. Biol. Appl. 56, 501–510. https://doi.org/10.1016/j.msec.2015.07.017
- Gomez-Gomez, B., Perez-Corona, M.T., Madrid, Y., 2020. Using single-particle ICP-MS for unravelling the effect of type of food on the physicochemical properties and gastrointestinal stability of ZnONPs released from packaging materials. Anal. Chim. Acta 1100, 12–21. https://doi.org/10.1016/j.aca.2019.11.063
- Grasso, A., Ferrante, M., Arena, G., Salemi, R., Zuccarello, P., Fiore, M., Copat, C., 2021. Chemical Characterization and Quantification of Silver Nanoparticles (Ag-NPs) and Dissolved Ag in Seafood by Single Particle ICP-MS: Assessment of Dietary Exposure. Int. J. Environ. Res. Public. Health 18, 4076. https://doi.org/10.3390/ijerph18084076
- Grasso, A., Ferrante, M., Zuccarello, P., Filippini, T., Arena, G., Fiore, M., Cristaldi, A., Conti, G.O., Copat, C., 2020. Chemical Characterization and Quantification of Titanium Dioxide Nanoparticles (TiO_2-NPs) in Seafood by Single-Particle ICP-MS: Assessment of Dietary Exposure. Int. J. Environ. Res. Public. Health 17, E9547. https://doi.org/10.3390/ijerph17249547
- Grillo, R., Rosa, A.H., Fraceto, L.F., 2015. Engineered nanoparticles and organic matter: a review of the state-of-the-art. Chemosphere 119, 608–619. https://doi.org/10.1016/j.chemosphere.2014.07.049
- Gurunathan, B., Ravi, A., 2015. Biodiesel production from waste cooking oil using copper doped zinc oxide nanocomposite as heterogeneous catalyst. Bioresour. Technol. 188, 124–127. https://doi.org/10.1016/j.biortech.2015.01.012
- Hao, L., Chen, L., 2012. Oxidative stress responses in different organs of carp (Cyprinus carpio) with exposure to ZnO nanoparticles. Ecotoxicol. Environ. Saf. 80, 103–110. https://doi.org/10.1016/j.ecoenv.2012.02.017
- Hao, L., Chen, L., Hao, J., Zhong, N., 2013. Bioaccumulation and sub-acute toxicity of zinc oxide nanoparticles in juvenile carp (Cyprinus carpio): a comparative study with its bulk counterparts. Ecotoxicol. Environ. Saf. 91, 52–60. https://doi.org/10.1016/j.ecoenv.2013.01.007
- He, L., Liu, Y., Mustapha, A., Lin, M., 2011. Antifungal activity of zinc oxide nanoparticles against Botrytis cinerea and Penicillium expansum. Microbiol. Res. 166, 207–215. https://doi.org/10.1016/j.micres.2010.03.003
- He, X., Zhang, H., Shi, H., Liu, W., Sahle-Demessie, E., 2020. Fates of Au, Ag, ZnO, and CeO2 Nanoparticles in Simulated Gastric Fluid Studied using Single-Particle-Inductively Coupled Plasma-Mass Spectrometry. J. Am. Soc. Mass Spectrom. 31, 2180–2190. https://doi.org/10.1021/jasms.0c00278
- Himoto, T., Masaki, T., 2018. Associations between Zinc Deficiency and Metabolic Abnormalities in Patients with Chronic Liver Disease. Nutrients 10, 88. https://doi.org/10.3390/nu10010088

- Hou, J., Wu, Y., Li, X., Wei, B., Li, S., Wang, X., 2018. Toxic effects of different types of zinc oxide nanoparticles on algae, plants, invertebrates, vertebrates and microorganisms. Chemosphere 193, 852–860. https://doi.org/10.1016/j.chemosphere.2017.11.077
- Jeon, Y.-R., Yu, J., Choi, S.-J., 2020. Fate Determination of ZnO in Commercial Foods and Human Intestinal Cells. Int. J. Mol. Sci. 21, 433. https://doi.org/10.3390/ijms21020433
- Jue, M., Lee, S., Paulson, B., Namgoong, J.-M., Yu, H.Y., Kim, G., Jeon, S., Shin, D.-M., Choo, M.-S., Joo, J., Moon, Y., Pack, C.-G., Kim, J.K., 2019. Optimization of ZnO Nanorod-Based Surface Enhanced Raman Scattering Substrates for Bio-Applications. Nanomater. Basel Switz. 9. https://doi.org/10.3390/nano9030447
- Ju-Nam, Y., Lead, J.R., 2008. Manufactured nanoparticles: an overview of their chemistry, interactions and potential environmental implications. Sci. Total Environ. 400, 396–414. https://doi.org/10.1016/j.scitotenv.2008.06.042
- Kaya, H., Aydın, F., Gürkan, M., Yılmaz, S., Ates, M., Demir, V., Arslan, Z., 2015. Effects of zinc oxide nanoparticles on bioaccumulation and oxidative stress in different organs of tilapia (Oreochromis niloticus). Environ. Toxicol. Pharmacol. 40, 936–947. https://doi.org/10.1016/j.etap.2015.10.001
- Khosravi-Katuli, K., Lofrano, G., Pak Nezhad, H., Giorgio, A., Guida, M., Aliberti, F., Siciliano, A., Carotenuto, M., Galdiero, E., Rahimi, E., Libralato, G., 2018. Effects of ZnO nanoparticles in the Caspian roach (Rutilus rutilus caspicus). Sci. Total Environ. 626, 30–41. https://doi.org/10.1016/j.scitotenv.2018.01.085
- Król, A., Pomastowski, P., Rafińska, K., Railean-Plugaru, V., Buszewski, B., 2017. Zinc oxide nanoparticles: Synthesis, antiseptic activity and toxicity mechanism. Adv. Colloid Interface Sci., Recent nanotechnology and colloid science development for biomedical applications 249, 37–52. https://doi.org/10.1016/j.cis.2017.07.033
- Lambert, S.A., Jolma, A., Campitelli, L.F., Das, P.K., Yin, Y., Albu, M., Chen, X., Taipale, J., Hughes, T.R., Weirauch, M.T., 2018. The Human Transcription Factors. Cell 172, 650–665. https://doi.org/10.1016/j.cell.2018.01.029
- Lee, S., Bi, X., Reed, R.B., Ranville, J.F., Herckes, P., Westerhoff, P., 2014. Nanoparticle Size Detection Limits by Single Particle ICP-MS for 40 Elements. Environ. Sci. Technol. 48, 10291–10300. https://doi.org/10.1021/es502422v
- MacDonald, R., 2000. The Role of Zinc in Growth and Cell Proliferation. J. Nutr. 130, 1500S-1508S. https://doi.org/10.1093/jn/130.5.1500S
- McClements, D.J., Xiao, H., Demokritou, P., 2017. Physicochemical and colloidal aspects of food matrix effects on gastrointestinal fate of ingested inorganic nanoparticles. Adv. Colloid Interface Sci. 246, 165–180. https://doi.org/10.1016/j.cis.2017.05.010

- Miranda, R.R., Damaso da Silveira, A.L.R., de Jesus, I.P., Grötzner, S.R., Voigt, C.L., Campos, S.X., Garcia, J.R.E., Randi, M. a. F., Ribeiro, C.A.O., Filipak Neto, F., 2016. Effects of realistic concentrations of TiO_2 and ZnO nanoparticles in Prochilodus lineatus juvenile fish. Environ. Sci. Pollut. Res. Int. 23, 5179–5188. https://doi.org/10.1007/s11356-015-5732-8
- Pappalardo Am, Copat C, Ferrito V, Grasso A, Ferrante M, 2017. Heavy metal content and molecular species identification in canned tuna: insights into human food safety. Mol. Med. Rep. 15, 3430–3437. https://doi.org/10.3892/mmr.2017.6376
- Pappalardo, A.M., Copat, C., Raffa, A., Rossitto, L., Grasso, A., Fiore, M., Ferrante, M., Ferrito, V., 2020. Fish-Based Baby Food Concern—From Species Authentication to Exposure Risk Assessment. Molecules 25, 3961. https://doi.org/10.3390/molecules25173961
- Raliya, R., Chadha, T.S., Hadad, K., Biswas, P., 2016. Perspective on nanoparticle technology for biomedical use. Curr. Pharm. Des. 22, 2481–2490.
- Read, S.A., Obeid, S., Ahlenstiel, C., Ahlenstiel, G., 2019. The Role of Zinc in Antiviral Immunity. Adv. Nutr. Bethesda Md 10, 696–710. https://doi.org/10.1093/advances/nmz013
- Sohal, I.S., Cho, Y.K., O'Fallon, K.S., Gaines, P., Demokritou, P., Bello, D., 2018. Dissolution Behavior and Biodurability of Ingested Engineered Nanomaterials in the Gastrointestinal Environment. ACS Nano 12, 8115–8128. https://doi.org/10.1021/acsnano.8b02978
- Taboada-López, M.V., Herbello-Hermelo, P., Domínguez-González, R., Bermejo-Barrera, P., Moreda-Piñeiro, A., 2019. Enzymatic hydrolysis as a sample pre-treatment for titanium dioxide nanoparticles assessment in surimi (crab sticks) by single particle ICP-MS. Talanta 195, 23–32. https://doi.org/10.1016/j.talanta.2018.11.023
- Taboada-López, M.V., Iglesias-López, S., Herbello-Hermelo, P., Bermejo-Barrera, P., Moreda-Piñeiro, A., 2018a. Ultrasound assisted enzymatic hydrolysis for isolating titanium dioxide nanoparticles from bivalve mollusk before sp-ICP-MS. Anal. Chim. Acta 1018, 16–25. https://doi.org/10.1016/j.aca.2018.02.075
- Taboada-López, M.V., Iglesias-López, S., Herbello-Hermelo, P., Bermejo-Barrera, P., Moreda-Piñeiro, A., 2018b. Ultrasound assisted enzymatic hydrolysis for isolating titanium dioxide nanoparticles from bivalve mollusk before sp-ICP-MS. Anal. Chim. Acta 1018, 16–25. https://doi.org/10.1016/j.aca.2018.02.075
- Tapiero, H., Tew, K.D., 2003. Trace elements in human physiology and pathology: zinc and metallothioneins. Biomed. Pharmacother. Biomedecine Pharmacother. 57, 399–411.
- Tighe-Neira, R., Carmora, E., Recio, G., Nunes-Nesi, A., Reyes-Diaz, M., Alberdi, M., Rengel, Z., Inostroza-Blancheteau, C., 2018. Metallic

nanoparticles influence the structure and function of the photosynthetic apparatus in plants. Plant Physiol. Biochem. PPB 130, 408–417. https://doi.org/10.1016/j.plaphy.2018.07.024

- Vale, G., Mehennaoui, K., Cambier, S., Libralato, G., Jomini, S., Domingos, R.F., 2016. Manufactured nanoparticles in the aquatic environment-biochemical responses on freshwater organisms: A critical overview. Aquat. Toxicol. Amst. Neth. 170, 162–174. https://doi.org/10.1016/j.aquatox.2015.11.019
- Vandebriel, R.J., De Jong, W.H., 2012. A review of mammalian toxicity of ZnO nanoparticles. Nanotechnol. Sci. Appl. 5, 61–71. https://doi.org/10.2147/NSA.S23932
- Xiong, D., Fang, T., Yu, L., Sima, X., Zhu, W., 2011. Effects of nano-scale TiO_2, ZnO and their bulk counterparts on zebrafish: acute toxicity, oxidative stress and oxidative damage. Sci. Total Environ. 409, 1444–1452. https://doi.org/10.1016/j.scitotenv.2011.01.015
- Xu, L., Wang, Z., Zhao, J., Lin, M., Xing, B., 2020a. Accumulation of metal-based nanoparticles in marine bivalve mollusks from offshore aquaculture as detected by single particle ICP-MS. Environ. Pollut. 260, 114043. https://doi.org/10.1016/j.envpol.2020.114043
- Xu, L., Wang, Z., Zhao, J., Lin, M., Xing, B., 2020b. Accumulation of metal-based nanoparticles in marine bivalve mollusks from offshore aquaculture as detected by single particle ICP-MS. Environ. Pollut. 260, 114043. https://doi.org/10.1016/j.envpol.2020.114043
- Yin, C., Zhao, W., Liu, Rui, Liu, Rong, Wang, Z., Zhu, L., Chen, W., Liu, S., 2017. TiO_2 particles in seafood and surimi products: Attention should be paid to their exposure and uptake through foods. Chemosphere 188, 541–547. https://doi.org/10.1016/j.chemosphere.2017.08.168
- Zhang, Y., Leu, Y.-R., Aitken, R.J., Riediker, M., 2015. Inventory of Engineered Nanoparticle-Containing Consumer Products Available in the Singapore Retail Market and Likelihood of Release into the Aquatic Environment. Int. J. Environ. Res. Public. Health 12, 8717–8743. https://doi.org/10.3390/ijerph120808717
- Zhou, Q., Liu, L., Liu, N., He, B., Hu, L., Wang, L., 2020. Determination and characterization of metal nanoparticles in clams and oysters. Ecotoxicol. Environ. Saf. 198, 110670. https://doi.org/10.1016/j.ecoenv.2020.110670

10.4 CHAPTER 4: DNA damage, and apoptosis induced by titanium dioxide nanoparticles (TiO_2-NPs) and the food additive E171 in colon cancer cells: HCT-116 and Caco-2.

Alfina Grasso[1], Rossella Salemi[2], Massimo Libra[2], Margherita Ferrante[1], Chiara Copat[1].

[1] Department of Medical, Surgical and Advanced Technologies "G.F. Ingrassia", University of Catania, Catania, Italy.

[2] Department of Biomedical and Biotechnological Sciences, University of Catania, Catania, Italy.

Abstract

This study investigated the DNA damage and apoptosis induced by an engineered TiO_2-NPs (60 nm) and a food additive E171 in colon cancer cells HCT-116 and Caco-2. The question of whether food grade TiO_2 is more toxic than general grade TiO_2 needs to be answered.

MTT assays showed that TiO_2-NPs (60 nm) and the food additive E171 significantly reduced cancer cells viability in a dose-dependent manner, particularly E171. In HCT116 cells exposed to a concentration of 500 mg/L of both compounds, a significant induction of DNA damage was detected by Comet assay. A low level of genotoxicity was observed in Caco-2 cells, especially when treated with TiO_2 60 nm. Western blot analysis showed that HCT116 and Caco-2 treated cells did not overexpress apoptotic markers such as cleaved Caspasi 3 and cleaved Parp. Moreover, further analysis by quantitative real-time PCR (qRT-PCR) showed that TiO_2-NPs and E171 did not promote expression of Bax or downregulation of Bcl-2, nor did they increase the Bax/Bcl-2 ratio.

The assays data provide clear evidence that TiO_2-NPs and E171 can cause DNA damage but do not induce apoptosis or decrease long-term cell proliferation. In addition, the results show that E171 has a slightly higher level of cytotoxicity and genotoxicity. This suggests that exposure to E171 may be hazardous to health and that further research on biological effects is needed to promote safer practices in the use of this compound. These results may be an important contribution to the risk assessment of the food additive E171.

Keywords: TiO_2; E171; HCT-116; Caco-2; apoptosis; genotoxicity;

4.1 Introduction

Nanoparticles are important components of the biogeochemical system, but their natural cycle has been altered by the introduction of artificial nanoparticles (Lespes et al., 2020). In fact, nanoparticles have achieved incredible success in more and more fields, such as pharmaceutical, cosmetic, biomedical, food, automotive and military industries due to their special properties such as resistance, reactivity, electrical conductivity and incredible flexibility (Piccinno et al., 2012). Food additives with a nanoparticle structure are an important component of processed foods. Consumers have been expressing concern about their potential adverse health effects for some time (Partridge et al., 2019) and want to be better informed about their potential health consequences.

Our study focuses on titanium dioxide (TiO_2-NPs), one of the most common nanoparticles used as a white pigment and opacifier in paints, pharmaceuticals, cosmetics, and foods (Weir et al., 2012). It occurs in three different varieties: as rutile, anatase and, less commonly, as brookite (Hanaor and Sorrell, 2011). It is also used as a food additive that has no nutritional value and is listed as E171 to provide a white colour or to tint other pigments, approved by the European Union in anatase and rutile in uncoated form and is not allowed to exceed 1% of food weight, according to the Food and Drug Administration (FDA) (Pedata et al., 2019). It is estimated that about 4 million tonnes of E171 are consumed worldwide each year (Winkler et al., 2018). Specifically, as a food additive, E171 consists of approximately 40% nano-sized TiO_2 particles (< 100 nm) and 60% micro-sized TiO_2 particles (> 100 nm). It is not a nanomaterial according to European Commission Recommendation 2011/696/EU, which defines a nanomaterial as a compound containing more than 50% nanoparticles. The uncertainties regarding the identity and characterisation of E171 were highlighted and it was noted that no particle size limits for E171 were set in the EU specifications. EFSA noted that more data are needed, information on the particle size

distribution of E171 as well as information on the percentage (in number and mass) of nanoscale particles, which is only possible after accurate detection and characterisation by an appropriate analytical method. Although it has long been considered safe due to its low solubility, toxicity, and inertness (Shi et al., 2013), the latest EFSA safety assessment concluded that E171 can no longer be considered safe for use as a food additive (EFSA, 2021) due to several uncertainties regarding its genotoxic potential.

For all the above-mentioned reasons, the use of E171 in food has become a topic of discussion. In particular, the proportion of nano-sized particles (< 100 nm), as there is evidence that they can be distributed through the bloodstream or lymphatic system, alter the intestinal barrier and accumulate in organs. Over the last year, a growing number of studies have investigated the effects of E171 and identified several potential adverse effects (Bischoff et al., 2020). Little is also known about TiO_2-NPs metabolism in our body. However, it seems that these molecules manage to be absorbed in a dose-dependent manner from the gastrointestinal tract and enter other organs (Jovanović, 2015). Studies in rats and mice have shown that nanoparticles can cross the intestinal barrier, accumulate in the gut and cause preneoplastic lesions (Bettini et al., 2017), promote anxiety, increase the number of adenomas in the colon, induce hypertrophy and hyperplasia of goblet cells (Viaud et al., 2015), and disrupt the composition and function of the gut microbiota. Despite several toxicological studies conducted in recent years, a robust risk assessment of oral exposure to E171 has not yet been satisfactorily achieved.

Human exposure to TiO_2-NPs may occur during both manufacture and use. Inhalation is thought to be the main route of TiO_2-NPs exposure in the workplace, followed by dermal exposure. Dermal exposure is also important for customers as TiO_2-NPs are the most common nanomaterial in skin care products (Shi et al., 2013). The oral route is the least studied, although E171 is widely used. Furthermore, in addition to food-grade titanium, attention must be

paid to titanium that unintentionally enters the environment. The anatase form of TiO_2 is most commonly used in food and is the main source of exposure for the general population (Skocaj et al., 2011). In general, children appear to be the most exposed group, as they have lower body weight and consume more products containing E171 (Bischoff et al., 2020). Indeed, little is known about the potential bioaccumulation of TiO_2- NPs along the food chain and the dietary intake dose to the general population.
Taking into account all the doubts expressed in the scientific literature and in accordance with the recommendations of EFSA, the aim of this study was to investigate the toxicological effects of E171 against TiO_2-NPs (60 nm) on colon cancer cells, Caco-2 and HCT-116, with particular interest in genotoxic effects that may lead to carcinogenic effects.

4.2 Materials and methods

4.2.1 Preparation and characterization of stock suspensions

TiO_2-NPs standard (60 nm TiO_2 Nano Powder, rutile, 99.9%, AEM) was purchased from Nanovision (Brugherio, MB, Italy), while E171 (anatase) was obtained from an Italian supplier of food colouring for bakeries.
Particles were weighed into 50 mL polypropylene vials, suspended in cell culture medium at a concentration of 1000 mg/L, sonicated at 300 W for 15 min to prevent aggregation, and then used to prepare the dilutions needed for exposure. In this way, three independent replicates were prepared for both to allow characterization of nanoparticles in solution.
The characterization of number of particles/mL, size and size distribution were examined using a spICP-MS (NexION® 350D, Perkin Elmer, USA). The instrument parameters and operational conditions are the same given in chapter 1.

Transport efficiency was calculated using a certified reference material PELCO (Ag-NPs, 39 ± 5nm, 110 ng/L, monitoring m/z 107), obtaining values ranging from 2.7 to 5.54%.
In cell culture medium the size distribution of TiO_2-NPs 60 nm showed a size range of 44-85 nm with a mean size of 66.2 ± 3.0 and a most frequent size of 56.6 ± 4.4 and a particle concentration/mL of $4.1 \times 10^{12} \pm 6.2 \times 10^{8}$; while for E171 we obtained a size range of 40-360 nm with a mean size of 150.0 ± 20.5 and a most frequent size of 176.3 ± 24.4 and a particle concentration/mL of $0.12 \times 10^{12} \pm 3.5 \times 10^{8}$. In E171, the percentage of nanoparticles < 100 nm was 32.1% and the percentage of microparticles was 67.9%. All stock suspensions were freshly prepared before each experiment.

4.2.2 Cell culture and treatment

Human colon cancer Caco-2 and HCT116 cells were obtained from the American Type Culture Collection (ATCC) (Rockville, MD, United States). The cell lines were cultured in RPMI-1640 medium supplemented with 10% foetal bovine serum (FBS), 100 IU penicillin, 2 mmol/L L-glutamine and 100 mg/ml streptomycin and incubated at 37 °C in a humidified incubator containing 5% CO_2. Mediums and all the supplements were provided by Lonza (Walkersville, USA).
A dispersing agent such FBS is needed to stabilise and disperse E171 and TiO_2-NPs, as already shown for different nanomaterials including TiO_2 (Bihari et al., 2008) and has been applied in larger harmonized studies on nanomaterials genotoxicity.
Cells were seeded in 25cm^2 flasks with vent cap and then passaged by 1:10 ratios using trypsin–EDTA 0.05% every 72 h. For all the experiments, the cells were trypsinized and sub-cultured in cell culture medium supplemented with TiO_2 (E171, 60 nm) according to the selection of experiment.
For MTT assay, TiO_2-NPs 60 nm and E171 were suspended in cell culture medium by pulse sonication for 5 min to avoid particle agglomeration and used at increased doses (0.001; 0.01; 0.1; 1; 10; 100;

1000 mg/L) according to the MTT assay.
For Western blot analysis, comet assay, clonogenic assay, and quantitative real-time PCR, cells were treated with various concentrations of each form of TiO_2 (E171, TiO2- NPs 60 nm) ranging from 0.1-500 mg/L.
For each experiment, cells not treated with titanium dioxide were used as controls. All experiments were performed in triplicate.

4.2.3 Cell viability and proliferation

The viability of two cancer cell lines was assessed by the MTT assay. The Caco-2 and HCT-116 were seeded in 96-well plates in 200 µl of complete RPMI-1640 medium at the density of 5.0×10^3 and 3.0×10^3 cells per well respectively and incubated for 24 h. After an exposure for 72 h with increasing doses of E171 and TiO_2 60 nm (0.001; 0.01; 0.1; 1; 10; 100; 1000 mg/L), cells were incubated at 37 °C in 5% CO_2. After removing the medium 100 µL of MTT working solution [5 mg/mL in RPMI] was added to each well for 4 h at 37 °C in a humidified incubator. Then 100 µL of the solution of 2-propanol and hydrochloric acid (50 mL + 167 µL) was supplied to each well to solubilize formazan blue crystals. The absorbance was measured at 590 nm with the ELISA Tecan Sunrise Reader according to the manufacturers' instructions. Cell viability was calculated as follows:

$$\text{Cell viability percentage} = [(\text{sample OD} - \text{blank OD} / \text{control OD} - \text{blank OD})] \times 100$$

4.2.4 Western Blot

All cells were cultured at a density of 1×10^6 cells/well in 6-well culture plates and incubated for 24 hours at 37 °C and 5% CO_2. Cells were seeded with various concentrations of E171 or TiO_2 60 nm (0.1; 1; 10; 100; 500 mg/L) for 48 hours. Cells without TiO_2-NPs and puromycin 0.5 µg/mL were used as positive controls for apoptosis.

Cells were then trypsinized with trypsin EDTA 0.05% and centrifuged.
Proteins were extracted from cellular pellets lysed in cell lysis buffer (NP40) (150 mM NaCl, 1.0% NP40, pH 8.0 50mM Tris), supplemented with protease and phosphatase inhibitors (Roche Diagnostics, Indianapolis, IN). After the lysis, the supernatant enriched of interest proteins was centrifugated. The Quick StartTM Bradford 1X Dye Reagent (Biorad Laboratories, Inc., Hercules, CA, USA) assay was performed on well-diluted proteins. This colorimetric assay exploits a dye, able to bind to alkaline residues of the proteins leading to a bathochromic shift, from 465 nm to 595 nm. A standard curve was realized using increasing doses of bovine serum albumin (BSA) (0.3125, 0.625, 1.25, 2.5, 5, 10 and 20 μg/μl) and a blank with NP40 diluted 1:10 with water.
Sample's proteins concentration was determined by placing in separate wells (containing 5μl of diluted protein + 250 μl of dye reagent) different dilution of the protein extract. After incubation at room temperature for 5 minutes, the absorbance was measured at 595 nm with the Tecan Sunrise ELISA reader and the concentration calculated.
For each sample, 30 μg of proteins were separated through vertical electrophoresis using 4–15% Mini Protean TGX Precast Gels (cat. n. 4561083 - Bio-Rad Laboratories, Inc., Hercules, CA, United States).
Bio-Rad Trans-Blot Turbo was used to transfer the gel proteins into a nitrocellulose membrane (Bio-Rad Laboratories, Inc.). The transfer of protein was assessed with the Red Ponceau dye. Afterward, the membrane was left for one hour in 5% semi-skimmed milk, after being rinsed with TBS-T (0.1% Tween 20, 20 mMTris–HCl pH 7.6, 137 mMNaCl).
Two apoptosis markers, cleaved Caspase-3 and total / cleaved PARP proteins were detected by using the anti- Cleaved Caspase-3 (Asp175) (5A1E) Rabbit mAb (Cell Signaling, #9664) and Anti-PARP (46D11) Rabbit mAb #9532 (Cell Signaling), after being incubated overnight. The anti-beta Tubulin rabbit Ab (diluted 1:1000 – cat. n.

15568- Abcam, Cambridge, United Kingdom) was used to detect Tubulin housekeeping protein. Then, the membrane was rinsed thrice for 10 minutes by using TBS-T solution and incubated for one hour at room temperature with anti-mouse or anti-rabbit secondary antibodies conjugated with horseradish peroxidase (HRP) (diluted 1:10000). Again, the membrane was rinsed thrice by using TBS-T solution.
The Clarity Western ECL Substrate (cat. n. 1705060 - Bio-Rad Laboratories, Inc., Hercules, CA, United States) was used to detect the chemiluminescence. Western blot images were acquired by Bio-Rad ChemiDoc Touch Imaging System and then analyzed with ImageJ software (National Institutes of Health, Bethesda, MD, United States). All Western Blot experiments were performed in triplicate.

4.2.5 Clonogenic assay

After 72 hours exposure to TiO2-NPs, the Caco-2 and HCT116 were seeded at 200 cells per well onto 24-well culture plates for 7 days in complete RPMI-1640 media. After being washed two times with ice cold PBS, cells were fixed with ice-cold methanol for 20 minutes.
Then methanol was removed from plates and these were rinsed with water. 0.5% crystal violet solution was added before incubating the plates at room temperature for 5 minutes. Finally, plates were rinsed again with water. Colony-forming assays were performed at least twice in quadrupled.

4.2.6 Comet assay

The analysis of genotoxicity was assessed by standard alkaline comet assay on Caco-2 and HCT-116 treated for 48 h with either TiO_2 nanoparticles or E171.
According to Tomasello et al., (2017) cell suspension was mixed with 0.7% low-melting point agarose at 37°C. Next, cell suspension was

spread onto microscope slides pre-coated with 1% normal-melting point agarose and two mini-gels were made on each slide. After the gels were maintained at 4°C for 10 min, the embedded cells were lysed in a freshly lysis buffer (2.5M NaCl, 0.1M EDTA, 1% Triton X-100, 1% N-laurosyl sarcosine, 10% DMSO, pH 10) for 1h in dark at 4°C. DNA unwinding was allowed for 20 min in fresh electrophoresis buffer (300 mM NaOH, 1 mM, Na2EDTA, pH = 13.1) followed by electrophoresis for 20min (1V/cm) in the same re-circulating pH 13.1 buffer. All the slides were neutralised 3×5min in 0.4M Tris, dipped in 70% ethanol and dried in air overnight. DNA was stained SYBR-green diluted in TAE buffer (1:10000). One hundred nucleoids per sample (50 for each of the two replicate slides) were randomly acquired using the Leica epifluorescence microscope. The DNA damage was quantified by CASP free software and the results were expressed as average percentage of fragmented DNA in the tail of comet (%TDNA).

4.2.7 Quantitative real-time PCR (qRT-PCR)

After 48h of treatment whit increasing doses of TiO_2-NPs and E171 (0.1; 1; 10; 100; 500 mg/L), in HCT116 and Caco-2 cell lines we determined the mRNA expression of apoptotic regulators such as Bax and Bcl-2 in survival or cytotoxicity of HCT116 and Caco-2 treated cells.

Total RNA extraction was carried out by Invitrogen™ PureLink™ RNA Mini Kit from treated cells according to the manufacturers' instructions. The ratio of absorbance at 260 nm and 280 nm was studied using a Nanodrop 1000 spectrophotometer (Thermo Fisher Scientifc, Canada) to assess the RNA concentration and purity spectrophotometrically in molecular-grade water. Then, for each sample, 2 μg of total RNA were treated with DNase I, RNase-free (Cat. N. EN0525 - Thermo Fisher ScientificTM) to remove possible DNA contamination. The cDNA was converted from the isolated total RNA by SuperScriptTM IV Reverse Transcriptase kit (Cat. N.

18090050 - Thermo Fisher ScientificTM). In brief, 1 μg RNA from each sample was added to 50 μM Random hexamers, 2.5 mM dNTPs and the reaction volume become 13 μL with RNase free water and mixed gently. Next, the mixtures were incubated at 65 °C for 5 min. After, the mixtures were supplemented with 4 μL 5x Super Script Bufer, 100 mM DTT, 1 μL Super Script IV Enzyme and RNase free water to obtain 20 μL reaction volume. The whole was incubated at 23 °C for 10 min, 55 °C for 10 min in order to start the reverse transcriptase enzyme and incubated in 85 °C for 5 s to block the reaction. After reverse transcription reactions, cDNA was applied for real-time quantitative RT-PCR on 7300 Real-Time PCR System (Applied Biosystems). The RT-PCR was carried out in a final volume of 20 μL containing 10 μL SYBR green master mix, 50 ng cDNA, 0.18 μL forward primer (10 μM), 0.18 μL reverse primer (10 μM), and nuclease free water to bring at volume (Luminaris Color HiGreen qPCR Master Mix, high ROX, Cat. N. K0362 - Thermo Fisher ScientificTM).

Sequences of primers are provided in Table 4.1. The thermal cycling program for all target and reference genes was as follows: pre-denaturation (2 min. at 50 °C), denaturation (10 min. at 95 °C), annealing, and extension (15 s at 95 °C, 30 s at 60 °C, 30 s at 72 °C) for 50 cycles. The melting curve analysis condition was as follows: 15 s at 95 °C, 1 min at 60 °C, and 15 s at 95 °C. Duplicate experiments were carried out for each data set. GAPDH mRNA was amplified as a reference gene, and fold changes in each target mRNA expression were calculated relative to GAPDH mRNA expression via $2^{-\Delta\Delta CT}$ method.

Table 4.1 Sequence of the primers applied for qRT-PCR

Primer	Forward	Reverse
BAX	*5'-CCCCGAGAGGTCTTTTTCCG-3'*	*5'-TGGTTCTGATCAGTTCCGGC-3'*
BCL-2	*5'-TGAACTGGGGGAGGATTGTG-3'*	*5'-CGTACAGTTCCACAAAGGCA-3'*
GAPDH	*5'-AGAAGGCTGGGGCTCATTTG-3'*	*5'-AGGGGCCATCCACAGTCTTC-3'*

4.2.8 Statistical Analysis of Data

GraphPad Prism 6.0 software was applied for statistical data analysis. The Mean ± SEM of three independent tests are shown for each group. $P < 0.05$ was considered meaningful. One-way analysis of variance (ANOVA) and Student t test were performed for determining statistical differences among groups. Dunnett's' adjustment was used for multiple comparisons.

4.3 Results

4.3.1 Effects of TiO_2 NPs on HCT-116 and Caco-2 cell viability

The growth-inhibitory effect of two forms of TiO_2-NPs was examined in vitro against human colon cancer cells. All cell lines were treated with increasing concentrations of bacterial cell-free supernatants. MTT assay was used to evaluate cell survival after 72 h incubation.

The percentage of growth inhibition of increasing concentrations of TiO_2-NPs and E171 against human HCT-116 and Caco-2 colon cancer cell lines and A375 melanoma cell line is shown in Figure 4.1.

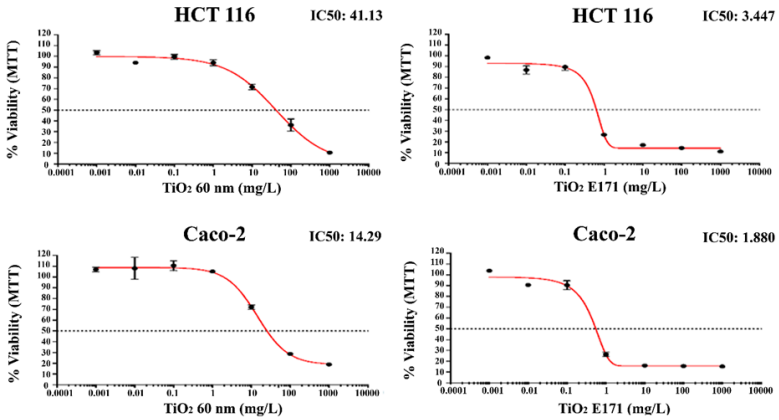

Figure 4.1. Inhibitory effect of TiO_2 NPs and E171 on the growth of HCT-116 and Caco-2 cell lines. Cells' viability evaluated through the MTT assay after 72 hrs of TiO2 NPs and E171 at different concentration (0.0001; 0.001; 0.01; 0.1; 1; 10; 100; 1000 mg/L). Data are expressed as mean ± SD of three separate experiments.

Both TiO_2-NPs and and E171 induce superimposable anti-proliferative effects in vitro and reduce the viability of HCT-116 and Caco-2 cell lines in a concentration-dependent manner.

Notably, the most pronounced anti-proliferative effect was induced by E171 on both cell lines. Indeed, the food additive E171, induced a peak collapse in the number of both cells with a reduction of more than 70% in the number of cells after exposure to 1 mg/L and of more than 80% with doses of 10, 100 and 1000 mg/L.

A lower cytotoxic effect was found after 72 h exposure to 60 nm TiO_2-NPs. As shown in Figure 4.1, a significant reduction occurred in both cells, only starting from 10 mg/L. However, even with 60 nm NPs, the reduction of cell number appears to be dose-dependent, with only 10-20% of living cells after exposure to 1000 mg/L.

Finally, although both cells show a similar pattern in the reduction of cell viability, Caco-2 appears to be more resistant to higher concentrations.

It is notable that HCT-116 cells showed a greater decrease in cell viability for both treatments with TiO_2-NPs (TiO_2 E171: IC50=3.447; TiO_2 60 nm: IC50=41.13) compared to Caco-2 cells (TiO_2 E171: IC50=1.880; TiO_2 60 nm: IC50=14.29).

4.3.2 Measurement of DNA damage by the comet assay

The genotoxic potential of TiO_2 (E171 and TiO_2 60 nm) was evaluated using comet assays.
The %TDNA-the relative DNA content of the comet tail was used for quantification. A significant concentration-dependent increase in DNA damage was observed in HCT-116 and Caco-2 cells at different TiO_2 concentrations (100 and 500 mg/L) after 48 hours of exposure.
Overall, a higher sensitivity of HCT-116 compared to CaCo2 cells can be observed.
As shown in Figure 4.2, we observed significant DNA damage in HCT-116 cells exposed to the high concentrations of the two compounds. A low level of genotoxicity was observed in Caco-2 cells, as shown in Figure 4.3 reported, especially when treated with TiO_2 60 nm.
This result seems to confirm what was observed in the MTT assay and underlines that Caco-2 seems to be more resistant.

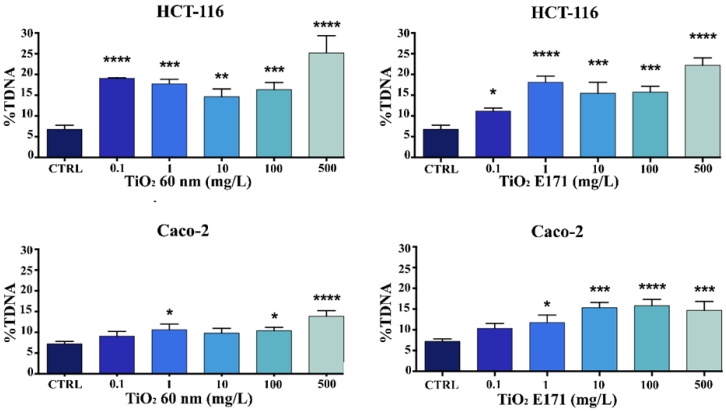

Figure 4.2 DNA damage was evaluated by alkaline comet assay. HCT-116 and Caco-2 cells were treated with different concentration of TiO2 60 nm and E171 for 48 h and investigated by alkaline comet assay. The results were expressed as the percentage of DNA present in the comet tail (%TDNA) and reported as mean ± SD. * $p < 0.05$ vs. control; ** $p < 0.01$ vs. control; *** $p < 0.001$; **** $P<0.0001$ vs. control.

4.3.3 Morphological changes of treated cells

Apoptotic cells are characterized by altered morphological and biochemical features.

For this reason, a morphological observation was performed to determine whether the cytotoxic effect of TiO_2-NPs and E171 correlates with the apoptotic process. The effect on the morphology of HCT116 and Caco-2 after 72-hour exposure to both forms of TiO_2 was not observed using inverted microscopy (Figure 4.4).

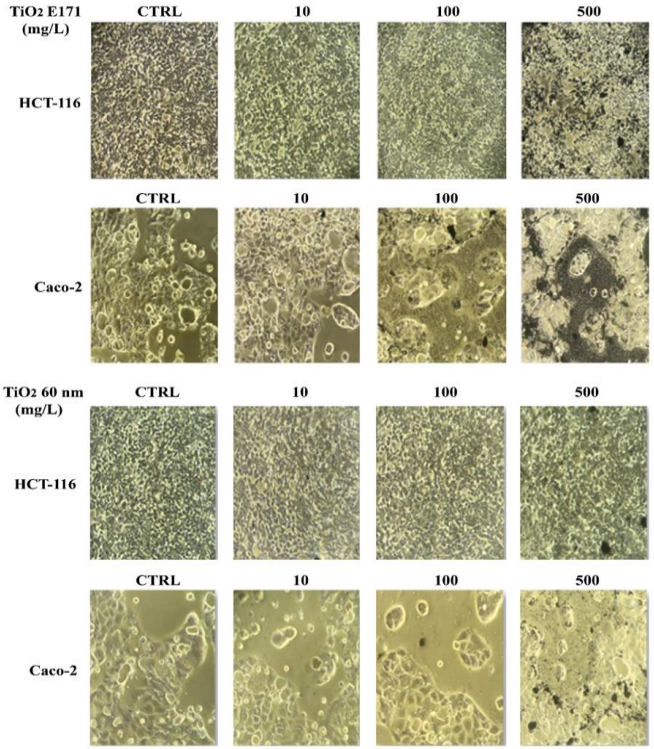

Figure 4.4. Evaluation of alteration in the Morphology of HCT116 and Caco-2 cells after after 48 h exposure to different concentration of TiO_2 NPs. Images were acquired by optical microscopy, original magnification 40x.

4.3.4 Effect of TiO_2 NPs on apoptosis-associated mRNA expression

The mRNA level of apoptotic markers (Bax, Bcl-2 and GAPDH) by RT-PCR was measured in cells (HCT116 and Caco-2) exposed to an increased concentration of TiO_2 as are shown in Figure 4.5.

The comparative differential expression of selected genes was examined by SYBR-Green Real-time PCR in TiO_2-treated HCT-116 and Caco-2 cells compared to non-treated cells. Transcription levels

of each gene were normalized with GAPDH Ct values.

After 48 hours of treatment with increasing doses of TiO_2-NPs and E171 (0.1-500 mg/L), in HCT116 and Caco-2 cell lines, the expression of Bcl-2 and BAX did not appear to be a critical marker of response to TiO_2-NPs and E171 (Figure 4.5).

While TiO_2 were able to decrease cell viability in both HT29 and Caco-2, they did not promote the upregulation of Bax as well as the downregulation of Bcl-2 and did not lead to an increase in the Bax/Bcl-2 ratio, as expected.

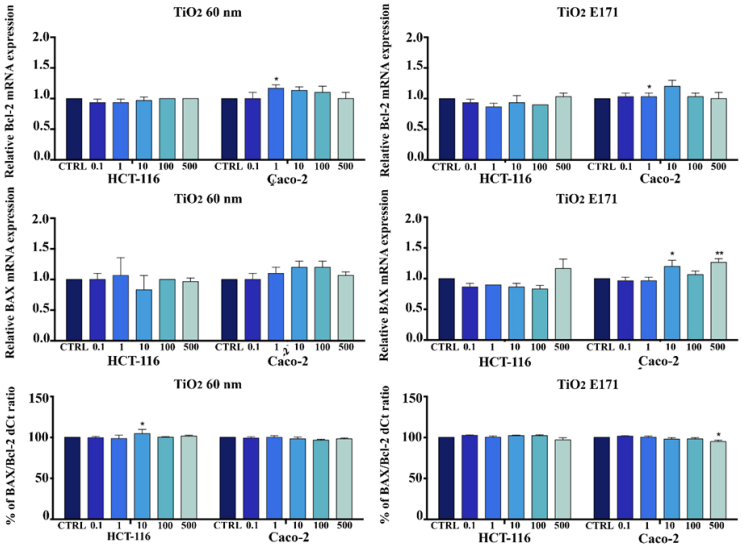

Figure 4.5. Bcl-2 and BAX mRNA expression: untreated vs treated (48h). Relative gene expression (mean fold change) of Bcl-2 and BAX in TiO_2-treated versus non-treated HCT-116 and Caco-2 cells. Both cell lines were cultured with increasing doses of TiO_2 (0; 0.1; 1; 10; 100; 500 mg/L) for 48hrs, and then RT-PCR was carried out with specific primers. For analysis, GAPDH was used as the internal reference and non-treated cells were used as the calibrator. mRNA relative expression for all genes was calculated by the comparative quantification Ct method ($\Delta\Delta$Ct). Results are representative of three independent experiments. * $p < 0.05$ vs. control; ** $p < 0.01$ vs. control.

4.3.5 TiO_2-NPs and E171 do not promote apoptotic cell death in cancer cells

To further investigate the TiO_2 anti-proliferative effects, whether the two TiO_2 form can promote apoptotic cell death was examined.
We performed a Western blot experiment to assess the expression of two different apoptotic markers, cleaved caspase-3 and total/cleaved PARP proteins. A treatment with Puromycin was added to determine a positive control (CTRL+) of cell death for apoptosis in order to ascertain the proper functioning of the antibody used.
As shown in Figure 4.6, we did not observe overexpression of either marker after 48 hours of exposure to TiO_2-NPs and E171. At all concentrations used, expression of total PARP was higher than control, while expression of cleaved PARP and cleaved caspase-3 downstream of the apoptotic pathway was lower than control.

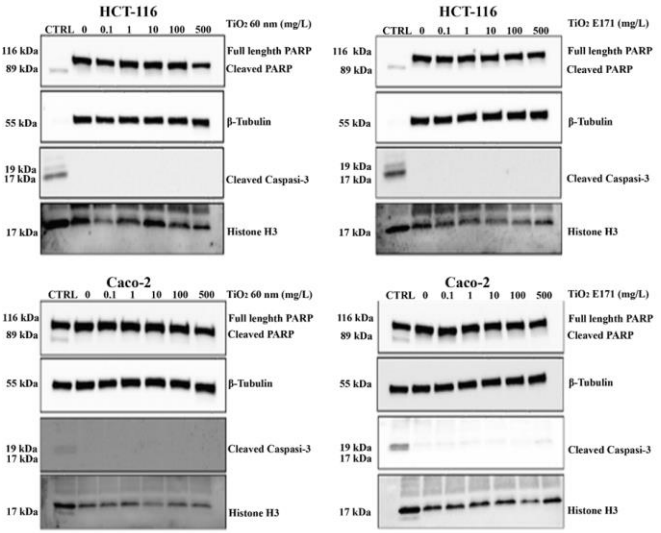

Figure 4.6. Effect of apoptosis in colon rectal cancer cell lines (HCT-116 and Cacp-2) of two apoptotic markers after 48 h exposure to different TiO_2 forms (E171, 60 nm NPs) (wester blot analysis).

Thus, the analysis of the protein expression of two markers of apoptosis, (cleaved Caspase-3 and total / cleaved PARP) confirmed that the treatment with TiO_2 did not cause apoptosis.

4.3.6 Clonogenic Assay

To investigate whether TiO_2-NPs and E171 are able to slow down the growth of cancer cells after treatment, a clonogenic assay was performed.
The results obtained showed that both cells proliferated again after treatment with TiO_2-NPs and E171 and that cell growth was comparable to that of the control (Figure 4.7). Although a minimal reduction in cell growth was observed in the HCT-116 cell line at higher doses, neither form of TiO_2 was able to slow the growth of the cancer cells, which is normally rapid.

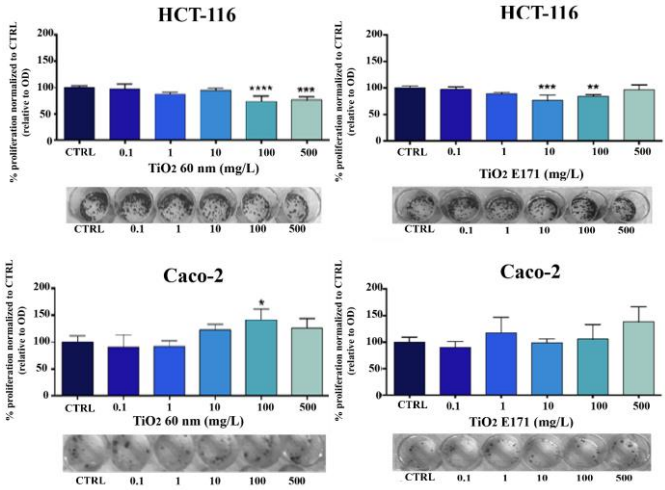

Figure 4.7. Clonogenic assay: HCT-116 and Caco-2 cell lines, 72 hours post treatment with TiO_2 NPs and E171 (0; 0.1; 1; 10; 100; 500 mg/L), were seeded at 200 cells per well onto 24-well culture plates and allowed to grow for a week in complete RPMI-1640 media. The cells treated with TiO_2 NPs were compare to cells untreated.

4.4 Discussion

Several authors have raised concerns about the possible risks of oral intake of food-grade titanium. However, the underlying mechanisms of these adverse effects are not yet fully understood (Gerloff et al., 2012; Song et al., 2015).

The toxicity of NPs has been associated with numerous physicochemical parameters such as size, shape, aspect ratio, charge and surface area (Zhao et al., 2011). Nano-sized TiO_2 has been found to be more toxic compared to larger particles (Gurr et al., 2005), as small nanoparticles have a larger total surface area and a higher total particle number, which may lead to increased toxicity. Although biokinetic behaviours of TiO_2 were found to be independent of particle size, but highly affected by the presence of biomatrices (Winkler et al., 2018).

In this study, we investigated the in vitro genotoxicity, and apoptosis of TiO_2-NPs 60 nm (rutile) and E171 (anatase) in colon cancer cells: HCT-116 and Caco-2. Both are colon cancer cell lines that have been used in many in vitro studies since the 1980s. Although these cells originate from colon carcinoma, they differentiate when cultured under certain conditions and simulate the normal enterocytes of our intestine (Hidalgo et al., 1989). The current results show that TiO_2-NPs and E171 had an antiproliferative effect on Caco-2 and HCT 116 cells in a concentration-dependent manner, indicating a possible toxic effect, with a statistically significant effect from 1 mg/L for E171 and from 10 mg/L for NPs 60 nm. This is in accordance with the results of the work done by other researchers (Wang et al., 2007).

Li et al (2020) reported a 20% reduction in HCT116 cell number after 24 h exposure to 60 μg/ml 25 nm TiO_2-NPs.

Some studies reported that differentiated Caco-2 cells were found to be more resistant than undifferentiated Caco-2 cells (Song et al., 2015), while E171 demonstrated toxicity in Caco-2 cells but not in HCT116 cells after 24 h exposure to 1000 μg/ml (Proquin et al., 2017). Both cells were found to be more resistant to 60 nm TiO_2-NPs than to

E171, as evidenced by the fact that the IC50 was approximately tenfold higher after exposure to 60 nm TiO_2 NPs. This could be due to the fact that the two forms of TiO_2 studied have different crystalline structures, which may lead to different toxicity. In particular, the anatase form of TiO_2 (E171) showed a slightly higher effect on cell viability than the rutile form of TiO_2 60 nm.

As reported in the literature, anatase TiO_2 particles are significantly more potent than rutile in producing negative biological effects such as cytotoxicity, inflammatory responses and formation of ROS in a variety of cell types and tissues and have higher surface reactivity (Prasad et al., 2013).

Furthermore, Proquin et al. (2017) have shown that a mixture of nano- and micro-sized TiO_2 particles, such as those found in E171, cause more adverse effects than the individual fractions alone. This confirms the importance of testing food-grade TiO_2 particles as a whole and not just their nano- and micro-fractions.

However, after removing the two forms of titanium, we found that cell proliferation returned to normal. For this reason, we hypothesize that the titanium dioxide nanoparticles and titanium food grade have no real cytotoxic effect. It is plausible that the deposition of the TiO_2 on the well bottom inhibited cell growth due to lack of space and/or limited cell adhesion to the well bottom. This theory is supported by the fact that when the effects of these two forms on apoptosis were assessed, the pro-apoptotic proteins caspase-3 and cleaved PARP were downregulated in all samples compared to the control. This suggests that TiO_2-NPs and E171 do not affect or are likely to reduce apoptosis.

Similar results were reported by Kukia et al., (2018) showing a reduction in apoptotic cells in a sample of HCT116 cells and a reduction in the Bax/BCL-2 ratio.

The results of the comet assay showed that E171 and TiO_2-NPs are genotoxic by inducing single strand DNA breaks. Likewise, Proquin et al. (2017) found in their work that TiO_2 particles, such as those contained in the food additive E171, can induce the formation of

ROS and DNA damage in the colon-derived cell lines Caco-2 and HCT116.

The genotoxic effect findings are also consistent with the safety assessment report for TiO_2 (E171) published by the EFSA Panel on 6 May 2021. In this report, the Panel concluded that, taking into account the available evidence, a suspicion of genotoxicity cannot be excluded and TiO_2 can therefore no longer be considered as a safe food additive.

Furthermore, genotoxicity is known to play an important role in triggering carcinogenesis, as it can lead to alterations in genetic material, which in turn leads to changes in cellular signalling pathways related to cell proliferation and apoptosis (Nogueira et al., 2012).

However, it should be noted that the concentrations exhibiting cytotoxicity and genotoxicity are too high to be absorbed by TiO_2 present in foods in commercial products, as its oral absorption is extremely low. Nevertheless, we should keep in mind that the potential total amount of TiO_2-NP entering human tissues after oral ingestion might be influenced by the extreme conditions in our digestive system, which certainly affect particle size distribution, surface properties and fate (Walczak et al., 2015).

4.5 Conclusion

Overall, the results of the present study indicate that despite the impairment of cell viability by E171 and TiO_2 60 nm, both chemical forms of TiO_2 do not induce apoptosis but genotoxic effect.

Furthermore, the resumption of cell proliferation after particle removal supports the notion that a better understanding of the biological effects of TiO_2-NPs is needed to promote safer practices in the use of nanomaterials.

Further in vitro and in vivo studies need to be conducted to draw conclusions about the mechanisms behind the potentially carcinogenic effects of E171.

Furthermore, it is important to carefully study and analyze the physicochemical properties of TiO_2 particles in their carrier as well as in the surrounding matrix as the final environment to ensure a sound evaluation of the potential adverse health effects of E171 and to adequately compare different studies in the context of risk assessment.

These findings could be relevant for the risk assessment of the food additive E171 and contribute to the implementation of the European Food Safety Authority (EFSA) risk assessment for the application of nanoscience and nanotechnologies in the food and feed chain.

References

- Bettini et al., 2017. Food-grade TiO_2 impairs intestinal and systemic immune homeostasis, initiates preneoplastic lesions and promotes aberrant crypt development in the rat colon [WWW Document]. URL https://www.ncbi.nlm.nih.gov/pmc/articles/PMC5247795/ (accessed 11.13.21).

- Bihari, P., Vippola, M., Schultes, S., Praetner, M., Khandoga, A.G., Reichel, C.A., Coester, C., Tuomi, T., Rehberg, M., Krombach, F., 2008. Optimized dispersion of nanoparticles for biological in vitro and in vivo studies. Part Fibre Toxicol 5, 14. https://doi.org/10.1186/1743-8977-5-14

- Bischoff, N.S., de Kok, T.M., Sijm, D.T.H.M., van Breda, S.G., Briedé, J.J., Castenmiller, J.J.M., Opperhuizen, A., Chirino, Y.I., Dirven, H., Gott, D., Houdeau, E., Oomen, A.G., Poulsen, M., Rogler, G., van Loveren, H., 2020. Possible Adverse Effects of Food Additive E171 (Titanium Dioxide) Related to Particle Specific Human Toxicity, Including the Immune System. Int J Mol Sci 22, 207. https://doi.org/10.3390/ijms22010207

- EFSA, 2021. Re-evaluation of titanium dioxide (E 171) as a food additive | EFSA [WWW Document]. URL https://www.efsa.europa.eu/en/efsajournal/pub/4545 (accessed 11.13.21).

- Gerloff, K., Fenoglio, I., Carella, E., Kolling, J., Albrecht, C., Boots, A.W., Förster, I., Schins, R.P.F., 2012. Distinctive toxicity of TiO_2 rutile/anatase mixed phase nanoparticles on Caco-2 cells. Chem Res Toxicol 25, 646–655. https://doi.org/10.1021/tx200334k

- Gurr, J.-R., Wang, A.S.S., Chen, C.-H., Jan, K.-Y., 2005. Ultrafine titanium dioxide particles in the absence of photoactivation can induce oxidative damage to human bronchial epithelial cells. Toxicology 213, 66–73. https://doi.org/10.1016/j.tox.2005.05.007

- Hanaor, D.A.H., Sorrell, C.C., 2011. Review of the anatase to rutile phase transformation. J Mater Sci 46, 855–874. https://doi.org/10.1007/s10853-010-5113-0

- Hidalgo et al., 1989. Characterization of the human colon carcinoma cell line (Caco-2) as a model system for intestinal epithelial permeability - PubMed [WWW Document]. URL https://pubmed.ncbi.nlm.nih.gov/2914637/ (accessed 11.13.21).

- Jovanović, B., 2015. Critical review of public health regulations of titanium dioxide, a human food additive. Integrated Environmental Assessment and Management 11, 10–20. https://doi.org/10.1002/ieam.1571

- Kukia, N.R., Rasmi, Y., Abbasi, A., Koshoridze, N., Shirpoor, A., Burjanadze, G., Saboory, E., 2018. Bio-Effects of TiO_2 Nanoparticles on Human Colorectal Cancer and Umbilical Vein Endothelial Cell Lines. Asian Pac J Cancer Prev 19, 2821–2829. https://doi.org/10.22034/APJCP.2018.19.10.2821

- Lespes, G., Faucher, S., Slaveykova, V.I., 2020. Natural Nanoparticles, Anthropogenic Nanoparticles, Where Is the Frontier? Front. Environ. Sci. 8. https://doi.org/10.3389/fenvs.2020.00071

- Nogueira, C.M., de Azevedo, W.M., Dagli, M.L.Z., Toma, S.H., Leite, A.Z. de A., Lordello, M.L., Nishitokukado, I., Ortiz-Agostinho, C.L., Duarte, M.I.S., Ferreira, M.A., Sipahi, A.M., 2012. Titanium dioxide induced inflammation in the small intestine. World J Gastroenterol 18, 4729–4735. https://doi.org/10.3748/wjg.v18.i34.4729

- Partridge, D., Lloyd, K.A., Rhodes, J.M., Walker, A.W., Johnstone, A.M., Campbell, B.J., 2019. Food additives: Assessing the impact of exposure to permitted emulsifiers on bowel and metabolic health – introducing the FADiets study. Nutr Bull 44, 329–349. https://doi.org/10.1111/nbu.12408

- Pedata, P., Ricci, G., Malorni, L., Venezia, A., Cammarota, M., Volpe, M.G., Iannaccone, N., Guida, V., Schiraldi, C., Romano, M., Iacomino, G., 2019. In vitro intestinal epithelium responses to titanium dioxide nanoparticles. Food Res Int 119, 634–642. https://doi.org/10.1016/j.foodres.2018.10.041

- Piccinno, F., Gottschalk, F., Seeger, S., Nowack, B., 2012. Industrial production quantities and uses of ten engineered nanomaterials in Europe and the world. J Nanopart Res 14, 1109. https://doi.org/10.1007/s11051-012-1109-9

- Prasad, R.Y., Chastain, P.D., Nikolaishvili-Feinberg, N., Smeester, L.M., Kaufmann, W.K., Fry, R.C., 2013. Titanium dioxide nanoparticles activate the ATM-Chk2 DNA damage response in human dermal fibroblasts. Nanotoxicology 7, 10.3109/17435390.2012.710659. https://doi.org/10.3109/17435390.2012.710659

- Proquin, H., Rodríguez-Ibarra, C., Moonen, C.G.J., Urrutia Ortega, I.M., Briedé, J.J., de Kok, T.M., van Loveren, H., Chirino, Y.I., 2017. Titanium

dioxide food additive (E171) induces ROS formation and genotoxicity: contribution of micro and nano-sized fractions. Mutagenesis 32, 139–149. https://doi.org/10.1093/mutage/gew051

- Shi, H., Magaye, R., Castranova, V., Zhao, J., 2013. Titanium dioxide nanoparticles: a review of current toxicological data. Part Fibre Toxicol 10, 15. https://doi.org/10.1186/1743-8977-10-15

- Skocaj et al., 2011. Titanium dioxide in our everyday life; is it safe? [WWW Document]. URL https://www.ncbi.nlm.nih.gov/pmc/articles/PMC3423755/ (accessed 11.13.21).

- Song, B., Liu, J., Feng, X., Wei, L., Shao, L., 2015. A review on potential neurotoxicity of titanium dioxide nanoparticles. Nanoscale Res Lett 10, 342. https://doi.org/10.1186/s11671-015-1042-9

- Tomasello, B., Malfa, G.A., Strazzanti, A., Gangi, S., Di Giacomo, C., Basile, F., Renis, M., 2017. Effects of physical activity on systemic oxidative/DNA status in breast cancer survivors. Oncol Lett 13, 441–448. https://doi.org/10.3892/ol.2016.5449

- Viaud, S., Daillère, R., Boneca, I.G., Lepage, P., Langella, P., Chamaillard, M., Pittet, M.J., Ghiringhelli, F., Trinchieri, G., Goldszmid, R., Zitvogel, L., 2015. Gut microbiome and anticancer immune response: really hot Sh*t! Cell Death Differ 22, 199–214. https://doi.org/10.1038/cdd.2014.56

- Walczak, A.P., Kramer, E., Hendriksen, P.J.M., Helsdingen, R., van der Zande, M., Rietjens, I.M.C.M., Bouwmeester, H., 2015. In vitro gastrointestinal digestion increases the translocation of polystyrene nanoparticles in an in vitro intestinal co-culture model. Nanotoxicology 9, 886–894. https://doi.org/10.3109/17435390.2014.988664

- Wang, J., Zhou, G., Chen, C., Yu, H., Wang, T., Ma, Y., Jia, G., Gao, Y., Li, B., Sun, J., Li, Y., Jiao, F., Zhao, Y., Chai, Z., 2007. Acute toxicity and biodistribution of different sized titanium dioxide particles in mice after oral administration. Toxicol Lett 168, 176–185. https://doi.org/10.1016/j.toxlet.2006.12.001

- Weir, A., Westerhoff, P., Fabricius, L., von Goetz, N., 2012. Titanium Dioxide Nanoparticles in Food and Personal Care Products. Environ Sci Technol 46, 2242–2250. https://doi.org/10.1021/es204168d

- Winkler, H.C., Notter, T., Meyer, U., Naegeli, H., 2018. Critical review of the safety assessment of titanium dioxide additives in food. J Nanobiotechnology 16, 51. https://doi.org/10.1186/s12951-018-0376-8

- Zhao, L., Wang, H., Huo, K., Cui, L., Zhang, W., Ni, H., Zhang, Y., Wu, Z., Chu, P.K., 2011. Antibacterial nano-structured titania coating incorporated with silver nanoparticles. Biomaterials 32, 5706–5716. https://doi.org/10.1016/j.biomaterials.2011.04.040

10.5 CHAPTER 5: Preliminary results of Fish Embryo test (FET) on zebrafish (*Danio rerio*) exposed to metallic nanoparticles (Titanium dioxide - TiO_2, Silver – Ag - and Zinc Oxide – ZnO) and food additive (TiO_2 - E171 - and Ag - E174).

Alfina Grasso[1], Margherita Ferrante[1], Maria Violetta Brundo[2], Roberta Pecoraro[2], Elena Scalisi[2], Fabio Marino[3] and Chiara Copat[1]

[1] Department of Medical, Surgical and Advanced Technologies "G.F. Ingrassia", University of Catania, Italy.

[2] Department of Biological, Geological and Environmental Science, University of Catania, Catania, Italy.

[3] Department of Chemical, Biological, Pharmaceutical and Environmental Sciences, University of Messina, Messina, Italy

Abstract

Metallic nanoparticles are used in many fields. For this reason, it is necessary to study their toxicity and potential hazards to human's health.

Zebrafish (*Danio rerio*) is a promising animal model for nanoparticle toxicity assessment, thank to its numerous features such as short life cycle, high fecundity transparency of embryos and genetic data similarity with human.

This study sought to find responses to acute toxicity in zebrafish (*Danio rerio*) exposed to three metallic nanoparticles (titanium dioxide TiO_2-NPs 60 nm, zinc oxide ZnO-NPs 30 nm and silver Ag NPs 40 nm) currently used in various consumer, household and industrial products. Furthermore, two food additives approved in the European Union, E171 and E174, were also tested for acute embryotoxicity.

The fish embryotoxicity test (FET) was conducted in accordance with the OECD test guidelines (TG) 236 at a concentration of 100 mg/L for all chemicals, with the except for Ag-NPs, which was tested also at different concentrations, 50 mg/L, 25 mg/L, 12.5 mg/L, and 6.25 mg/L, to better investigate the acute embryotoxicity observed.

Our results showed no acute embryotoxicity for TiO_2 suspensions of 60 nm, E171 and E174. A delay in development was observed after exposure to a ZnO-NPs suspension of 30 nm at the end of 96 hours after fertilization. Ag-NPs solutions of 50 nm were found to be toxic with a lethal concentration (LC50) of 9.604 mg/L.

Keywords: Fish Embryo test (FET); Zebrafish; Nanoparticles; Embriotoxicity.

5.1 Introduction

Metallic nanoparticles (MNPs) have found a wide range of industrial applications, from biomedicine to mechanical engineering to the food industry, thanks to their large surface-to-volume ratio, extremely small size, size-dependent optical properties, and physiochemical properties that make them superior to their larger counterparts (Mody et al., 2010).

In recent decades, human production and thus exposure to MNPs has radically increased. Moreover, studies on the inherent toxicity of some MNPs have increased, showing that they can affect biological systems at cellular and subcellular levels (Li and Ju, 2018; Rodríguez-Hernández et al., 2020; Stone et al., 2007; Zhang et al., 2016). However, as different MNPs may coexist in the natural environment, the findings on the toxicity of individual MNPs may not reflect the actual effects on the environment and human health (Zhang et al., 2020). Furthermore, far from it is the knowledge about the concentrations of MNPs released in the environment, nor about the MNPs concentrations to which humans are exposed by oral, inhalation or dermal exposure.

This research was focused to determine acute toxicity on zebrafish (Danio rerio) exposed to three molecular compounds and/or metallic element in the nanoparticle scale dimension (1-100) and as food additive. In particular, titanium dioxide (TiO_2), zinc oxide (ZnO) and silver (Ag), currently used in several consumer, household and industrial products, which are likely to end up being discarded into water bodies, were studied. The chemicals chosen are widely uses in household and consumers products. TiO_2-NPs is adopted as an additive for development of plastic packaging (EFSA Panel on Food Contact Materials, Enzymes and Processing Aids (CEP) et al., 2019), it is added in toothpaste, sun cream, creams, lip balm, paints, catalysts for air and water purification, medical applications, and energy storage (Rompelberg et al., 2016; Ruszkiewicz et al., 2017;

Schneider and Lim, 2019). Until May 2021, TiO_2 was authorized as a food additive (E 171) for whitening and brightening purpose, and it may contain up to 3.2% of its weight in nanoparticles, but there is not an established limit of E171 amount for food products Until date, there is a need for more data on the reproductive toxicity of E171 in order to establish an acceptable daily intake (ADI)(EFSA Panel on Food Additives and Nutrient Sources added to Food (ANS), 2016). Nevertheless, based on the last safety assessment, EFSA Panel on Food Additives and Flavourings concluded that E171 can no longer be considered as safe, because a concern for genotoxicity could not be ruled out (EFSA Panel on Food Additives and Flavourings (FAF) et al., 2021). ZnO-NPs have received much attention in cancer therapy, electrochemical DNA biosensors, antibiofilm action, industrial packaging, urban wastewater treatment, seed treatment, and UV-blocking products (Abbas et al., 2019; Abu-Salah et al., 2010; Elhaj Baddar and Unrine, 2018; Khan et al., 2020; Liu et al., 2020; Murcia Mesa et al., 2019; Olson et al., 2019). Finally, Ag-NPs are used in food industry, as food-contact plastics (Han et al., 2011) or food additive (E174) in its elemental form (EFSA Panel on Food Additives and Nutrient Sources added to Food (ANS), 2016). In addition, they are widely applied in biomedicine, pharmaceuticals, health care, drug and gene delivery, environmental research, water treatment, and many other fields, although their main application is their antimicrobial property (Fontecha-Umaña et al., 2020; Jha et al., 2017; Shimabuku et al., 2017; Valsalam et al., 2019; Vines et al., 2018).

The developmental process by which cells acquire distinct identities, and thus embryotoxicity, from NPs is of particular interest to scientists in the field of nanotoxicology, and various animal models have proven useful for this purpose, from invertebrates to vertebrates. Furthermore, the study of zebrafish embryonic development is much less expensive than embryonic development of higher vertebrate models in terms of the amount of material required, time, manipulation, cost, and accessibility (Bai and Tang,

2020), and for the above reasons, it represent attractive animal model for screening toxic effects of environmental pollutants. In particular, the Fish Embryo Acute Toxicity Test (ZFET) on the zebrafish (Danio rerio), OECD Test Guideline (TG) 236, is useful in bridging a gap between cell culture and small animal models. It can be used as an alternative to the Acute Fish Toxicity Test (AFT), OECD Test Guideline 203, as it is more sensitive and more closely resembles humans than other whole-organism models (von Hellfeld et al., 2020), as about 85% of its genes are homologous with human counterparts (Renier et al., 2007).

5.2 Material and Methods

5.2.1 Zebrafish Maintenance and Embryo Collection

Zebrafish of strain AB (wild type) were obtained from the Center of Experimental Ichthyiopathology of Sicily (CISS), University of Messina, Italy, where they were kept in a "Fish facility" (Stand Alone Unit, Tecniplast) with a closed-circuit system allowing continuous monitoring of vital signs. They were reared in a circulating aquarium system in an environmentally controlled room (28°C, 80% humidity), with the photoperiod set to a 14-h light/10-h dark cycle. Adult zebrafish were fed twice a day with Artemia sp (hatched from eggs in saline water). For the experiments, fertilized eggs were collected and selected under a stereomicroscope (Leica M0205C, Multifocus) within 4-hour post fertilization (hpf). All embryos were derived from the same eggs.

5.2.2 Fish Embryo Toxicity (FET) Test

Fish Embryo Toxicity (FET) test was performed according to OECD (2013). Zebrafish embryos exposed to TiO_2-NPs with a nominal size of 60 nm, TiO_2 used as a food additive (E171), ZnO-NPs with a nominal size of 30 nm, Ag-NPs with a certified value of 39±5 nm and

Ag used as a food additive (E174) at concentrations of 100 mg/L for all the chemicals, and at 50 mg/L, 25 mg/L, 12.5 mg/L, and 6.25 mg/L only for Ag-NPs. Experiments lasted for 4–96 hpf, and measured for embryonic/larval mortality and hatching rate every 24 h. Healthy embryos were placed in 24-well culture plates (1 embryo in 2 ml solution/well). with internal plate controls (negative control). Each group had five replicate wells. Each experiment was replicated four times. During the exposure period (4–96 hpf), photographs of the embryos were captured under a stereomicroscope (Leica M0205C, Multifocus) and the percentage of abnormal embryos was counted every 24 h. Tests were considered valid if at least 90% of the negative control embryos survived.

5.4 Results and Discussion

5.4.1 Acute toxicity test on zebrafish embryos exposed to TiO_2 suspension of 60 nm and E171.

The two chemical forms of TiO_2 showed low solubility at the concentration studied. Therefore, it was difficult to observe the embryos throughout the experimental period, as the chorion was uniformly covered by the studied molecules. Moreover, no spontaneous movement was observed at 48 hpf in 75% of the embryos exposed to TiO_2 60 nm. As it is found in literature, it seems that metallic NPs such as zinc oxide, titanium dioxide, silicon dioxide, copper and silver, tend to accumulate on or in chorion structures of zebrafish eggs (Brun et al., 2018; Fent et al., 2010; Lin et al., 2011; Osborne et al., 2013), although the chorionic pore size ranging from 0.5 to 1 μm is large enough to allow nanoparticle entry to the chorionic sac. Until now, the potential process of particle uptake from the chorionic and vitelline membranes has been difficult to interpret due to the limitations of the detection techniques used (Brinkmann et al., 2021). Furthermore, the reactivity and toxicity of different metallic nanoparticles varies depending on the type and size of the particles, and particle size has an inverse effect on the

dissolution of metal NPs or the ionic strength of the media (Lacave et al., 2016). Chorion-attached nanoparticles, observed in TiO_2 exposed embryos, can interfere in several ways with embryo development, as the leaching of toxic ion onto the developing embryos (Batel et al., 2018), interference with the microbial chorion community, which play a predominant role in normal neurobehavioral development (Phelps et al., 2017), and the obstruction of gas exchange across the chorion surface (Duan et al., 2020). The accumulation of TiO_2 particles on zebrafish eggs was confirmed by Brinkmann et al. (2021) by exposing them to 2, 5 and 10 mg/L of TiO_2 with primary particle sizes around 15-24 nm. Although the adsorbed particles did not exert antimicrobial effects, they led to an overall increase in microbial abundance, which could have a cascading effect on later life stages (Brinkmann et al., 2021). Nevertheless, at the end of the 96-hour exposure, embryos hatched in 85% exposed to TiO_2 60nm and in 90% exposed to E171 (Table 5.1), with proper separation of the tail bud, resorption of the yolk, and somite formation. Embryos exposed to E171 were observed to hatch earlier than controls, in 65% at 48 hpf (Table 5.1). Overall, the results suggest no acute embryotoxicity of the chemicals, although coagulation of the fertilized eggs was observed in 10% for embryos exposed to both TiO_2 chemical forms, without significant differences with the control group.

Table 5.1. Lethality and hatching recorded for zebrafish embryos exposed to 100 mg/L TiO_2- NPs and 100 mg/L E171 from 24 hpf to 96 hpf.

100 mg/L TiO_2 60 nm	**TiO_2 60 nm**	**Control group**
% Lethality 24h	5	5
% Lethality 48h	10	5
% Lethality 72h	10	10
% Lethality 96h	10	10
100 mg/L TiO_2 60 nm	**TiO_2 60 nm**	**Control group**
% Hatching 24h	0	0
% Hatching 48h	0	0
% Hatching 72h	25	15
% Hatching 96h	85	80
100 mg/L E171	**E171 60 nm**	**Control group**
% Lethality 24h	0	5
% Lethality 48h	0	5
% Lethality 72h	0	10
% Lethality 96h	5	10
100 mg/L E171	**E171 60 nm**	**Control group**
% Hatching 24h	0	0
% Hatching 48h	0	0
% Hatching 72h	65	15
% Hatching 96h	95	80

Toxicity studies inherent developing zebrafish (Danio rerio) embryos exposed to TiO_2 are often inconsistent. The findings reported by Kansara et al., (2020), who tested the survival rate of zebrafish embryos from 0 to 96 hpf, showed that 100% of embryos died at an exposure concentration of 100 mg/L P25 TiO_2 after 72 hpf, versus an increase of ROS generation. Conversely, Zhu et al., (2008) tested the effects of exposure to smaller diameter TiO_2 (< 20 nm) at a concentration of 500 mg/L on early development and recorded a 100% successful hatching rate at 84 hours post-fertilization (hpf), which was no different from exposure to bulk TiO_2 and had no significant malformations. As well, Tang et al., (2019) found that zebrafish embryos exposed to 100 mg/L of TiO_2 (25 nm) had no effect on hatching rate and showed no signs of malformations at 96 hpf, although long-term adult exposure can cause oxidative damage. At the same exposure concentration of 100 mg/L, it was found that P25

TiO_2, with an average primary particle size of 21 nm, led to a significant premature hatching, with an EC value of 107.2 mg/L at 62 hpf (Samaee et al., 2015).

Lower exposure concentrations of 0.1 to 10 mg/L of P25 TiO_2 did not affect hatchability, survival, and malformation rate to 120 hpf, although subtle behavioral changes were observed in larvae of the low concentration groups (Chen et al., 2011).

Furthermore, it seems that combined exposure of zebrafish embryos to TiO_2 suspension with other parameters brought to different results. Bar-Ilan et al. (2012) exposed for 5 days fertilized eggs to a concentration of 100-1000 mg/L P25 TiO_2, revealed how increased ROS and toxicity was entirely dependent on illumination, given the high photocatalytic property of this molecule (Bar-Ilan et al., 2012, p.). This was also confirmed in the long-term test, where zebrafish exposed to as little as 1 ng/mL showed a significant increase in mortality, as well as a significant increase in aggregation, uptake and toxicity with increasing exposure concentration (Bar-Ilan et al., 2013). Accordingly, the life stage of yolk-sac larvae was found to be the most sensitive to TiO_2 phototoxicity than embryos, free-swimming larvae and juvenile life stage (Ma and Diamond, 2013). Kansara et al. (2020) found a decreased mortality in the presence of humic acid and a mixture of HA and clay, versus a decreased of ROS generation, indicating a mitigation of toxicity in presence of organic matter.

Results obtaining related TiO_2 developmental toxicity at the chosen exposure concentrations confirm some literature results. A preliminary approach on reproductive endpoint E171 toxicity was carried on, but there is still a gap on the in vivo evidence of hepatotoxicity, hematotoxicity, genotoxicity and immunotoxicity, because some effects are expected to be similar TiO_2 nanoparticles, as it was confirmed by in vitro studied (Medina-Reyes et al., 2020), although with different purity, shape and size distribution because the synthesis is different.

5.4.2 Acute toxicity test on zebrafish embryos exposed to ZnO suspension of 30 nm

ZnO-NPs (30nm) was also tested for acute developmental toxicity in zebrafish. The exposure concentration of 100 mg/L showed good solubility in the test medium and provided good visibility. Somite formation with lateral contractions and incipient erection of the tail around the yolk sac was clearly observed from 24 hpf. One embryo had a shorter body length than the others after the first 24 hours, and this endpoint of ZnO-NPs toxicity grew up to 25% at the end of 96 hpf.

Overall, 95% of the fertilized eggs had not hatched (Table 5.2), and the heartbeat indicated that they were alive, showing correct morphogenesis of the primary organ systems. In the end, only one embryo hatched in which the yolk sac was completely resorbed and the tail bud was properly detached. Therefore, the results do not suggest acute effects of lethality, although the delay in development should be further investigated.

Table 5.2. Lethality and hatching recorded for zebrafish embryos exposed to 100 mg/L ZnO-NPs from 24 hpf to 96 hpf.

100 mg/L ZnO 30 nm	**ZnO 30 nm**	**Control group**
% Lethality 24h	0	5
% Lethality 48h	0	5
% Lethality 72h	0	10
% Lethality 96h	0	10
100 mg/L ZnO 30 nm	**ZnO 30 nm**	**Control group**
% Hatching 24h	0	0
% Hatching 48h	0	0
% Hatching 72h	0	15
% Hatching 96h	5	80

Our results confirm the findings in the literature on the toxic effect of ZnO in altering hatching rate with concentration between 10 and 120 mg/L (Bai Wei et al., 2010; Kteeba et al., 2017; Lacave et al., 2016;

Zhao et al., 2016; Zhu et al., 2008), probably linked to an effect on the metalloprotease, ZHE 1, which is responsible for degradation of the chorionic membrane (Lin et al., 2013).

In particular, it was estimated that exposure concentrations of ZnO (30 nm primary particle size) in the range of 25-50 mg/L resulted in significant delay in hatching of embryos after 96 hpf, along with a reduction in larval body length and tail malformation, but mortality was observed between 50 and 100 mg/L (Bai Wei et al., 2010). The reduction in body size, malformation and delay in hatching was also observed by Kteeba et al., (2017), who also revealed how different organic compound classes can attenuate the endpoints of ZnO-NPs toxicity. In particular, humic acid or humic acid containing NOMs were the best mitigators of ZnO-NPs reductions in hatching rate.

The effects of ZnO (20 nm) on early development were tested at a concentration of 1 mg/L. This revealed 75.3% of successful hatching rate at 84 hpf and 71.6% of survival rate at 96 hpf (Zhu et al., 2008). These parameters decrease significantly with higher concentration, resulting in delayed development of zebrafish embryos and larvae. The EC50 value for hatching rate was calculated to be 2.065 mg/L at 84 hpf, while the 96-h LC50 value of the ZnO suspension was 1.793 mg/L, with no significant differences from ZnO bulk, versus an LC50 >10 mg/L calculated by Lacave et al. (2016), probably due to the differences in particle size used.

Other observed endpoints of ZnO are the acceleration of heartbeat at 120 mg/L exposure, indicating a probable physiological mechanism compensating for body hypoxia (Zhao et al., 2016), generation of reactive oxygen species (ROS) (Zhao et al., 2016, 2013) cell apoptosis (Zhao et al., 2016) and DNA damage (Zhao et al., 2013; Zhu et al., 2008).

5.4.3 Acute toxicity test on zebrafish embryos exposed to Ag suspension of 40 nm and E174

Ag-NPs 40 nm showed early signs of acute toxicity from the first 24 hpf, with coagulation of 100% of embryos. In contrast, embryos exposed to elemental Ag (E174) showed normal development with proper somite formation, detachment of the tail and normal heartbeat. At 72 hpf, 35% of the embryos hatched alive, with 85% reaching at the end of the exposure. Only one 15% of embryos were coagulated at 96 hpf (Table 5.3).

Table 5.3. Lethality and hatching recorded for zebrafish embryos exposed to 100 mg/L Ag E174 from 24 hpf to 96 hpf.

100 mg/L Ag E174	**Ag E174**	**Control group**
% Lethality 24h	5	5
% Lethality 48h	5	5
% Lethality 72h	5	10
% Lethality 96h	15	10
100 mg/L Ag E174	**Ag E174**	**Control group**
% Hatching 24h	0	0
% Hatching 48h	5	0
% Hatching 72h	35	15
% Hatching 96h	85	80

To improve the information on the acute toxicity of Ag-NPs 40 nm to embryos, additional ZFET tests were performed with exposure concentrations of 50 mg/L, 25 mg/L, 12.5 mg/L, and 6.25 mg/L.

At the concentrations of 50 mg/L and 25 mg/L, 100% of the embryos coagulated in the first 24 hpf. After 48 hpf to 12.5 mg/L, 65% of the embryos hatched, but the heartbeat was not clearly observed. After 72 hpf, 85% of the embryos were dead and reached 95% after 96 hpf (Table 5.4).

After 48 hpf to 6.5 mg/L, 100% of the exposed embryos were alive and of these, 75% had hatched. In comparison, the embryos in the control group were alive and had not yet hatched. At the end of the 96 hpf, 95% of the exposed embryos had hatched alive. The evaluated LC50 for Ag 40 nm was 9.604 mg/L but experimental condition needs to be repeated with further concentration between 6 and 12 mg/L to better study endpoints of Ag 40 nm toxicity.

Table 5.4. Lethality and hatching recorded for zebrafish embryos exposed to Ag-NPs 40 nm (concentration range: 6.25-100 mg/L) from 24 hpf to 96 hpf.

100 mg/L Ag 40 nm	**Ag 40 nm**	**Control group**	**100 mg/L Ag 40nm**	**Ag 40 nm**	**Control group**
% Lethality 24h	100	0	% Hatching 24h	0	0
50 mg/L Ag 40 nm	**Ag 40 nm**	**Control group**	**50 mg/L Ag 40 nm**	**Ag 40 nm**	**Control group**
% Lethality 24h	100	0	% Hatching 24h	0	0
25 mg/L Ag 40 nm	**Ag 40 nm**	**Control group**	**25 mg/L Ag 40nm**	**Ag 40 nm**	**Control group**
% Lethality 24h	100	0	% Hatching 24h	0	0
12.5 mg/L Ag 40 nm	**Ag 40 nm**	**Control group**	**12.5 mg/L Ag 40nm**	**Ag 40 nm**	**Control group**
% Lethality 24h	0	0	% Hatching 24h	0	0
% Lethality 48h	0	0	% Hatching 48h	60	0
% Lethality 72h	85	0	% Hatching 72h	-	100
% Lethality 96h	95	0	% Hatching 96h	-	100
6.25 mg/L Ag 40 nm	**Ag 40 nm**	**Control group**	**6.25 mg/L Ag 40nm**	**Ag 40 nm**	**Control group**
% Lethality 24h	0	0	% Hatching 24h	0	0
% Lethality 48h	0	0	% Hatching 48h	75	0
% Lethality 72h	5	0	% Hatching 72h	95	100
% Lethality 96h	5	0	% Hatching 96h	95	100

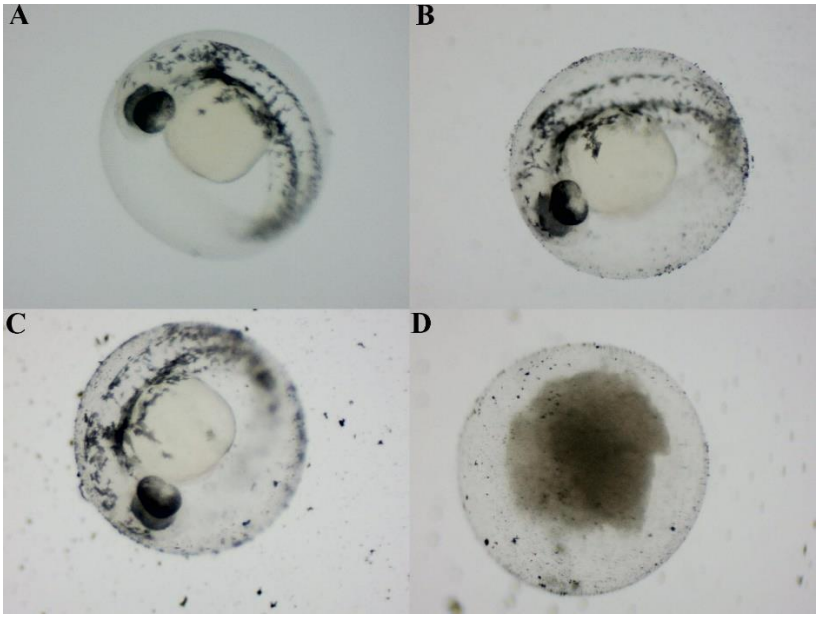

Figure 5.1. Embryos at 24 hpf. A: CTR; B: exposure level 6.25 mg/L; C: exposure level 12.5 mg/L; D: coagulated embryo at exposure level 50 mg/L.

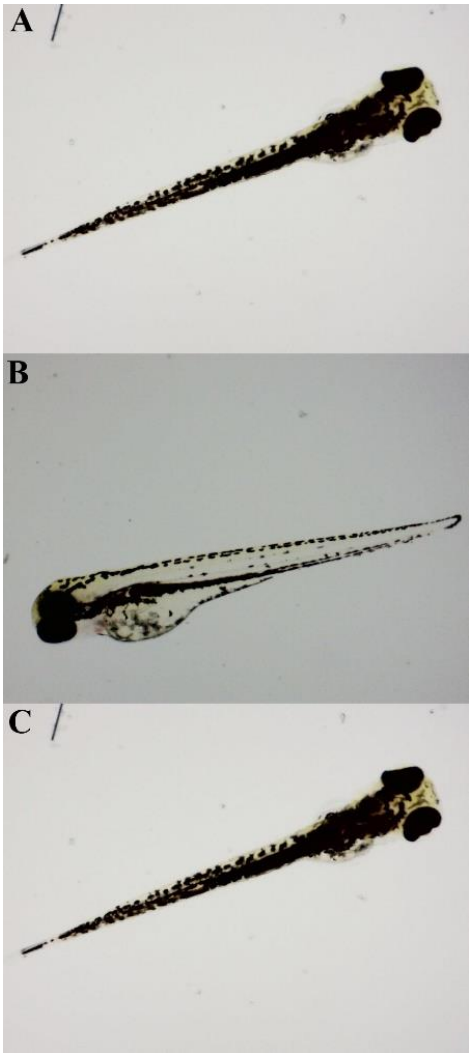

Figure 5.2. Hatched embryos at 76 hpf. A: CTRL; B: exposure level 6.25 mg/L; C: exposure level 12.5 mg/L

Ag-NPs are among the most studied metallic nanoparticles, as acute and chronic toxicity in various animal models is becoming increasingly known. Accordingly, early developmental stages and lethality are affected in a concentration- and size-dependent manner, with smaller NPs exerting higher toxic effects than those of larger size (Lacave et al., 2016; Powers et al., 2007), or in the form of nanoplates, as the low leaching of Ag+ (George et al., 2012), although several disagreements on this topic can be found.

Most studies in literature focus on the toxicity of coated Ag-NPs. The LC50 calculated in the early developmental stage of zebrafish for maltose-coated Ag-NPs of different sizes showed a progressively higher concentration from the smaller size (40 nm; 0.529 mg/L) to the highest one (100 nm; 1.973 mg/L)(Lacave et al., 2016). It seems that that coating Ag-NPs may reduce toxicity in different ways. For example, coating 10 nm Ag with citrate or fulvic acid significantly reduced toxicity, while 35 nm Ag without coating was significantly more toxic than 10 nm Ag (respectively, 5 and 50 μg/L the lowest effect concentration at 48 hpf) (Osborne et al., 2013).

5.4 Conclusion

Results obtained from ZFET related to TiO_2 and ZnO are in line with literature findings but they need further investigations. Unfortunately, there is a deep gap in the knowledge of E174 toxicity, compared to what is known of the Ag-NPs. Recently, the nanoparticle fraction in E174 and in products containing E174 was sized and quantified showing that E174 itself contains up to 23% of Ag nanoparticles while E174-containing food products up to 16% of Ag-NPs with a mean of 15.3–22.5 nm (Waegeneers et al., 2019), but data about the E174 exposure risk remain unknown. Reproductive toxicity and many others endpoint of toxicity should be enhanced both in vitro and in vivo.

References

- Abbas, M., Buntinx, M., Deferme, W., Peeters, R., 2019. (Bio)polymer/ZnO Nanocomposites for Packaging Applications: A Review of Gas Barrier and Mechanical Properties. Nanomater. Basel Switz. 9, E1494. https://doi.org/10.3390/nano9101494
- Abu-Salah, K.M., Alrokyan, S.A., Khan, M.N., Ansari, A.A., 2010. Nanomaterials as analytical tools for genosensors. Sensors 10, 963–993. https://doi.org/10.3390/s100100963
- Bai, C., Tang, M., 2020. Toxicological study of metal and metal oxide nanoparticles in zebrafish. J. Appl. Toxicol. 40, 37–63. https://doi.org/10.1002/jat.3910
- Bai Wei, Zhang Zhiyong, Tian Wenjing, He Xiao, Ma Yuhui, Zhao Yuliang, Chai Zhifang, 2010. Toxicity of zinc oxide nanoparticles to zebrafish embryo: a physicochemical study of toxicity mechanism. J. Nanoparticle Res. 12, 1645–1654.
- Bar-Ilan, O., Chuang, C.C., Schwahn, D.J., Yang, S., Joshi, S., Pedersen, J.A., Hamers, R.J., Peterson, R.E., Heideman, W., 2013. TiO_2 Nanoparticle Exposure and Illumination during Zebrafish Development: Mortality at Parts per Billion Concentrations. Environ. Sci. Technol. 47, 4726–4733. https://doi.org/10.1021/es304514r
- Bar-Ilan, O., Louis, K.M., Yang, S.P., Pedersen, J.A., Hamers, R.J., Peterson, R.E., Heideman, W., 2012. Titanium dioxide nanoparticles produce phototoxicity in the developing zebrafish. Nanotoxicology 6, 670–679. https://doi.org/10.3109/17435390.2011.604438
- Batel, A., Borchert, F., Reinwald, H., Erdinger, L., Braunbeck, T., 2018. Microplastic accumulation patterns and transfer of benzo[a]pyrene to adult zebrafish (Danio rerio) gills and zebrafish embryos. Environ. Pollut. 235, 918–930. https://doi.org/10.1016/j.envpol.2018.01.028
- Brinkmann, B.W., Beijk, W.F., Vlieg, R.C., van Noort, S.J.T., Mejia, J., Colaux, J.L., Lucas, S., Lamers, G., Peijnenburg, W.J.G.M., Vijver, M.G., 2021. Adsorption of titanium dioxide nanoparticles onto zebrafish eggs affects colonizing microbiota. Aquat. Toxicol. 232, 105744. https://doi.org/10.1016/j.aquatox.2021.105744
- Brun, N.R., Koch, B.E.V., Varela, M., Peijnenburg, W.J.G.M., Spaink, H.P., Vijver, M.G., 2018. Nanoparticles induce dermal and intestinal innate immune system responses in zebrafish embryos. Environ. Sci. Nano 5, 904–916. https://doi.org/10.1039/C8EN00002F
- Chen, T.-H., Lin, C.-Y., Tseng, M.-C., 2011. Behavioral effects of titanium dioxide nanoparticles on larval zebrafish (Danio rerio). Mar. Pollut. Bull., 6th International Conference on Marine Pollution and Ecotoxicology 63, 303–308. https://doi.org/10.1016/j.marpolbul.2011.04.017

- Duan, Z., Duan, X., Zhao, S., Wang, X., Wang, J., Liu, Y., Peng, Y., Gong, Z., Wang, L., 2020. Barrier function of zebrafish embryonic chorions against microplastics and nanoplastics and its impact on embryo development. J. Hazard. Mater. 395, 122621. https://doi.org/10.1016/j.jhazmat.2020.122621
- EFSA Panel on Food Additives and Flavourings (FAF), Younes, M., Aquilina, G., Castle, L., Engel, K.-H., Fowler, P., Frutos Fernandez, M.J., Fürst, P., Gundert-Remy, U., Gürtler, R., Husøy, T., Manco, M., Mennes, W., Moldeus, P., Passamonti, S., Shah, R., Waalkens-Berendsen, I., Wölfle, D., Corsini, E., Cubadda, F., De Groot, D., FitzGerald, R., Gunnare, S., Gutleb, A.C., Mast, J., Mortensen, A., Oomen, A., Piersma, A., Plichta, V., Ulbrich, B., Van Loveren, H., Benford, D., Bignami, M., Bolognesi, C., Crebelli, R., Dusinska, M., Marcon, F., Nielsen, E., Schlatter, J., Vleminckx, C., Barmaz, S., Carfí, M., Civitella, C., Giarola, A., Rincon, A.M., Serafimova, R., Smeraldi, C., Tarazona, J., Tard, A., Wright, M., 2021. Safety assessment of titanium dioxide (E171) as a food additive. EFSA J. 19, e06585. https://doi.org/10.2903/j.efsa.2021.6585
- EFSA Panel on Food Additives and Nutrient Sources added to Food (ANS), 2016. Scientific opinion on the re-evaluation of silver (E 174) as food additive: Re-evaluation of silver (E 174) as food additive. EFSA J. 14, 4364. https://doi.org/10.2903/j.efsa.2016.4364
- EFSA Panel on Food Contact Materials, Enzymes and Processing Aids (CEP), Silano, V., Barat Baviera, J.M., Bolognesi, C., Brüschweiler, B.J., Chesson, A., Cocconcelli, P.S., Crebelli, R., Gott, D.M., Grob, K., Lampi, E., Mortensen, A., Steffensen, I.-L., Tlustos, C., Van Loveren, H., Vernis, L., Zorn, H., Castle, L., Cravedi, J.-P., Kolf-Clauw, M., Milana, M.R., Pfaff, K., Tavares Poças, M. de F., Svensson, K., Wölfle, D., Barthélémy, E., Rivière, G., 2019. Safety assessment of the substance, titanium dioxide surface treated with fluoride-modified alumina, for use in food contact materials. EFSA J. 17, e05737. https://doi.org/10.2903/j.efsa.2019.5737
- EFSA Panel on Food Additives and Nutrient Sources added to Food (ANS), 2016. Re-evaluation of titanium dioxide (E 171) as a food additive. EFSA J. 14, e04545. https://doi.org/10.2903/j.efsa.2016.4545
- Elhaj Baddar, Z., Unrine, J.M., 2018. Functionalized-ZnO-Nanoparticle Seed Treatments to Enhance Growth and Zn Content of Wheat (Triticum aestivum) Seedlings. J. Agric. Food Chem. 66, 12166–12178. https://doi.org/10.1021/acs.jafc.8b03277
- Fent, K., Weisbrod, C.J., Wirth-Heller, A., Pieles, U., 2010. Assessment of uptake and toxicity of fluorescent silica nanoparticles in zebrafish (Danio rerio) early life stages. Aquat. Toxicol. Amst. Neth. 100, 218–228. https://doi.org/10.1016/j.aquatox.2010.02.019
- Fontecha-Umaña, F., Ríos-Castillo, A.G., Ripolles-Avila, C., Rodríguez-Jerez, J.J., 2020. Antimicrobial Activity and Prevention of Bacterial Biofilm Formation of Silver and Zinc Oxide Nanoparticle-Containing Polyester

Surfaces at Various Concentrations for Use. Foods Basel Switz. 9. https://doi.org/10.3390/foods9040442
- George, S., Lin, Sijie, Ji, Z., Thomas, C.R., Li, L., Mecklenburg, M., Meng, H., Wang, X., Zhang, H., Xia, T., Hohman, J.N., Lin, Shuo, Zink, J.I., Weiss, P.S., Nel, A.E., 2012. Surface Defects on Plate-Shaped Silver Nanoparticles Contribute to Its Hazard Potential in a Fish Gill Cell Line and Zebrafish Embryos. ACS Nano 6, 3745–3759. https://doi.org/10.1021/nn204671v
- Han, W., Yu, Y., Li, N., Wang, L., 2011. Application and safety assessment for nano-composite materials in food packaging. Chin. Sci. Bull. 56, 1216–1225. https://doi.org/10.1007/s11434-010-4326-6
- Jha, P.K., Jha, R.K., Rout, D., Gnanasekar, S., Rana, S.V.S., Hossain, M., 2017. Potential targetability of multi-walled carbon nanotube loaded with silver nanoparticles photosynthesized from Ocimum tenuiflorum (tulsi extract) in fertility diagnosis. J. Drug Target. 25, 616–625. https://doi.org/10.1080/1061186X.2017.1306534
- Kansara, K., Kumar, A., Karakoti, A.S., 2020. Combination of humic acid and clay reduce the ecotoxic effect of TiO_2 NPs: A combined physico-chemical and genetic study using zebrafish embryo. Sci. Total Environ. 698, 134133. https://doi.org/10.1016/j.scitotenv.2019.134133
- Khan, F., Lee, J.-W., Pham, D.N.T., Khan, M.M., Park, S.-K., Shin, I.-S., Kim, Y.-M., 2020. Antibiofilm Action of ZnO, SnO2 and CeO2 Nanoparticles Towards Grampositive Biofilm Forming Pathogenic Bacteria. Recent Pat. Nanotechnol. 14, 239–249. https://doi.org/10.2174/1872210514666200313121953
- Kteeba, S.M., El-Adawi, H.I., El-Rayis, O.A., El-Ghobashy, A.E., Schuld, J.L., Svoboda, K.R., Guo, L., 2017. Zinc oxide nanoparticle toxicity in embryonic zebrafish: Mitigation with different natural organic matter. Environ. Pollut. 230, 1125–1140. https://doi.org/10.1016/j.envpol.2017.07.042
- Lacave, J.M., Retuerto, A., Vicario-Parés, U., Gilliland, D., Oron, M., Cajaraville, M.P., Orbea, A., 2016. Effects of metal-bearing nanoparticles (Ag, Au, CdS, ZnO, SiO2) on developing zebrafish embryos. Nanotechnology 27, 325102. https://doi.org/10.1088/0957-4484/27/32/325102
- Li, Y., Ju, D., 2018. The Role of Autophagy in Nanoparticles-Induced Toxicity and Its Related Cellular and Molecular Mechanisms. Adv. Exp. Med. Biol. 1048, 71–84. https://doi.org/10.1007/978-3-319-72041-8_5
- Lin, Sijie, Zhao, Y., Ji, Z., Ear, J., Chang, C.H., Zhang, H., Low-Kam, C., Yamada, K., Meng, H., Wang, X., Liu, R., Pokhrel, S., Mädler, L., Damoiseaux, R., Xia, T., Godwin, H.A., Lin, Shuo, Nel, A.E., 2013. Zebrafish high-throughput screening to study the impact of dissolvable metal oxide nanoparticles on the hatching enzyme, ZHE1. Small Weinh. Bergstr. Ger. 9, 1776–1785. https://doi.org/10.1002/smll.201202128
- Lin, Sijie, Zhao, Y., Xia, T., Meng, H., Zhaoxia, J., Liu, R., George, S., Xiong, S., Wang, X., Zhang, H., Pokhrel, S., Mädler, L., Damoiseaux, R., Lin, Shuo,

Nel, A.E., 2011. High Content Screening in Zebrafish Speeds up Hazard Ranking of Transition Metal Oxide Nanoparticles. ACS Nano 5, 7284–7295. https://doi.org/10.1021/nn202116p

- Liu, M., Peng, Y., Nie, Y., Liu, P., Hu, S., Ding, J., Zhou, W., 2020. Co-delivery of doxorubicin and DNAzyme using ZnO@polydopamine core-shell nanocomposites for chemo/gene/photothermal therapy. Acta Biomater. 110, 242–253. https://doi.org/10.1016/j.actbio.2020.04.041
- Ma, H., Diamond, S.A., 2013. Phototoxicity of TiO_2 nanoparticles to zebrafish (Danio rerio) is dependent on life stage. Environ. Toxicol. Chem. 32, 2139–2143. https://doi.org/10.1002/etc.2298
- Medina-Reyes, E.I., Rodríguez-Ibarra, C., Déciga-Alcaraz, A., Díaz-Urbina, D., Chirino, Y.I., Pedraza-Chaverri, J., 2020. Food additives containing nanoparticles induce gastrotoxicity, hepatotoxicity and alterations in animal behavior: The unknown role of oxidative stress. Food Chem. Toxicol. 146, 111814. https://doi.org/10.1016/j.fct.2020.111814
- Mody, V.V., Siwale, R., Singh, A., Mody, H.R., 2010. Introduction to metallic nanoparticles. J. Pharm. Bioallied Sci. 2, 282–289. https://doi.org/10.4103/0975-7406.72127
- Murcia Mesa, J.J., Arias Bolivar, L.G., Sarmiento, H.A.R., Martínez, E.G.Á., Páez, C.J., Lara, M.A., Santos, J.A.N., Del Carmen Hidalgo López, M., 2019. Urban wastewater treatment by using Ag/ZnO and Pt/TiO_2 photocatalysts. Environ. Sci. Pollut. Res. Int. 26, 4171–4179. https://doi.org/10.1007/s11356-018-1592-3
- Olson, E., Li, Y., Lin, F.-Y., Miller, A., Liu, F., Tsyrenova, A., Palm, D., Curtzwiler, G.W., Vorst, K.L., Cochran, E., Jiang, S., 2019. Thin Biobased Transparent UV-Blocking Coating Enabled by Nanoparticle Self-Assembly. ACS Appl. Mater. Interfaces 11, 24552–24559. https://doi.org/10.1021/acsami.9b05383
- Osborne, O.J., Johnston, B.D., Moger, J., Balousha, M., Lead, J.R., Kudoh, T., Tyler, C.R., 2013. Effects of particle size and coating on nanoscale Ag and TiO_2 exposure in zebrafish (Danio rerio) embryos. Nanotoxicology 7, 1315–1324. https://doi.org/10.3109/17435390.2012.737484
- Phelps, D., Brinkman, N.E., Keely, S.P., Anneken, E.M., Catron, T.R., Betancourt, D., Wood, C.E., Espenschied, S.T., Rawls, J.F., Tal, T., 2017. Microbial colonization is required for normal neurobehavioral development in zebrafish. Sci. Rep. 7, 11244. https://doi.org/10.1038/s41598-017-10517-5
- Powers, K., Palazuelos, M., Moudgil, B., Roberts, S., 2007. Characterization of the size, shape, and state of dispersion of nanoparticles for toxicological studies. Nanotoxicology 1, 42–51.
- Renier, C., Faraco, J.H., Bourgin, P., Motley, T., Bonaventure, P., Rosa, F., Mignot, E., 2007. Genomic and functional conservation of sedative-hypnotic targets in the zebrafish. Pharmacogenet. Genomics 17, 237–253. https://doi.org/10.1097/FPC.0b013e3280119d62

- Rodríguez-Hernández, A.G., Vazquez-Duhalt, R., Huerta-Saquero, A., 2020. Nanoparticle-plasma Membrane Interactions: Thermodynamics, Toxicity and Cellular Response. Curr. Med. Chem. 27, 3330–3345. https://doi.org/10.2174/0929867325666181112090648
- Rompelberg, C., Heringa, M.B., van Donkersgoed, G., Drijvers, J., Roos, A., Westenbrink, S., Peters, R., van Bemmel, G., Brand, W., Oomen, A.G., 2016. Oral intake of added titanium dioxide and its nanofraction from food products, food supplements and toothpaste by the Dutch population. Nanotoxicology 10, 1404–1414. https://doi.org/10.1080/17435390.2016.1222457
- Ruszkiewicz, J.A., Pinkas, A., Ferrer, B., Peres, T.V., Tsatsakis, A., Aschner, M., 2017. Neurotoxic effect of active ingredients in sunscreen products, a contemporary review. Toxicol. Rep. 4, 245–259. https://doi.org/10.1016/j.toxrep.2017.05.006
- Samaee, S.-M., Rabbani, S., Jovanović, B., Mohajeri-Tehrani, M.R., Haghpanah, V., 2015. Efficacy of the hatching event in assessing the embryo toxicity of the nano-sized TiO_2 particles in zebrafish: A comparison between two different classes of hatching-derived variables. Ecotoxicol. Environ. Saf. 116, 121–128. https://doi.org/10.1016/j.ecoenv.2015.03.012
- Schneider, S.L., Lim, H.W., 2019. A review of inorganic UV filters zinc oxide and titanium dioxide. Photodermatol. Photoimmunol. Photomed. 35, 442–446. https://doi.org/10.1111/phpp.12439
- Shimabuku, Q.L., Arakawa, F.S., Fernandes Silva, M., Ferri Coldebella, P., Ueda-Nakamura, T., Fagundes-Klen, M.R., Bergamasco, R., 2017. Water treatment with exceptional virus inactivation using activated carbon modified with silver (Ag) and copper oxide (CuO) nanoparticles. Environ. Technol. 38, 2058–2069. https://doi.org/10.1080/09593330.2016.1245361
- Stone, V., Johnston, H., Clift, M.J.D., 2007. Air pollution, ultrafine and nanoparticle toxicology: cellular and molecular interactions. IEEE Trans. Nanobioscience 6, 331–340. https://doi.org/10.1109/tnb.2007.909005
- Tang, T., Zhang, Z., Zhu, X., 2019. Toxic Effects of TiO_2 NPs on Zebrafish. Int. J. Environ. Res. Public. Health 16, 523. https://doi.org/10.3390/ijerph16040523
- Valsalam, S., Agastian, P., Esmail, G.A., Ghilan, A.-K.M., Al-Dhabi, N.A., Arasu, M.V., 2019. Biosynthesis of silver and gold nanoparticles using Musa acuminata colla flower and its pharmaceutical activity against bacteria and anticancer efficacy. J. Photochem. Photobiol. B 201, 111670. https://doi.org/10.1016/j.jphotobiol.2019.111670
- Vines, J.B., Lim, D.-J., Park, H., 2018. Contemporary Polymer-Based Nanoparticle Systems for Photothermal Therapy. Polymers 10. https://doi.org/10.3390/polym10121357
- von Hellfeld, R., Brotzmann, K., Baumann, L., Strecker, R., Braunbeck, T., 2020. Adverse effects in the fish embryo acute toxicity (FET) test: a catalogue

of unspecific morphological changes versus more specific effects in zebrafish (Danio rerio) embryos. Environ. Sci. Eur. 32, 122. https://doi.org/10.1186/s12302-020-00398-3

- Waegeneers, N., De Vos, S., Verleysen, E., Ruttens, A., Mast, J., 2019. Estimation of the Uncertainties Related to the Measurement of the Size and Quantities of Individual Silver Nanoparticles in Confectionery. Mater. Basel Switz. 12, E2677. https://doi.org/10.3390/ma12172677
- Zhang, H., Shi, J., Su, Y., Li, W., Wilkinson, K.J., Xie, B., 2020. Acute toxicity evaluation of nanoparticles mixtures using luminescent bacteria. Environ. Monit. Assess. 192, 484. https://doi.org/10.1007/s10661-020-08444-6
- Zhang, Y.-N., Poon, W., Tavares, A.J., McGilvray, I.D., Chan, W.C.W., 2016. Nanoparticle-liver interactions: Cellular uptake and hepatobiliary elimination. J. Control. Release Off. J. Control. Release Soc. 240, 332–348. https://doi.org/10.1016/j.jconrel.2016.01.020
- Zhao, X., Ren, X., Zhu, R., Luo, Z., Ren, B., 2016. Zinc oxide nanoparticles induce oxidative DNA damage and ROS-triggered mitochondria-mediated apoptosis in zebrafish embryos. Aquat. Toxicol. Amst. Neth. 180, 56–70. https://doi.org/10.1016/j.aquatox.2016.09.013
- Zhao, X., Wang, S., Wu, Y., You, H., Lv, L., 2013. Acute ZnO nanoparticles exposure induces developmental toxicity, oxidative stress and DNA damage in embryo-larval zebrafish. Aquat. Toxicol. Amst. Neth. 136–137, 49–59. https://doi.org/10.1016/j.aquatox.2013.03.019
- Zhu, X., Zhu, L., Duan, Z., Qi, R., Li, Y., Lang, Y., 2008. Comparative toxicity of several metal oxide nanoparticle aqueous suspensions to Zebrafish (Danio rerio) early developmental stage. J. Environ. Sci. Health Part A Tox. Hazard. Subst. Environ. Eng. 43, 278–284. https://doi.org/10.1080/10934520701792779

10.6 CHAPTER 6: Behaviour and fate of Ag-NPs, TiO_2-NPs and ZnO-NPs in an in vitro digestion model of the human gastrointestinal tract and calculation of the biopersistence rate.

Alfina Grasso[1], Margherita Ferrante[1], Gianluca Giuberti[2], Margherita Dall'Asta[2], Edoardo Puglisi[2], Chiara Copat[1]

[1] Department of Medical, Surgical and Advanced Technologies "G.F. Ingrassia", University of Catania, Italy.

[2] Department for Sustainable Food Process-DiSTAS, Università Cattolica del Sacro Cuore, Piacenza, Italy.

Abstract

Metallic nanoparticles (MNPs) have attracted incredible attention in many fields and especially in the food industry to develop products that have the potential to extend shelf life, increase nutritional value of food, and prevent bacterial contamination. This indiscriminate use has led to an increase in these contaminants in the environment, while increasing the likelihood of human exposure through consumption of fish products. Considering that oral ingestion is one of the most important routes of exposure, the main toxic effects of MNPs most likely involve the gastrointestinal tract.

This study provides information on the behaviour of MNPs (Ag-NPs, TiO_2-NPs, ZnO-NPs) naturally present in cannes seafood compared to a standard concentration (Ag-NPs 40 nm, TiO_2-NPs 60 nm, ZnO-NPs 30 nm) during static digestion in vitro. The aim was to evaluate the biopersistence rate according to the formula of the EFSA guidance published in 2018.

sp-ICP-MS was performed to determine particle number concentrations, particle size distribution, and ionic metal concentrations in oral, gastric, and intestinal digests at different stages.

Our results have highlighted important phenomena of agglomeration and dispersion that may occur depending on the conditions of the environment and sample matrix studied. Among standard suspensions, ZnO-NPs seem to be more degradable than Ag-NPs and TiO_2-NPs, which have lower biopersistence rates, while among NPs naturally present in the food matrix, Ag-NPs were found to be more degradable than ZnO-NPs and TiO_2-NPs.

However, the calculated biopersistence rates are higher than the limit set by EFSA (12%), indicating that the investigated metallic nanoparticles are stable under gastrointestinal conditions and cannot be considered as readily degradable.

Keywords: Nanoparticles; Food; Static digestion; Biopersistance.

6.1 Introduction

Although nanoparticles are widespread in nature, it was only with technological advances and the development of powerful instruments that humans were able to study them.

Nanoparticles are not only found in their natural form (Schaming et al., 2015), but nowadays they are also widely manufactured and processed by humans to be used in various industrial production sectors, in countless production areas, including energy, electronics and computers, biology, medicine, and everyday consumer goods, including food (Thiruvengadam et al., 2018).

The interesting thing about nanotechnology is that the reduction of a material to the nanoscale results in that material having very different properties from the same material in bulk form, such as higher reactivity and optical, thermal, catalytic, electronic and mechanical properties such as strength, flexibility and deformability (Tiede et al., 2008; Trindade et al., 2001).

The use of nanomaterials and nanoparticles in the food industry is increasing. They may be present directly in food as additives, pigments and supplements or used in the manufacture of products intended to come into contact with food, such as packaging, kitchen utensils, containers, etc., with a significant risk of release into food (Singh et al., 2017).

Titanium dioxide (TiO_2) is used in large quantities in the food industry, mainly in the form of E171, a white food pigment containing up to 36% TiO_2-NPs (Weir et al., 2012). In its nanoscale form, it is also used in food packaging to extend the shelf life of products due to its antimicrobial properties (Chawla et al., 2019).

Ag-NPs have great antimicrobial and fungistatic properties, which is why they are widely used in the food industry, especially in food preservation, packaging, and water treatment (Zorraquín-Peña et al., 2020).

ZnO-NPs are widely used in food industry for zinc supplementation in various foods, as it is an essential micronutrient for human health

(Jung et al., 2021), as well as in packaging, thanks to its antimicrobial action (Jones et al., 2009).
According to the 2011 European Commission definition, a nanomaterial (NM) is a material that consists of at least 50% of particles or aggregates of particles with a size of 1 to 100 nm (EFSA Scientific Committee et al., 2011).
Because of this intensive use, attention should be focused on the extent of exposure to these nanoparticles and their possible effects on the human organism, which may come into contact with them mainly through inhalation, ingestion and skin absorption (De Matteis, 2017).
Despite the interest of the scientific community and the efforts that have been made to study these risks and the various biological interactions between ingested nanoparticles and the host organism, little is known about them.
Indeed, the behaviour of nanoparticles is subject to enormous variability in the gastrointestinal tract, resulting from the properties of the particles themselves, such as size, shape, surface properties and aggregate state, but also from the specificities of the environment in which they are found (Taboada-López et al., 2021).
In the case of ingested NPs, these factors include pH changes between the different sections of the gastrointestinal lumen; physical forces such as peristalsis and chewing to which the ingested material is subjected; the action of the gut microbiota and digestive enzymes; interactions with the food matrix (components such as proteins, carbohydrates and lipids) and biochemical constituents of the medium that can adsorb on the surface of the NPs and form a so-called corona that can alter the resulting complex properties and fate of the NP (Bellmann et al., 2015). The formation of aggregates can affect various aspects of the behaviour of NPs such as reactivity and possible toxicity, in addition to size (Hotze et al., 2010).
Therefore, it is not easy to account for all these variables in studies investigating the interactions between ingested NPs and the gut, and to predict with certainty the behaviour of man-made nanoparticles

(Hotze et al., 2010).
Furthermore, the doses of NPs studied are often significantly higher than the actual estimated levels of daily oral intake, so further efforts need to be made to address the lack of knowledge on this topic (McCracken et al., 2016).
The aim of this work was to study metallic nanoparticles, in particular Ag-NPs, TiO_2-NPs and ZnO-NPs under gastrointestinal conditions naturally present in samples of canned tuna and clams compared to a standard concentration (Ag-NPs 40 nm, TiO_2-NPs 60 nm, ZnO NPs 30 nm) and to calculate the biopersistence rate according to the formula from the EFSA guidance published in 2018 (EFSA Scientific Committee et al., 2018).
The standard concentrations were chosen in accordance with the estimated dietary intake presented in the previous works for canned tuna and clams.
According to EFSA guidance, a nanomaterial is considered to be highly degradable if 12% or less of the material remains as NPs in the intestine at the end of the 30-minute simulated digestion than at the start of the experiment (T0).
sp-ICP-MS was performed to determine particle number concentrations, particle size distribution, and ionic metal concentrations in oral, gastric, and intestinal digests at different stages to evaluate possible changes in nanoparticle behaviour between these different stages.

6.2 Material and method

6.2.1 Reagents

The Ag-NPs solution of size 40 nm was prepared from an Ag-NPs reference material (PELCO® 40 nm, Citrate, NanoXactTM, Ted Pella Inc.). TiO_2-NPs solution of 60 nm was prepared from a TiO_2-NPs standard (TiO_2 Nano Powder 60 nm, Rutile, 99.9%, AEM). ZnO-NPs solution of 30 nm was prepared from a reference nano powder

material (AEM®, purity 98.8%, size 30 nm, Changsha, Hunan, China). The above three reference materials were all obtained from Nanovision (Brugherio, MB, Italy).
Zinc (Zn) ion standard solution (1000 mg/L), Ti ion standard (1000 mg/L) and Ag ion standard (1000 mg/L) were purchased from CPAchem S.r.l. (Roma, Italy) and used for sp-ICP- MS calibration.
Ultrapure water, 0.22μm filtered, was obtained from a Milli-Q purifier (Merck Millipore, Bedford, MA, USA).
Certified reference material for silver nanoparticles (Ag-NPs) (PELCO® 39±5 nm, Citrate, NanoXactTM, 6.1×1010 particles/mL, monitoring m/z 107, Ted Pella Inc., Redding, CA, U.S.A.) was purchased from Nanovision S.r.l (Brugherio, MB, Italy) and used for transport efficiency calculations.
Salivary-α-amylase from human saliva type IX -A, pepsin from porcine gastric mucosa, pancreatin from porcine pancreas and bile salts were obtained from Sigma.

6.2.2. Selected samples

The study was conducted with three different brands of canned tuna and clams purchased from Italian supermarket chains. Each sample was homogenized and stored at -80 °C until in vitro digestion assay.

6.2.3. In vitro gastrointestinal digestion

The in vitro gastrointestinal digestion, simulating the oral, gastric and intestinal digestion phases, was applied to samples and standards according to the static method detailed by Minekus et al., (2014).
Standards were prepared in polypropylene tubes in 50 ml ultrapure water to give a concentration of 2.8x105 part/ml for Ag-NPs, 8.4x104 part/ml for TiO_2-NPs, 1.3x105 part/ml for ZnO-NPs.
Seafood samples were weighed (5 g) and mixed with 50 ml ultrapure water. All samples were homogenized with 5 mL of simulated

salivary fluid (SSF) with a pH of 7.0, and salivary-α-amylase solution was added from the SSF electrolyte stock solution to achieve a final concentration of 75 U/mL in the final volume. The oral step was performed at 37 °C for 2 min. Then, the oral bolus samples (1:1 ratio) were mixed with simulated gastric fluid (SGF) with a pH of 3.0 and porcine pepsin stock solution from SGF electrolyte stock solution was added to reach 2000 U/mL in the final digestion mixture, followed by CaCl2 to reach 0.075 mM in the final digestion mixture. 1 M HCl was added to adjust the pH to 3.0. The gastric phase was performed at 37 °C for 2 hours.
Gastric chyme was mixed (1:1) with simulated intestinal fluid (SIF) electrolyte stock solution at pH 7.0, then pancreatin and bile salts were added to reach 100 U/ml in the final volume (based on trypsin activity) and a final concentration of 10 mM in the final volume, respectively. CaCl2 was added to reach 0.3 mM in the final digestion mixture.
We performed two replicates for sample and two blanks for each batch of digestion in vitro.
A new replicate of the sample (experiment T0) was prepared to measure the concentration of NPs, particle size distribution and dissolved content after a pH of 7.0 and the addition of salivary-α-amylase solution.
Aliquots of 5 ml were taken after 2 min in the oral phase (S), after 60 and 120 (G60, G120) in the gastric phase and after 30, 60 and 120 min in the intestinal phase.
Seafood digest fractions were subjected to centrifugation (3500 rpm, 5°C, 15 min) to obtain the supernatant and were stored with the digest fractions of the standards at -20°C until analysis.

6.2.4. sp-ICP-MS analysis

Ag-NPs, TiO_2-NPs, ZnO-NPs were evaluated using a NexION® 350D (Perkin Elmer, USA) with Syngistix Nano Application Software. The instrumental operating conditions for the

determination of metallic NPs are given in Table 6.1.

Table 6.1. NexION® 350D ICP-MS instrumental condition for single particles determination.

Analyte	Ti	Ag	Zn
Nebulizer, Flow	Meinhard, 1 mL/min	Meinhard, 1 mL/min	Meinhard, 0.92 mL/min
Spray chamber	Glass cyclonic	Glass cyclonic	Glass cyclonic
Sample uptake rate	0.26-0.28 mL/min	0.26-0.28 mL/min	0.26-0.29 mL/min
RF power	1600W	1600W	1600W
Analysis mode	Standard	Standard	Standard
Sampling time	100s	100s	100s
Mass	Ti 49	Ag 107	Zn 64
Dwell time	60 μs	50 μs	50 μs
Data acquisition time	60 sec	60 sec	60 sec
Density	4.23 g/cm^3	10.49 g/cm^3	7.14 g/cm^3
Ag mass fraction	60%	100%	80%

The Single Particle - Inductively Coupled Plasma technique (spICP-MS) allows the identification of the number of particles, the size and the size distribution of the metallic NPs under investigation with simultaneous quantification of the concentration of the dissolved elements.
This is possible using TE% value, ionic calibration fit, the sample flow rate, NPs density and mass fraction.
The transport efficiency was determined using a certified reference material (AgNPs 39±5 nm, 6.1 x 1010 particles/mL, monitoring m/z 107), obtaining values in the range 2.9-5.1%
Calibration standards were prepared in water solution covering the range 0-10 μg/L for Ag and ionic Ti and 0-50 μg/L for ionic Zn.
All digested samples at different time points were analysed after a 1:10 dilution with ultrapure water and sonicated for 20 minutes before analysis.
The limit of detection (LOD) and the limit of quantification (LOQ) were calculated by analysing ten blanks, in the same analytical condition of the samples, and based respectively on the mean ± 3 SD

and the mean ± 10 SD criterion of the number of particles/mL obtained.
In the case of TiO_2-NPs LOD was 2.4 × 103 particles/ml, while LOQ was 3.6 ×103 particles/ml, whereas LOD and LOQ values for dissolved Ti were 0.4 μg L-1 and 0.8 μg/L, respectively.
The valued for Ag-NPs LOD and LOQ were 2.6 × 103 particles/ml and 4.1 × 103 particles/ml and Ag 0.4 ng/L and 0.9 ng/L for dissolved Ag.
As regard ZnO-NPs and dissolved Zn LOD and LOQ values were 2.5 × 103 particles/mL and 4.4 × 103 particles/ml and 4 μg/L and 9 μg/L, respectively.
In addition, LOD in size (LOD nm) was estimated applying the following equation (1) (Lee et al., 2018):

$$\mathrm{LODnm} = \sqrt[3]{\frac{6 \times 3\sigma_{blank}}{R \times f_a \times \rho \times \pi}} \quad (1)$$

Where, 3σ_blank is three times the standard deviation of counts/dwell time of the blanks, R is the slope of the calibration curve of the ionic solution, fa is the mass fraction of the analysed metallic element in the NPs, and ◎ the density of the NPs under investigation.
For TiO_2-NPs, Ag-NPs, ZnO-NPs LOD in sizes were 37 nm, 19 nm and 29 nm, respectively.

6.2.5. Statistical Analysis

The software package IBM SPSS 20.0 (IBM, Armonk, NY, USA) was used to perform one-way ANOVA and post hoc Tukey test for comparison of NPs concentration, mean size and dissolved content (a p-value of less than 0.05 indicates a statistically significant difference in standard deviation) between digestion phases.

6.3. Results and Discussion

6.3.1 Ag-NPs in canned clams, canned tuna and standard and calculation of biopersistence rate

The results concerning Ag-NPs concentration, particle size distribution and ion content for oral, gastric and intestinal digestion in vitro at different time points in canned clams, canned tuna and Ag-NPs standard 40 nm are summarised in Table 6.2 and shown in Figure 6.1, 6.2 and 6.3.

Regarding the digestion in vitro in samples of clams (Table.6.2 and Figure 6.1), an increase in the concentration of Ag-NPs was observed in the gastric digests (mainly G120, G120 vs T0, $p < 0.001$) compared to the beginning of the experiment (T0). These results do not seem to correlate with the mean sizes, which were larger in the gastric tract than in stage T0 (G60 and G120 vs T0, $p<0.001$). This behaviour could be consistent with the simultaneous presence of smaller Ag-NPs and large Ag-NPs agglomerates at this stage. Under intestinal conditions, we observed an increase in Ag-NPs concentrations, especially at stage I30 (I30 vs G120, $p<0.001$), while mean size decreased and remain constant over the process (I30 vs G120, $p<0.001$). This could be consistent with a dispersion under intestinal conditions reported in literature. The trend of ionic Ag content was similar to Ag-NPs, increasing in the stomach (mainly G120, G120 vs G60 $p <0.01$) and remaining high in the intestinal tract (I30, I60, I120 vs G60 $p<0.01$). This could be an explanation for the strong tendency of Ag-NPs to ionize at low pH.

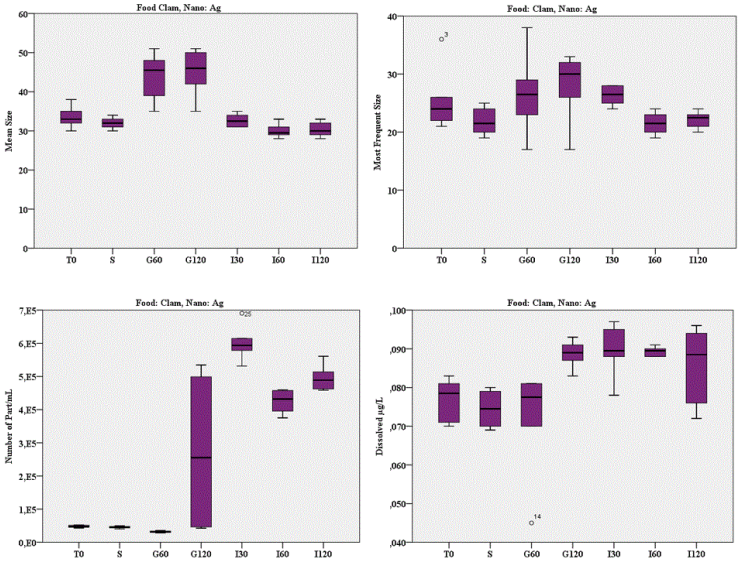

Figure 6.1. Characterization of Ag-NPs in Clam for each digestion phase.

The concentration of Ag-NPs in canned tuna (Table.6.2 and Figure 6.2), showed a different behaviour, being lower in the gastric digests than at the beginning of the experiment (G60 and G120 vs T0, $p<0.001$) with a higher mean size as in clams (G120 vs T0, $p<0.001$). The content of NPs increased during the intestinal process (mainly I30 vs G120, $p<0.001$) and remained constant at the end of the same stages, while the mean size of Ag-NPs decreased significantly compared to the oral phase (I120 vs S $p<0.05$) and was similar to that at the beginning of the experiment (T0). The content of ionic Ag is higher in the intestinal digests than in the gastric digests (mainly I30, I60 vs G60, $p<0.05$) and at stage T0 and S (I30 > T0 and S, not significant).

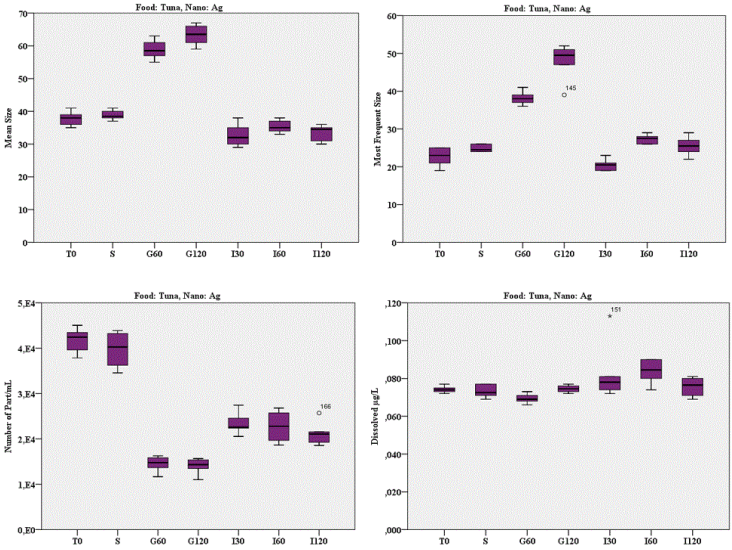

Figure 6.2. Characterization of Ag-NPs in Tuna for each digestion phase.

The results from in vitro digestion of Ag standard 40 nm (Table.6.2 and Figure 6.3), do not provide a clear trend. The gastric process leads to a slight decrease in the concentration of Ag-NPs than the initial digestion stage (T0), which is accompanied by a significant increase in mean size (G60 and G120 vs T0 $p<0.001$). Differently, the ionic Ag in gastric phase increases significantly (mainly G120 vs T0, $p<0.001$). Thereafter, the concentration of Ag-NPs in the intestinal stage increased slightly than the original value (T0) and decreases in average size (mainly I30, I30 vs G120 $p<0.001$), similar to the initial stage (T0, S). An increase in the number of Ag-NPs can be seen in stage I120 compared to I30 and I60. However ionic Ag in intestinal digests is significantly lower than in the last gastric stage (I30 vs G120, $p<0.01$) but significantly higher than at the beginning of the experiment (I30 vs T0 $p<0.001$).

In both seafood and standard experiments, no changes in concentration and size were observed in the oral phase (S), which is consistent with the results reported in the literature (Laloux et al.,

2020).

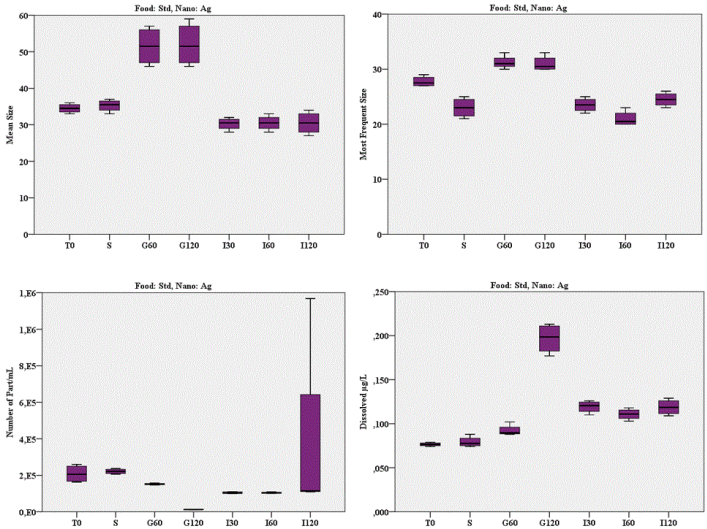

Figure 6.3. Characterization of AgNPs standard for each digestion phase

Regarding the gastric phase, most studies have reported a clear tendency towards aggregation, resulting in an increase in hydrodynamic diameter and a lower concentration of Ag-NPs, both in tests with pure Ag-NPs and in those with the presence of food matrix (Pinďáková et al., 2017; Ramos et al., 2017; Walczak et al., 2015). In some cases, clusters were formed only by silver (Laloux et al., 2020), while in others, the presence of AgCl was highlighted, probably formed by the interaction between Ag+ and Cl- ions released in the highly acidic gastric environment (Mwilu et al., 2013; Rogers et al., 2012; Walczak et al., 2015).

In contrast to the behaviour shown in the gastric phase, Ag-NPs showed a tendency to disperse after entering a simulated intestinal environment where the pH was significantly higher than in the gastric phase. This is evidenced by the almost constant decrease in the mean size of Ag-NPs and the increased percentage concentration

of NPs, indicating the dissolution of previously formed clusters in favour of a larger number of nanoparticles dissolved in the medium (Laloux et al., 2020; Pinďáková et al., 2017; Ramos et al., 2017; Taboada-López et al., 2021).
In the study of Taboada-Lòpez et al. (2021) Ag-NPs showed less constant behaviour. Authors exposed Ag-NPs standards in two different sizes (40 and 60 nm) to a simulated gastric and intestinal phase and then repeated the same procedure with samples from molluscs in which Ag-NPs were naturally present.
Experiments with Ag-NPs standards showed a rather size- and concentration-dependent behaviour, without a clear aggregation and dissolution tendency as in the experiment we performed.
The experiment with mollusc samples also gave similar results to our study, with a tendency of NPs to aggregate in the gastric phase and to dissolve in the intestinal phase.
This difference between the behaviour of Ag-NPs standards and food samples may indicate the important influence that the food matrix exerts on the fate of Ag-NPs during the digestive process.
Following the EFSA protocol, we calculated the biopersistence rates for each experiment. For canned tuna and 40 nm Ag-NPs standard, values of 56% and 48% were obtained. However, for clams, the biopersistence rate was higher than 100%.
The levels found are above the limit set by EFSA (12%), which means that Ag-NPs are difficult to degrade under gastrointestinal tract conditions.
In their study, Taboada-López et al. reported a biopersistence rate of less than 60% for an Ag-NPs standard of 40 nm, which is in agreement with the results of this study, while values of 20% and more than 100% were calculated for oysters and variegated mussels, confirming the concept that the matrix is a crucial factor for the fate of NPs.

Table 6.2. Descriptive statistics concerning the chemical characterization and quantification of AgNPs in Clam, Tuna and AgNPs Standard for each digestion phase.

Clam		Mean	SD	Min.	Max.	Tuna		Mean	SD	Min.	Max.	Ag-NPs Standard		Mean	SD	Min.	Max.
Mean Size nm	T0	33.50	2.739	30	38	Mean Size nm	T0	37.83	2.229	35	41	Mean Size nm	T0	34.50	1.291	33	36
	S	32.00	1.414	30	34		S	38.83	1.472	37	41		S	35.25	1.708	33	37
	G60	44.00	6.000	35	51		G60	58.83	2.858	55	63		G60	51.50	5.323	46	57
	G120	45.00	5.899	35	51		G120	63.33	3.011	59	67		G120	52.00	6.055	46	59
	I30	32.67	1.633	31	35		I30	32.67	3.386	29	38		I30	30.25	1.708	28	32
	I60	30.00	1.789	28	33		I60	35.33	1.862	33	38		I60	30.50	2.082	28	33
	I120	30.33	1.966	28	33		I120	33.50	2.429	30	36		I120	30.50	3.109	27	34
Most Frequent Size nm	T0	25.50	5.468	21	36	Most Frequent Size nm	T0	22.67	2.338	19	25	Most Frequent Size nm	T0	27.75	.957	27	29
	S	21.83	2.317	19	25		S	24.83	.983	24	26		S	23.00	1.826	21	25
	G60	26.67	6.947	17	38		G60	38.17	1.835	36	41		G60	31.25	1.258	30	33
	G120	28.00	5.933	17	33		G120	48.00	4.817	39	52		G120	31.00	1.414	30	33
	I30	26.33	1.633	24	28		I30	20.50	1.517	19	23		I30	23.50	1.291	22	25
	I60	21.50	1.871	19	24		I60	27.33	1.211	26	29		I60	21.00	1.414	20	23
	I120	22.17	1.472	20	24		I120	25.50	2.429	22	29		I120	24.50	1.291	23	26
Number of Part/mL	T0	4.8E+04	3.6E+03	4.3E+04	5.2E+04	Number of Part/mL	T0	4.2E+04	2.6E+03	3.8E+04	4.5E+04	Number of Part/mL	T0	2.1E+05	4.8E+04	1.6E+05	2.6E+05
	S	4.5E+04	3.3E+03	4.0E+04	4.9E+04		S	4.0E+04	4.0E+03	3.5E+04	4.4E+04		S	2.2E+05	1.4E+04	2.1E+05	2.4E+05
	G60	3.1E+04	2.8E+03	2.8E+04	3.5E+04		G60	1.5E+04	1.7E+03	1.2E+04	1.6E+04		G60	1.5E+05	4.9E+03	1.5E+05	1.6E+05
	G120	2.7E+05	2.5E+05	4.2E+04	5.3E+05		G120	1.4E+04	1.7E+03	1.1E+04	1.6E+04		G120	1.3E+04	1.5E+03	1.1E+04	1.5E+04
	I30	6.0E+05	5.3E+04	5.3E+05	6.9E+05		I30	2.3E+04	2.4E+03	2.1E+04	2.7E+04		I30	1.0E+05	5.2E+03	9.9E+04	1.1E+05
	I60	4.3E+05	3.5E+04	3.8E+05	4.6E+05		I60	2.3E+04	3.3E+03	1.9E+04	2.7E+04		I60	1.0E+05	3.8E+03	1.0E+05	1.1E+05
	I120	5.0E+05	3.9E+04	4.6E+05	5.6E+05		I120	2.1E+04	2.5E+03	1.9E+04	2.6E+04		I120	3.8E+05	5.3E+05	1.1E+05	1.2E+06
Dissolved µg/L	T0	0.077	0.005	0.070	0.083	Dissolved µg/L	T0	0.074	0.002	0.072	0.077	Dissolved µg/L	T0	0.077	0.002	0.074	0.079
	S	0.075	0.005	0.069	0.080		S	0.073	0.003	0.069	0.077		S	0.079	0.006	0.074	0.088
	G60	0.072	0.014	0.045	0.081		G60	0.069	0.002	0.066	0.073		G60	0.092	0.007	0.088	0.102
	G120	0.089	0.004	0.083	0.093		G120	0.075	0.002	0.072	0.077		G120	0.197	0.017	0.177	0.213
	I30	0.090	0.007	0.078	0.097		I30	0.083	0.015	0.072	0.113		I30	0.119	0.007	0.110	0.126
	I60	0.089	0.001	0.088	0.091		I60	0.084	0.007	0.074	0.090		I60	0.111	0.006	0.103	0.118
	I120	0.086	0.010	0.072	0.096		I120	0.076	0.005	0.069	0.081		I120	0.119	0.009	0.109	0.129

6.3.2 TiO_2-NPs in canned clams, canned tuna and standard and calculation of biopersistence rate

Table 6.3 summarises the results of the descriptive statistics for chemical characterization and quantification of TiO_2-NPs in clams, tuna, and TiO_2-NPs standard 60 nm for each digestion phase. In addition, TiO_2-NPs concentrations, size distribution (most and mean size), and ionic Ti for different samples are shown in Figures 6.4, 6.5 and 6.6, respectively.

Regarding the digestion in vitro in samples of clam (Table 6.3 and Figure 6.4), some differences were found in the different experiments.

No significant changes in concentration and size of TiO_2-NPs in the clam samples were observed in the oral phase (S) compared to the beginning of the experiment (T0). In the gastric condition, the number of TiO_2-NPs was slightly higher (mainly in G120) than at the beginning of the experiment (T0). The mean sizes in the gastric digests were significantly higher than at oral stage, supporting the idea of agglomeration of TiO_2-NPs at this stage (G60 and G120 vs S, $p<0.001$). At stages I60, I120 and especially I30, TiO_2-NPs are higher than during gastric digestion, confirming that intestinal digestion promotes the dispersion of TiO_2-NPs. However, the average size decreases significantly compared to the value before starting digestion T0 (I30, I60, I120 vs T0, $p <0.01$). As can be read in the literature, pH is a crucial parameter of this process (De Matteis, 2017). An acidic pH in the stomach and a neutral pH in the intestine promote the aggregation and dispersion of NPs, respectively, as confirmed by the results obtained. The ionic Ti content is similar throughout the experiment, supporting the fact that the dissolution of TiO_2-NPs was absent and not significant.

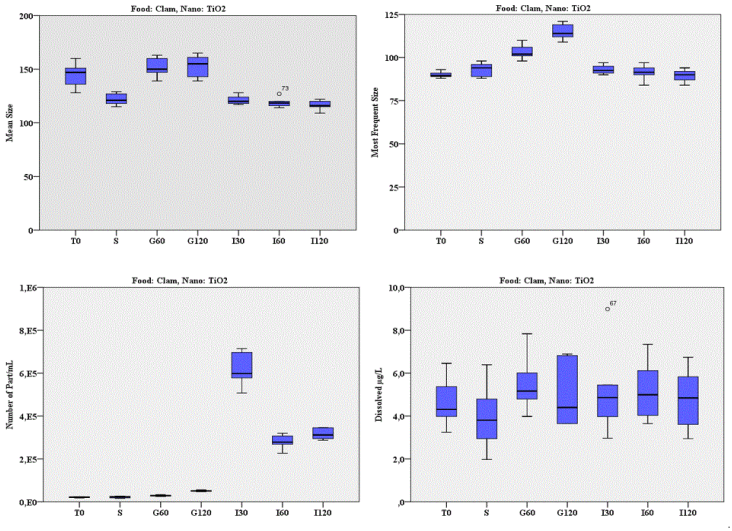

Figure 6.4. Characterization of TiO_2NPs in Clam for each digestion phase.

Different behaviour was observed in the in vitro digestion of canned tuna (Table 6.3 and Figure 6.5). We first observed a significant increase in the concentrations of TiO_2-NPs at stage G60 (G60 vs T0, $p<0.001$), followed by a marked decrease at stage G120 (G120 vs T0, $p<0.001$). At both stages the mean size was higher than at T0, as in clams (G60 and G120 vs T0, $p<0.001$). In the intestinal digests, there is a significant increase in the concentrations of TiO_2-NPs compared to the gastric digests (I30, I60 and I120 vs G120, $p<0.01$), but this increase is not significant compared to the beginning of the experiment, as the concentration of NPs returns to the original value. The ionic Ti concentration also remains constant throughout the digestion process, as in the clams.

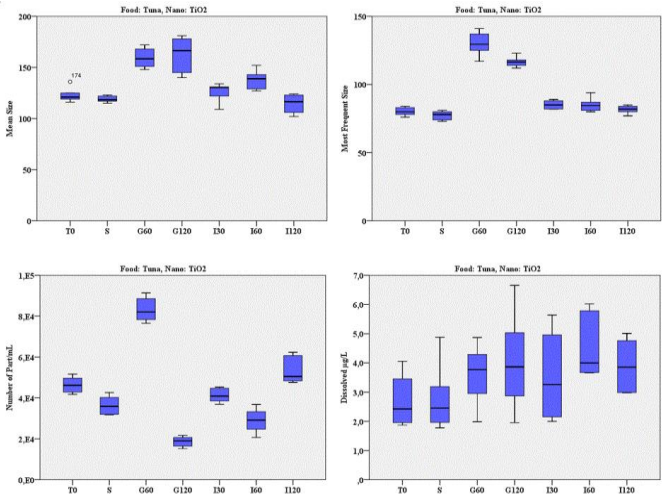

Figure 6.5. Characterization of TiO_2-NPs in Tuna for each digestion phase.

For the standard TiO_2-NPs 60 nm (Table.6.3 and Figure 6.6), no significant changes in concentration and size were observed in the oral phase (S) than at the beginning of the experiment (T0). The results of the standard of TiO_2-NPs 60 nm are partially similar to those of the experiments with clams, confirming a possible aggregation of nanoparticles under gastric conditions (G60 and G120) associated with a significant increase in mean size of TiO_2-NPs (G60 and G120 vs T0, $p<0.01$), a dispersion phenomenon under intestinal conditions (mainly I60 and I120 vs T0, $p<0.01$), as well as the absence of ionisation throughout the process.

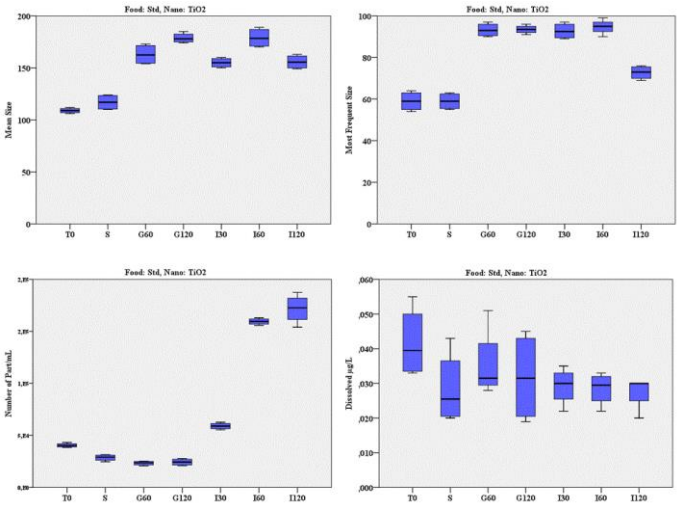

Figure 6.6. Characterization of TiO_2NPs standard for each digestion phase.

Some recent work has investigated the interactions between TiO_2-NPs and various food matrices when subjected to simulated digestion in vitro, and the results are in some cases comparable to ours.

A discrepancy exists in the salivary phase where TiO_2-NPs spiked with corn oil and protein powder showed better dispersion than the control, probably due to the steric effects and physicochemical changes caused by the biological corona formed by proteins or oil droplets adsorbed on the surface of the NPs (Taboada-López et al., 2021; Zhou et al., 2021).

From the literature, TiO_2-NPs showed a significant tendency to aggregate in the gastric phase with an increase in average size and a decrease in NPs concentration, while increased dispersion of TiO_2-NPs was observed in the intestinal phase, except in the experiments with fresh mussel samples and those in which protein powders were.

These results seem to show that the intestinal environment could favours the dissolution of the clusters formed in the gastric phase,

causing the dispersion and ionization of the TiO_2-NPs, which may also affect toxicity (Taboada-López et al., 2021; Zhou et al., 2021).
Our results show a different behaviour of TiO_2-NPs during in vitro digestion, probably related to the different foods studied.
For example, digestion of clams does not show a clear decrease in TiO_2-NPs in the gastric condition, and digestion of tuna does not show a clear increase of TiO_2-NPs concentration in intestinal condition, in contrast to the standard where this trend is more evident.
The biopersistence rate was calculated and the results obtained are higher than 100% for clams and standard TiO_2 60 nm and higher than 80% for tuna samples. A value of more than 100% can be explained by the fact that a dispersion of NPs occurs in the intestine
The values obtained are well above the limit set by EFSA (12%), which means that the TiO_2-NPs are unchanged and non-degradable under gastrointestinal tract conditions.
In their study, Taboada-López et al. (2021) reported a biopersistence rate of higher than 80% and 100% for TiO_2-NPs standards of 50 nm and 100 nm respectively, which is in agreement with our results, while values higher than 100% were calculated for mollusc and surimi, confirming the concept that the matrix is a crucial factor for the fate of NPs.

Table 6.3. Descriptive statistics concerning the chemical characterization and quantification of TiO_2-NPs in Clam, Tuna and TiO_2-NPs Standard for each digestion phase.

Clam		Mean	SD	Min.	Max.	Tuna		Mean	SD	Min.	Max.	TiO_2-NPs Standard		Mean	SD	Min.	Max.
Mean Size nm	T0	144.83	11.321	128	160	Mean Size nm	T0	123.00	7.014	116	136	Mean Size nm	T0	109.00	2.582	106	112
	S	121.83	5.456	115	129		S	119.00	3.033	115	123		S	117.00	7.528	110	124
	G60	151.50	8.803	139	163		G60	159.33	9.374	148	172		G60	163.00	9.899	154	173
	G120	153.00	10.198	139	165		G120	162.83	17.128	140	181		G120	178.75	4.856	174	185
	I30	121.17	4.167	117	128		I30	126.17	9.326	109	134		I30	155.00	4.761	150	160
	I60	119.00	4.472	114	127		I60	138.17	9.239	127	152		I60	179.00	9.416	170	189
	I120	116.33	4.546	109	122		I120	114.67	8.937	102	124		I120	155.75	6.801	149	163
Most Frequent Size nm	T0	90.00	1.789	88	93	Most Frequent Size nm	T0	80.17	3.061	76	84	Most Frequent Size nm	T0	59.00	4.761	54	64
	S	93.17	3.971	88	98		S	77.33	3.266	73	81		S	59.00	4.082	55	63
	G60	103.17	4.262	98	110		G60	129.83	8.589	117	141		G60	93.25	3.304	90	97
	G120	114.83	4.491	109	121		G120	116.67	3.777	112	123		G120	93.50	2.082	91	96
	I30	93.00	2.608	90	97		I30	85.17	3.189	82	89		I30	92.75	3.862	89	97
	I60	91.33	4.367	84	97		I60	85.17	5.037	80	94		I60	94.75	3.686	90	99
	I120	89.50	3.619	84	94		I120	81.67	2.944	77	85		I120	72.75	3.304	69	76
Number of Part/mL	T0	2.1E+04	2.1E+03	1.9E+04	2.4E+04	Number of Part/mL	T0	4.6E+04	4.0E+03	4.2E+04	5.2E+04	Number of Part/mL	T0	4.1E+04	2.1E+03	3.8E+04	4.3E+04
	S	2.2E+04	4.1E+03	1.6E+04	2.6E+04		S	3.6E+04	4.6E+03	3.2E+04	4.3E+04		S	2.9E+04	3.1E+03	2.5E+04	3.1E+04
	G60	2.9E+04	3.1E+03	2.5E+04	3.3E+04		G60	8.3E+04	5.9E+03	7.7E+04	9.1E+04		G60	2.3E+04	2.1E+03	2.1E+04	2.5E+04
	G120	5.1E+04	2.9E+03	4.7E+04	5.6E+04		G120	1.9E+04	2.5E+03	1.5E+04	2.2E+04		G120	2.4E+04	3.3E+03	2.1E+04	2.8E+04
	I30	6.2E+05	7.8E+04	5.1E+05	7.1E+05		I30	4.1E+04	3.4E+03	3.7E+04	4.5E+04		I30	5.9E+04	3.2E+03	5.5E+04	6.3E+04
	I60	2.8E+05	3.3E+04	2.3E+05	3.2E+05		I60	2.9E+04	6.0E+03	2.1E+04	3.7E+04		I60	1.6E+05	3.2E+03	1.6E+05	1.6E+05
	I120	8.7E+05	1.4E+06	2.9E+05	3.7E+06		I120	5.3E+04	6.5E+03	4.8E+04	6.2E+04		I120	1.7E+05	1.4E+04	1.5E+05	1.9E+05
Dissolved µg/L	T0	4.612	1.146	3.245	6.460	Dissolved µg/L	T0	2.697	0.920	1.870	4.056	Dissolved µg/L	T0	0.042	0.010	0.033	0.055
	S	3.954	1.527	1.976	6.391		S	2.787	1.137	1.776	4.876		S	0.029	0.011	0.020	0.043
	G60	5.491	1.328	3.985	7.834		G60	3.606	1.019	1.987	4.870		G60	0.036	0.010	0.028	0.051
	G120	4.968	1.512	3.650	6.890		G120	4.041	1.744	1.956	6.654		G120	0.032	0.013	0.019	0.045
	I30	5.183	2.059	2.970	8.987		I30	3.546	1.525	1.996	5.640		I30	0.029	0.005	0.022	0.035
	I60	5.188	1.370	3.650	7.340		I60	4.521	1.082	3.655	6.020		I60	0.029	0.005	0.022	0.033
	I120	4.802	1.392	2.947	6.740		I120	3.908	0.987	2.980	5.012		I120	0.028	0.005	0.020	0.030

6.3.4. ZnO-NPs in canned clams, canned tuna and standard and calculation of biopersistence rate

Table 6.4 shows the descriptive statistics of the chemical characterization and quantification of ZnO-NPs and dissolved Zn in clams, tuna samples, and a standard of ZnO-NPs 30 nm. The naturally occurring ZnO-NPs in the samples showed different behaviour than the ZnO-NPs standard, confirming once again the importance of the influence of the matrix on the fate of this compound. Concentrations of ZnO-NPs and average sizes are similar in both seafood samples under oral, gastric and intestinal condition.

In clams (Table 6.4 and Figure 6.7), mean sizes at the oral stage were significantly smaller than at the beginning of the experiment (S vs T0 $p< 0.05$). This increase in mean size is also significant in the gastric digests when the oral stage is considered (G60 and G120 vs S, $p < 0.001$).

In tuna (Table 6.4 and Figure 6.8), the mean size in the oral phase and in gastric stage was smaller than at the beginning of the experiment (S and G120 vs T0, $p <0.001$). The results do not correlate with the concentrations of ZnO in oral and gastric digests NPs found for both seafood samples similar to stage T0.

Thereafter, an increase in the mean size in intestinal condition was observed for both seafood products compared to the oral phase (I30, I60 and I120 vs S, $p<0.001$) accompanied by a slight increase in NPs concentration marked in stage I120 (Figure 6.7 and 6.8).

The increase in mean sizes in intestinal condition may be attributed to the fact that a protein corona can form on the surface of the ZnO-NPs due to the rapid binding of proteins, as reported in the literature (Bae et al., 2018). This would decrease the electrostatic repulsion and space resistance between NPs and increase the agglomeration of NPs. This was mainly due to the fact that protein digested by gastric juice could be continuously digested in the small intestine phase due to the presence of pancreatin.

In tuna digested samples, the trend of ionic Zn concentration showed a constant concentration in oral and gastric condition and a significant increase in intestinal digests (mainly I60 vs T0, $p<0.001$) (Figure 6.8).
In clams, the results are similar, but a significant increase in ionic Zn concentration was observed first in gastric condition (G120 vs G60, T0 and S, $p<0.01$) and then in intestinal digests (I30, I60 and I120 vs T0, $p<0.001$) (Figure 6.7).

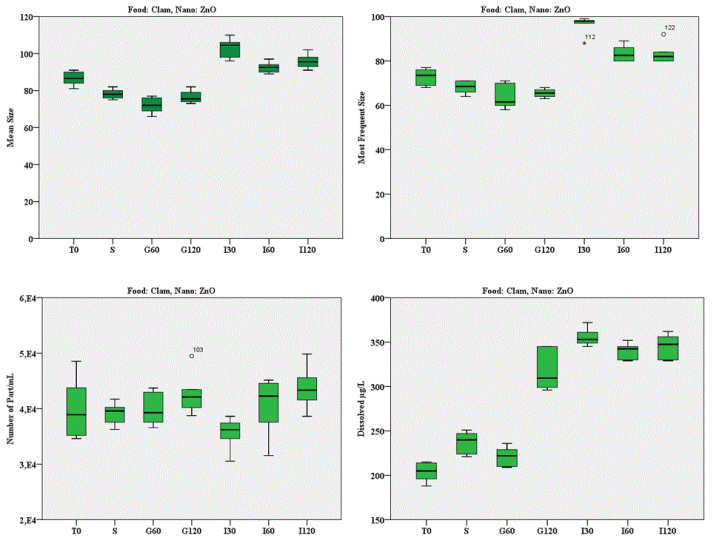

Figure 6.7. Characterization of ZnO-NPs in Clam for each digestion phase.

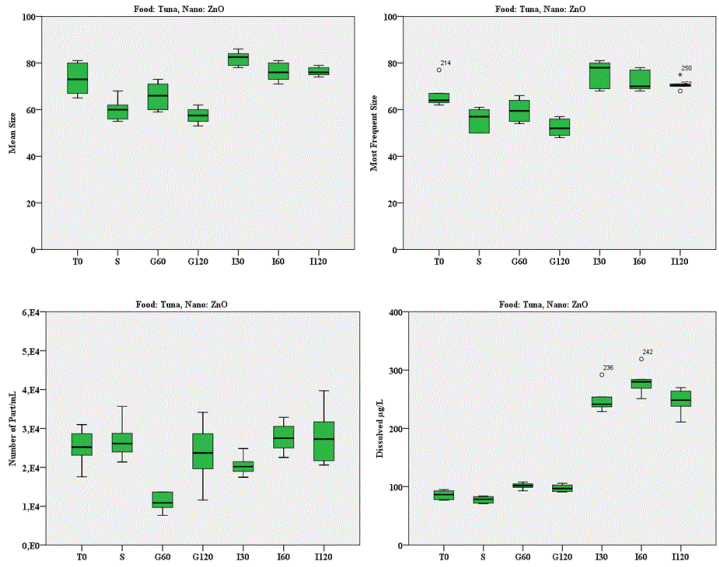

Figure 6.8. Characterization of ZnO-NPs in Tuna for each digestion phase.

Biopersistence rates according to EFSA criteria were similar for both samples (89% for the clams and 84% for the tuna samples). These high values indicate that ZnO-NPs is hardly degraded in the presence of this type of matrix during the gastrointestinal process.

Results regarding the digestion in vitro of a standard of ZnO-NPs are plotted in Figure 6.9. The gastric condition resulted in a significant decrease in the concentration of ZnO-NPs, compared to the oral phase and the beginning of the experiment (mainly G60 vs T0 and S, $p < 0.05$). These results are consistent with an increase in the mean size of the particles (G60 and G120 vs T0, $p<0.001$). The same significant decrease is observed in intestinal digests (I30, I60 and I120 vs G60 and G120, $p<0.001$), where a smaller mean size was found than in the gastric stages. In addition, the ionic Zn content is also higher at these stages compared to the values measured in the gastric tract (mainly I60 vs G60, $p<0.001$) and at the beginning of the experiment (I30, I60, I120 vs T0, $p<0.001$).

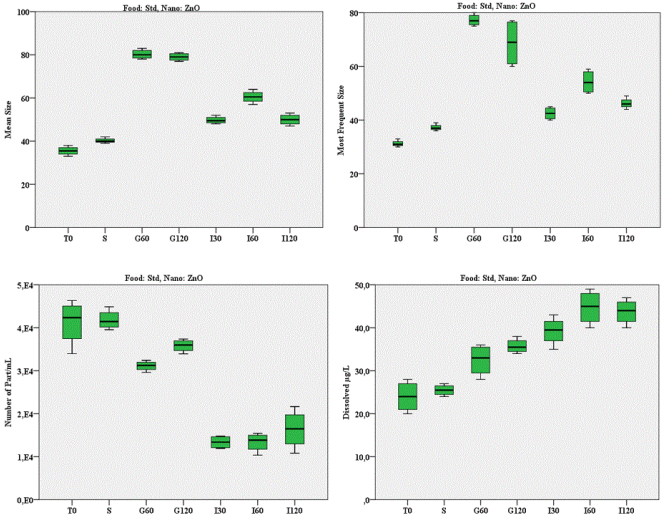

Figure 6.9. Characterization of ZnONPs standard for each digestion phase.

All three experiments show high concentrations of ionic zinc at the end of digestion, which is probably largely due to the composition of the foods studied, as was evident in the study conducted previously and reported in Chapter 3, in which dissolved zinc is also determined prior to alkaline digestion.

To a lesser extent, this could also be related to an ionization phenomenon originating from the zinc nanoparticles present in the matrix or standard.

What has just been said is evident in the digestion carried out with the standard, whereas it is less evident in the two food matrices containing other components such as lipids, carbohydrates and proteins, which probably influence the fate of the nanoparticles.

Studies in the literature report data slightly different from those obtained.

During simulated digestion in vitro ZnO-NPs tend to undergo no particular changes in the oral phase and then dissolve completely or partially in the gastric phase, depending on the concentrations studied, which is consistent with the high solubility of zinc

compounds in acidic medium (Bae et al., 2018).
In the intestinal phase, ZnO-NPs show a lower dissolution rate and in some cases an increase in particle size (Gomez-Gomez et al., 2020; Zhou et al., 2021) or de novo NPs formation after complete dissolution under gastric conditions (Voss et al., 2020).
The release of Zn+ ions proved to be maximal in the gastric phase, which may be attributed to the significant dissolution of ZnO-NPs in the highly acidic environment of the stomach (Duan et al., 2020; Voss et al., 2020).
ZnO-NPs standard (30 nm), which have a biopersistence rate of 30%, appear to be more degradable than ZnO-NPs in clam and tuna samples with biopersistence rates of 89% and 84%, respectively. However, this is higher than the limit set by EFSA and indicates moderate stability of ZnO-NPs under gastrointestinal conditions.

Table 6.4. Characterization of ZnO-NPs standard for each digestion phase.

Clam		Mean	SD	Min.	Max.	Tuna		Mean	SD	Min.	Max.	ZnO-NPs Standard		Mean	SD	Min.	Max.
Mean Size nm	T0	86.50	3.834	81	91	Mean Size nm	T0	73.17	7.250	65	81	Mean Size nm	T0	35.50	2.082	33	38
	S	78.17	2.639	75	82		S	60.17	4.708	55	68		S	40.25	1.258	39	42
	G60	72.00	4.195	66	77		G60	65.83	5.947	59	73		G60	80.25	2.217	78	83
	G120	76.50	3.391	73	82		G120	57.50	3.391	53	62		G120	79.00	1.826	77	81
	I30	103.17	5.307	96	110		I30	82.00	3.033	78	86		I30	49.75	1.708	48	52
	I60	92.50	2.881	89	97		I60	76.17	3.920	71	81		I60	60.50	2.887	57	64
	I120	95.83	3.869	91	102		I120	76.33	1.966	74	79		I120	50.00	2.582	47	53
Most Frequent Size nm	T0	72.83	3.764	68	77	Most Frequent Size nm	T0	66.17	5.565	62	77	Most Frequent Size nm	T0	31.25	1.258	30	33
	S	68.17	2.787	64	71		S	55.83	4.956	50	61		S	37.25	1.258	36	39
	G60	63.67	5.465	58	71		G60	59.67	4.844	54	66		G60	77.25	2.217	75	80
	G120	65.50	1.871	63	68		G120	52.33	3.670	48	57		G120	68.75	8.995	60	77
	I30	96.33	4.131	88	99		I30	75.67	5.715	68	81		I30	42.50	2.380	40	45
	I60	83.33	3.670	80	89		I60	72.00	4.382	68	78		I60	54.25	4.425	50	59
	I120	83.33	4.546	80	92		I120	70.83	2.317	68	75		I120	46.25	2.062	44	49
Number of Part/mL	T0	4.0E+04	5.3E+03	3.5E+04	4.9E+04	Number of Part/mL	T0	2.5E+04	4.7E+03	1.8E+04	3.1E+04	Number of Part/mL	T0	4.1E+04	5.3E+03	3.4E+04	4.6E+04
	S	3.9E+04	1.9E+03	3.6E+04	4.2E+04		S	2.7E+04	5.0E+03	2.1E+04	3.6E+04		S	4.2E+04	2.3E+03	4.0E+04	4.5E+04
	G60	4.0E+04	2.9E+03	3.7E+04	4.4E+04		G60	2.2E+04	2.9E+04	7.6E+03	8.1E+04		G60	3.1E+04	1.2E+03	3.0E+04	3.2E+04
	G120	4.3E+04	3.7E+03	3.9E+04	4.9E+04		G120	2.4E+04	7.9E+03	1.2E+04	3.4E+04		G120	3.6E+04	1.5E+03	3.4E+04	3.7E+04
	I30	3.6E+04	2.9E+03	3.1E+04	3.9E+04		I30	2.1E+04	2.5E+03	1.7E+04	2.5E+04		I30	1.3E+04	1.5E+03	1.2E+04	1.5E+04
	I60	4.1E+04	5.2E+03	3.2E+04	4.5E+04		I60	2.8E+04	3.9E+03	2.3E+04	3.3E+04		I60	1.3E+04	2.2E+03	1.0E+04	1.5E+04
	I120	4.4E+04	3.9E+03	3.9E+04	5.0E+04		I120	2.8E+04	7.0E+03	2.1E+04	4.0E+04		I120	1.6E+04	4.6E+03	1.1E+04	2.2E+04
Dissolved µg/L	T0	203.83	11.32	188.00	215.00	Dissolved µg/L	T0	86.00	8.20	77.00	95.00	Dissolved µg/L	T0	24.00	3.65	20.00	28.00
	S	237.17	12.42	221.00	251.00		S	77.83	5.49	71.00	84.00		S	25.50	1.29	24.00	27.00
	G60	221.33	10.84	209.00	236.00		G60	101.50	5.21	93.00	108.00		G60	32.50	3.70	28.00	36.00
	G120	741.00	1051.47	296.00	2887.00		G120	97.67	6.44	91.00	106.00		G120	35.75	1.71	34.00	38.00
	I30	355.50	9.85	345.00	372.00		I30	249.17	22.52	229.00	292.00		I30	39.25	3.30	35.00	43.00
	I60	340.17	9.11	329.00	352.00		I60	280.50	22.43	251.00	319.00		I60	44.75	4.03	40.00	49.00
	I120	345.33	13.62	329.00	362.00		I120	246.67	21.81	211.00	270.00		I120	43.75	2.99	40.00	47.00

6.4. Conclusion

This study is important because it highlights the contribution of the food matrix to the digestive process, which has not been adequately studied in the literature.

Studies using NPs for oral exposure only may therefore lead to misinterpretation of results, and it is necessary to evaluate the synergistic effects of NPs in a complex system and the potential interactions between NPs and food ingredients when considering the safety of NPs in food.

Important phenomena of agglomeration and dispersion can occur depending on the conditions of the environment studied, such as pH, ionic strength or organic matter.

Interactions between NPs and food components are also very likely, affecting the physicochemical properties of NPs and possibly causing undesirable biological reactions or even toxicity in humans.

The results obtained in our study partly follow the different studies in the literature present.

ZnO-NPs appear to be more degradable than Ag-NPs and TiO_2-NPs, which have lower biopersistence rates. However, the biopersistence rates calculated in this work are higher than the limit set by EFSA (12%), indicating that the metallic nanoparticles studied are stable under gastrointestinal conditions and cannot be considered as highly degradable.

Further studies are needed to better understand the behaviour of the metallic NPs under different conditions.

The size of the NPs should be studied as this is an important factor to consider when evaluating stability and degradability under gastrointestinal conditions and at different levels.

A TEM - EDX analysis could be useful to detect and confirm the presence of agglomerates that we suspect in the different stages studied (oral, gastric and intestinal).

References

- Bae, S.-H., Yu, J., Lee, T.G., Choi, S.-J., 2018. Protein Food Matrix–ZnO Nanoparticle Interactions Affect Protein Conformation, but May not Be Biological Responses. Int J Mol Sci 19, 3926. https://doi.org/10.3390/ijms19123926
- Bellmann, S., Carlander, D., Fasano, A., Momcilovic, D., Scimeca, J.A., Waldman, W.J., Gombau, L., Tsytsikova, L., Canady, R., Pereira, D.I.A., Lefebvre, D.E., 2015. Mammalian gastrointestinal tract parameters modulating the integrity, surface properties, and absorption of food-relevant nanomaterials. Wiley Interdiscip Rev Nanomed Nanobiotechnol 7, 609–622. https://doi.org/10.1002/wnan.1333
- Chawla, R., Filippini, T., Loomba, R., Cilloni, S., Dhillon, K.S., Vinceti, M., 2019. Exposure to a high selenium environment in Punjab, India: Biomarkers and health conditions. Science of The Total Environment 134541. https://doi.org/10.1016/j.scitotenv.2019.134541
- De Matteis, V., 2017. Exposure to Inorganic Nanoparticles: Routes of Entry, Immune Response, Biodistribution and In Vitro/In Vivo Toxicity Evaluation. Toxics 5, E29. https://doi.org/10.3390/toxics5040029
- Duan, Z., Duan, X., Zhao, S., Wang, X., Wang, J., Liu, Y., Peng, Y., Gong, Z., Wang, L., 2020. Barrier function of zebrafish embryonic chorions against microplastics and nanoplastics and its impact on embryo development. Journal of Hazardous Materials 395, 122621. https://doi.org/10.1016/j.jhazmat.2020.122621
- EFSA Scientific Committee, Hardy, A., Benford, D., Halldorsson, T., Jeger, M.J., Knutsen, H.K., More, S., Naegeli, H., Noteborn, H., Ockleford, C., Ricci, A., Rychen, G., Schlatter, J.R., Silano, V., Solecki, R., Turck, D., Younes, M., Chaudhry, Q., Cubadda, F., Gott, D., Oomen, A., Weigel, S., Karamitrou, M., Schoonjans, R., Mortensen, A., 2018. Guidance on risk assessment of the application of nanoscience and nanotechnologies in the food and feed chain: Part 1, human and animal health. EFSA Journal 16. https://doi.org/10.2903/j.efsa.2018.5327
- Gomez-Gomez, B., Perez-Corona, M.T., Madrid, Y., 2020. Using single-particle ICP-MS for unravelling the effect of type of food on the physicochemical properties and gastrointestinal stability of ZnONPs released from packaging materials. Analytica Chimica Acta 1100, 12–21. https://doi.org/10.1016/j.aca.2019.11.063
- Hotze, E.M., Phenrat, T., Lowry, G.V., 2010. Nanoparticle Aggregation: Challenges to Understanding Transport and Reactivity in the Environment. Journal of Environmental Quality 39, 1909–1924. https://doi.org/10.2134/jeq2009.0462

- Jones, G., Jacobs, D.S., Kunz, T.H., Willig, M.R., Racey, P.A., 2009. Carpe noctem: the importance of bats as bioindicators. Endangered Species Research 8, 93–115. https://doi.org/10.3354/esr00182
- Jung, E.-B., Yu, J., Choi, S.-J., 2021. Interaction between ZnO Nanoparticles and Albumin and Its Effect on Cytotoxicity, Cellular Uptake, Intestinal Transport, Toxicokinetics, and Acute Oral Toxicity. Nanomaterials 11, 2922. https://doi.org/10.3390/nano11112922
- Laloux, L., Kastrati, D., Cambier, S., Gutleb, A.C., Schneider, Y.-J., 2020. The Food Matrix and the Gastrointestinal Fluids Alter the Features of Silver Nanoparticles. Small 16, e1907687. https://doi.org/10.1002/smll.201907687
- Lee, P.-K., Chang, H.J., Yu, S., Chae, K.H., Bae, J.-H., Kang, M.-J., Chae, G., 2018. Characterization of Cr (VI) - Containing solid phase particles in dry dust deposition in Daejeon, South Korea. Environ. Pollut. 243, 1637–1647. https://doi.org/10.1016/j.envpol.2018.09.127
- McCracken, C., Dutta, P.K., Waldman, W.J., 2016. Critical assessment of toxicological effects of ingested nanoparticles. Environ. Sci.: Nano 3, 256–282. https://doi.org/10.1039/C5EN00242G
- Minekus, M., Alminger, M., Alvito, P., Ballance, S., Bohn, T., Bourlieu, C., Carrière, F., Boutrou, R., Corredig, M., Dupont, D., Dufour, C., Egger, L., Golding, M., Karakaya, S., Kirkhus, B., Feunteun, S.L., Lesmes, U., Macierzanka, A., Mackie, A., Marze, S., McClements, D.J., Ménard, O., Recio, I., Santos, C.N., Singh, R.P., Vegarud, G.E., Wickham, M.S.J., Weitschies, W., Brodkorb, A., 2014. A standardised static in vitro digestion method suitable for food – an international consensus. Food Funct. 5, 1113–1124. https://doi.org/10.1039/C3FO60702J
- Mwilu, S.K., El Badawy, A.M., Bradham, K., Nelson, C., Thomas, D., Scheckel, K.G., Tolaymat, T., Ma, L., Rogers, K.R., 2013. Changes in silver nanoparticles exposed to human synthetic stomach fluid: effects of particle size and surface chemistry. Sci Total Environ 447, 90–98. https://doi.org/10.1016/j.scitotenv.2012.12.036
- Pinďáková, L., Kašpárková, V., Kejlová, K., Dvořáková, M., Krsek, D., Jírová, D., Kašparová, L., 2017. Behaviour of silver nanoparticles in simulated saliva and gastrointestinal fluids. Int J Pharm 527, 12–20. https://doi.org/10.1016/j.ijpharm.2017.05.026
- Ramos, K., Ramos, L., Gómez-Gómez, M.M., 2017. Simultaneous characterisation of silver nanoparticles and determination of dissolved silver in chicken meat subjected to in vitro human gastrointestinal digestion using single particle inductively coupled plasma mass spectrometry. Food Chem 221, 822–828. https://doi.org/10.1016/j.foodchem.2016.11.091
- Rogers, K.R., Bradham, K., Tolaymat, T., Thomas, D.J., Hartmann, T., Ma, L., Williams, A., 2012. Alterations in physical state of silver nanoparticles exposed to synthetic human stomach fluid. Sci Total Environ 420, 334–339. https://doi.org/10.1016/j.scitotenv.2012.01.044

- Schaming, D., Remita, H., 2015. Nanotechnology: from the ancient time to nowadays. Found Chem 17, 187–205. https://doi.org/10.1007/s10698-015-9235-y
- Singh, T., Shukla, S., Kumar, P., Wahla, V., Bajpai, V.K., Rather, I.A., 2017. Application of Nanotechnology in Food Science: Perception and Overview. Frontiers in Microbiology 8, 1501. https://doi.org/10.3389/fmicb.2017.01501
- Taboada-López, M.V., Vázquez-Expósito, G., Domínguez-González, R., Herbello-Hermelo, P., Bermejo-Barrera, P., Moreda-Piñeiro, A., 2021. Biopersistence rate of metallic nanoparticles in the gastro-intestinal human tract (stage 0 of the EFSA guidance for nanomaterials risk assessment). Food Chem 360, 130002. https://doi.org/10.1016/j.foodchem.2021.130002
- Thiruvengadam, M., Rajakumar, G., Chung, I.-M., 2018. Nanotechnology: current uses and future applications in the food industry. 3 Biotech 8, 74. https://doi.org/10.1007/s13205-018-1104-7
- Tiede, K., Boxall, A.B.A., Tear, S.P., Lewis, J., David, H., Hassellov, M., 2008. Detection and characterization of engineered nanoparticles in food and the environment. Food Addit Contam Part A Chem Anal Control Expo Risk Assess 25, 795–821. https://doi.org/10.1080/02652030802007553
- Trindade, T., O'Brien, P., Pickett, N.L., 2001. Nanocrystalline Semiconductors: Synthesis, Properties, and Perspectives. Chem. Mater. 13, 3843–3858. https://doi.org/10.1021/cm000843p
- Voss, L., Saloga, P.E.J., Stock, V., Böhmert, L., Braeuning, A., Thünemann, A.F., Lampen, A., Sieg, H., 2020. Environmental Impact of ZnO Nanoparticles Evaluated by in Vitro Simulated Digestion. ACS Appl. Nano Mater. 3, 724–733. https://doi.org/10.1021/acsanm.9b02236
- Walczak, A.P., Kramer, E., Hendriksen, P.J.M., Helsdingen, R., van der Zande, M., Rietjens, I.M.C.M., Bouwmeester, H., 2015. In vitro gastrointestinal digestion increases the translocation of polystyrene nanoparticles in an in vitro intestinal co-culture model. Nanotoxicology 9, 886–894. https://doi.org/10.3109/17435390.2014.988664
- Weir, A., Westerhoff, P., Fabricius, L., von Goetz, N., 2012. Titanium Dioxide Nanoparticles in Food and Personal Care Products. Environ Sci Technol 46, 2242–2250. https://doi.org/10.1021/es204168d
- Zhou, P., Guo, M., Cui, X., 2021. Effect of food on orally-ingested titanium dioxide and zinc oxide nanoparticle behaviors in simulated digestive tract. Chemosphere 268, 128843. https://doi.org/10.1016/j.chemosphere.2020.128843
- Zorraquín-Peña, I., Cueva, C., Bartolomé, B., Moreno-Arribas, M.V., 2020. Silver Nanoparticles against Foodborne Bacteria. Effects at Intestinal Level and Health Limitations. Microorganisms 8, 132. https://doi.org/10.3390/microorganisms8010132

11 Conclusion

The improper use of metallic nanoparticles has resulted in an increasing number of nanomaterials entering the environment through various channels. Despite their useful and numerous applications, nanoparticles have the potential to endanger human health and the environment. Since food is an important route for human exposure to nanoparticles, their actual concentrations need to be assessed, focusing on small nanoparticles that have higher toxicity than larger particles and can enter the bloodstream more easily. Therefore, we considered it useful to conduct this study to obtain data on the level of contamination of processed fish products for the evaluation of oral exposure data, as well as data on the biopersistence of these compounds and possible toxic effects.

Our study revealed the presence of metal compounds in the form of nanoparticles less than 100 nm in diameter and dissolved elements in processed canned seafood among the best-selling brands of major supermarket chains, to which the additives E174 and E171 were not intentionally added and were not present in the food contact material. This confirms contamination with nanoparticles from the aquatic environment, which is a receptor for bioaccumulation of these contaminants, which could originate from numerous activities in different sectors or from contamination during industrial processing of food. Moreover, we do not exclude the possibility that they originate from the chemical transformation of these compounds once they have entered the body regions of organisms. A limitation of the study was that we were not able to determine the origin of the metallic NPs, i.e. whether they were formed naturally or anthropogenically.

The present work highlights the importance of proper characterization and quantification of metallic nanoparticles, made

possible by the emerging technique of single particle inductively coupled plasma (spICP- MS). This technique allows the determination of particle number concentration with rapid simultaneous characterization of elemental composition, number of particles, size and size distribution, and solute concentration, with prior alkaline extraction of nanoparticles from samples. This was challenging because food samples are a heterogeneous matrix in terms of composition, structure and properties, and the food matrix may alter the original properties of the NPs. In this regard, the method was successfully optimized and validated, showing good sensitivity, low LOD and LOQ and analytical recovery for each metallic nanoparticle studied.

The choice of two trophic levels of organisms was advantageous for the objective of assessing the risk of environmental contamination and the risk of human exposure via the oral route. Furthermore, since very few studies report on the content of nanoparticles in marine organisms, this study is an important contribution to the limited data available in the scientific literature.

In general, the measured concentrations of metallic nanoparticles are consistent with the trophic level studied and are significantly higher in the larger pelagic fish, tuna and mackerel, than in anchovy, which is the smallest pelagic fish. A similar trend was observed for ion content. Otherwise, the mean size of metallic nanoparticles showed no trend with respect to trophic level and is comparable in all fishes studied, except for TiO_2-NPs, which had the highest mean diameters in canned anchovies and clams.

The studies on benthonic species (bivalves) showed higher concentration and larger size of TiO_2-NPs and ZnO-NPs and dissolved ions among all seafoods. These data are supported by the sedimentation ability and long-term persistence of these metallic compounds in aquatic systems with a high chloride content and low natural organic matter, as well as by the filtration behaviour of these

organisms.

These results therefore support the fact that smaller diameter nanoparticles have a higher potential for bioaccumulation and biomagnification along the food chain in aquatic systems.

Proper characterization of the metallic nanoparticles and ion content was critical to the goal of providing initial data on estimated daily intake for adults and children from consumption of processed seafood. To date, available studies have focused on the oral intake of metallic nanoparticles added during food manufacturing, rather than those naturally present in foods. Our results indicate that consumption of the selected foods could be an important route for the ingestion of these metallic compounds, especially for a vulnerable group such as children, due to the low body weight of the age group considered. This can be inferred from the estimated meal intake (EMI), which was significantly higher in children than in adults for all the studied MNPs and the dissolved fractions. Moreover, the increased exposure is almost always due to the consumption of tuna or clams, which were found to be more contaminated, especially for Ti and Zn (NPs and dissolved). For Ag (NPs and dissolved), anchovies and mackerel showed higher contamination than clams. In addition, the estimated Target Hazard Quotient (THQ) for ionic silver and zinc showed that the exposure level is below the established oral reference dose (RfD) for both substances, which means that they are unlikely to cause adverse effects during human lifetime

Although seafood is a valuable dietary source of unsaturated fatty acids, proteins, and various micronutrients, it represents only a small fraction of the total human diet. Nevertheless, our results represent an important first step in understanding MNP exposure in the human population. Moreover, the observed small average size could be of great concern for human health because, as shown in the literature, the smaller the diameter, the higher the toxicity after oral exposure, as the nanoparticles can better enter the bloodstream.

Further studies are needed to characterize and quantify them in a wide range of foods, both processed and unprocessed, and where MNPs are added at the industrial level. They will provide a realistic assessment of exposure useful for understanding whether the toxicity levels of MNPs observed in the literature are close to those that can actually be estimated from food consumption, and will provide data useful to risk assessors in developing the provisional tolerable daily intake of MNPs.

To better understand the fate of metallic nanoparticles and the chemical reactions that occur in the digestive tract due to their chemical composition and different digestive conditions, we performed several experiments simulating the static digestion of nanoparticle standard, tuna and clam samples in vitro.This study was important because it highlights the contribution of the food matrix to the digestion process, which has not been adequately studied in the literature. This suggests an interaction between NPs and food dietary components that affect the physicochemical properties of NPs, possibly causing undesirable biological responses or even toxicity in humans. The results obtained in our study are partially consistent with the limited number of studies available in the literature, confirming in most experiments a possible aggregation of nanoparticles under gastric conditions, associated with a higher mean size of MNPs, and a dispersion phenomenon under intestinal conditions, with a sometimes lower mean size.

The absence of ionisation throughout the digestive process was observed only for ionic Ti. While Ag and Zn showed elevated levels in the stomach and intestine, probably due to the high ionisation capacity of these two elements, caused in part by the nanoparticles present in the food matrix.

The assessment of the degradation of metallic nanoparticles in food is particularly complicated by the fact that they are associated with matrix components in their initial state, which affects their dissolution and aggregation rates and alters their behaviour upon

entry into the gastrointestinal tract and possibly toxicity.

ZnO-NPs appear to be more degradable in the absence of a food matrix (biopersistence rate 30%) than Ag-NPs and TiO_2-NPs, which have lower biopersistence rates. On the other hand, in the presence of tuna as food matrix, the Ag-NPs have lower biopersistence rate (56%) than the Zn-NPs and TiO_2-NPs, which have higher values.

However, the biopersistence rates calculated in this work are always higher than the limit set by EFSA (12%), indicating that the metallic nanoparticles studied are stable under gastrointestinal conditions and cannot be considered as readily degradable and may be able to pass through the gastrointestinal epithelium and enter the bloodstream and other organs. The results obtained provide the basis for further studies to evaluate the percentage bioavailability of MNPs from seafood using an in vitro model of the gastrointestinal tract.

This work also focused on the investigation of possible toxic effects of nanoparticles through in vitro and in vivo studies, which have been extensively studied in the literature, but often with contradictory results, depending on different factors that characterise nanoparticles and their behaviour (size, concentration, chemical composition, surface properties, released ions, solubility, aggregation behaviour, and biopersistence).

One objective was to find an answer to the question whether the most commonly used food-grade TiO_2 in anatase form (E171) is more toxic than general TiO_2 (60 nm) by performing an in vitro study with different concentrations of both on colon cancer cells: HCT-116 and Caco-2, to obtain data for risk assessment. The work performed suggests that exposure to E171 may be more harmful to health than TiO_2-NPs causing DNA damage.

This confirmed the concern about the higher genotoxicity of a mixture of nano- (32%) and micro-sized TiO_2 particles (68%) contained in E171 compared to a single fraction alone, and suggests that further studies on different molecular mechanisms triggered by

TiO_2 particles are needed to promote safer practises in the use of this compound. However, it is important to emphasise that the concentrations at which genotoxicity is observed are too high to be absorbed by TiO_2 present in foods in commercial products, as its oral absorption is undoubtedly lower.

In vivo toxicity was evaluated using the fish embryotoxicity test (FET) on zebrafish (*Danio rerio*) in accordance with OECD test guideline (TG) 236. The results showed that Ag-NPs (40 nm) was embryotoxic with a lethal concentration (LC50) of 9.604 mg/L, while TiO_2 (60 nm), E171 and E174 showed no acute embryotoxicity at 100 mg/l. As regard ZnO-NPs 30 nm, developmental delay was observed at the end of 96 h post fertilization.

This study suggests that metallic NPs in seafood are indicative of the presence of these new emerging contaminants in the environment, which need to be addressed and assessed to provide data to competent authorities for appropriate risk assessment and management, for sustainable and safe use of nanomaterials, and for the protection, restoration and support of the environment and thus human health.

Overall, the study provides the first quantitative indication of the extent to which humans are orally exposed to NPs through the consumption of contaminated seafood. The results confirm that the NPs in these particular foods, once they enter the gastrointestinal tract, are poorly degradable and thus pose a risk to human health. However, it is extremely important to quantify NPs in more foods and to study the behaviour of nanoparticles in each type of food under static in vitro digestion, since the behaviour of NPs strongly depends on the food matrix. In addition, the toxicological study confirms the concerns about the genotoxicity of TiO_2 60nm and TiO_2 E171 and the developmental delay of ZnO-NPs, while the toxicity of Ag-NPs should be studied in more detail to reach more robust conclusions, especially uncapped Ag-NPs, which are very poorly studied.

Further studies are currently underway to evaluate the effects of NPs on the composition of the faecal microbiota and a metabolomica analysis on Caco-2 cell lines after contact with faeces in the presence of NPs, to evaluate if metabolic processes are affected by the presence of nanoparticles, and to measure markers of oxidative stress.

Deepening the study of nanotoxicology and the characterization of NPs, as well as the development of harmonized methodologies, is essential to better investigate the toxicity, genotoxicity and biopersistence aspects of NPs of different sizes in relation to their different properties and under the different conditions that may occur.